

Transcriptome analyses of *Staphylococcus aureus* grown in platelet concentrates with focus on virulence

Carina Paredes

A thesis submitted to the University of Ottawa in partial fulfillment of the requirements for the PhD degree in Microbiology and Immunology

Department of Biochemistry, Microbiology, and Immunology,
Faculty of Medicine, University of Ottawa

© Carina Paredes, Ottawa, Canada, 2026

Abstract

Platelet concentrates (PCs), used to treat bleeding disorders, are stored at $22 \pm 2^\circ\text{C}$ under agitation to maintain platelet function; however, these conditions favor growth of bacteria introduced during venipuncture. *Staphylococcus aureus* is a predominant PC contaminant and has been involved in septic transfusion reactions. The Ramirez' lab has demonstrated that PC storage elicits differential regulation of bacterial virulence genes. I therefore hypothesized that the PC storage environment triggers transcriptional changes in *S. aureus* resulting in enhanced antibiotic resistance. Furthermore, these transcriptional changes result in enhanced virulence of *S. aureus* grown in PCs. These hypotheses were tested with two objectives: (1) assess differential expression of antibiotic resistance genes in *S. aureus* grown in PCs compared to tryptic soy broth (TSB), and (2) study the role of the NorB efflux pump on the virulence of *S. aureus* grown in PCs. Four transfusion relevant *S. aureus* strains (TRS) were grown in PCs and TSB and subjected to comparative transcriptome analyses. These studies revealed that the *norB* gene (encodes for the efflux pump NorB, which is implicated in quinolone resistance and negatively regulated by MgrA) was upregulated in PC-grown TRS compared to TSB cultures. Furthermore, Minimal Bactericidal Concentration (MBC) assays showed increased quinolone resistance in PC cultures of TRS versus TSB cultures. MBC and RT-qPCR assays with non-transfusion relevant strains (*S. aureus* RN6390, RN6390 Δ *norB*, and RN6390 Δ *mgrA*) indicated that not only NorB, but also efflux pumps NorA and NorC, may be involved in enhanced quinolone resistance in PC-grown *S. aureus*. The impact of the PC storage environment on regulation of quinolone resistance driven by Nor efflux pumps has not been reported before. Furthermore, NorB was shown to be implicated in

S. aureus virulence using a silkworm model. The use of silkworm larvae to evaluate virulence of *S. aureus* driven by NorB is novel and inform the research and transfusion medical communities about potential targets to minimize the risk of transfusing contaminated blood products. My research has open venues for further investigation on the role of efflux pumps in quinolone resistance and virulence in *S. aureus* grown in PCs, which could be used to propose mechanisms to enhance the safety of transfusion patients.

Dedication

I dedicate this work to my grandma, Adelaide,
whose strength, kindness and eternal love continue to inspire me every day.

Eu dedico este trabalho a minha avó, Adelaide,
cuja a força, bondade e amor eterno continuam a inspirar-me todos os dias.

Acknowledgements

I am grateful to Canadian Blood Services for funding my research and providing an inclusive, supportive, and inspiring environment throughout my doctoral studies. I would like to particularly thank the leadership of the Innovation and Portfolio Management, Donor Policy and Studies, Knowledge Mobilization and Strategies Alliances, netCAD and donors.

Words can not express my heartfelt gratitude to my supervisor, Dr. Sandra Ramirez-Arcos, for giving me the invaluable opportunity to pursue my PhD and for providing continuous guidance and support throughout this journey. Thank you for your kindness, guidance and for being the mentor of a lifetime.

I would like to extend my gratitude to the members of my Thesis Advisory Committee – Dr. Franco Pagotto, Dr. Mads Kaern, and Dr. Nicolas Pineault – for their valuable suggestions, constructive feedback and all the time they dedicated to my research work throughout this journey.

I sincerely thank all members of the Ramirez Lab. I am beyond grateful to Adriana Zapata, Dr. Sylvia Ighem Chi and Mr. Yuntong Kou (MSc). I am truly grateful for your companionship and support, both academically and personally. The stimulating scientific discussions and shared moments of encouragement have been invaluable and will remain cherished memories. In addition, I would like to thank our former lab members, Dr. Basit Yousuf and Tamiko Stewart, for their contributions to my research and their warm friendship during my time in the lab.

I would like to thank, Lidia Warth, Andreia Neves and Dr. Virgilio Cadete for their endless support when I decided to adventure myself through grad school. I would like to extend my heartfelt gratitude to Dr. Dilini Kumaran for her unconditional support and friendship since day one, all the tough conversations and the funniest moments ever (*tra la la*) in the past years, this journey would have not been the same without you.

Someone once said friends are the family that the heart chooses, and I am so grateful for my fam-friends, Renata Casais, Jose Casais, Nancy Robitaille, Paul Birch, Hala Najm, Christina Preece, Kevin Preece, Nan and Tiffany Ladder. I have been blessed with amazing friends who have supported throughout the good and hard days, laugh at my lab stories, heard me and helped me wiping my tears, looked out for my wellbeing and never let me give up, specially in the hard days. Thank you all for always believing in me.

Finally, I extend my heartfelt gratitude to my parents, Manuel and Manuela, my sisters Rita and Marta, brothers in law, Nel and Mark, my godson Rodrigo, my niece Lara and extended family for being my biggest supporters. Although we were separated by great distance, their unwavering spiritual, and emotional support made this journey possible.

“Tudo vale a pena quando a alma não é pequena”

“All is worth when the soul is not small”

– translated from Mensagem, Fernando Pessoa

Table of Contents

Abstract.....	ii
Dedication.....	iv
Acknowledgements.....	v
List of Tables.....	xiii
List of Figures.....	xiv
List of Abbreviations.....	xvi
Copyright contents.....	xviii
1. Introduction and Literature review.....	1
1.2 Platelets.....	3
1.2.1 Structure and Thrombopoiesis	3
1.2.2 Role of Platelets in Hemostasis	5
1.2.3 Role of Platelets in Immunity	5
1.2.4 Role of Platelets in Bacterial Clearance	6
1.3 Platelet Concentrates	7
1.3.1 Platelet Storage Lesion	11
1.4 Adverse Transfusion Reactions Involving PCs	11
1.4.1 Non-infectious Adverse Transfusion Reactions.....	11
1.4.2 Infectious Adverse Transfusion Reactions	12
1.5 Bacterial Contamination of PCs	13
1.6 Safety Strategies to Prevent Septic Transfusion Reactions.....	14
1.7 Near Misses and Septic Transfusion Reactions despite PC screening with the BACT/ALERT system and INTERCEPT treatment	17
1.8 <i>Staphylococcus aureus</i>	18
1.8.1 Epidemiology.....	18

1.8.2	Clinical significance	19
1.8.2.1	Platelet interaction with <i>Staphylococcus aureus</i>	19
1.8.3	Virulence factors.....	22
1.8.3.1	Expression and Regulation of virulence factor expression in <i>Staphylococcus aureus</i>	23
1.8.3.2	Cell surface-localized virulence factors involved in host cell adhesion and colonization.....	23
1.8.3.3	Secreted virulence factors	24
1.8.3.4	Biofilm formation by <i>Staphylococcus aureus</i>	26
1.8.3.5	Antibiotic Resistance	27
1.8.3.5.1	Mechanisms of Antibiotic Resistance in <i>Staphylococcus aureus</i>	27
1.8.3.5.2	Changes in membrane permeability	28
1.8.3.5.3	Antibiotic enzymatic inactivation	30
1.8.3.5.4	Antibiotic target modification.....	31
1.8.3.5.5	Efflux pumps.....	31
1.8.3.5.6	The Nor family efflux pumps	34
1.8.3.5.6.1	Regulation of efflux pump <i>nor</i> genes	35
1.8.3.5.6.2	MgrA: Regulation Mechanism and Target Genes	36
1.8.3.5.6.3	NorG: Regulation Mechanism and Target Genes	37
1.8.4	Models to study <i>Staphylococcus aureus</i> virulence	39
1.8.4.1	Vertebrate models	39
1.8.4.2	Invertebrate models.....	40
1.8.4.3	In vitro models	43
1.9	Rationale	43

1.10 Hypotheses	44
1.10.1 Objectives.....	44
2. Materials and Methods.....	45
2.1 Phenotypic characterization of <i>Staphylococcus aureus</i> strains	46
2.1.1 <i>Staphylococcus aureus</i> strains.....	46
2.1.2 Pooled Platelet Concentrates.....	48
2.1.3 Media and Reagents	48
2.1.4 Morphological Characterization of <i>Staphylococcus aureus</i> strains.....	49
2.1.5 Biochemical characterization of <i>Staphylococcus aureus</i> strains	50
2.1.6 Growth curve studies of <i>Staphylococcus aureus</i> strains	51
2.1.7 Biofilm formation assays of <i>Staphylococcus aureus</i> strains	52
2.1.8 Comparative genomic analyses of <i>Staphylococcus aureus</i> strains	54
2.1.8.1 Whole genome sequencing (WGS)	54
2.1.8.2 Comparative genomic analyses.....	55
2.1.8.3 Virulence genes identification	55
2.1.8.4 Antibiotic resistance genes identification	56
2.1.9 Comparative Transcriptome Analysis of TRS grown in PCs vs TSB	56
2.1.9.1 <i>Staphylococcus aureus</i> RNA isolation, library construction and sequencing	56
2.1.9.2 Transcriptome assembly and differential gene expression analyses	57
2.1.9.3 Validation of RNA-seq data using quantitative reverse transcription PCR (RT-qPCR)	58
2.2 Creation of a <i>norB</i> knockout mutant in <i>Staphylococcus aureus</i>	59

2.2.1	Preparation of competent cells	59
2.2.2	Transformation of bacterial competent cells	61
2.2.3	Mutagenesis of <i>Staphylococcus aureus norB</i> using CRISPR-Cas9 methodology	62
2.2.3.1	Plasmid incompatibility analysis	65
2.2.4	Mutagenesis of <i>Staphylococcus aureus norB</i> using allelic recombination exchange	66
2.2.5	Overexpression of <i>Staphylococcus aureus norB</i>	67
2.3	Antibiotic resistance studies	68
2.3.1	Minimum Inhibitory Concentration (MIC)	69
2.3.2	Minimal Bactericidal Concentration (MBC).....	69
2.4	Silkworm Rearing	70
2.4.1	Determination of Lethal Dose 50 (LD50)	70
2.4.2	Virulence studies with PC- and media-derived <i>Staphylococcus aureus</i>	71
2.5	Statistical Analyses	72
3.	Results	73
3.1	Phenotypic characterization of <i>Staphylococcus aureus</i> isolates	74
3.1.1	Microscopic characterization	74
3.1.2	Macroscopic characterization	75
3.1.3	Hemolysis characterization and biochemical identification	75
3.1.4	<i>Staphylococcus aureus</i> growth curves in TSB	77
3.1.5	<i>Staphylococcus aureus</i> growth curves in PCs.....	79
3.1.6	<i>Staphylococcus aureus</i> biofilm formation in TSB and PCs.....	84
3.1.7	Comparative genomic analyses of <i>Staphylococcus aureus</i> strains	87
3.1.8	<i>Staphylococcus norB</i> genomic analysis	90

3.1.9 Comparative analysis of virulence genes in <i>Staphylococcus aureus</i> genomes.....	90
3.1.9.1 <i>Staphylococcus aureus</i> genes involved in adherence and biofilm formation.....	92
3.1.9.2 <i>Staphylococcus aureus</i> genes encoding exotoxins	92
3.1.9.3 <i>Staphylococcus aureus</i> genes encoding enzymes	93
3.1.9.4 <i>Staphylococcus aureus</i> genes encoding antibiotic resistance genes	94
3.2 Global Comparative transcriptome analysis of <i>Staphylococcus aureus</i> TRS grown in PCs and TSB.....	95
3.2.1 Transcriptome analysis of antibiotic resistance genes in <i>Staphylococcus aureus</i>	95
3.2.2 Mutagenesis and overexpression of <i>Staphylococcus aureus norB</i>	98
3.2.2.1 Deletion of <i>norB</i> via CRISPR-Cas9 technology	98
3.2.2.2 Deletion of <i>norB</i> via allelic exchange recombination.....	101
3.2.2.3 Overexpression of the <i>norB</i> gene in <i>Staphylococcus aureus</i>	103
3.2.2.4 <i>norB</i> expression in non-transfusion relevant strains of <i>Staphylococcus aureus</i>	104
3.3 Quinolone resistance assays of <i>Staphylococcus aureus</i> grown in media and PCs.....	106
3.3.1 MIC of ciprofloxacin and norfloxacin.....	106
3.3.2 MBC of ciprofloxacin and norfloxacin	107
3.4 <i>Staphylococcus aureus</i> virulence studies using a <i>Bombyx mori</i> model ..	110

3.4.1	NorB involvement in increased proliferation of <i>Staphylococcus aureus</i> in PCs.....	110
3.4.2	NorB involvement in virulence of <i>Staphylococcus aureus</i>	111
3.4.3	Virulence assays in PC- versus TSB-derived <i>Staphylococcus aureus</i>	112
4.	Discussion	114
4.1.	Role of NorB in quinolone resistance in <i>Staphylococcus aureus</i>	115
4.2.	Role of NorB in growth of <i>Staphylococcus aureus</i> in PCs	116
4.3.	Role of NorB in virulence of <i>Staphylococcus aureus</i>	118
5.	Concluding Remarks.....	121
6.	Future work.....	122
7.	Appendices	123
	References.....	158

List of Tables

Table 1 – Pathogen Reduction Technology (PRT) systems details, mechanism of action and targets.....	16
Table 2 – <i>Staphylococcus aureus</i> ' mechanisms of changes in membrane permeability	29
Table 3 – <i>Staphylococcus aureus</i> ' mechanisms of enzymatic inactivation of antibiotics	30
Table 4 – <i>Staphylococcus aureus</i> ' mechanisms of antibiotic target modification.....	32
Table 5 – <i>Staphylococcus aureus</i> efflux pump families.....	33
Table 6 – MgrA regulatory effect and target genes	37
Table 7 – NorG regulatory effect and target genes	38
Table 8 – Immune response to <i>Staphylococcus aureus</i> infection in <i>Bombyx mori</i> in comparison to human immune response.....	42
Table 9 – <i>Staphylococcus aureus</i> strains used in this study.	47
Table 10 – Phenotypic classification of <i>Staphylococcus aureus</i> TRS, and <i>S. aureus</i> RN6390, RN6390 Δ <i>norB</i> and RN6390 Δ <i>mgrA</i>	76
Table 11 – Summary of Growth rate (slope) and Doubling time parameters..	83
Table 12 – Biofilm formation assay results for all isolates in TSB and PCs, biofilm capability classification and statistical comparison (PCs vs TSB).....	86
Table 13 – Overview of <i>Staphylococcus aureus</i> genome features of all isolates in study	88
Table 14 – Steps of CRISPR-Cas9 protocol to obtain a <i>norB</i> mutant in <i>Staphylococcus aureus</i> PS/BAC/169/17/W.....	100
Table 15 – Steps of allelic recombination exchange protocol to obtain a <i>norB</i> mutant in <i>Staphylococcus aureus</i> RN6390.	102
Table 16 – Steps of overexpression protocol for <i>Staphylococcus aureus</i> RN6390.	103
Table 17 – Minimal Inhibitory Concentration (MIC) of ciprofloxacin and norfloxacin in <i>Staphylococcus aureus</i> grown in Müller Hinton.....	107
Table 18 – Minimal Bactericidal Concentration (MBC) of ciprofloxacin and norfloxacin in <i>Staphylococcus aureus</i> grown in TSB and PCs.	109
Table 19 – LD50 results for wild type and mutants <i>norB</i> and <i>mgrA</i> <i>Staphylococcus aureus</i> strains in a silkworm animal model	112

List of Figures

Figure 1 – Schematic representation of thrombopoiesis.....	4
Figure 2 – Platelet pro-inflammatory and anti-inflammatory immune mediators.....	6
Figure 3 – Collection process of apheresis PCs at Canadian Blood Services..	9
Figure 4 – Manufacturing process of buffy coat PCs at Canadian Blood Services.....	10
Figure 5 –Simplified algorithm used for categorization of BACT/ALERT 3D results obtained during PC screening.	15
Figure 6 – Schematic representation of <i>Staphylococcus aureus</i> virulence factors.....	22
Figure 7 – <i>Staphylococcus aureus</i> molecular antibiotic resistance mechanisms.	28
Figure 8 – Proposed model for the regulatory cascade for the Nor efflux pump family genes in <i>Staphylococcus aureus</i>	35
Figure 9– CRISPR-Cas9 experimental protocol to create a <i>norB</i> mutant in <i>Staphylococcus aureus</i> PS/BAC/169/17/W.....	65
Figure 10 – Protocol overview for overexpression of <i>norB</i> in <i>Staphylococcus aureus</i> CBS2016-05.....	68
Figure 11- Gram staining of TRS and laboratory <i>Staphylococcus aureus</i> isolates.	74
Figure 12- Growth curve studies of TRS <i>Staphylococcus aureus</i> strains.....	81
Figure 13- Growth curve studies of <i>Staphylococcus aureus</i> RN6390 and RN6390 Δ <i>norB</i> and RN6390 Δ <i>mgrA</i>	82
Figure 14 – Biofilm formation by <i>Staphylococcus aureus</i>	85
Figure 15 – Multiple genome alignment of <i>Staphylococcus aureus</i> TRS and <i>Staphylococcus aureus</i> RN6390 using Mauve progressive algorithm.	89
Figure 16 – Schematic representation of the orientation of <i>Staphylococcus aureus norB</i> and neighboring ORFs.....	90
Figure 17 – Virulence factors category and number of genes detected in <i>Staphylococcus aureus</i> (four TRS – CBS 2016-05, CI/BAC/25/13/W, PS/BAC/169/17/W and PS/BAC/317/16/W, and <i>S. aureus</i> RN6390.....	91
Figure 18 – Heatmap of <i>Staphylococcus aureus</i> differentially expressed genes encoding antibiotic resistance mechanisms (PCs vs. TSB)	96
Figure 19 – RT-qPCR of <i>norB</i> expression in PCs compared to TSB.....	98
Figure 20 – Electroporation of <i>Staphylococcus aureus</i> RN4220 (CRISPR-Cas9).....	101
Figure 21 – Electroporation of <i>Staphylococcus aureus</i> RN4220 (Allelic Exchange)	102
Figure 22 – Electroporation of <i>Staphylococcus aureus</i> RN4220 (Overexpression).....	104

Figure 23 – Expression of efflux pumps genes *norA*, *norB*, and *norC* measured by RT-qPCR... 105

Figure 24 – Comparison of silkworm larvae survival after inoculation with *Staphylococcus aureus* derived from TSB and PCs..... 113

List of Abbreviations

AACs	Acetyltransferases
ABC	ATP-Binding Cassette
ADP	Adenosine Diphosphate
AHTR	Acute Hemolytic Transfusion Reaction
AMEs	Aminoglycoside Antibiotics
Amp	Ampicillin
ANTs	Nucleotidyltransferases
APHs	Phosphotransferases
ATP	Adenosine Triphosphate
ATR	Adverse Transfusion Reaction
BA	Sheep Blood Agar
BHI	Brain Heart Infusion
BLASTn	Basic Local Alignment Search Tool - nucleotides
CA-MRSA	Community-associated Methicillin Resistant <i>Staphylococcus aureus</i>
CARD-RGI	The Comprehensive Antibiotic Resistance Database
CD62P	P-Selectin
CFU	Colony Forming Unit
CHIPS	Chemotaxis Inhibitory Protein of <i>Staphylococcus aureus</i>
CLSI	Clinical and Laboratory Standards Institute
CM	Chloramphenicol
CPD	Citrate Phosphate Dextrose
CRISPR	Clustered Regularly Interspaced Short Palindromic Repeats
DTS	Dense Tubular System
FNHTR	Febrile Non-hemolytic Transfusion Reaction
HA-MRSA	Hospital-associated Methicillin Resistant <i>Staphylococcus aureus</i>
HDR	Homologous Direct Recombination
HLA	Human Leukocyte Antigens
HNA	Human Neutrophil Antigens
Kan	Kanamycin
LB	Lysogeny Broth
LBA	Lysogeny Broth Agar
MATE	Multidrug and Toxin Extrusion
MBC	Minimum Bactericidal Concentration
MFS	Major Facilitator Superfamily
MGE	Mobile Genetic Elements
MHB cat+	Muller Hinton Broth, cationic adjusted
MIC	Minimum Inhibitory Concentration
MLSB	Macrolides, Lincosamides and Streptogramin B
MSCRAMMs	Microbial Surface Component Recognizing Adhesive Matrix Molecules
NCBI	National Center for Biotechnology Information

NETs	Neutrophil Extracellular Traps
NHSBT	National Health Service Blood and Transfusion (England)
OCS	Open Canicular System
OD	Optical Density
PAMPs	Pathogen-associated Molecular Patterns
PAS	Platelet Additive Solution
PBPs	Penicillin-binding Proteins
PBS	Phosphate Buffered Saline
PCR	Polymerase Chain Reaction
PCs	Platelet Concentrates
PIA	Polysaccharide intercellular adhesin
PMPs	Platelet Microbicidal Proteins
PRT	Pathogen Reduction Technology
PSL	Platelet Storage Lesion
PSMs	Phenol-soluble Modulins
PVL	Panton-Valentine Leucocidine
RBC	Red Blood Cell
RBCC	Red Blood Cell Concentrate
RNAP	RNA Polymerase Holoenzyme
RND	Resistance-nodulation-division
ROS	Reactive Oxygen Species
rRBCs	Residual Red Blood Cell
RT-qPCR	Reverse Transcription quantitative Polymerase Chain Reaction
SAGM	Saline Adenine Glucose Mannitol
SAs	Superantigens
SCC	Staphylococcal Cassette Chromosomes
SE	Staphylococcal Enterotoxins
SE/s	Enterotoxin-like Proteins
SMR	Small Multidrug Resistance
TCS	Two Component System
TLRs	Toll-like Receptors
TRALI	Transfusion-related Acute Lung Injury
TRS	Transfusion Relevant Strains
TSA	Tryptic Soy Agar
TSB	Trypticase Soy Broth
TSST-1	Toxic Shock Toxin-1
VFDB	Virulence Factor Data Base
vWF	von Willbrand Factor
WBC	White Blood Cells
WGS	Whole Genome Sequencing

Copyright Contents

As a disclaimer, the work presented in this thesis has been partially published in the journal *Antibiotics* (MDPI), in which I am the first author ^[1]. Dr. Sandra Ramirez-Arcos was involved in the conception of the study, designing the experiments, data analysis and interpretation, and in editing the published manuscript.

Citation:

Paredes, C., Truong-Bolduc, Q. C., Wang, Y., Hooper, D. C., & Ramirez-Arcos, S. (2025). Enhanced Quinolone Resistance and Differential Expression of Efflux Pump *nor* Genes in *Staphylococcus aureus* Grown in Platelet Concentrates. *Antibiotics*, 14(7), 635.

DOI: <https://doi.org/10.3390/antibiotics14070635>

Copyright permission was obtained from the journal *Antibiotics* for reproduction of the content of my manuscript in this thesis. The next four pages contain:

1. The email communication about copyright permission
2. The first page of the published manuscript
3. The email communication informing us that the manuscript was selected for the cover of the July issue of *Antibiotics*
4. A copy of the cover of the July issue of *Antibiotics*

Carina Paredes

From:
Sent: 2025-06-26 8:33 PM
To: Sandra Ramirez
Cc: Carina Paredes
Subject: Re: [Antibiotics] Manuscript ID: antibiotics-3687635 - Final Proofreading Before Publication

ATTENTION: This email originated from outside of Canadian Blood Services. Do not click links or open attachments unless you recognize the sender or believe the content is safe.

Dear Dr. Ramirez,

Thank you very much for your reply.

This article is an open access article distributed under the terms and conditions of the Creative Commons Attribution {CC BY} license (<https://creativecommons.org/licenses/by/4.0/>). The authors hold the copyright for published materials. You are free to 1) Share - copy and redistribute the material in any medium or format for any purpose, even commercially;

2) Adapt - remix, transform, and build upon the material for any purpose, even commercially under the certain terms

(see more details via above link).

If you have any questions, please do not hesitate to contact us.

Kind regards,
Karina Yang
Assistant Editor
MDPI (Beijing)

www.mdpi.com

News in Antibiotics:

Antibiotics Impact Factor: 4.6 (2024)

17/137 (Q1) in 'Infectious Diseases'

57/352 (Q1) in 'Pharmacology & Pharmacy'

You are welcome to follow us on Twitter and LinkedIn:

Twitter: <https://twitter.com/antibioticsmdpi>

LinkedIn: <https://www.linkedin.com/company/antibiotics-mdpi/>



Facebook: [https://www.facebook.com/people/Antibiotics-M DPI/100094528824345/](https://www.facebook.com/people/Antibiotics-M%20DPI/100094528824345/)

The information and files contained in this message are confidential and intended solely for the use of the individual or entity to whom they are addressed. If you have received this message in error, please notify me and delete this message from your system. You may not copy this message in its entirety or in part, or disclose its content to anyone.



Article

Enhanced Quinolone Resistance and Differential Expression of Efflux Pump *nor* Genes in *Staphylococcus aureus* Grown in Platelet Concentrates

Carina Paredes ^{1,2}, Que Chi Truong-Bolduc , Yin Wang ³, David C. Hooper ³ and Sandra Ramirez-Arcos ^{1,2,*} 

¹ Department of Biochemistry, Microbiology, and Immunology (BMI), Faculty of Medicine, University of Ottawa, Ottawa, ON K1G 4J5, Canada

² Donation Policy & Studies, Canadian Blood Services, Ottawa, ON K1G 4J5, Canada

³ Division of Infectious Diseases, Massachusetts General Hospital, Harvard Medical School, Boston, MA 02114, USA

* Correspondence:

Abstract

Background/Objective: Platelet concentrates (PCs) are used in transfusion medicine to treat bleeding disorders. *Staphylococcus aureus*, a predominant PC contaminant, has been implicated in several adverse transfusion reactions. The aim of this study was to investigate the impact of PC storage on *S. aureus* resistance to quinolones, which are commonly used to treat *S. aureus* infections. **Methods/Results:** Four transfusion-relevant *S. aureus* strains (TRSs) were subjected to comparative transcriptome analyses when grown in PCs vs. trypticase soy broth (TSB). Results of these analyses revealed differentially expressed genes involved in antibiotic resistance. Of interest, the *norB* gene (encodes for the NorB efflux pump, which is implicated in quinolone resistance and is negatively regulated by MgrA) was upregulated (1.2–4.7-fold increase) in all PC-grown TRS compared to TSB cultures. Minimal Bactericidal Concentration (MBC) of ciprofloxacin and norfloxacin in PC-grown TRS compared to TSB showed increased resistance to both quinolones in PC cultures. Complementary studies with non-transfusion-relevant strains *S. aureus* RN6390 and its *norB* and *mgrA* deletion mutants were conducted. MBC of ciprofloxacin and norfloxacin and RT-qPCR assays of these strains showed that not only *norB*, but also *norA* and *norC* may be involved in enhanced quinolone resistance in PC-grown *S. aureus*. The role of *norB* in *S. aureus* virulence was also tested using the silkworm *Bombyx mori* animal model; lethal dose 50 (LD₅₀) assays revealed slightly higher virulence in larvae infected with the wild-type strain compared to the *norB* mutant. **Conclusions:** The PC storage environment enhances quinolone resistance in *S. aureus* and induces differential expression of efflux pump *nor* genes. Furthermore, our preliminary data of the involvement of NorB in virulence of *S. aureus* using a silkworm model merit further investigation with other systems such as a mammal animal model. Our results provide mechanistic insights to aid clinicians in the selection of antimicrobial treatment of patients receiving transfusions of *S. aureus*-contaminated PCs.

Keywords: *Staphylococcus aureus*; platelet concentrates; quinolone resistance by *Staphylococcus aureus*; *Staphylococcus aureus* virulence; silkworm animal model



Academic Editor: William R. Schwan

Received: 22 May 2025

Revised: 10 June 2025

Accepted: 16 June 2025

Published: 21 June 2025

Citation: Paredes, C.; Truong-Bolduc, Q.C.; Wang, Y.; Hooper, D.C.; Ramirez-Arcos, S. Enhanced Quinolone Resistance and Differential Expression of Efflux Pump *nor* Genes in

Staphylococcus aureus Grown in Platelet Concentrates. *Antibiotics* **2025**, *14*, 635. <https://doi.org/10.3390/antibiotics14070635>

Copyright: © 2025 by the authors.

Licensee MDPI, Basel, Switzerland.

This article is an open access article distributed under the terms and conditions of the Creative Commons

Attribution (CC BY) license

(<https://creativecommons.org/licenses/by/4.0/>).

From: Ms. Sonnier Xu/MDPI

Sent: July 13, 2025 10:24 PM

To: Sandra Ramirez-Arcos

Cc:

Subject: [Antibiotics] Doi Number: 10.3390/antibiotics14070635 - Your paper has been selected as an issue cover - Confirmation Required

Attention : courriel externe | external email

Dear Dr. Ramirez-Arcos,

I am Sonnier from the Marketing team of Antibiotics journal.

Thank you for publishing with us,

Manuscript ID: *antibiotics-3687635*

Title: Enhanced Quinolone Resistance and Differential Expression of Efflux Pump nor Genes in Staphylococcus aureus Grown in Platelet Concentrates

Website: <https://www.mdpi.com/2079-6382/14/7/635>

We are pleased to inform you that your paper is selected by the editors as the cover of the forthcoming issue. The issue cover will be displayed on the issue page: <https://www.mdpi.com/2079-6382/14/7>, and promoted in the issue released notification which will be sent to the journal subscribers together with the table of contents.

To help us prepare the cover, please kindly provide us with the following materials before 20 July 2025:

1. A high-resolution graphical abstract. Our inhouse designers will redesign the picture to fit the specific requirements of issue covers, and the final version will be sent to you for confirmation before online.
2. A short introduction with up to 850 characters including the spaces.
3. A shorten title with up to 80 characters including the spaces.

As the schedule is very tight, it will be highly appreciated if you can send us a short confirmation upon receiving this email.

Thank you for your cooperation and understanding. I am looking forward to your prompt reply.

--

Best regards,

Sonnier Xu

Marketing Assistant

MDPI (Beijing)

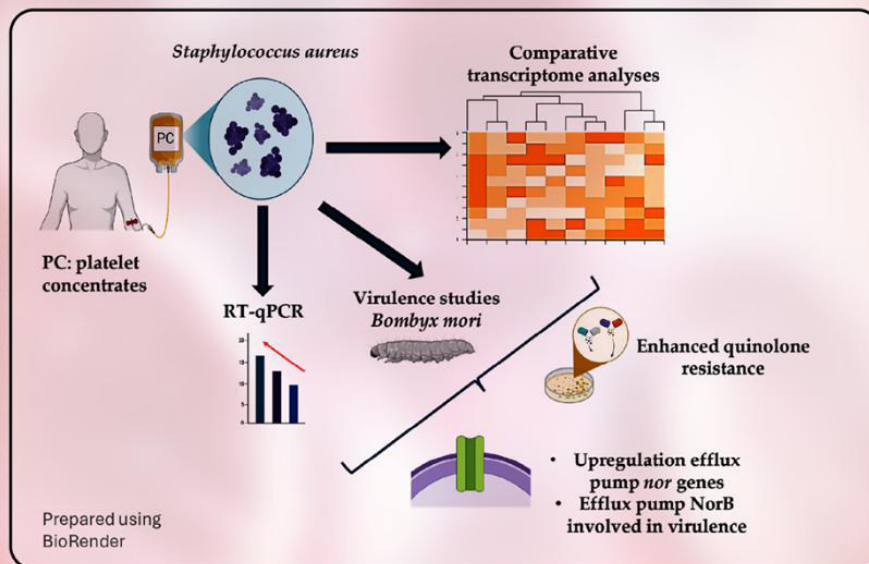
www.mdpi.com

Data Protection Notes <<http://www.mdpi.com/about/data-protection>>

The information and files contained in this message are confidential and intended solely for the use of the individual or entity to whom they are addressed. If you have received this message in error, please notify me and delete this message from your system. You may not copy this message in its entirety or in part, or disclose its contents to anyone.

NorB Confers Quinolone Resistance to *Staphylococcus aureus* Grown in Platelets

Volume 14 · Issue 7 July 2025



1. Introduction and Literature review

As a disclaimer, images presented in this chapter have been published in the journal Antibiotics (MDPI), in which I am the first author ^[1].

1.1 Blood components

Transfusion medicine and blood banking was initiated and gradually established during the 19th and 20th centuries. The first transfusion of human blood was reported in 1818 by Dr. James Blundell, a physician of the Medical Chirurgical Society of London [2]. Some of the main issues identified in blood transfusion in the 19th century included blood clotting and increased risk of transmission of blood-borne diseases (e.g., syphilis) to transfusion patients; therefore, improving blood storage to assure product quality and safety was deemed essential [3]. World War I and World War II intensified the need for blood, leading to significant advances in the transfusion medicine field. Whole blood was initially stored in glass containers, however in the 1960s, sterile plastic storage bags were implemented, permitting the separation of whole blood into blood components such as red blood cell (RBC) concentrates (RBCC), plasma, and platelet concentrates (PCs) [3,4].

Canadian Blood Services manufactures and supplies a trio of blood components (RBCCs, Plasma and PCs) to all provinces and territories of Canada (excluding Québec). Donor blood is collected into bags containing Citrate Phosphate Dextrose (CPD) and then each component is extracted through a combination of centrifugation and filtration processes that separates whole blood into RBCs, plasma, and buffy coat which contains white blood cells and platelets. Each of this fraction is further processed to prepare the three blood components. RBCCs are important for the treatment of anemic patients, with RBC functionality preserved by suspending the RBCC in additive solutions such as saline adenine glucose mannitol (SAGM) and storage at 1-6 °C for a maximum of 42 days. Plasma is used to treat patients with coagulation factor and plasma protein deficiencies;

plasma units are stored for a maximum of one year at temperatures ≤ -18 °C. Finally, PCs are used to treat patients with bleeding disorders and could be suspended in 100% plasma or a mix of plasma and platelet additive solution (PAS). Platelet functionality in PCs is maintained during storage in gas-permeable containers at 22 ± 2 °C under constant agitation [5,6]. Platelet characteristics and PCs are described in more detail in the following sections.

1.2 Platelets

1.2.1 Structure and Thrombopoiesis

Platelets are small, colorless, discoid anucleate cellular fragments originating from megakaryocytes and released into the bloodstream in counts that can range from $150 \times 10^9/L$ to $400 \times 10^9/L$. The lifetime of platelets in the bloodstream is roughly seven to ten days, and platelet levels in the bloodstream are continuously being replenished [7,8]. Platelets are formed from cytoplasmic fragments of megakaryocytes, this mechanism is named thrombopoiesis [9,10], and takes place in the bone marrow with the differentiation of a hemopoietic stem cell into the myeloid branch of hematopoiesis (progenitor cells). They evolve as precursor cells (megakaryoblast, promegakaryocyte), resulting in the development of megakaryocytes [10]. Megakaryocytes undergo cytoplasmatic maturation (cytoplasm expansion), forming proplatelets that are then subject to fragmentation leading to the release of platelets into the blood stream (Figure 1).

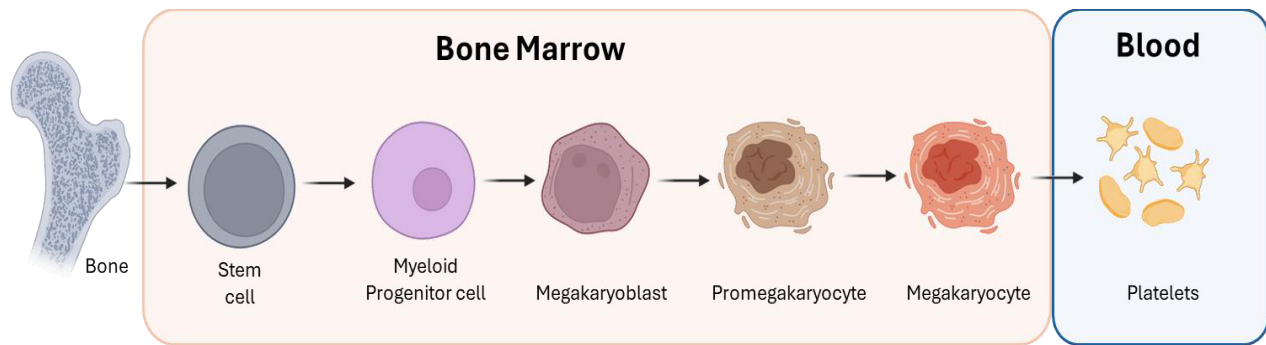


Figure 1 – Schematic representation of thrombopoiesis. Schematic representation of platelet production from hematopoietic stem cells along a continuum into the megakaryocytic lineage. Image prepared using BioRender.

Platelets contain cytoplasmic organelles present in eucaryotic cells including mitochondria, endoplasmic reticulum (in platelets known as dense tubular system (DTS)), and an open canicular system (OCS). Moreover, platelets carry a wide variety of biomolecules in alpha granules (proteins, hemostatic factors, growth factors, and cytokines), dense granules (ADP, serotonin, and calcium) and lysosomes (hydrolytic enzymes) [8].

Platelet activation is triggered by vascular injury, presence of pathogens or contact with other activated platelets. Activation causes a morphological change in platelets from a discoid to a sticky irregular shape, and prompts the release of granules' contents, enabling hemostatic and immunomodulatory responses [7]. Platelets play an important role of managing vascular integrity, regulating hemostasis and monitoring their surrounding environment via a wide array of receptors [8].

1.2.2 Role of Platelets in Hemostasis

Platelets play a major role in hemostasis, a physiological response mechanism coordinated to act upon vascular injury, blood vessel repair, and thrombus plug formation [8,11]. Vascular damage triggers the release of collagen and von Willebrand factor (vWF), which bind to platelet glycoprotein VI and glycoprotein Ib-V-IX complex, respectively, initiating platelet adhesion, activation and aggregation [11]. Activation elicits platelet degranulation (release of alpha and dense granules contents), and a morphological change from discoid to a sticky star-like shape as mentioned above. Moreover, activated platelets aggregate and form a hemostatic plug [7,8]. During activation, platelets release several biomolecules including cytokines and chemokines, thromboxane A₂, adenosine diphosphate (ADP), serotonin, and numerous α-granule proteins, driving inflammatory response vascular repair, and tissue regeneration [12].

1.2.3 Role of Platelets in Immunity

Platelets play a pivotal role in the immune system; they contain a wide array of immune modulators stored within their α-granules, dense granules, and lysosomes, and express several surface receptors, including Toll-like receptors (TLRs), FcγRIIA, and integrins [11,12]. Vascular injury or pathogen-associated molecular patterns (PAMPs) lead to platelet activation and consequently the release of a variety of immune modulators (Figure 2) [8,13]. Platelets have a major role in leukocyte and neutrophil recruitment, for instance platelet interaction with neutrophils trigger the formation of aggregates involved in bacterial phagocytosis and release of reactive oxygen species (ROS) [14]. Platelets induce the formation of neutrophil extracellular traps (NETs) contributing to bacterial elimination [15],

and promote monocyte differentiation into macrophages contributing to an increase in the production of pro-inflammatory cytokines like TNF- α and IL-6, promoting phagocytic activity [8,13,13,14].

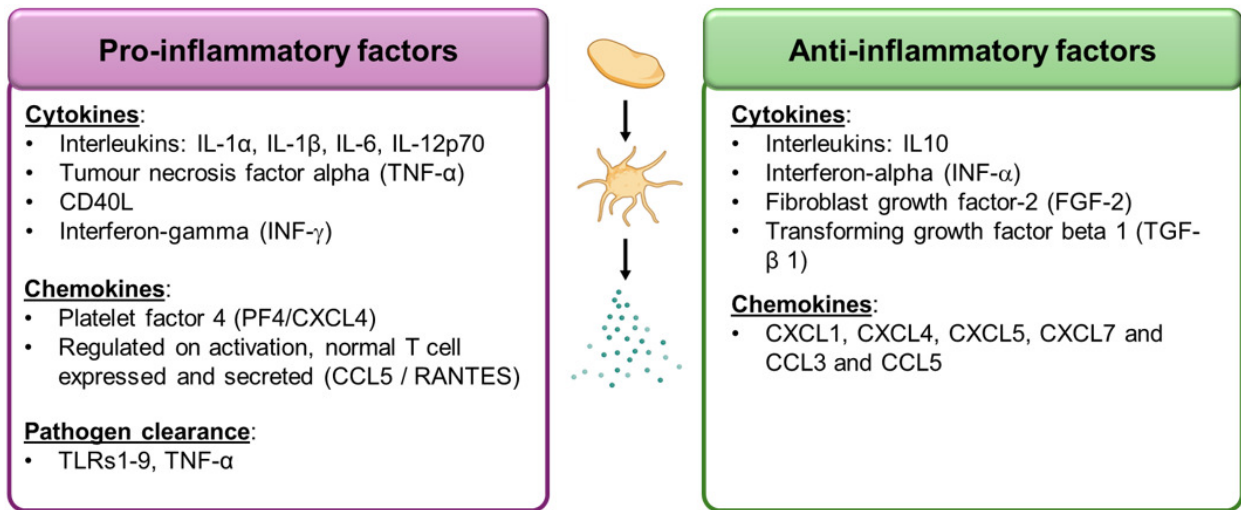


Figure 2 – Platelet pro-inflammatory and anti-inflammatory immune mediators [8,13,13,14]. Image prepared using BioRender.

1.2.4 Role of Platelets in Bacterial Clearance

Platelets express multiple pattern recognition receptors, including TLR2 and TLR4 that recognise bacterial cell wall components such as peptidoglycan and lipoproteins (Gram-positive bacteria), and lipopolysaccharide (Gram-negative bacteria), respectively [16,17]. In the presence of pathogens, TLRs prompt platelet activation, degranulation and release of immunomodulatory biomolecules, and expression of surface receptors such as GPIIb/IIIa, GPIb α , and Fc γ RIIA [15,18]. Activated platelets secrete antimicrobial peptides, including thrombocidins, and platelet microbicidal proteins (PMPs), that contribute to pathogen clearance [18].

Notably, platelets can bind to bacteria forming free-floating aggregates that can circulate in the bloodstream and later attach to tissues such as cardiac valves promoting formation of bacterial aggregates (i.e., biofilms) and bacterial survival, consequently contributing to infection (e.g., endocarditis) ^[19]. Furthermore, the impact of platelet interaction with pathogens can lead to acute infection. For instance, in sepsis, increased platelet activation leads to host response imbalance, due to excessive production of pro-inflammatory cytokines (e.g. TNF- α , IL6, IL β 1) causing inflammation, tissue damage and organ failure ^[20]. Overall, platelet immunomodulatory response plays a major role in the global immune response upon pathogen infection.

1.3 Platelet Concentrates

Platelet concentrates (PCs) are a therapeutic blood component that contains platelets (approximately 251×10^9 platelets per unit) suspended in 100% plasma or 40% plasma plus 60% of PAS ^[21]. Platelet function and quality is maintained in the well-established PC storage conditions. PCs are stored in gas-permeable plastic bags, at 20-24 °C, under constant agitation, in a glucose rich media (324mg/dl in plasma-PCs and 144mg/dl in PAS-PCs) and neutral pH for up to seven days ^[5,22].

Currently, at Canadian Blood Services, PCs are obtained through apheresis, which are collected directly from a single donor (Figure 3) or from individual whole blood donations which are pooled via the buffy coat method (Figure 4).

Single-donor hyperconcentrated apheresis PC are aseptically collected from a single donor using an automated equipment (Terumo Trima apheresis collection system) ^[21].

Platelets are leukoreduced at the time of collection by the automatic collection system and suspended in a mix of donor plasma and PAS in a ratio of approximately 40:60 (plasma:PAS). The units are then split into two and the remaining blood components are returned to the donor's bloodstream ^[23,24]. Split units are subjected to pathogen reduction as described in section 1.6 of this chapter (Figure 3).

Since 2022, the buffy coat method involves pooling and suspending seven ABO matched buffy coat fractions in a mix of plasma and PAS in a 40:60 ratio to produce a double dose PC, which is subjected to residual RBC removal and leukoreduction by filtration^[23], prior to splitting it into two PC units. Split units are subjected to pathogen reduction as described in section 1.6 of this chapter (Figure 4A).

Prior to the implementation of PAS, PC were units suspended in 100% plasma. Specifically buffy coat PC pools were prepared by pooling four buffy coat fractions which were suspended in the plasma of one of the donations (Figure 4B). In my thesis, I used this last product, PC buffy coat pools suspended in 100% plasma, for all the experiments described in the following chapters.

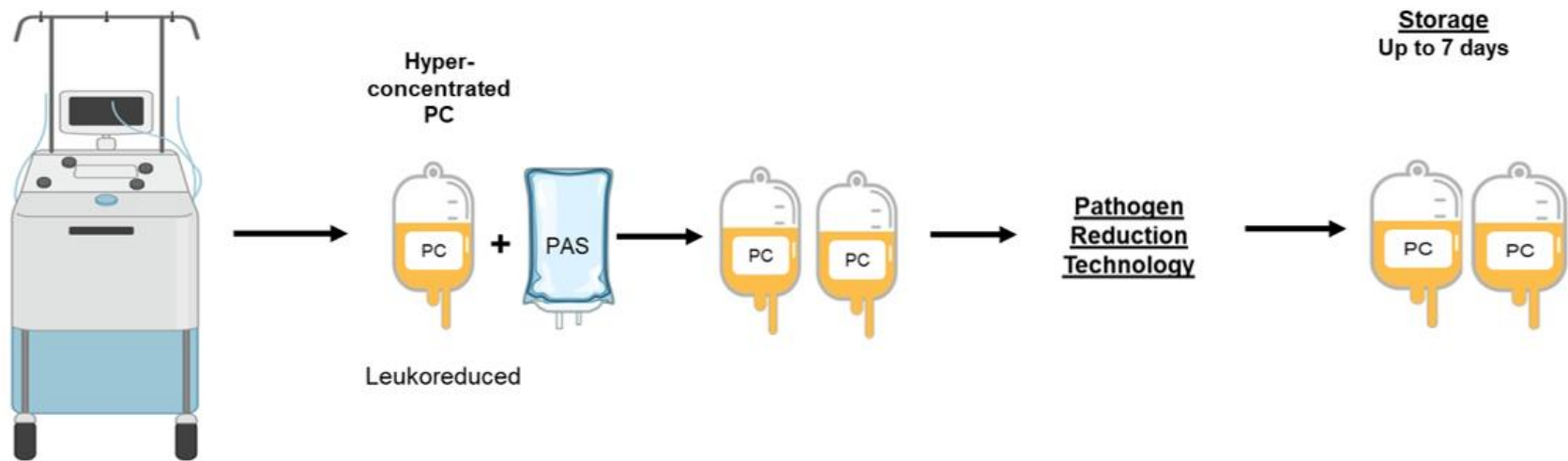


Figure 3 – Collection process of apheresis PCs at Canadian Blood Services. Apheresis PCs are produced using an automated equipment that draws blood from the donor and separates the blood components via centrifugation, platelets are retained and suspended in a mix of plasma (~40%) and platelet additive solution (PAS, ~60%), RBC and plasma are returned to the donor's bloodstream. Removal of white blood cells (WBC) (i.e., leukoreduction) is done via filtration. Image prepared using BioRender.

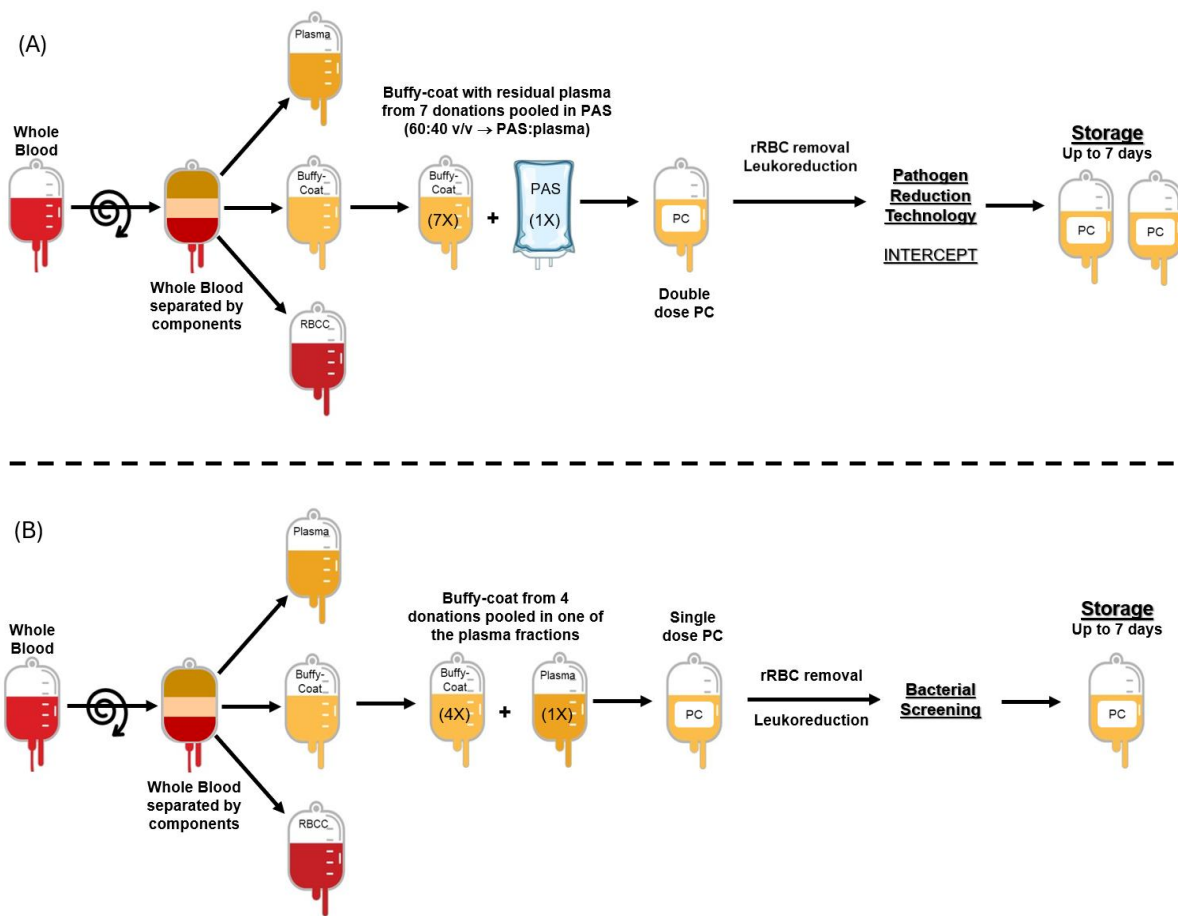


Figure 4 – Manufacturing process of buffy coat PCs at Canadian Blood Services. (A) Current method: Buffy coat PCs manufactured by resuspending seven buffy coats in a mix of plasma (~40%) and platelet additive solution (PAS, ~60%). (B) Old method: Buffy coat PCs manufactured by resuspending four buffy coats into the plasma of one donation. The PC units in both processes are centrifuged to remove residual red blood cells (rRBCs). Removal of white blood cells (WBC) (i.e., leukoreduction) is done via filtration. Image prepared using BioRender.

1.3.1 Platelet Storage Lesion

PC production and storage can elicit biochemical, structural, and functional deterioration of platelets compromising the final quality of PCs due to a phenomenon called platelet storage lesion (PSL) [25,26]. One of the major contributors for PSL is metabolic stress due to glucose consumption and lactate production by platelets during storage, leading to acidification of the storage medium and a decline in pH, reducing platelet viability [27]. Moreover, a reduction in surface membrane glycoproteins due to platelet activation triggers the expression of activation markers such as P-selectin (CD62P) and the release of immune factors (degranulation) [28]. Collectively, these factors affect the functionality of the platelets in the PC bag posing a reduction in the quality of the transfusable product.

1.4 Adverse Transfusion Reactions Involving PCs

An adverse transfusion reaction (ATR) is an unintended and harmful response in an infused patient that occurs during or after the transfusion of a blood product [29]. ATRs can be non-infectious or infectious reactions and involve a wide range of symptoms from mild allergic reactions to severe life-threatening events [29,30].

1.4.1 Non-infectious Adverse Transfusion Reactions

Non-infectious reactions are ATRs caused by immune or physiological incompatibility between the patient and the transfused blood product and can be acute or delayed depending on the symptoms' evolution. Examples of non-infectious reactions and symptoms are briefly described below:

- *Febrile non-hemolytic transfusion reaction (FNHTR)* – mild reaction caused by the patient’s immune response to white blood cells or cytokines present in the transfused PCs. Patient symptoms include fever and chills [29].
- *Allergic reactions* – recipient’s hypersensitivity reaction to proteins in the donated PCs, symptoms can be mild (itchiness, urticaria) to severe anaphylactic shock [29].
- *Acute hemolytic transfusion reaction (AHTR)* – caused by ABO incompatibility, resulting from recipient’s antibodies attacking the donor platelets, leading to their destruction. Patient symptoms can range from fever, back pain, hemoglobinuria and potential kidney failure [29].
- *Transfusion-related acute lung injury (TRALI)*: rare reaction marked by an abrupt respiratory distress due to an immune-mediated response in the infused patient’s lungs, usually associated to the activation of patient’s neutrophils by antibodies present in the PC plasma that target human leukocyte antigens (HLA) or human neutrophil antigens (HNA) [29].

1.4.2 Infectious Adverse Transfusion Reactions

Infectious ATRs result from transfusion of blood components contaminated with pathogens (bacteria, viruses, or parasites), causing mild to serious and potentially life-threatening transfusion complications [5]. Bacterial contamination poses the major infectious transfusion risk to susceptible patients as these pathogens can proliferate during blood component storage in contrast to other pathogenic agents such as viruses and parasites.

1.5 Bacterial Contamination of PCs

Adverse transfusion reactions caused by the infusion of bacterially contaminated PCs have been reported globally at rates ranging from 1/100,000 to 1/300,000 transfused units [6,31,32]. However, these data are obtained from passive surveillance monitoring, resulting in underreports of septic transfusion reactions. For example, a study by Hong et al., using an active surveillance approach, revealed that 20 out of 51,440 PC transfused in the US between 2007 and 2013 were contaminated with bacteria resulting in adverse transfusion events, which were missed during passive surveillance [33]. Many ATRs have been associated with contaminated PCs by both Gram-negative and Gram-positive bacteria [20,34–38][39].

Gram-negative bacteria (e.g., *Serratia marcescens*, *Escherichia coli* and *Klebsiella* species) liberate endotoxins (lipopolysaccharide), that stimulate the production of pro-inflammatory cytokines such as tumor necrosis factor (TNF), interleukin-1 β (IL-1 β), gamma interferon (IFN γ) and several chemokines, which can cause severe tissue damage and contribute to increased mortality [40,41]. Gram-positive bacteria (e.g. *Staphylococcus aureus*, *Streptococcus* spp.) in the other hand can release a wide variety of toxins (e.g., exotoxins) that prompt a dysregulated immune response that can also lead to septic shock [42].

1.6 Safety Strategies to Prevent Septic Transfusion Reactions

To minimize the risk of transfusing bacterially contaminated PCs, blood centers, including Canadian Blood Services, have implemented several strategies to increase PC safety [6,37,43].

- Mandatory blood donor evaluation questionnaire and temperature measurement to assess donor's health condition, and medical and travel history prior to blood donation [44].
- Disinfection of the venipuncture site to decrease contamination derived from donor skin flora with disinfectants such as one-step Chloraprep used at Canadian Blood Services, which contains 2% chlorhexidine gluconate and 70% isopropyl alcohol. The antiseptic is applied to the antecubital region for 30 seconds followed by a 30 second drying time prior to venipuncture [45]. Arms of donors allergic to Chloraprep are disinfected with 70% isopropyl alcohol followed by 10% povidone-iodine [45].
- Diversion of the initial aliquot of collected blood (30-40 ml) to decrease skin flora contamination. Diversion of the initial aliquot of blood (30-40 ml) collected during venipuncture aims at reducing skin flora contamination in the donated PCs [46].
- PC Screening with the automated BACT/ALERT 3D culture system to detect bacterial contamination in PCs. This system is based on colorimetric detection of CO₂ produced during bacterial growth in BACT/ALERT 3D culture bottles. The sensitivity of the BACT/ALERT 3D system is estimated to be 1-10 colony forming units per ml (CFU/mL) [47,48]. At Canadian Blood Services, PC samples are taken at least 36 hours post-blood collection and inoculated into aerobic and anaerobic

culture bottles, which are incubated into the BACT/ALERT system until flagging positive or up to 7 days [6]. Results are categorized based on microbial detection by the system and bacterial growth upon culturing (Figure 5).

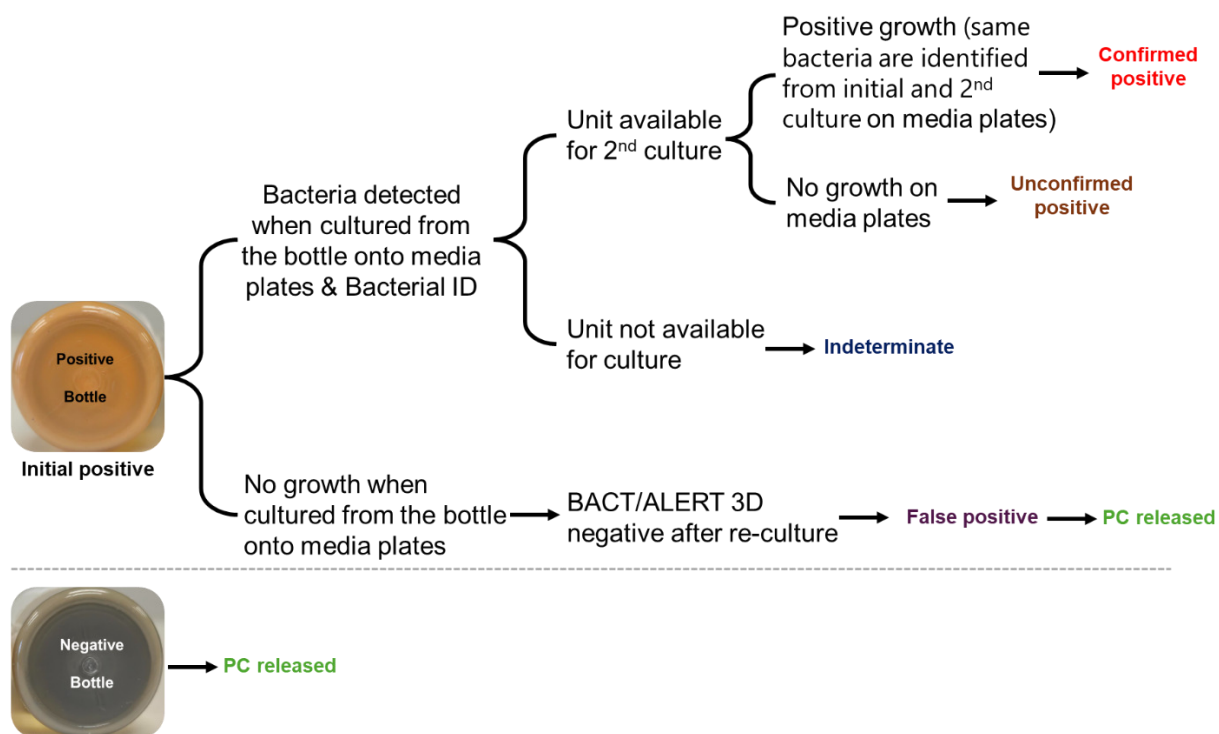


Figure 5 – Simplified algorithm used for categorization of BACT/ALERT 3D results obtained during PC screening [6].

- PC treatment with pathogen reduction technologies (PRT) is a proactive approach designed to impair pathogen viability by targeting nucleic acids with different approaches. Currently, there are three pathogen reduction technology systems available: Mirasol (Terumo BCT Inc. USA), THERAFLEX (MacoPharma, France) and INTERCEPT (Cerus Corp, USA). Each company presents a solution based in UV radiation combined with either a photosensitizer or agitation as described in Table 1. Canadian Blood Services fully implemented INTERCEPT treatment for apheresis and buffy coat PCs in 2024.

Table 1 – Pathogen Reduction Technology (PRT) systems details, mechanism of action and targets.

PRT System	Photoreactive compound	Mechanism of Action	Target	Reference
Mirasol	Riboflavin ↓ <u>Exposure</u> UVB/UVA 265-370 nm 6.2 J/mL	<ul style="list-style-type: none"> ◆ Nonspecific binding of riboflavin and nucleotides ◆ UV exposure ◆ Nucleic acids permanent alteration (oxidation of guanine) 	<ul style="list-style-type: none"> ◆ Bacteria ◆ Viruses ◆ Parasites 	[49]
THERAFLEX	N/A ↓ <u>Exposure</u> UVC 254 nm 0.2 – 0.3 J/mL	<ul style="list-style-type: none"> ◆ UVC exposure & severe agitation ◆ Selective nucleic acids alteration (inhibiting DNA transcription) 	<ul style="list-style-type: none"> ◆ Bacteria ◆ Viruses ◆ Parasites 	[49]
INTERCEPT	Amotosalen ↓ <u>Exposure</u> UVA 320 – 400 nm 3 J/mL	<ul style="list-style-type: none"> ◆ Amotosalen intercalates with DNA bases, crosslinking and blocking DNA ◆ Inhibition of bacterial replication 	<ul style="list-style-type: none"> ◆ Bacteria ◆ Viruses ◆ Parasites 	[49]

1.7 Near Misses and Septic Transfusion Reactions despite PC screening with the BACT/ALERT system and INTERCEPT treatment

At Canadian Blood Services, there have been false negative BACT/ALERT screening transfusion reactions involving PCs contaminated with *Staphylococcus aureus* (two cases), *Serratia marcescens* and *S. epidermidis*. [6,50].

Although no transfusion reactions have been reported since the recent implementation of the PRT INTERCEPT to treat PCs at Canadian Blood Services, some breakthroughs have been reported by other blood centers including l'Établissement Français du Sang in France and the American Red Cross in the US. Organisms involved in these breakthrough cases included *S. aureus*, *Bacillus* spp., *Acinetobacter baumannii* and coagulase negative *Staphylococcus* [51,52].

In the two false negative BACT/ALERT screening cases involving *S. aureus* reported by Canadian Blood Services [34,35], staphylococcal enterotoxins were detected in the transfused products, which were likely responsible for the septic shock symptoms experienced by the patients [34,35]. More recently, a near miss case was documented by Canadian Blood Services involving PCs contaminated with *S. aureus* [53]. Similarly, near misses or ATRs cases involving *S. aureus* contaminated PCs have been reported by other countries including the US, the UK and Ireland [31,54,55].

S. aureus has therefore become an important safety risk to PC transfusion recipients worldwide due to its ability to escape detection during routine PC screening, to grow to

clinically significant levels and produce exotoxins during PC storage, and to resist INTERCEPT treatment [31,34,35,51,54,55]. Due to the predominance of this species as a PC contaminant and causative agent of septic transfusion reactions, it was chosen as a model organism for my research studies and the next section discusses characteristics of this bacterium in more detail.

1.8 *Staphylococcus aureus*

1.8.1 Epidemiology

S. aureus was first identified in 1880 by Sir Alexander Ogston and later named for its golden-colored colonies [56]. This bacterium is often considered a pathogen, however, it commonly exists harmlessly in the human mucosa flora, particularly in the nose and the gut [57–60]. *S. aureus*, a member of the *Staphylococcaceae* family, is a non-motile, non-sporulating Gram-positive coccus, with a cell envelope that comprises a cytoplasmic membrane, surrounded by a cell wall mainly composed of peptidoglycan, teichoic acids, and surface-associated proteins [60]. The peptidoglycan layer (thick cross-linked network) preserves cell shape, and contributes to osmotic balance, permeability and cell protection [61]. Several *S. aureus* strains secrete polysaccharide-based microcapsules over of the peptidoglycan layer as a protective coat against host defenses [62]. The chromosome of *S. aureus* is circular (~ 2.8M bp), and this bacterium carries a plethora of mobile genetic elements (MGE), such as pathogenicity islands, staphylococcal cassette chromosomes (SCCs), prophages, transposons, insertion sequences, and plasmids [63]. Genes encoding for virulence factors are located both on the chromosome and MGEs [63,64]. *S.*

aureus genes encoding virulence factors are transferred within staphylococcal species and across other species, both vertically (during cell division from a parent cell to progeny) and horizontally (transformation, transfection and conjugation), contributing to rapid bacterial adaptation to environmental stressors [60,64,65].

1.8.2 Clinical significance

S. aureus emerged as a major concern over the past years due to widespread outbreaks in both hospital and community settings, and enhanced resistance to antibiotics [57,60].

Notably, platelet – *S. aureus* aggregation is paramount in bacterial infections such as infective endocarditis where the bacteria colonize heart valves by adhering to platelet-fibrin thrombi, resisting shear stress and immune attack [19]. Interactions between platelets and *S. aureus* are also important for the development of sepsis contributing to intravascular coagulation, vascular damage, and organ dysfunction. Furthermore, *S. aureus*-platelets association aids bacterial persistence during biofilm formation [66]. A recent study investigated the impact of *S. aureus* on platelet function in contaminated PCs with results demonstrating that *S. aureus* triggers platelet activation, impacting mitochondrial disfunctions and eliciting platelet apoptosis [67].

1.8.2.1 Platelet interaction with *Staphylococcus aureus*

The interaction between *S. aureus* and platelets occurs in stages: initial adhesion of *S. aureus* to platelets, followed by platelet activation and aggregation, and then by *S. aureus* evasion from host immune clearance [68]. This dynamic multistep process combines both

bacterial virulence factors and platelet receptors, that may lead to transient adherence and formation of stable *S. aureus*-platelet aggregates that pose a high risk for patients. These aggregates are the scaffold for infective endocarditis, colonization of indwelling medical devices, and prosthetic joint infections [19,39].

Adhesion to platelets: S. aureus Microbial Surface Component Recognizing Adhesive Matrix Molecules (MSCRAMMs) bind to platelet receptors such as GPIIb/IIIa (integrin α IIb β 3) and Fc γ RIIa. MSCRAMMs involved in interactions with platelets include clumping factors A and B (ClfA and ClfB), fibronectin-binding proteins (FbBD A and B), collagen adhesin (Can), and serine-aspartate repeat proteins (C, D and E) [69,70]. Protein A binds the Fc region of immunoglobulins contributing to the interaction with Fc γ RIIa platelet receptors [71]. Clumping factors, A and B (ClfA and ClfB) can bind the platelet receptor GPIIb/IIIa directly or by bridging with fibrinogen [72]. Fibronectin-binding proteins (FnBPA and FnBPB) contribute to endocytic uptake of the bacteria by host cells, these proteins bind to fibronectin-coated surfaces and play a crucial role in colonization of non-phagocytic cells [73]. Collagen-binding protein (Can) plays a role in infection by promoting the attachment to collagen-rich tissues, and the Serine-Aspartate repeat proteins (SdrC/D/E) participate in the formation of surface-attached bacterial aggregates known as biofilms[70].

Furthermore, shear flow may result in the binding of other adhesins such as Eap (extracellular adherence protein) and IsdB (iron-regulated surface determinant B) to platelets via interaction with plasma proteins like fibrinogen and vitronectin [74,75].

Platelet activation and aggregation: S. aureus induces the activation and aggregation of platelets, triggering platelet degranulation (release of granules contents: cytokines,

antimicrobial peptides, ADP, among others) promoting thrombus formation and host immune responses [76]. Importantly, platelet activation can be mediated via immune complexes or Protein A–IgG interaction using FcγRIIIa signaling, TLRs (e.g., TLR2) stimulation, and engagement of integrins through MSCRAMMs-platelet surface markers complexes [70]. During activation, platelets release proinflammatory factors such as platelet factor 4 (PF4), and serotonin that increase inflammation and recruit immune cells to the infection site [77]. Additionally, *S. aureus* α-toxin can prompt calcium mobilization and cytoskeletal rearrangement in platelets (shape change), contributing to increased platelet aggregation [78].

Immune evasion: The aggregation of *S. aureus* and platelets provides this bacterium with an advantage to evade immune clearance. Platelet-rich thrombi may act as a scaffold for bacterial biofilm formation, contributing to bacterial antibiotic resistance and evasion from host immune factors (i.e., acting as a shield preventing phagocytosis) [79]. Additionally, *S. aureus* secretes toxins (e.g., α-hemolysin, leukocidins) that can modulate the host immune response and induce platelet apoptosis [67,80,81]. Staphylococcal biofilm formation can result in altered metabolic activity, resulting in reduced susceptibility to antibiotic penetration [82]. Moreover, *S. aureus* secretes staphylococcal complement inhibitor (SCIN) and chemotaxis inhibitory protein (CHIPS), that inhibit opsonization and leukocyte recruitment, promoting bacterial immune evasion inside platelet-bacterial aggregates [83].

1.8.3 Virulence factors

S. aureus is a bacterium that harbors a plethora of virulence factors involved in host colonization, tissue damage and immune evasion [68]. The virulence factors produced by *S. aureus* include cell surface-localized virulence factors such as Protein A and MSCRAMMs, secreted virulence factors like superantigens (SAs), pore-forming toxins, phenol-soluble modulins, and enzymes (Figure 6) [57,63,65].

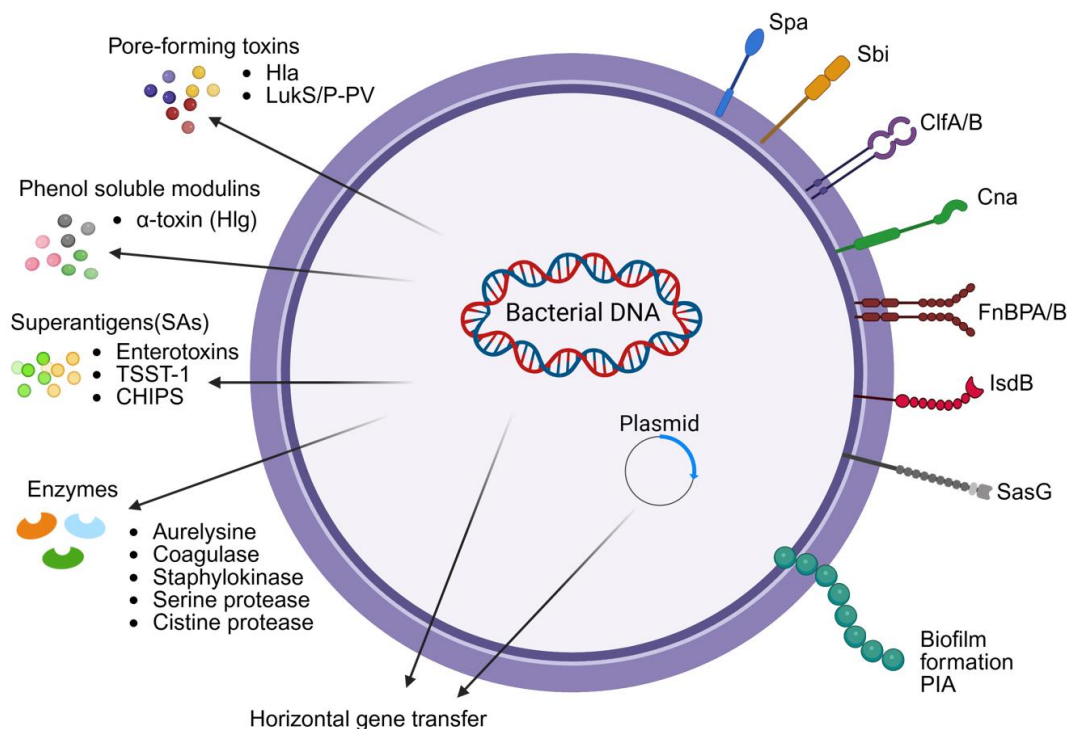


Figure 6 – Schematic representation of *Staphylococcus aureus* virulence factors. Cell surface-localized virulence factors represented on the right-hand side: Sap - protein A; Clf A/B - Clumping factors A and B, Cna - collagen-binding protein; FnBPA/B - fibronectin-binding protein A and B; IsdB - iron-regulated surface determinant B and SasG, *S. aureus* surface protein G. Secreted virulence factors represented on the left-hand side: Pore-forming toxins: Hla - α-Hemolysin, LukS/P- PV - Panton-Valentine leucocidin, phenol-soluble modulins, superantigens: TSST-1 - Toxic shock syndrome toxin-1, CHIPS - Chemotaxis inhibitory protein of *S. aureus* and enzymes. PIA - Polysaccharide intercellular adhesin. Image prepared using BioRender.

1.8.3.1 Expression and Regulation of virulence factor expression in *Staphylococcus aureus*

S. aureus virulence factors can be divided into two functional groups responsible for colonization and infection, giving the bacterium the capability to shift from a harmless commensal colonizer to a deadly invasive pathogen [84]. These virulence factors are either encoded in the genome or acquired via horizontal gene transfer, and their modulation is driven by the action of two-component regulatory systems (TCS) and the accessory genome regulator (Agr) system. The AgrC-AgrA two-component transcriptional quorum (i.e., bacterial cell density) sensing system responds to an extracellular signal, a post-transcriptional modified autoinducing thiolactone-containing cyclic peptide. At high cell density, Agr is responsible for increased expression of extracellular virulence factors (e.g., exotoxins) while at low bacterial cell density, Agr triggers the transcription of virulence factors involved in adhesion and chronic infections (e.g., MSCRAMMs proteins and biofilm formation)^[85,86].

1.8.3.2 Cell surface-localized virulence factors involved in host cell adhesion and colonization

S. aureus expresses several surface proteins, also known as cell adhesion markers, that play a major role in bacterial virulence contributing to adhesion to host cells and medical devices, and immune evasion [63–65,69]. MSCRAMMs contribute to the binding to host extracellular matrices, enabling bacterial aggregation and adherence favoring tissue colonization [67,70]. *S. aureus* surface proteins play a pivotal role in attachment and

immune evasion, facilitating bacterial infection (acute and chronic) [65,69]. *S. aureus* surface proteins are key in host tissue colonization by binding to host extracellular markers such as collagen, fibronectin or fibrinogen [63]. For instance, Protein A contributes to immune evasion and has a role in opsonization and phagocytosis by binding to the Fc portion of immunoglobulin G (IgG) and B-cell receptors triggering B-cell apoptosis [71].

1.8.3.3 Secreted virulence factors

In addition to surface proteins, secreted virulence factors play a major role in colonization and immune evasion promoting systemic inflammation. *S. aureus* secretes pore-forming toxins, phenol-soluble modulins, superantigens and enzymes that contribute to bacterial colonization, evasion to immune defenses and damage to host cells [65,87,88]. This group of virulence factors act in a similar fashion to surface-associated virulence components, primarily by impairing phagocytic uptake and thereby inhibiting opsonophagocytic clearance [88,89]. Secreted virulence factors include:

Pore-forming toxins can be grouped in two classes: α -hemolysin (alpha-toxin - Hla) and leukocidins. Hla binds to host cells plasma membrane, forming pores and therefore, this toxin compromises the integrity of the membrane leading to damage and cell lysis. Interestingly, Hla depicts pro-inflammatory properties and bind to epithelial, endothelial and immune cells [90]. Leukocidins are bi-component toxins that target protein receptors in the host cell membrane and form pores. *S. aureus* leukocidins have been categorized into five subgroups based on specific protein receptor and target (host specificity): LukSF-

PV (also known as Panton-Valentine leucocidin – PVL), LukE, γ -hemolysins AB and CD (HlgAB and HlgCB), and LukAB (also known as LukGH) [80].

Phenol-soluble modulins (PSMs) are short peptides that display surfactant-like activity and amphipathic properties, playing a multitude of roles in infection, such as triggering pro-inflammatory cytokines, damage in neutrophils, and biofilm formation [91].

Superantigens (SAs) are exotoxins that disturb the adaptive immune response by hyper-stimulating T lymphocytes contributing to toxic shock syndrome, respiratory track infections (e.g., pneumonia) and sepsis [63,92]. Interestingly, in the clinical setting, SAs are involved in inflammatory syndromes that can range from mild symptoms (fever and rash) to severe symptoms (cytokine storm and multiorgan failure) [93]. *S. aureus* carries an array of genes encoding for staphylococcal enterotoxins (SE), enterotoxin-like (SE/s) proteins and toxic shock toxin-1 (TSST-1) [92]. Remarkably, it has been shown that SE are frequently organized in clusters that facilitate bacterial infection and immune evasion [88]. Whilst some SE are chromosomally encoded, most genes encoding SEs reside in mobile genetic elements (e.g., pathogenicity islands), facilitating horizontal gene exchange [63].

Exoenzymes are secreted by *S. aureus* to aid in bacterial pathogenicity, via host cell invasion and immune clearance evasion. Prominent examples of enzymes released by *S. aureus* are lipases, phospholipases, proteases, esterases and hyaluronidases [81]. For instance, chemotaxis inhibitory protein of *S. aureus* (CHIPS) is encoded by *chp* and binds

to human neutrophils compromising calcium intake, which has a crucial role in neutrophil physiology (activation, degranulation, phagocytosis) [94].

Staphyloxanthin is a carotenoid pigment produced by *S. aureus*, which is responsible for the golden-yellow colony color of this species. This carotenoid offsets reactive oxygen species (ROS) released by host immune cells (e.g., neutrophils) acting as a powerful antioxidant enabling bacterial survival and contributing significantly to the pathogen's overall virulence^[95,96]. Yu et al. (2025) have recently shown a key role of staphyloxanthin not only in ROS resistance but also in promoting biofilm formation [97].

1.8.3.4 Biofilm formation by *Staphylococcus aureus*

In 1978, Bill Costerton highlighted the impact of biofilms in medical settings and the study of biofilm formation by *S. aureus* has been the scope of many molecular and functional characterization studies [36,79,97,98]. *S. aureus* biofilm cells produce a matrix of extracellular polymeric substances, allowing for aggregation and adherence to biotic and abiotic surfaces. The *S. aureus* biofilm matrix is primarily composed of the polysaccharide intercellular adhesin (PIA), encoded by the *icaADBC* operon and regulated by IcaR^[99]. In addition to PIA, the biofilm matrix contains proteins and extracellular DNA (eDNA). Importantly, there are *ica*-independent biofilm-positive *S. aureus* strains which form proteinaceous biofilm matrices [98,99]. *S. aureus* biofilms are involved in most of the infections caused by this organism and are very difficult to eradicate due to increased resistance to antibiotic treatment and immune clearance [98]. Biofilm formation by *S. aureus* is controlled by several regulatory systems involving quorum-sensing (*agr*), the

cytoplasmic regulator *sarA*, the alternative sigma factor *sigB*, and the two-component system *saeRS* [100]. *S. aureus* biofilms are important for the colonization of indwelling medical devices, including intravascular catheters, prosthetic heart valves, prosthetic joints, artificial pacemakers and several organs, causing severe infections [19,101]. Moreover, evidence collected in the Ramirez' laboratory demonstrated that the PC storage environment triggers biofilm formation by *S. aureus* [50,79].

1.8.3.5 Antibiotic Resistance

Hospital-associated methicillin resistant *S. aureus* (HA-MRSA) outbreaks have been documented since the 1970s due to a rise in infections after patient hospital admission [60,102,103]. Later, MRSA infections spread to communities contributing to outbreaks of community-associated methicillin resistant *S. aureus* (CA-MRSA)[102–104]. Data from the Public Health Agency of Canada related to infections caused by MRSA showed an increase in the incidence of CA-MRSA between 2016 and 2020 [105]. Hospital associated infections are mostly associated with respiratory track infections, whereas community associated infections usually present as skin and soft tissue infections [102].

1.8.3.5.1 Mechanisms of Antibiotic Resistance in *Staphylococcus aureus*

S. aureus carries an array of antibiotic resistance mechanisms to withstand a wide spectrum of antimicrobial drugs [91,98], which include changes in membrane permeability, enzymatic inactivation, target modification and efflux pump activity (Figure 7). Notably, genes encoding for resistance mechanisms can be exchanged via mobile genetic elements [107,108].

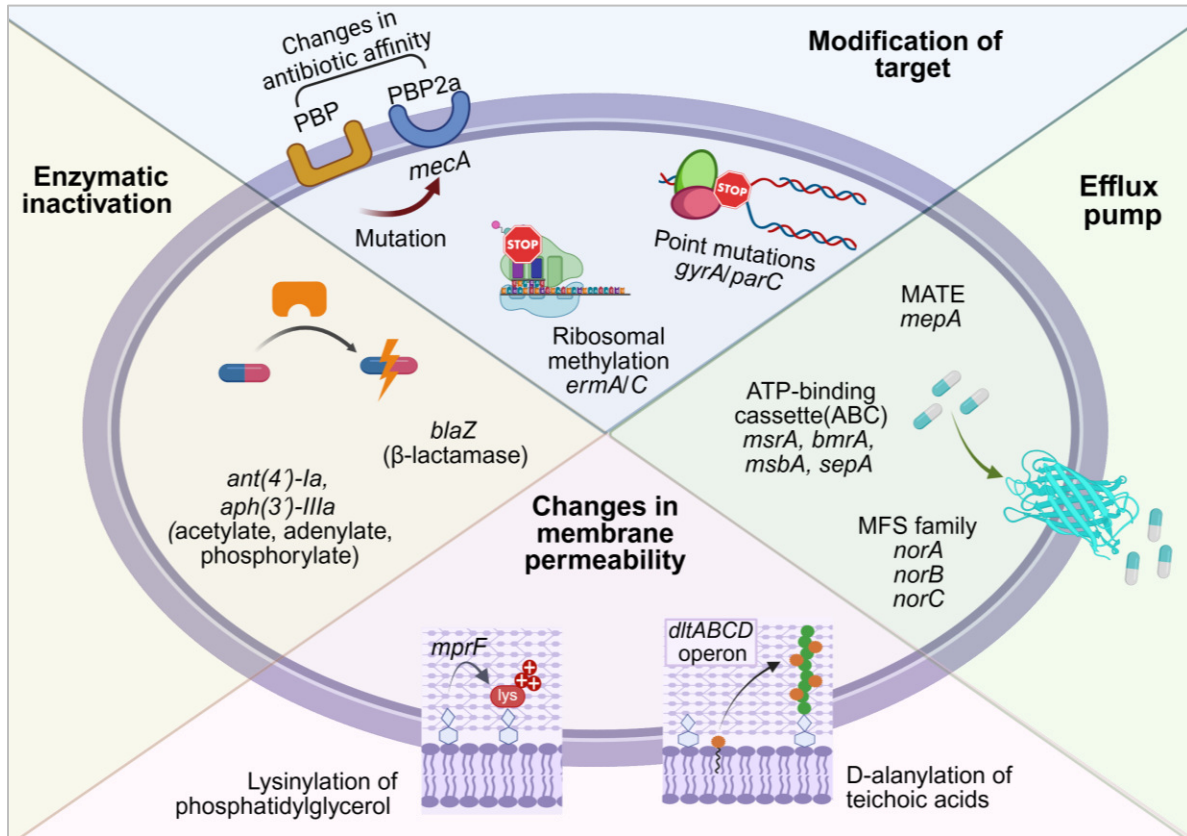


Figure 7 – *Staphylococcus aureus* molecular antibiotic resistance mechanisms. Visual representation of four different resistance mechanisms: Modification of target; Enzymatic inactivation, Changes in membrane permeability, and Efflux pumps. Pills represent antibiotics. Image prepared using BioRender.

1.8.3.5.2 Changes in membrane permeability

S. aureus can modify its membrane permeability to resist drugs and reduce antimicrobials uptake. Changes in membrane permeability typically involves lipid modifications limiting the passive diffusion of antibiotics into the cells. Modification of membrane permeability are particularly important in the resistance to hydrophilic antibiotics, like certain β -lactams

and aminoglycosides [107]. The mechanisms of antibiotic resistance based on changes of membrane permeability are summarized in Table 2.

Table 2 – *Staphylococcus aureus*' mechanisms of changes in membrane permeability

Target	Genes	Mechanism	Result	Ref.
Lysinylated of phosphatidylglycerol	<i>mprF</i>	MprF adds L-lysine (from lysyl-tRNA) to phosphatidylglycerol in the inner membrane and spins lysyl-phosphatidylglycerol to the outer leaflet	Positive surface charge is increased repelling cationic antibiotics (e.g., daptomycin) and host AMPs	[109]
D-alanylation of teichoic acids	<i>dltABCD</i> operon	DltA activates D-alanine, transported by DltB and attached to wall and lipoteichoic acids by DltD	Reduction of cell wall negative charge, limiting binding of cationic antibiotics and AMPs	[110]
Alteration of fatty acid composition	<i>fabD, fabG, fabI, fabF, fabZ</i> and <i>acc</i> genes (e.g., <i>accA, accD</i>)	Adjustment of the saturated/unsaturated and long-chain fatty acids ratio to alter membrane rigidity and packing density	Modified membrane fluidity hinders insertion or aggregation of lipopeptide antibiotics such as daptomycin.	[111, 112]

1.8.3.5.3 Antibiotic enzymatic inactivation

S. aureus enzymes are instrumental in bacterial defense and strongly influence the classification of this bacterium as a “superbug”, two of the mechanisms of enzymatic inactivation are summarized in Table 3. For instance, the expression of β -lactamases that hydrolyze the β -lactam ring of penicillin and related antibiotics, compromises the drug’s ability to bind to the target penicillin-binding proteins (PBPs) [113,114]. This inhibition mechanism confers resistance to a wide range of β -lactam antibiotics. Furthermore, enzymes such as acetyltransferases (AACs), phosphotransferases (APHs), and nucleotidyltransferases (ANTs), play a crucial role in resistance to aminoglycoside antibiotics (AMEs) [115] by modifying its structure via phosphorylation, acetylation or adenylation preventing the drugs from binding its target (ribosome) [115].

Table 3 – *Staphylococcus aureus*’ mechanisms of enzymatic inactivation of antibiotics

Target	Genes	Mechanism	Result	Ref
β -lactam hydrolysis	<i>blaZ</i> (β - <i>lactamase</i>)	β -lactamase cleaves the β -lactam ring inactivating the antibiotic before reaching PBPs.	Resistance to penicillins and narrow-spectrum β -lactams.	[116]
Aminoglycoside modification	<i>aac(6')-Ie-aph(2'')-Ia</i> , <i>ant(4')-Ia</i> , <i>aph(3')-IIIa</i>	Enzymes acetylate, adenylate, phosphorylate aminoglycosides, blocking their binding to the ribosome.	Resistance to gentamicin, kanamycin, and tobramycin.	[117]

1.8.3.5.4 Antibiotic target modification

S. aureus resistance to drugs by target modification are presented in Table 4. Some of the target modifications include modifications in the penicillin-binding proteins (PBPs) in MRSA driven by the *mecA* gene that encodes for a modified PBP, known as PBP2a, enabling the synthesis of peptidoglycan that is poorly cross-linked with reduced affinity for β -lactams such as methicillin and oxacillin [113,118].

S. aureus has a similar strategy to resist quinolones, by mutating the DNA gyrase (encoded by *gyrA*, *gyrB*) and the topoisomerase IV (encoded by *parC*, *parE*), decreasing binding affinity and conferring resistance to this family of antibiotics [119]. Moreover, mutations in ribosomal proteins (23S rRNA) provide resistance to macrolides, lincosamides, and streptogramin B (MLSB resistance) [120]. Target mutations allow *S. aureus* to preserve cellular functions while escaping antibiotics.

1.8.3.5.5 Efflux pumps

Efflux pumps are transmembrane proteins that actively expel antibiotics from the bacterial cytoplasm reducing their intracellular concentration to sub-lethal levels [124,125]. Notably, low antibiotic concentrations can promote efflux pump expression and induce other mechanisms of resistance (target modification) leading to higher levels of resistance [125]. Beyond the role in antibiotic resistance, efflux pumps activity has been associated to bacterial survival and virulence [124,126]. A variety of roles, such as evasion to host defenses, cellular signaling and bacterial basal functions under stressful conditions have been attributed to efflux pumps, posing a major challenge for the development of novel antimicrobial approaches that target this mechanism of resistance [127].

Efflux pumps of *S. aureus* are divided into families according to their substrate specificity and energy source as described in Table 5^[128].

Table 4 – *Staphylococcus aureus*' mechanisms of antibiotic target modification

Target	Genes	Mechanism	Result	Ref.
Penicillin-binding proteins (PBPs)	<i>mecA</i> (encodes PBP2a)	<i>mecA</i> encodes a low-affinity PBP2a that continues peptidoglycan synthesis even when β -lactams inhibit native PBPs.	Resistance to β -lactam antibiotics (e.g., methicillin, oxacillin, cephalosporins).	[121]
Ribosomal methylation	<i>ermA</i> / <i>ermC</i>	Methylation of 23S rRNA by Erm methyltransferases prevents macrolide–lincosamide–streptogramin B antibiotic binding.	Resistance to erythromycin, clindamycin, and other antibiotics.	[122]
DNA gyrase and topoisomerase IV	<i>gyrA</i> / <i>parC</i> point mutations	Point mutations in quinolone resistance-determining regions reduce fluoroquinolone binding.	Resistance to fluoroquinolones such as ciprofloxacin and levofloxacin.	[123]

Table 5 – *Staphylococcus aureus* efflux pump families.

Efflux Pump Family	Role in Resistance	Substrate Specificity	Representative Genes	Energy Source
Major Facilitator Superfamily (MFS)	Major contributor to multidrug resistance, especially fluoroquinolones	Quinolones, dyes, biocides, antibiotics	<i>norA, norB, norC, mdeA, lmrS</i>	Proton motive force (H ⁺ gradient)
ATP-Binding Cassette (ABC)	Provides resistance through active drug efflux using ATP. Important in nutrient and toxin transport. Contributes to stress survival and virulence.	Macrolides, peptide antibiotics, various xenobiotics	<i>msrA, bmrA, msbA, sepA</i>	ATP hydrolysis
Multidrug and Toxin Extrusion (MATE)	Contributes to resistance by exporting toxic compounds.	Quinolones, aminoglycosides	<i>mepA</i>	Sodium or proton gradient
Small Multidrug Resistance (SMR)	Confers resistance to biocides and disinfectants.	Quaternary ammonium compounds, antiseptics	<i>sepA</i>	Proton motive force
Resistance-Nodulation-Division (RND)	Confer resistance to antimicrobial fatty acids by exporting them from the cell	Broad-spectrum substrates	<i>farE, femT, secDF</i>	Proton motive force

1.8.3.5.6 The Nor family efflux pumps

The Nor family of *S. aureus* efflux pumps is described in more detail as it is relevant for my thesis as shown in subsequent chapters. Nor efflux pumps have a crucial role in the resistance to quinolones, such as norfloxacin and ciprofloxacin, contributing to bacterial survival upon antibiotic exposure^[119]. Notably, studies have shown that exposure to low concentrations of quinolones may contribute to upregulation of *nor* genes and consequently increased quinolone resistance in *S. aureus* ^[129–131]. Nor proteins use an ion-driven antiport mechanism in which the substrate and proton (H⁺) are moved across the membrane in opposite directions facilitating antibiotic movement to the outside of the cell ^[107,125]. *S. aureus* Nor family comprises three efflux pumps NorA, NorB and NorC ^[132].

- NorA is a well-characterized efflux pump; this protein contains 388 amino acids, and it is structurally organized in 12 transmembrane segments forming the efflux channel conferring resistance to quinolones, dyes and biocides ^[133]. It is involved in the extrusion of hydrophilic quinolones such as ciprofloxacin and norfloxacin ^[133].
- NorB is analogous to NorA; it is 463 amino acids long and is structured in 12 transmembrane segments ^[128]. NorB substrates include hydrophobic quinolones such as moxifloxacin and sparfloxacin, and hydrophilic quinolones such as ciprofloxacin and norfloxacin, dyes and biocides ^[133].
- NorC, a less studied protein; it comprises 462 amino acids, which are arranged in 12 transmembrane segments. This protein is involved in the resistance to hydrophilic and hydrophobic quinolones, such as ciprofloxacin, moxifloxacin and garenoxacin, and to the dye rhodamine ^[134].

1.8.3.5.6.1 Regulation of efflux pump *nor* genes

The expression of the *nor* genes is affected by the phosphorylation status of the multiple gene regulator A (MgrA, previously known as NorR) and the NorG regulator [132,135–140] (Figure 8 6).

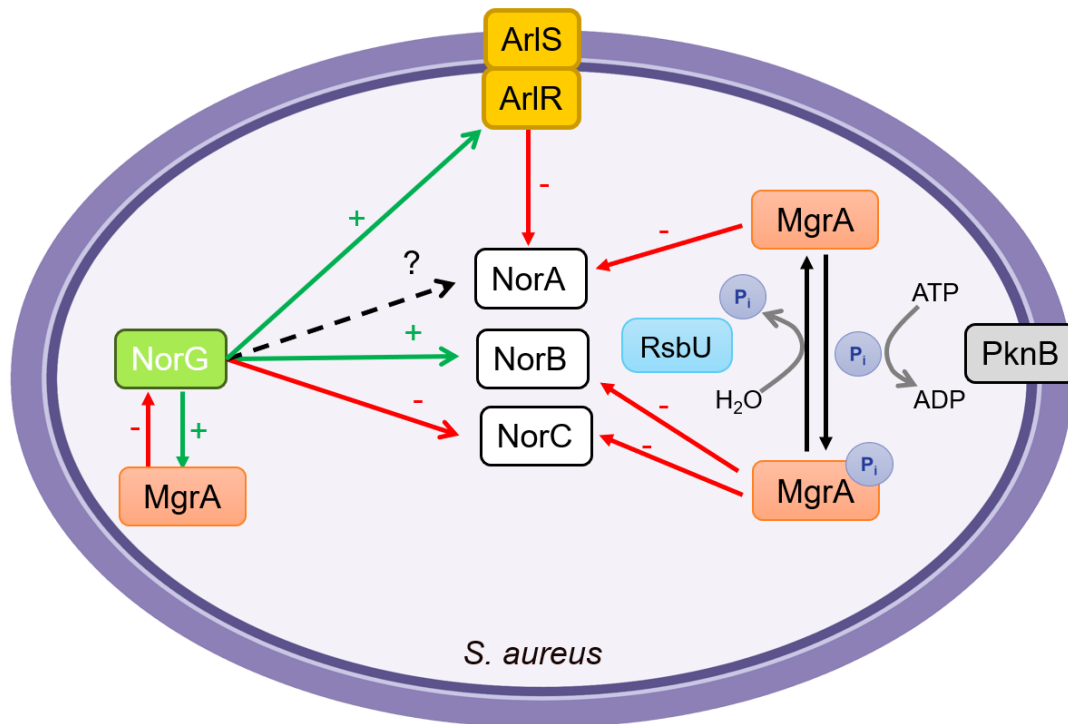


Figure 8 – Proposed model for the regulatory cascade for the *Nor* efflux pump family genes in *Staphylococcus aureus*. Image prepared using BioRender.

As shown in Figure 8, the GntR-family transcriptional regulator NorG is involved in the positive regulation of *nor* genes contributing to enhanced resistance to quinolones [140]. NorG binds to promoter regions of *norA*, *norB* and *norC* [135,140]. However, it has only been demonstrated to function as an activator of *norB*, triggering an increase in *norB* expression levels (Figure 8). Importantly, MgrA and NorG have opposite effects on *norB*

expression, phosphorylated MgrA represses *norB*, while NorG activates *norB* [135,140]. Additionally, MgrA represses *norG* expression [132,135].

Additionally, the PknB kinase phosphorylates MgrA [132] and phosphorylated MgrA (MgrA-P) binds to the promoter of *norB* acting as a repressor, whereas dephosphorylated MgrA represses *norA* expression [132,135,136]. The RsbU phosphatase has been reported to dephosphorylate MgrA [132]. This phosphatase RsbU has a key role in the alternative sigma factor SigB regulon, which consists of four proteins, RsbV, RsbW, RsbU and SigB [141]. RsbU dephosphorylates RsbV-P; dephosphorylated RsbV then binds to RsbW releasing SigB to form a complex with the RNA polymerase resulting in the holoenzyme RNAP [141,142]. This holoenzyme drives the transcription of genes involved in housekeeping functions, virulence, biofilm formation, persistence, cell internalization, membrane transport, and antimicrobial resistance [143]. In the absence of RsbU, RsbV remains phosphorylated and RsbW sequesters SigB, preventing the formation of RNAP and expression of virulence genes [132].

1.8.3.5.6.2 MgrA: Regulation Mechanism and Target Genes

MgrA is a global transcriptional regulator of the MarR family that has a central role in virulence, stress responses, and antibiotic resistance in *S. aureus* as shown in Table 6 [144]. MgrA activity is strongly regulated through redox-sensitive modifications, phosphorylation, and interactions with other global regulators [145,146]. Under oxidative stress conditions, MgrA conserved cysteine residue (Cys12) undergoes oxidation resulting in the loss of MgrA's DNA-binding and activation or repression of its target genes

[147,148]. Additionally, the serine/threonine kinase PknB phosphorylates the serine 110 (S110A) and 113 (S113A) residues of MgrA; these residues are replaced by alanine (Ala) at these positions leading to a decrease in the phosphorylation of MgrA. The phosphorylation of MgrA affects transcription of target genes (activate or repress) like efflux pumps contributing to a shift in this pathogen virulence and antibiotic resistance [132,135–139,146,147]. MgrA regulates several genes (Table 6) and participates in a complex regulatory network that includes other global regulators, such as SigB, SarA, and Rot [148].

Table 6 – MgrA regulatory effect and target genes [135,149]

Target	Effect	Function of Target
<i>norA</i>	Repressor	Encodes the NorA efflux pump, involved in quinolone resistance
<i>norB</i>	Activator	Encodes the NorB efflux pump, contributes to quinolone resistance
<i>norG</i>	Repressor	Encodes the NorG transcriptional regulator resistance
<i>cidA</i>	Repressor	Associated with autolysis, murein hydrolase activity, and cell death; important for biofilm dispersal
<i>cap5A-P</i>	Activator	Capsular polysaccharide synthesis enzyme
<i>ureA-G</i>	Repressor	Encodes urease, an enzyme that hydrolyzes urea to ammonia, contributing to pH neutralization and survival in acidic environments (e.g., phagosomes, urinary tract)
<i>spA</i>	Repressor	Encodes Protein A, an immune-evasion factor that binds IgG
<i>sarA</i>	Activator	Encodes the SarA regulator, another major global regulator of virulence genes

1.8.3.5.6.3 NorG: Regulation Mechanism and Target Genes

NorG is an HTH-type transcriptional regulator of the GntR family that regulates antibiotic resistance and metabolism in *S. aureus* [140]. NorG is a global sensor involved in the

bacterial response to environmental stressors, particularly by regulating the expression of several efflux pumps (Table 7) [135,140]. The activation of *norB* by NorG is well-established, while simultaneously acting as a repressor of other efflux genes like *norC* and *abcA* [140]. Furthermore, NorG is negatively regulated by MgrA, resulting in a complex regulatory network that contributes to *S. aureus* ability to resist antibiotics [135].

Table 7 – NorG regulatory effect and target genes [135,139,140,150]

Target	Effect	Function of Target
<i>norB</i>	Activator	Encodes the NorB efflux pump, contributes to quinolone resistance
<i>abcA</i>	Repressor	Encodes the AbcA transporter, involved in antimicrobial resistance
<i>norC</i>	Repressor	Encodes the NorC efflux pump, associated with quinolone resistance
<i>mgrA</i>	Activator	Encodes the major global regulator (indirect effect, creating a complex regulatory loop)
<i>arlS</i>	Activator	Encodes global regulators involved in virulence network

1.8.4 Models to study *Staphylococcus aureus* virulence

Virulence models are a key tool to investigate bacterial mechanisms of disease in a controlled environment. These models contribute to the understanding of virulence profile of pathogens like *S. aureus*. Clinical relevance and research goals are paramount in the selection of a model to study bacterial virulence [151].

1.8.4.1 Vertebrate models

The study of *S. aureus* virulence can be enhanced with the resource of experimental models, that can range from simple models to advanced mammalian systems, high-throughput invertebrates, and in vitro assays [161–165]. Mammalian models are required to study systemic and tissue-specific infections, as these models mimic human disease [163–165]. Mice are small, cost-effective, and genetically tractable animal models suitable for modeling a wide selection of *S. aureus* infections including pneumonia, sepsis, skin and soft tissue infections (SSTI), osteomyelitis, and abscesses [126,163]. Murine models have contributed greatly to the identification of virulence factors and characterization of the immune response, such as the discovery of alpha-hemolysin's critical role in pneumonia [164]. Species-specific limitations in virulence studies led to the development of humanized mouse models (carrying engrafted human hematopoietic stem cells and immune tissues), which are suitable to study secreted toxins like the Pantone-Valentine leukocidin (PVL) [165]. Rabbits are another example of mammalian animal models suitable to study skin infections, pneumonia, osteomyelitis, and endocarditis caused by *S. aureus*. Their size presents a big advantage as it facilitates surgical procedures, sample collection, and high-

yield antibody production. However, the use of rabbits presents disadvantages, such as higher costs, need for larger facilities, shortage in specialized research reagents (e.g., specific antibodies and knockout models) in comparison to what is available for murine models, and differences in drug interaction due to their foregut fermentation digestive system ^[166].

1.8.4.2 Invertebrate models

Invertebrate models emerged as a cost-effective and high-throughput option for virulence and antimicrobial studies of *S. aureus* ^[53,167]. The *Galleria mellonella* (greater wax moth) larvae display cellular and humoral immune response to infection that resembles the mammalian immune response. This model has been used to study Gram-positive and Gram-negative bacteria, including *S. aureus* to investigate antimicrobial resistance, test the efficacy of novel drugs and combination therapies, and the function of bacterial virulence factors and sRNAs in a living host ^[168–170]. *G. mellonella* has also been used to study biofilm formation on prosthetic implants and abscess development, contributing to the understanding of host-pathogen interactions ^[170,171].

Caenorhabditis elegans and *Drosophila melanogaster* models have also contributed to the study of staphylococcal virulence mechanisms and innate immune pathways post infection ^[161].

For instance, *C. elegans* has been used to study staphylococcal virulence factors, such as the *agr* system, *sarA*, and α -hemolysin, that play a major role in *S. aureus* infections and in the characterization of host innate immune responses ^[172,173]. Furthermore, *C.*

elegans is a useful model to investigate antimicrobials efficacy against *S. aureus*, offering valuable insights in the development of therapeutical approaches [174].

Additionally, *Drosophila melanogaster*, despite its simplicity, has been largely employed for the study of host-pathogen interactions due to a highly conserved innate immune response that include pathways similar to those in humans, such as the Toll and IMD [175,176]. *D. melanogaster* has shown efficiency in the identification and characterization of *S. aureus* virulence factors and host defense response mechanisms, shedding light on host immune responses and supporting the improvement of therapeutic treatments [177].

Bombyx mori silkworm larvae have been shown to be an effective model to study *S. aureus* virulence via killing assays [155,158,167,178]. The silkworm immune response comprises regulatory pathways that are conserved in the mammalian innate response closely in the mammalian immune response, but lacks adaptative immune response mechanisms [167,178]. The immune response of *B. mori* comprises of a cellular and humoral response. The cellular arm is driven by hemocytes (analogous to human phagocytes) and encompasses phagocytosis, encapsulation, and nodulation of invading microorganisms [179]. On the other hand, unlike in the mammalian system where the humoral system is part of the adaptative response, in silkworms humoral arm of the immune response is activated by JAK-STAT and Toll-receptor pathways resulting in the secretion of antimicrobial peptides, complement-like proteins and the activation of the prophenoloxidase (PPO) activating system, melanization and clotting [167,180,181]. Therefore, the silkworm provides a simplified yet effective model for studying fundamental aspects of human immune responses. The silkworm immune response to *S. aureus* infection, in comparison to human innate immune response is described in table 8.

Table 8 – Immune response to *Staphylococcus aureus* infection in *Bombyx mori* in comparison to human immune response [155,157,158,167,178,180].

Feature	Immunomodulators	Silkworm Response	Human Response
Pathogen Recognition	Peptidoglycan Recognition Proteins (PGRP), β -1,3-glucan Recognition Proteins (β GRPs)	Recognize lysine-type peptidoglycan, prompting downstream signaling cascades	Toll-like receptor 2 (TLR2) recognition of Gram-positive bacterial components
Toll Receptor	Toll receptors	Activation of Toll signaling that leads to the production of antimicrobial peptides (cecropins, moricins, defensins, and gloverins)	TLR–NF- κ B pathway in humans induce cytokine and AMP expression
Immune Deficiency pathway	IMD	Provides cross-regulation with Toll signaling during <i>S. aureus</i> infection to enhance AMP production	TNF receptor–NF- κ B pathway; secondary role in Gram-positive infections
JAK-STAT pathway	JAK-STAT, cytokine-like molecules	Modulates immune gene expression and maintains immune balance during prolonged infection	Cytokine-mediated immune regulation
Melanization Cascade	Prophenoloxidase (proPO), serine protease cascade, phenoloxidase (PO), melanin synthesis enzymes	Activated by PGRPs; promotes melanization around infection sites	Inflammatory oxidative responses in humans. Skin pigmentation, not an immune mechanism against <i>S. aureus</i>
Cellular Response	Hemocytes (granulocytes, plasmatocytes)	Phagocytosis, encapsulation, and nodulation at infection sites; release reactive oxygen species (ROS) and AMPs	Macrophage and neutrophil-mediated phagocytosis and oxidative killing in humans

1.8.4.3 In vitro models

In vitro models provide controlled environments for investigating specific host-pathogen interactions. Cell culture models, including two-dimensional (single layer on a flat surface) and three-dimensional systems (organoids, spheroids, co-culture), can be applied to investigate secreted toxins and *S. aureus* biofilm formation [182–184]. Moreover, human skin models and epithelial cells can be applied to describe colonization and the transcriptional response of *S. aureus* during infection [184]. Similarly, biofilm models are important for understanding chronic infections. Flow-based systems provide real-time biofilm formation insights whereas three-dimensional collagen-based models replicate staphylococcal abscess communities, which exhibit high tolerance to antibiotics [185].

1.9 Rationale

Bacterial contamination of PCs remains a significant challenge in transfusion medicine and poses a serious threat to patient safety. *S. aureus* is a predominant PC contaminant, which can escape detection during screening with culture methods and resist pathogen reduction treatment, resulting in septic transfusion reactions, and has therefore been chosen as the focus of my PhD research studies.

My thesis builds on previous findings from the Ramirez' lab that revealed that *S. aureus* grown in PCs display upregulation of virulence genes. However, a major knowledge gap remains as it is currently unknown if transcriptional changes translate into enhanced antibiotic resistance and virulence in the pathogen when grown in PCs. Hence, my work aims to expand the current knowledge by conducting functional assays to test whether

the increased gene expression observed under PC conditions translates into heightened antibiotic resistance and virulence potential of *S. aureus* by addressing the following research question:

Does the PC storage environment drive the transcriptional and functional adaptation of *S. aureus* for enhanced virulence and antibiotic resistance, thereby compromising the efficacy of standard antibiotic therapy and patient outcomes following transfusion?

1.10 Hypotheses

The PC storage environment triggers transcriptional changes in *S. aureus* resulting in increased resistance to antibiotics. Furthermore, these transcriptional changes result in enhanced virulence of *S. aureus* when grown in PCs.

1.10.1 Objectives

The objectives of my PhD research project are to:

1. Assess the differential gene expression of *S. aureus* grown in PCs compared to Tryptic Soy Broth (TSB) with focus on genes involved in antibiotic resistance using molecular biology approaches.
2. Study the role of the NorB efflux pump on the virulence of *S. aureus* grown in PCs using a *B. mori* (silkworm) model.

2. Materials and Methods

As a disclaimer, part of the work presented in this chapter has been published in the journal *Antibiotics* (MDPI), in which I am the first author ^[1]. Dr. Sandra Ramirez-Arcos was involved in the conception of the study, designing the experiments described in this chapter, and in editing the published manuscript. Post-doctoral fellow Dr. Basit Yousuf optimized RNA-seq extraction and RT-qPCR protocols that I used in my transcriptome studies. Post-doctoral fellow Dr. Sylvia Ighem Chi established the CRISPR-Cas9 method to create deletional mutants in *S. aureus* that I adopted to attempt the construction of a *norB* mutant in *S. aureus*. Minimal Bactericidal Concentration protocols were optimized in collaboration with Dr. Thien-Fah Mah in the University of Ottawa. Dr. Dilini Kumaran developed the silkworm killing assay protocol in *S. aureus* ^[159] that I used during my virulence studies.

2.1 Phenotypic characterization of *Staphylococcus aureus* strains

2.1.1 *Staphylococcus aureus* strains

Four transfusion relevant strains (TRS) and three laboratory strains were tested in my thesis. Out of the four TRS, *S. aureus* CBS2016-05 was involved in a septic transfusion event in Canada ^[34,186] (Table 9). The other three TRS were isolated in England by the National Health Service Blood and Transplant (NHSBT) (Table 3). These strains include *S. aureus* Cl/BAC/25/13/W ^[187], which was isolated from a unit recalled prior to transfusion (near-miss) due to the presence of aggregates, and *S. aureus* PS/BAC/169/17/W ^[188] and *S. aureus* PS/BAC/317/16/W ^[189], which were both detected during routine screening. In addition to the TRS, *S. aureus* RN6390 ^[190] and derived *norB* and *mgrA* mutants, which were kindly provided by Dr. David Hooper (Harvard University), were used for functional studies (Table 9). Furthermore, *S. aureus* RN4220 and *Escherichia coli* DC10b were used for mutagenesis protocols, and *S. aureus* ATCC 25923 and ATCC 29213 served as controls for biofilm formation and antimicrobial resistance assays, respectively (Table 9).

Table 9 – *Staphylococcus aureus* strains used in this study.

Strains	Characteristics	Origin	Reference
Transfusion Relevant Strains (TRS)			
CBS2016-05	Failed detection during PC screening Involved in a septic transfusion reaction. Isolated from patient samples and residual PCs	Canada, 2016	[34,186]
CI/BAC/25/13/W	Failed detection during PC screening. Near-miss captured prior to transfusion due to the presence of aggregates	England, 2013	[187]
PS/BAC/169/17/W	Detected during PC screening	England, 2017	[188]
PS/BAC/317/16/W	Detected during PC screening	England, 2016	[189]
Laboratory Strains			
RN6390	Wild type, descendent of NCTC8325-4 (<i>rsbU</i> mutant)		[190]
RN6390 Δ <i>norB</i>	RN6390 (<i>norB</i> deletion mutant)		[1]
RN6390 Δ <i>mgrA</i>	RN6390 (<i>mgrA</i> deletion mutant)		[191]
Other Strains			
ATCC 25923	American Type Culture Collection		
ATCC 29213	American Type Culture Collection		
<i>S. aureus</i> RN4220	Mutation in the " <i>sau1 hsdR</i> " gene		
<i>Escherichia coli</i> DC10b	<i>dcm</i> deletion mutation (cytosine methylation)		

2.1.2 Pooled Platelet Concentrates

Leukocyte-reduced buffy coat pooled PCs suspended in 100% plasma were used for this study following standard manufacturing protocols established at the Canadian Blood Services netCAD Blood4Research Facility (netCAD, Vancouver, BC, Canada). This study was granted ethical approval by the Canadian Blood Services Research Ethical Board (REB 2015.024, 24 June 2019).

2.1.3 Media and Reagents

Media: Frozen stocks of all isolates were prepared in Brain Heart Infusion (BHI) broth (BD) with 15% glycerol (v/v) and stored at -80 °C. Tryptic Soy Agar (TSA) plates (TSB – BD; agar - Fisher) were used to sub-culture frozen stocks and for bacterial enumeration. Tryptic Soy Broth (TSB) (supplier) was used for growth curve studies, Minimal Bactericidal Concentration (MBC) assays and bacterial culturing for RNA extraction and virulence assays. TSB supplemented with 0.5% glucose (TSBg) was used for biofilm formation experiments. Müller Hinton Broth cationic adjusted (MHB^{ca+}) (Sigma) was the media used for Minimal Inhibitory Concentration (MIC) assays. Blood Agar (BA) (Oxoid) was used to determine the hemolysis profile of *S. aureus* isolates. Lysogeny Broth (LB) (LB – BD) and Lysogeny Broth agar (LBA) (LB – BD; Agar – Fisher) were used to subculture *E. coli*.

Bacterial frozen stocks: Bacterial frozen stocks were prepared by re-suspending a full loop of a fresh culture of each *S. aureus* strain in BHI with 15% glycerol (v/v). Enumerated frozen stocks were prepared by incubating *S. aureus* overnight (18 ± 2 h) in TSB at 37°C with agitation (160 rpm). Overnight cultures were mixed with 50% glycerol in an 8:2 ratio

(culture:glycerol), thoroughly vortexed and aliquoted into previously labeled cryovials and store at -80 °C. After 24h, one vial per isolate was used to determine bacterial load as follows: one vial of frozen stocks was thawed, serial diluted (1:10), plated on TSA plates, and incubated for 16 ± 2 h at 37°C. After incubation, colonies were counted, and bacterial load was determined based on the number of colonies and dilution factor. Bacterial frozen stocks were retrieved and thawed only once for downstream applications to avoid repeated freeze-thaw cycles.

Antibiotics: Ciprofloxacin – CIP (TCI), and Norfloxacin – NOR (Sigma) were used MIC and MBC assays. Kanamycin - Kan (Sigma), Chloramphenicol – CM (Sigma), and Ampicillin – Amp (Sigma) were used to supplement TSA, TSB and LB in mutagenesis experiments and will be described in the respective protocols as “media+antibiotic+ concentration” (e.g., TSB containing 10 ug/mL of chloramphenicol would be TSB+CM10 or LB containing 50 ug/mL of kanamycin would be LB+Kan50).

2.1.4 Morphological Characterization of *Staphylococcus aureus* strains

Gram staining and microscopy: Bacterial smears were prepared by placing a small number of bacteria on a glass slide with a droplet of water, which was spread into a thin layer, allowed to air-dry, and fixed with 99.9% methanol. Gram stain was performed using the BD Gram Stain kit (BD). Briefly, crystal violet was applied onto the slide (1 minute), rinsed with distilled water, followed by application of the mordant iodine solution (1 minute) and rinsing with distilled water, before decolorization with acetone: Isopropanol, 25/75(v/v) for 10 seconds, and contrast staining with safranin (1 minute). After staining,

the slides were subjected to a final rinsing with distilled water and air drying. Slides were observed under the microscope (Olympus BX53) using oil immersion lens (100x objective) and pictures were captured with an Infinity 3 Teledyne Lumera camera and processed with the Infinity Analyser 7 software (version 7.1.0.1215).

Colony morphology and hemolysis: a loopful of bacteria was collected from a frozen stock vial and streak onto BA using the quadrant method and incubated 37 °C for a minimum of 24h. Plates were separately prepared for each isolate and examined under the light to identify yellow/golden colony pigmentation (indicator of staphyloxanthin production) and zones of hemolysis. A clear halo, around colonies was classified as beta hemolysis, while no change in the agar coloration around the colonies was classified as gamma hemolysis [192].

2.1.5 Biochemical characterization of *Staphylococcus aureus* strains

Biochemical characterization of the strains was performed using Gram-positive cards (VITEK®2 GP) which were incubated in the VITEK®2 compact system (bioMérieux) as per manufacturer's specifications. The VITEK®2 system is a closed automatic system that fills, seals, and incubates the cards at 37 °C for up to 24 hours. During incubation, the system monitors bacterial growth and metabolic kinetics periodically, measuring fluorescence, turbidity, and color in the wells. Once incubation is complete, the collected data are analyzed by the system, and results are compared with the system validated database to determine isolate identification [193].

2.1.6 Growth curve studies of *Staphylococcus aureus* strains

Growth in TSB: Overnight cultures were prepared by re-suspending 1 or 2 colonies of *S. aureus* fresh cultures into 15 ml of TSB followed by incubation at 37° C under agitation at 160 rpm for 18 ± 2 hours. These fresh cultures were used to inoculate 70 mL of TSB at an initial inoculum of OD₆₀₀ = 0.002 (corresponds to approximately 10⁵ to 10⁶ CFU/ml) in T75 culture flasks, which were incubated at 37 °C under agitation (160 rpm), for 12 hours. Optical density (OD₆₀₀) of the cultures was determined using a spectrophotometer (Ultraspec3100, Biochrom). Samples were collected every 2 hours for OD₆₀₀ measurements and bacterial load determination by plating serial dilutions (1:10) onto TSA plates in duplicated followed by incubation at 37 °C, 18 ± 2 hours. After incubation, CFU/mL were calculated for each sampling point.

Growth curves were analysed using MS Excel to determine growth rate (SLOPE function) and doubling time ^[194]. Briefly, the slope function calculates the steepness of the growth curve based on linear regression (k). The Excel tool determines the growth rate (k) between time points using the formula (x = time and y = Log (CFU/mL)):

$$\text{Slope } (k) = \frac{y_2 - y_1}{x_2 - x_1}$$

Doubling time was determined using the formula:

$$\text{Doubling time} = \frac{\ln(2)}{k}$$

The data analysed represent the average resulting from the analysis of three growth curves obtained from independent cultures.

Growth in PCs: PC cultures were prepared in T75 culture flasks containing 70 mL of PCs and incubated under PC storage conditions (22 ±2 °C, 60 rpm) for up to 144 hours (six days). *S. aureus* PC cultures of TRS started with an initial inoculum ranging from 10⁵ to 10⁶ CFU/ml (based on adjusted OD₆₀₀ in TSB). In contrast, *S. aureus* RN6390 and derived *norB* and *mgrA* mutants were inoculated with ~30 CFU per flask to mimic real-life bacterial loads in PCs, which are less than 1 CFU/mL. Samples from PC cultures were collected every 24 hours and bacterial load was determined by plating samples on TSA in duplicated followed by incubation (37 °C, 18 ± 2 hours).

Growth curves were analysed using MS Excel to determine growth rate (SLOPE function) and doubling time [194]. Briefly, the slope function calculates the steepness of the growth curve based on linear regression (k). The Excel tool determines the growth rate (k) between time points using the formula (x = time and y = Log (CFU/mL)):

$$\text{Slope } (k) = \frac{y_2 - y_1}{x_2 - x_1}$$

Doubling time was determined using the formula:

$$\text{Doubling time} = \frac{\ln(2)}{k}$$

The data analysed represent the average resulting from the analysis of three growth curves obtained from independent cultures.

2.1.7 Biofilm formation assays of *Staphylococcus aureus* strains

S. aureus biofilm formation was determined using a crystal violet assay method previously optimized in the Ramirez' laboratory [34]. Overnight cultures were prepared by re-suspending 1 or 2 colonies of *S. aureus* in 15 mL of TSB followed by incubation at 37° C,

under agitation at 160 rpm for 18 ± 2 hours. TSBg and PC cultures were inoculated at an initial inoculum of $OD_{600} = 0.1$ ($\sim 1.0 \times 10^8$ CFU/mL) and then dispensed onto 6-well culture plates. Three wells were loaded each with 3 mL of inoculated cultures and three wells were loaded with 3ml of unspiked TSBg or PCs (negative controls). TBSg cultures were incubated at 37°C for 24h with no agitation, while PC cultures were incubated at $22 \pm 2^\circ\text{C}$, with agitation at 60 rpm for 5 days. After incubation, plates were treated as follows: each well was washed three times with 3 ml of phosphate buffered saline (PBS) to remove planktonic cells. Wells were stained with 3 ml of 0.3% crystal violet followed by incubation at room temperature for 30 min under agitation (~ 60 rpm). Thereafter, the wells were washed three times with PBS to wash the excess of crystal violet. Lastly, 3 mL of a destaining solution (20% acetone and 80% ethanol) was added to each well and plates were incubated at room temperature for 30 min under agitation (~ 60 rpm) to elute the crystal violet staining. Crystal violet staining is directly related to attached bacterial aggregates (i.e., biofilms) in the plate culture wells. Subsequently, 200 μl aliquots of the eluted solution from each well were transferred in triplicate to a 96-well plate and the absorbance was read at a wavelength 492 nm in a microplate reader (Spectra MAX190, Molecular Devices). *S. aureus* ATCC 25923 served as positive control for biofilm formation while unspiked TSBg and PCs served as negative controls. Quantification of biofilm formation was determined by normalizing optical density data: (OD values of uninoculated TSB and PCs were subtracted from absorbance readings of test samples). The isolates capability of producing biofilm was determined as per Lin, M.F., et al (2020)

[195] :

Cutt-off value \rightarrow $OD_c = \text{Average OD of negative control} + 3 \times \text{Standard deviation}$

- $\hookrightarrow OD \leq OD_c \rightarrow$ negative (not a biofilm former)
- $\hookrightarrow OD_c < OD_{492} \leq 2 \times OD_c \rightarrow$ weak biofilm producer
- $\hookrightarrow 2 \times OD_c < OD_{492} \leq 4 \times OD_c \rightarrow$ moderate biofilm producer
- $\hookrightarrow 4 \times OD_c < OD_{492} \rightarrow$ strong biofilm producer

2.1.8 Comparative genomic analyses of *Staphylococcus aureus* strains

2.1.8.1 Whole genome sequencing (WGS)

WGS of the TRS used in this study were performed and published by the Ramirez' lab in collaboration with colleagues from Health Canada. I was directly involved in the WGS of TRS *S. aureus* CI/BAC/25/13/W and *S. aureus* PS/BAC/169/17/W [187,188]. The other two TRS (*S. aureus* CBS 2016-05 and *S. aureus* PS/BAC/317/16/W [186,189].) were sequenced following the same procedure by post-doctoral fellow Dr. Basir Yousuf Briefly, paired-end Illumina whole-genome shotgun sequencing was performed using Nextera XT DNA libraries run on a MiSeq instrument (v3 chemistry, 2×300 bp reads) per manufacturer guidelines (Illumina). Nanopore WGS sequencing libraries were obtained with a rapid barcoding sequencing kit (SQK-RBK004), a FLO-MIN106 flow cell (R9.4) and a 1D MinION system (Oxford Nanopore Technologies). The raw Illumina reads were processed using FastP (v0.20.1) to extract adapter and barcode sequences, correct out of place bases in overlaps, and filter low-quality reads ($Q < 20$). Long-read signal processing, base calling, demultiplexing, and adapter trimming were performed using

Guppy GPU v5.0.16+b9fcd7b and reads of <1 kb were discarded using Filtlong v0.2.0 (<https://github.com/rrwick/Filtlong>). A *de novo* hybrid assembly was performed using Unicycler (v 0.4.8) at default settings. Annotation was performed with PGAP v 2021-01-11. build5132 (best placed reference protein set, GeneMarkS-2+) (github.com/ncbi/pgap) and analysed with QUAST v 5.0.2 (github.com/ablab/quast) ^[196]. The genome of *S. aureus* RN6390 was published by Garret et al ^[190].

2.1.8.2 Comparative genomic analyses

The genomes of five *S. aureus* isolates, the four TRS and RN6390, were aligned and visualized using Mauve Progressive (Mauve 2015226 built10, last accessed on May 28th, 2025). Genome files (FASTA format) were uploaded onto the software for comparison using a guide tree constructed from pairwise comparisons and identify conserved segments, insertions, deletions, and rearrangements within the genomes. The *norB* gene and neighbour genes (upstream and downstream) were identified by manual search using published genomes ^[186–190]. Sequences were analysed using the Operon Mapper online bioinformatics tool (https://biocomputo.ibt.unam.mx/operon_mapper, last accessed on November 6th, 2025) to determine if *norB* was part of an operon ^[197].

2.1.8.3 Virulence genes identification

Virulence genes encoded in the bacterial genomes were obtained using the Virulence Factor Database (VFDB 2022) VFAnalyzer9 (accessed on May 28th, 2025) under default parameters. Genes listed by VFDB were aligned against the whole genome sequenced using BLASTn ^[198].

2.1.8.4 Antibiotic resistance genes identification

Genes encoding for antibiotic resistance mechanisms were gathered using the Comprehensive Antibiotic Resistance Database (CARD-RGI, The Comprehensive Antibiotic Resistance Database, McMaster University, accessed on May 28th, 2025), under default parameters to curate the genes generating gene accession numbers. Compiled genes were verified by alignment against the whole genome sequenced using BLASTn [198].

2.1.9 Comparative Transcriptome Analysis of TRS grown in PCs vs TSB

2.1.9.1 *Staphylococcus aureus* RNA isolation, library construction and sequencing

For RNA isolation, 70 mL PC and TSB cultures were inoculated with each of the four TRS (Table 3), with an initial inoculum of approximately 4×10^6 CFU/ culture, followed by incubation under PC storage conditions (22 ± 2 °C, 60 rpm, 144 h) to allow the comparison of gene expression in TSB and PCs in similar culture conditions. *S. aureus* isolates were sampled during stationary phase to increase the yield of extracted RNA in PC-cultured isolates and capture the gene expression of virulence factors that contribute to increased pathogenicity [63,67,92,199,200]. Subsequently, the cultures were pelleted by centrifugation at 4°C and subjected to RNA extraction using the miRNeasy Mini Kit (Qiagen), as per the manufacturer's instructions. To eliminate genomic DNA, the RNA samples from three independent biological replicates were treated with TURBO™ DNase Ambion™ (Thermo Fisher Scientific). Furthermore, the RNA samples from spiked PCs underwent an additional treatment using the MICROBEnrich™ kit (Ambion) to remove eukaryotic

RNA. RNA sequencing was performed at the Ottawa Hospital Research Institute (OHRI) sequencing facility. Briefly, quality and quantity of the RNA samples were assessed using a Biodrop μ LITE and Fragment Analyzer™, and samples with an RNA Quality Number (RQN) ranging between 8.7 and 10 were chosen for next steps. Subsequently, cDNA libraries were generated using Illumina® Stranded Total RNA Prep, Ligation with Ribo-Zero Plus (Illumina 20040525). Quantification of the libraries was performed with the Qubit Double Stranded DNA HS kit (Thermo Q32854) and ran on the AATI Fragment Analyzer to verify the size distribution. The libraries were normalized, pooled, and diluted as required to achieve acceptable cluster density on the NextSeq 500 sequencer (Illumina SY-414-1001). The library pool then underwent 75 Cycle High Output (Illumina 20024906).

2.1.9.2 Transcriptome assembly and differential gene expression analyses

Genome sequences of the four TRS (Table 3) were used as reference genomes for transcriptome assembly. Sequence quality control analysis was performed using FastQC and fastp to determine the quality of the reads. Transcript quantification was conducted using Salmon and the reads were aligned to the genome using bowtie2. For differential expression analysis, the transcript quantification data for all samples were imported into R. In the subsequent stages of the analysis, genes encoding rRNA and tRNA were filtered out from the read count matrix, and non-expressed genes (genes with fewer than two replicates with five or more assigned reads) were excluded. DESeq2 was employed to estimate size factors for count scaling based on library size and to calculate dispersion

parameters to assess the deviation of expression variance from the mean across the dataset [201]. The DESeq 'rlog()' function was applied to perform a regularized log transformation of the count values, which were then used in DESeq's plotPCA() function to generate a PCA plot visualizing the clustering of the replicates. Hierarchical clustering was conducted using the rlog-transformed values to depict similarities between samples. Following the normalization procedure, differentially expressed gene (DEG) analysis was carried out between the PC and TSB conditions for each bacterial strain. The 'lfcShrink()' function in DESeq2 was employed for this analysis, which calculates the log2 fold change between the conditions while shrinking the value in cases of high uncertainty in the estimated fold change, often arising from low read counts assigned to the gene. The transcriptome dataset of antibiotic resistance genes was further analyzed considering a log2-fold difference of ≥ 1.0 as a significant change in DGE. This cut-off was chosen to capture relatively small but biologically meaningful gene expression changes.

2.1.9.3 Validation of RNA-seq data using quantitative reverse transcription PCR (RT-qPCR)

RNA-seq data was validated by performing RT-qPCR. Briefly, complementary DNA (cDNA) synthesis was performed with 1 μ g of DNase-treated total RNA using the iScript cDNA synthesis kit (Bio-Rad) following manufacturer's instructions and using the following protocol: Priming 5 min at 25°C; Reverse transcription 20 min at 46°C; Reverse transcriptase inactivation 1 min at 95°C. The qRT-PCR reaction was carried out in a CFX96 Thermal cycler (Bio-Rad) using iQ SYBR Green super mix (Bio-Rad) as recommended by the manufacturer. Oligonucleotide primers were designed using the

PrimerQuest tool at IDT website efficiency of the primers was determined by the dilution method (100 ng – 0.01 ng) using the following protocol: 3 min at 95°C; 40 cycles (10 sec at 95°C; 25 sec at 57°C); 10 sec at 95°C; 5 sec at 65°C (Appendices A1 and A2 show primer melting curves to assess primer specificity and efficiency; Appendix 6 lists all primers used in this work). The 16S RNA was used as an internal control to normalize the target gene mRNA expression. Fold change in gene expression between TSB and PC samples were calculated using cycle threshold (Ct) values of each gene and the $2^{-\Delta\Delta Ct}$ method [63,67,92]

2.2 Creation of a *norB* knockout mutant in *Staphylococcus aureus*

Two methods were attempted for the construction of a *norB* knockout mutant in *S. aureus*, CRISPR-Cas9 and allelic recombination exchange.

2.2.1 Preparation of competent cells

Escherichia coli DC10b competent cells

E. coli DC10B was selected because it does not produce a DNA cytosine methyltransferase, and therefore plasmids produced in this strain bypass the *S. aureus* type IV restriction barrier, a major foreign DNA restriction system.

E. coli was streak from a frozen stock onto LB agar plates and incubated overnight (16 to 20 h) at 37 °C. Thereafter, one colony was inoculated in 3 mL LB and incubated overnight (16 to 20 h) at 37 °C with agitation at 250 rpm. The overnight culture was diluted 1:100

by adding 1 mL of the overnight culture into 100 mL LB media in a T75 flask and incubated at 37°C with agitation at 250 rpm until optical density $OD_{600} = 0.5 - 1.0$. Cells were harvested by centrifugation (6000g for 10 minutes at room temperature). Supernatant was discarded and the pellet was resuspended in 10 mL of sterile ice-cold ddH₂O and chilled on ice for 15 mins. Cells were pelleted, supernatant was decanted, and the pellet was gently resuspended in 40 mL ice-cold ddH₂O and centrifuged at 6000g for 10 minutes at 4 °C. Thereafter, the supernatant was carefully discarded, and the pellet was gently resuspended in 20 mL ice-cold 100 mM CaCl₂ followed by centrifugation at 6000g for 10 minutes at 4 °C. This wash was repeated with 2 mL of ice-cold solution of 85% v/v 100 mM CaCl₂ and 15% v/v glycerol. Finally, supernatant was decanted, and cells were resuspended in 0.5 mL ice-cold solution of 85% v/v 100 mM CaCl₂ and 15% v/v glycerol. Competent cells were aliquoted (50 µl) onto pre-chilled microcentrifuge tubes and stored at -80 °C freezer. The viability of the competent cells was confirmed after 24 hours of storage: one vial was thawed in ice and plated onto LB plates, which were incubated at 37 °C, for 16 to 20h. The viability was confirmed by the presence of colonies in the LBA plates.

Staphylococcus aureus electrocompetent cells

S. aureus RN4220 was selected because this isolate carries a mutation in the *sau1 hsdR* gene making it highly transformable and an ideal intermediate for successful transformation of other *S. aureus* strains [202,203]. *S. aureus* was streak from a frozen stock onto TSA plates and incubated overnight (16 to 20 h) at 37 °C. Thereafter, one colony

was inoculated in 10 mL TSB and incubated overnight (16 to 20 h) at 37 °C with agitation at 160 rpm. The overnight culture was diluted to an optical density of $OD_{578} = 0.2$, this was obtained by diluting the overnight culture in a 1:20 ratio (5mL of culture into 95 mL TSB media in a T75 flask) and incubated at 37°C under agitation at 160 rpm until they reached an $OD_{578} = 0.6$. Cultures were separated into Oakridge tubes and placed in ice for 15 minutes. All subsequent steps were performed at 4 °C. The cells were harvested (15000 g, 15 min, 4 °C) and supernatant discarded. Cells were washed with 20 mL of ice-cold autoclaved water and centrifuged to pellet cells (15000 g, 15 min, 4 °C). Pellets were then combined in one tube using 10 mL of autoclaved ice-water and centrifuged (15000 g, 15 min, 4 °C). Thereafter, cells were washed twice using 10 ml of ice-cold sterile 10% (w/v) glycerol, followed by two washes with 2 ml and 1 ml of ice-cold sterile 10% (w/v) glycerol, respectively. Cells were harvested by centrifugation (13000 g, 5 min, 4 °C). The pellets were resuspended in 700 μ l of ice-cold 10% (w/v) glycerol and aliquots of 70 μ l were frozen at -80 °C. This protocol was performed on different days for *S. aureus* RN4220, *S. aureus* PS/BAC/169/17/W, *S. aureus* CBS 2016-05, and *S. aureus* RN6390 to avoid potential contamination.

2.2.2 Transformation of bacterial competent cells

Escherichia coli transformation with the heat shock method

E. coli competent cells were thawed on ice (~15 – 20 min) prior to the addition of 50 pg to 100 ng of plasmid DNA (10 to 15 μ l). Cells were then transferred to a heat block at 42°C for 45 seconds and immediately transferred back to ice and incubated for 2 minutes. LB (950 μ l) was added to the transformation vials followed by incubation at 37°C

for 2h with agitation (250 rpm) to allow the cells to recover. Transformed cells were plated on LB supplemented with appropriate antibiotic(s) and incubated under specific conditions depending on specific experiments as described in subsequent sections.

Staphylococcus aureus transformation by electroporation

Electrocompetent cells were thawed on ice for ~5 min and then incubated at room temperature for 10 minutes. Five hundred μ l of filter-sterilized electroporation buffer (0.5M sucrose in 10% glycerol) was added to the cells which were immediately centrifuged (10000 rpm for 5 min). Upon centrifugation, the supernatant was discarded, and the pellet was resuspended in 85 μ l of filter-sterilized electroporation buffer. Plasmid DNA (1 – 2 μ g in 10 – 15 μ l) was added to the cells, which were then transferred to a 1 mm gap electroporation cuvette (Bio-Rad) at room temperature, and pulsed three times at 23 kV/cm, 5ms (BTX 630, BTX or Xcell, GenePulsar I/II, Biorad). Electroporated cells were immediately transferred into 1 ml of TSB supplemented with filter-sterilized 0.5M sucrose and incubated tilted (45°) at plasmid optimal growth temperatures (30 °C or 37 °C, see below) for 2 h (160 rpm). Thereafter, 100 μ l aliquots were spread onto TSB and TSB+CM10 followed by incubation optimal growth temperatures depending on the plasmid for a maximum of 48 h.

2.2.3 Mutagenesis of *Staphylococcus aureus norB* using CRISPR-Cas9 methodology

CRISPR-Cas9 is a genome-editing tool that allows precise modification into the DNA of organisms. The system was designed to use guide RNA to direct the Cas9 enzyme to a

specific sequence of the DNA, herein Cas9 makes a cut, permitting genes to be inserted, mutated or modified [204]. *S. aureus* PS/BAC/169/17/W was chosen to create a *norB* mutant because the gene was highly upregulated in PC cultures of this strain compared to TSB cultures (see transcriptome results in the next chapter). Concurrently, this isolate had increased resistance to quinolones when grown in PCs (see MBC results in the next chapter). Generating a *S. aureus norB* knockout mutant allows the investigation of *norB*'s role in quinolone resistance and virulence, which was the focus of my studies.

Mutagenesis using the CRISPR technology and plasmid specific for *S. aureus* (pCasSA) obtained from Addgene was used to create the *norB* knockout mutant in *S. aureus* PS/BAC/169/17/W using a protocol recently optimized in the Ramirez' lab (Figure 9) [92]. CRISPR-Cas9 oligonucleotides including homologous recombination (HR) primers, small guide RNA (sgRNA) spacers and verification primers were designed using the PrimerQuest tool on IDT website (Appendix A7). PCR amplification and purification of the HR fragments from *S. aureus* genomic DNA was performed, using the following protocol: 30 sec at 94°C; 30 cycles (30 sec at 94°C; 60 sec at 59 °C); 60 sec at 68°C), 5 min at 68°C and ∞ at 94°C, followed by gel electrophoresis in 1% agarose gel to verify the size of each HR fragment. Parallely, pCasSA plasmid DNA was extracted using a Miniprep kit (Qiagen) followed by double digestion with XbaI and XhoI and purification with a PCR purification kit (Qiagen) as per manufacturer's instructions. HR fragments were cloned into the digested pCasSA plasmid using NEBuilder HiFi DNA Assembly Master Mix (BioLabs) to obtain plasmid pHR. The new plasmid pHR was transformed into *E. coli* DC10b and plated on LB+Kan50 for overnight incubation at 30 °C. Colonies grown on LB+Kan50 plates were selected to determine the presence of pHR by colony PCR, using

the following protocol: 3 min at 94°C; 30 cycles (30 sec at 94°C; 60 sec at 59 °C); 5 min at 68°C), 5 min at 68°C and ∞ at 94°C. PCR fragments were run in 1% agarose gels to verify the presence of pHR. Positive clones were cultured on LB+Kan50 plates and used to prepare frozen socks. Thereafter, previously designed sgRNA spacers were phosphorylated (to enhance stability and improve the efficiency), amplified and cloned into pHR using the Golden Gate assembly kit (BioLabs) to obtain plasmid pHR-sgRNA. *E. coli* DC10b was transformed with pHR-sgRNA. Transformants were plated onto LB+Kan50 plates followed by overnight incubation. Confirmation of the presence of the new pHR-sgRNA plasmid was done by colony PCR, using the following protocol: 3 min at 94°C; 30 cycles (30 sec at 94°C; 60 sec at 59 °C); 5 min at 68°C), 5 min at 68°C and hold at 4°C. PCR fragments were run in 1% agarose gels to verify the presence of pHR-sgRNA. The new pHR-sgRNA plasmid was used to transform *S. aureus* RN4220 competent cells by electroporation. Transformants were confirmed by colony PCR, using the following protocol: 10 min at 95°C; 30 cycles (30 sec at 95°C; 60 sec at 58 °C); 5 min at 68°C), 5 min at 68°C and hold at 4°C, and cultured on TSB+CM10 plates at 30 °C for up to 36 hours. pHR-sgRNA was isolated from *S. aureus* RN4220 using a Miniprep kit (Qiagen) as per manufacturer's instructions to electroporate *S. aureus* PS/BAC/169/17/W.

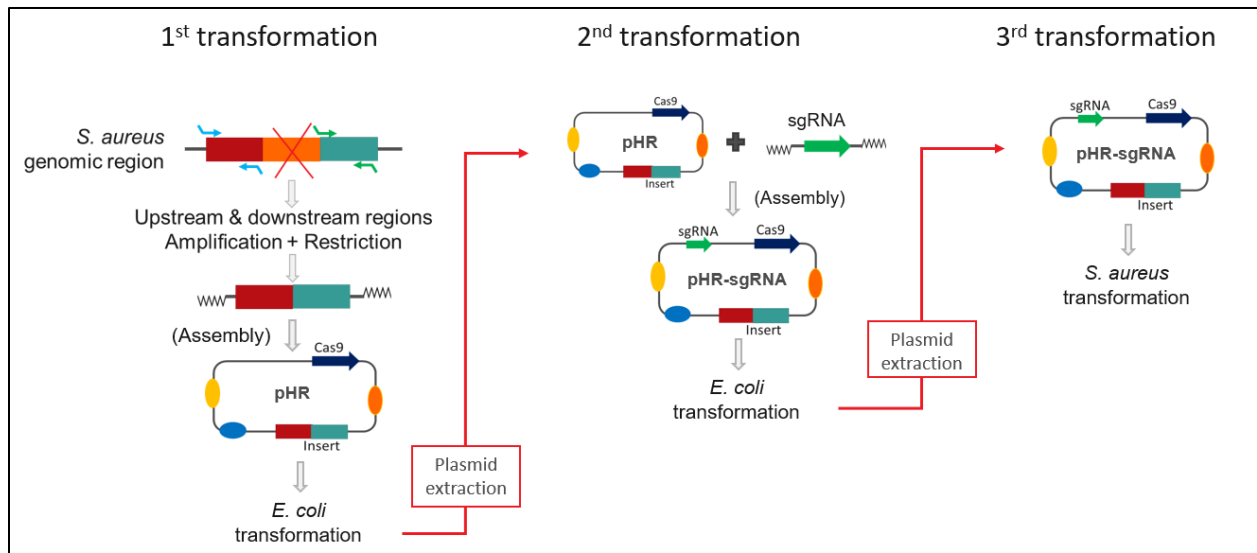


Figure 9– CRISPR-Cas9 experimental protocol to create a *norB* mutant in *Staphylococcus aureus* PS/BAC/169/17/W.

2.2.3.1 Plasmid incompatibility analysis

Construction of a *norB* deletion mutant using CRISPR-Cas9 was not successful despite troubleshooting and several repetitions. Therefore, it was important to determine if there was incompatibility between the 2,7 Kb plasmid carried by *S. aureus* PS/BAC/169/17/W^[188] and pCasSA^[205] that could compromise successful transformation of the PS/BAC/169/17/W strain. If both plasmids belong to the same compatibility group (i.e., have the same replicon and/or partitioning system), they cannot coexist in this strain. The sequence of pCasSA plasmid origin of replication (ColE1)^[205] was aligned with PS/BAC/169/17/W using NCBI BLASTn to determine homology. Additionally, to determine the presence of other incompatibility plasmid groups, replicon typing was performed using PlasmidFinder version 2.1, Center for Genomic Epidemiology (CGE) at the Technical University of Denmark (DTU) available at:

<https://www.google.com/search?q=https://cge.cbs.dtu.dk/services/PlasmidFinder/>, last accessed on November 12th, 2025 [206].

2.2.4 Mutagenesis of *Staphylococcus aureus norB* using allelic recombination exchange

Construction of a *norB* deletion mutant using CRISPR-Cas9 was not successful despite troubleshooting and several repetitions. I therefore attempted the construction of a *norB* in-frame deletion mutant in *S. aureus* RN6390 by allelic recombination exchange using a staphylococcal allelic exchange vector (pIMAY) obtained from Addgene (Appendix A7) [203], following the protocol optimized by Truong-Bolduc, et al (2022) [207]. Upstream and downstream sequences of *norB* were amplified from genomic DNA by overlay polymerase chain reaction (PCR), the two fragments were ligated by overlay PCR (primers used for this procedure are listed in Appendix A6). PCR products and plasmid pIMAY were double digested with KpnI and SacI, ligated using a New England Biolabs ligation kit as per manufacturer's instructions to construct pIMAY- Δ *norB*, and transformed into *E. coli* DC10B by the heat shock method. Transformed cells were plated on LB+CM10 and incubated at 37°C for 48 h. The presence of the pIMAY- Δ *norB* was confirmed by colony PCR, using the following protocol: 3 min at 94°C; 30 cycles (30 sec at 94°C; 60 sec at 57°C); 5 min at 68°C), 5 min at 68°C and hold at 4°C. Plasmid pIMAY- Δ *norB* was isolated from *E. coli* using a Miniprep kit (Qiagen) as per manufacturer's instructions, and transformed into *S. aureus* RN4220 by electroporation. Confirmation of the presence of pIMAY- Δ *norB* was done by colony PCR, using the following protocol: 3 min at 94°C; 30 cycles (30 sec at 94°C; 60 sec at 57 °C); 5 min at 68°C), 5 min at 68°C and hold at 4°C.

Transformed cells were plated on TSB+CM10 and incubated at 37°C for 48 h. Plasmid pIMAY- Δ *norB* was isolated from *S. aureus* RN4220 using a Miniprep kit (Qiagen) and electroporated into *S. aureus* strain RN6390.

2.2.5 Overexpression of *Staphylococcus aureus norB*

As construction of a *norB* deletion mutant using CRISPR-Cas9 and allelic exchange was unsuccessful, I undertook a different approach to test gene functionality and tried to overexpress *norB* in the transfusion relevant strain *S. aureus* CBS2016-05. Primers of *norB* and its promoter were amplified by PCR from *S. aureus* CBS2016-05, double digested with BamHI and KpnI, and cloned into the shuttle vector pSK5632 (Appendix A7) ^[208], resulting in the new 7.4 kb plasmid pSK::*norB*p. This plasmid was transformed into *E. coli* DC10B, which was plated on LB+Kan50. Colonies containing the construct were verified by colony PCR. Successful transformants were grown on LB+Kan50 for plasmid extraction using a Miniprep kit (Qiagen) as per manual. *S. aureus* CBS2016-05 competent cells were electroporated with the vector pSK5632 and with pSK::*norB*p and plated on TSA+Cm10 (Figure 10).

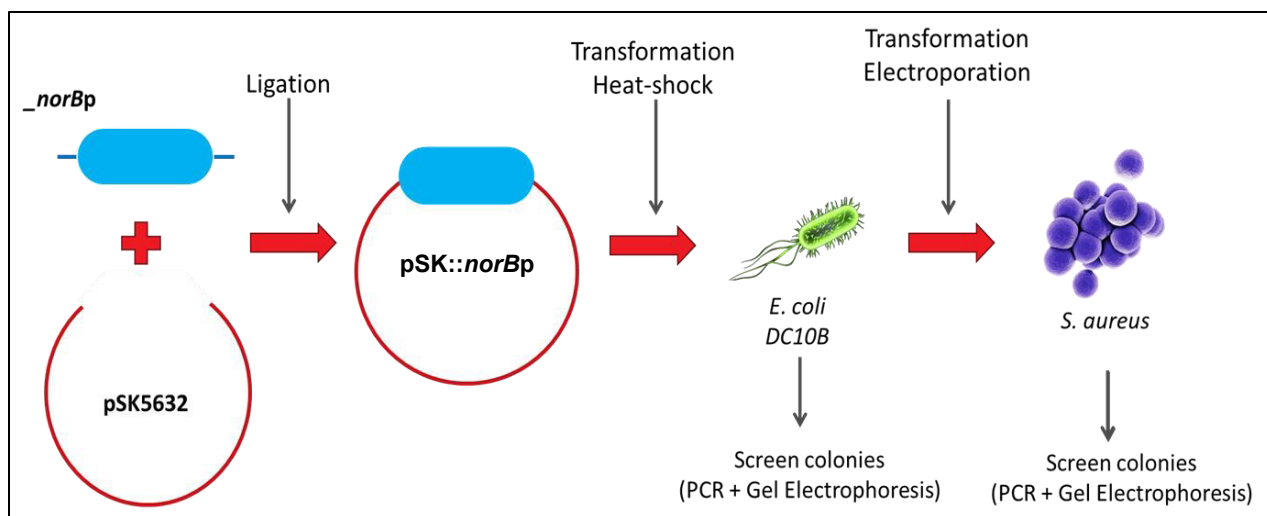


Figure 10 – Protocol overview for overexpression of *norB* in *Staphylococcus aureus* CBS2016-05.

Attempts to create a *norB* mutant or overexpress the gene in *S. aureus* were unsuccessful. Therefore, to proceed with functional assays, I obtained three non-transfusion relevant strains kindly provided by Dr. David Hooper (Harvard University), which included wild-type *S. aureus* RN6390 and derivative *norB* and *mgrA* mutants (*S. aureus* RN6390 Δ *norB* and *S. aureus* RN6390 Δ *mgrA*, respectively) (Table 3).

2.3 Antibiotic resistance studies

These assays were performed for seven *S. aureus* isolates (four TRS, RN6390, RN6390 Δ *norB* and RN6390 Δ *mgrA*, Table 3) to assess bacterial resistance to the quinolones ciprofloxacin and norfloxacin. *S. aureus* ATCC 29213 was used as a control for Minimum Inhibitory Concentration (MIC) and Minimum Bactericidal Concentration (MBC) assays.

2.3.1 Minimum Inhibitory Concentration (MIC)

MIC values were determined according to the microdilution broth method described in Clinical Laboratory Standards Institute (CLSI) guidelines [209]. Stock solutions of ciprofloxacin and norfloxacin were prepared as per manufacturers' specifications. Bacterial colonies were re-suspended in MHB^{ca+} to 0.5 Densimat, which corresponds to approximately 1×10^8 CFU/mL, and then diluted to a bacterial load of approximately 2×10^6 CFU/mL. Bacterial suspensions were distributed into a 96-well plate within 15 min of preparation. The 96-well plates were loaded as follows: wells of the outer rows and columns were filled with 200 μ L of MHB^{ca+} and the internal wells were filled with 100 μ L of serially diluted antibiotics in MHB^{ca+} to obtain antibiotic concentration gradients across the plates. Antibiotics were added in double concentration since they were diluted 2-fold once the bacterial suspensions were added (e.g., stock solution of 512 μ g/mL to ensure a final concentration of 256 μ g/mL in the well). Following antibiotic dispensing, 100 μ L of the bacterial suspensions were added to each well and were thoroughly mixed. The top only had unspiked MHB^{ca+} (negative control) while the last row was filled with the bacterial suspension without antibiotics (positive control). Plates were incubated for 24 h at 37 °C. After incubation, well absorbance (OD₆₀₀) was recorded using a plate reader and MIC values were determined as the lowest concentration of the antibiotic inhibiting bacterial growth.

2.3.2 Minimal Bactericidal Concentration (MBC)

The MBC protocol use was optimized in collaboration with Dr. Thien-Fah Mah's (University of Ottawa) [210]. MBC was performed as follow, a 2-fold antibiotic gradient was

prepared and 50 μL was pre-loaded onto 48-well plates, overnight bacterial cultures were adjusted to 0.5 Densimat and inoculated in TSB or PCs to approximately 5.5×10^5 CFU/mL, and 450 μL of culture was loaded onto the 48-well plates previously coated with an antibiotic and incubated. Plates seeded with inoculated TSB were incubated at optimal conditions for bacterial growth (37 °C, for 24 h without agitation) and plates seeded with PCs were incubated at PC conditions (22 \pm 2 °C, for 5 days with constant agitation). After incubation, samples from each well were spotted in TSA (~3.5 μL /spot) and incubated overnight at 37 °C. The presence or absence of bacterial growth was recorded to establish the MBC value.

2.4 Silkworm Rearing

Silkworm assays were established to study the role of NorB in *S. aureus* virulence following recently optimized protocols in the Ramirez' lab ^[159]. Briefly, *B. mori* eggs were acquired from Coastal Silkworms (Jacksonville, FL USA) and were kept at room temperature until hatched. Silkworm larvae were fed on commercially bought de-hydrated silkworm chow (coastal silk) supplemented with 300 mg of vancomycin/Kg upon re-hydration. Fifth in-star larvae (day 1 and 2 post molt) were fed food free of vancomycin for a minimum of 24 h prior to use in downstream assays.

2.4.1 Determination of Lethal Dose 50 (LD50)

S. aureus isolates were grown overnight aerobically at 37 °C with agitation in TSB media. The bacterial load required to kill 50% of the silkworm test population (LD₅₀) was

determined as recently described [159]. Briefly, overnight cultures were centrifuged, and the pellets were resuspended in insect saline (0.6% NaCl). TSB cultures of *S. aureus* were centrifuged, the supernatants were discarded, and bacterial pellets were resuspended in insect saline as per the protocol previously optimized at the Ramirez Lab [159]. The injection of TSB into silkworm larvae induces melanization and larvae lethargy and therefore media must be removed from the bacterial pellets prior to larvae injections to avoid false positive results. Suspensions were serially diluted (ten-fold) and inoculated into the haemolymph of silkworm larvae (30 µl/10 larvae/dilution). Bacterial load of each suspension was determined by plating on TSA plates followed by incubation at 37 °C for 24 h and colony counting. Silkworm larvae were incubated at 37 °C for three days (72 h) and inspected daily to assess larval survival and death (no movement when nudged with a pipette tip). Insect saline served as control; LD₅₀ studies were performed in triplicate.

2.4.2 Virulence studies with PC- and media-derived *Staphylococcus aureus*

Frozen enumerated stocks of *S. aureus* isolates (RN6390, RN6390Δ*norB* and RN6390Δ*mgrA*) were thawed on ice and serially diluted to reach ~300CFU/ml. TSB and PCs (30 ml) were dispensed in T25 flasks, which were inoculated with 100µl of the serially diluted cultures to obtain a bacterial load of ~1 CFU/ml and incubated at PC storage conditions (22 ±2 °C, 60 rpm, for 5 days). As described above, TSB-grown *S. aureus* cultures were centrifuged at 10,000 rpm for 5min at 4°C, after which the supernatants were discarded, and the pellets were gently resuspended with the same volume of sterile

insect saline (0.6% NaCl). TSB and PC samples were diluted with saline or unspiked PCs respectively to reach bacterial loads matching the previously established LD₅₀. Fifth instar larvae were fed antibiotic free chow for a minimum of 24 h and groups of 10 larvae/sample were injected with 30 µl of bacterial suspensions. Control groups were injected with un-spiked PCs or 0.6% NaCl. Larvae were incubated at 37°C and inspected daily (for a total of 72 h) to assess larval survival and death, and record mortality (no movement when nudged with a pipette tip). These experiments were performed at least three independent times.

2.5 Statistical Analyses

Statistical analysis of the RNA-seq data was performed in R, while statistical comparisons of biofilm formation, antibiotic resistance assays, and silkworm experiments were obtained using GraphPad Prism (version 9.0.0) software. The statistical method used in each analysis is indicated in the figure legends. Values were expressed as mean ± SE and a p-value of <0.05 was considered statistically significant.

3. Results

As a disclaimer, part of the work presented in this chapter has been published in the journal *Antibiotics* (MDPI), in which I am the first author ^[1]. Dr. Sandra Ramirez-Arcos was involved in data analysis and interpretation, and in editing the published manuscript. Biochemical assays for bacterial identification were performed by Mr. Yuntong Kou, M.Sc. (Senior Development Assistant in the Ramirez' lab). Growth curve data in TSB and PCs for *S. aureus* CBS2016-05 and PS/BAC/317/16/W were produced by post-doctoral fellows Dr. Sylvia Ighem Chi and Dr. Basit Yousuf. Biofilm formation results for *S. aureus* CBS2016-05 and PS/BAC/317/16/W in PCs was obtained by Dr. Basit Yousuf. Growth curves and biofilm formation results from other team members were included in this chapter for comparative purposes. Statistical analysis was performed with Dr. John Blake (Canadian Blood Services) guidance.

3.1 Phenotypic characterization of *Staphylococcus aureus* isolates

3.1.1 Microscopic characterization

Gram staining of the four TRS *S. aureus* (CBS2016-05, CI/BAC/25/13/W, PS/BAC/169/17/W and PS/BAC/317/16/W) and three *S. aureus* laboratory strains (wild-type RN6390, and derivative mutants RN6390 Δ *norB* and RN6390 Δ *mgrA*), showed the expected Gram-positive cocci shape forming grape-like clusters for all isolates (Figure 11, Table 10). These results merit further investigation using electron microscopy to investigate possible morphological changes such as modifications of the cell surface due to the deletion of *norB* or *mgrA*.

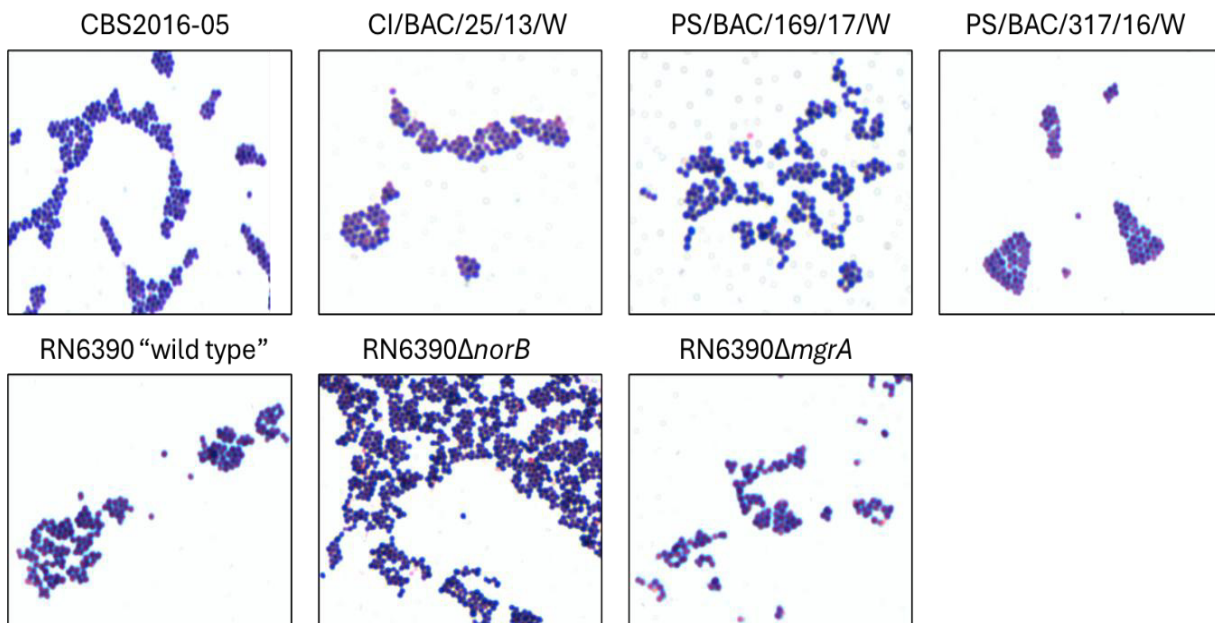


Figure 11- Gram staining of TRS and laboratory *Staphylococcus aureus* isolates. Gram-stained isolates showing purple-colored cocci clusters visualized using oil immersion at 1000x magnification.

3.1.2 Macroscopic characterization

All TRS and laboratory *S. aureus* isolates cultured on TSA formed round smooth, convex, and opaque colonies, with pigmentation varying from light yellow to bright yellow indicating different levels of staphyloxanthin production (Table 10, Appendix A3) Under identical growth conditions, *S. aureus* RN6390, RN6390 Δ *norB* and RN6390 Δ *mgrA* produced colonies with similar morphology compared to the TRS, and no difference in colony size between the wild-type and mutant strains.

3.1.3 Hemolysis characterization and biochemical identification

On BA plates, most isolates exhibited β -hemolysis, except for strain PS/BAC/169/17/W, which was non-hemolytic (δ -hemolysis) (Table 10, Appendix A3).

Bacterial identification based on biochemical and metabolic tests using the VITEK 2 system confirmed that all isolates were *S. aureus*, with confidence levels ranging from good to excellent identification (89% - 99%) (Table 10).

Table 10 – Phenotypic classification of *Staphylococcus aureus* TRS, and *S. aureus* RN6390, RN6390 Δ *norB* and RN6390 Δ *mgrA*. *S. aureus* ATCC 29213 was included as a reference strain.

<i>S. aureus</i> Isolate	Microscopic morphology	Colony pigmentation on TSA plates	Hemolysis on BA plates	Biochemical identification
ATCC 29213	Gram-positive Cocci Grape-like arrangement	Light yellow	β -hemolysis	Excellent 96%
CBS 2016-05	Gram-positive Cocci Grape-like arrangement	Light yellow	β -hemolysis	Good 90%
CI/BAC/25/13/w	Gram-positive Cocci Grape-like arrangement	Bright Yellow	β -hemolysis	Excellent 99%
PB/BAC/169/17/W	Gram-positive Cocci Grape-like arrangement	Bright Yellow	δ -hemolysis	Good 90%
PS/BAC/317/16/W	Gram-positive Cocci Grape-like arrangement	Bright Yellow	β -hemolysis	Very Good 94%
RN6390	Gram-positive Cocci Grape-like arrangement	Light yellow	β -hemolysis	Good 89%
RN6390 Δ<i>norB</i>	Gram-positive Cocci Grape-like arrangement	Light yellow	β -hemolysis	Excellent 99%
RN6390 Δ<i>mgrA</i>	Gram-positive Cocci Grape-like arrangement	Light yellow	β -hemolysis	Good 92%

3.1.4 *Staphylococcus aureus* growth curves in TSB

All TRS started at approximately 4×10^6 CFU/mL in TSB cultures. A clear lag phase of 2 hours was observed for strain CBS2016-05, while strains PS/BAC/317/16/W, CI/BAC/25/13/W and PS/BAC/169/17/W did not present a typical lag phase (Figure 12A). Overall, all isolates displayed rapid exponential growth under optimal nutrient and temperature conditions, however the growth pattern varied among strains. PS/BAC/169/17/W and CI/BAC/25/13/W demonstrated faster growth, achieving high cell densities ($\sim 1.13 \times 10^{12}$ CFU/mL and $\sim 1.37 \times 10^{12}$ CFU/mL, respectively) by 10–12 hours, whereas PS/BAC/317/16/W showed moderate growth and CBS 2016-05 grew slower, reaching lower final CFU ($\sim 5.10 \times 10^9$ CFU/mL and $\sim 2.25 \times 10^9$ CFU/mL, respectively). These kinetic patterns reflect differences in intrinsic metabolic fitness under the laboratory conditions. Additionally, growth kinetics of each TRS was analysed by determining their slope (growth rate) and doubling time (Table 11). This analysis revealed that *S. aureus* CI/BAC/25/13/W grew faster, with highest growth rate of 1.08/hour, and corresponding doubling time of 0.64 hours. Conversely, PS/BAC/169/17/W and CBS2016-05 grew at slower rates of 0.60/hour and 0.65/hour, respectively, and doubling times higher than one hour. The PS/BAC/317/16/W strain presented a growth rate and doubling time between the other strains (0.83/hour and 0.84 hours, respectively). Overall, the comparison of slopes and doubling time demonstrate that *S. aureus* CI/BAC/25/13/W was the isolate presenting faster growth in laboratory media, followed by PS/BAC/317/16/W, CBS2016-05 and PS/BAC/169/17/W. Statical comparison of slope (growth rate) among isolates grown in TSB did not showed significance, indicating no difference in the isolates growth in this media (Table 11).

Although the initial inocula of *S. aureus* RN6390, *S. aureus* RN6390 Δ *norB* *S. aureus* RN6390 Δ *mgrA* was adjusted to OD₆₀₀ = 0.002, colony counts showed that the RN6390 and RN6390 Δ *norB* isolates started at a bacterial load of $\sim 10^5$ CFU/mL while the initial inoculum of *S. aureus* RN6390 Δ *mgrA* was $\sim 10^6$ CFU/mL (Figure 13A). The three isolates showed similar growth patterns, displaying rapid growth and reaching comparable final CFU loads (RN6390 $\sim 3.35 \times 10^9$ CFU/mL, RN6390 Δ *norB* $\sim 3.60 \times 10^9$ CFU/mL and RN6390 Δ *mgrA* $\sim 2.97 \times 10^9$ CFU/mL) by 12 hours indicating start of stationary growth phase. Although RN6390 Δ *norB* showed an increase at around ~ 6 hours, this difference diminished as each isolate culture approached stationary phase. Despite starting 1-log higher, the RN6390 Δ *mgrA* mutant reached similar counts ($\sim 9.50 \times 10^8$ CFU/mL) around 8 hours of incubation, converging with the wild type and the RN6390 Δ *norB* strains ($\sim 7.33 \times 10^8$ and $\sim 1.23 \times 10^8$, CFU/mL, respectively). These results indicate that under nutrient-rich, optimal conditions, deletion of *mgrA* or *norB* does not impact bacterial proliferation. Growth rate analysis of these three strains showed that RN6390 displayed a growth rate of 0.65/hour comparable to CBS2016-05 (Table 11). The mutants RN6390 Δ *norB* and RN6390 Δ *mgrA* grew at comparable rates of 0.50/hour and 0.56/hour, respectively, which were slightly lower than that of the wild-type strain (0.65/hour). Doubling times for wild-type RN6390 was correspondingly slightly lower in *S. aureus* RN6390 (1.07 hours) compared to mutants RN630 Δ *norB* and RN6390 Δ *mgrA* strains (1.38 hours and 1.24 hours, respectively, Table 11). Similarly to the TRS, the statistical comparison of slopes (growth rate) among these isolates grown in TSB did not show statistical differences ($p > 0.05$, Table 11).

3.1.5 *Staphylococcus aureus* growth curves in PCs

In PC-cultures, all strains exhibited reduced growth rates in comparison to TSB consistent with the reduced temperature, nutrient limitations, and host immune factors present in PCs. This has been previously observed in the Ramirez' lab. The TRS started at approximately 4×10^6 CFU/mL and grew at the different rates (Figure 12B). In this milieu, CI/BAC/25/13/W achieved higher CFU/mL loads at 24 hours ($>10^9$ CFU/mL), whereas the other isolates grew to lower bacterial loads, particularly PS/BAC/169/17/W that reach a final bacterial load of $\sim 3.57 \times 10^8$ CFU/mL at 144h, showing different adaptation abilities to PC-associated stresses among TRS isolates. Growth curves depict a clear difference of *S. aureus* CI/BAC/25/13/W with faster growth rate 0.07/h and doubling time 10.19 hours, Table 11) compared to the other three isolates, which showed slower growth rates, ranging from 0.03 to 0.06/hour and extended doubling times ranging from 10.97 to 21.08 hours (Figure 12B and Table 11). Interestingly, PS/BAC/169/17/W presented the lowest growth rate (0.03/hour) and the longest doubling time (21.08 hours) indicating that the PC environment affects growth ability of *S. aureus* in a strain-dependent manner. Statistically significant differences were observed between strain CI/BAC/25/13/W and PS/BAC/169/17/W ($p = 0.003$) and PC/BAC/317/16/W ($p = 0.008$) (Table 11), confirming differential growth pattern of these strains in PCs

Comparison of growth rates in PC cultures all isolates displayed a prolonged lag phase that may be attributed to nutrient limitation, lower temperature, and stressors inherent to PCs. Wild-type *S. aureus* RN6390 and RN6390 Δ *norB* showed similar growth kinetics (Figure 13B). The wild-type strain increased steadily and reached the highest counts ($\sim 8.47 \times 10^7$ CFU/mL) by 96–144 hours, reflecting its effective adaptation to the PC

environment. The RN6390 Δ *norB* mutant showed impaired growth, particularly in the first 72 hours, suggesting that the NorB efflux pump contributes to early adaptation by exporting antimicrobial or toxic compounds present in PCs. In contrast, RN6390 Δ *mgrA* demonstrated a consistently reduced growth rate throughout the experiment, with lower colony counts during early and mid-log phases. Both *S. aureus* RN6390 and RN6390 Δ *norB* strains had the same growth rate of 0.08/h and similar doubling times (8.73 and 8.30 hours for *S. aureus* RN6390 and RN6390 Δ *norB*, respectively), while RN6390 Δ *mgrA* depicted a higher growth rate of 0.15/hour and shorter doubling time (4.56 hours) than the two other strains (Table 11). Despite these differences, the growth curves of the three strains overlap (except at the 72h sampling point) indicating no differences in growth between the three strains when grown in PCs. This attenuation supports the role of MgrA as a global regulator of stress responses, efflux systems, and virulence factors that collectively enhance survival in hostile environments. Although both mutants RN6390 Δ *norB* and RN6390 Δ *mgrA* eventually approached wild-type bacterial load levels ($\sim 1.01 \times 10^8$ CFU/mL and $\sim 1.32 \times 10^8$ CFU/mL, respectively) at 144 hours, the delayed growth emphasizes that *mgrA* and *norB* play important roles in optimizing bacterial fitness in blood-derived products. The statistical comparison of slopes (growth rate) among these isolates grown in PCs did not show statistical differences ($p > 0.05$, Table 11).

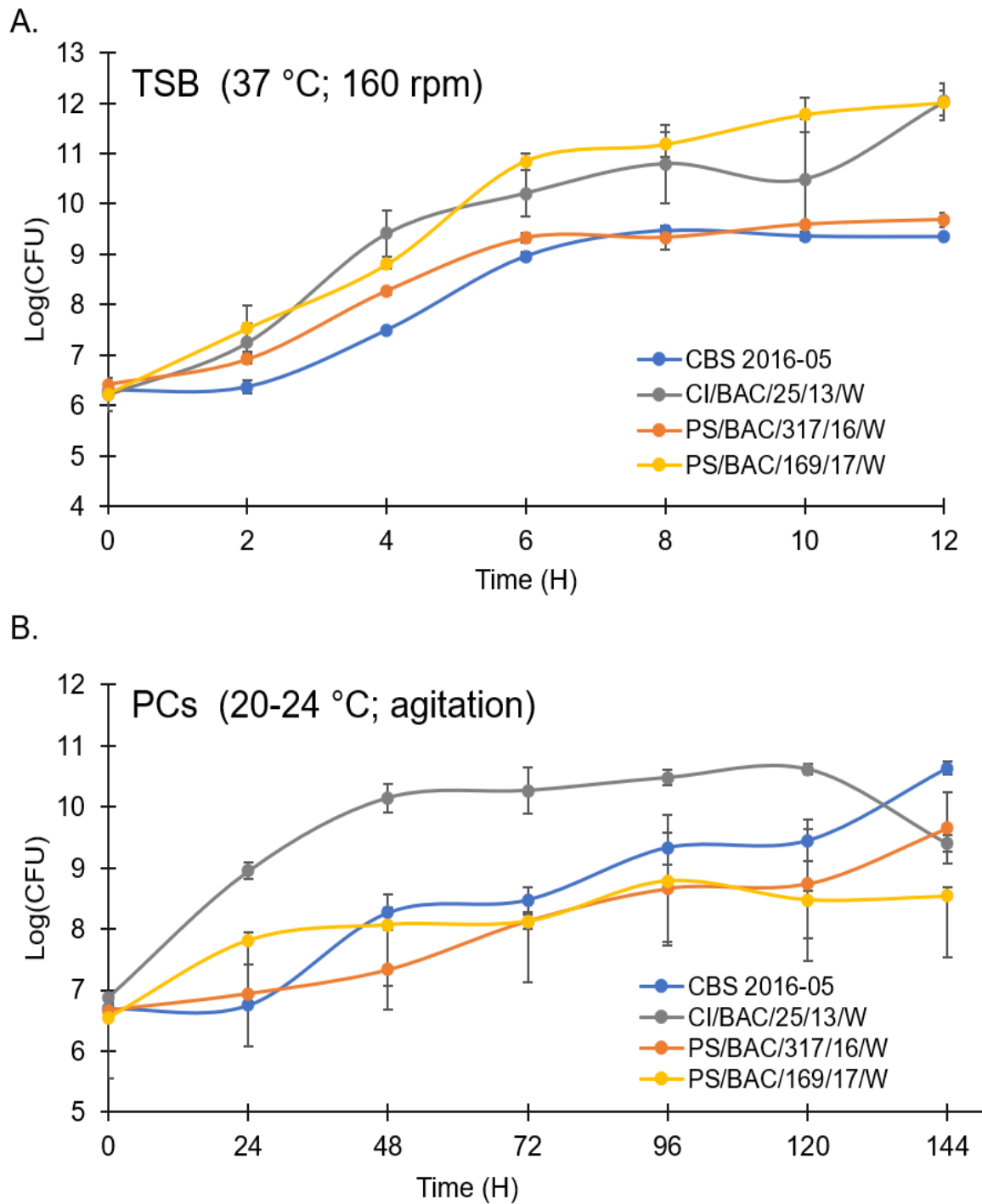


Figure 12- Growth curve studies of TRS *Staphylococcus aureus* strains A. TSB (37 °C, 160rpm) and B. PCs (22 ± 2 °C, 60rpm). Results are presented as a mean of 3 independent trials. Error bars with standard deviation ±SD.

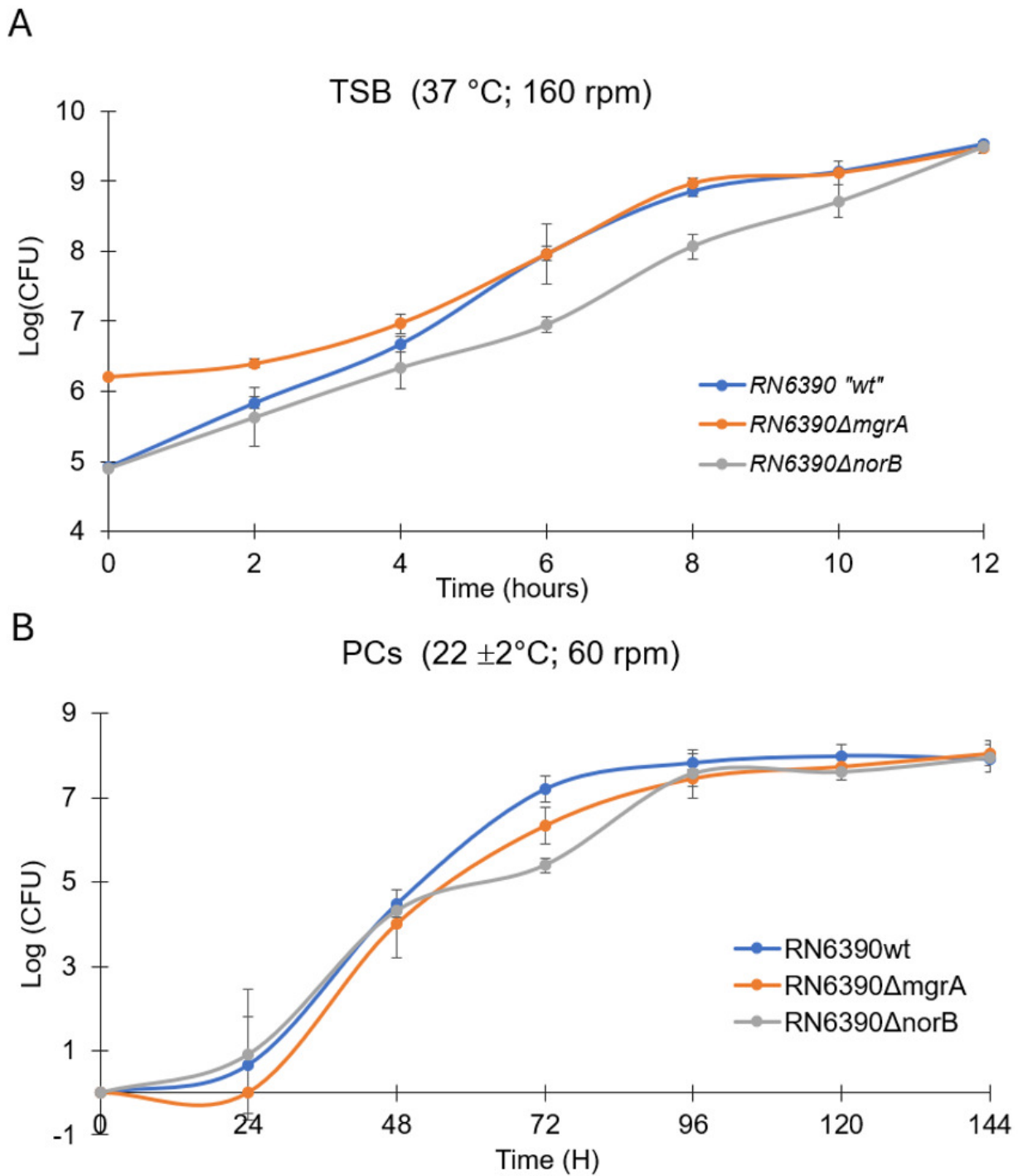


Figure 13- Growth curve studies of *Staphylococcus aureus* RN6390 and RN6390Δ*norB* and RN6390Δ*mgrA*. A. TSB (37 °C, 160rpm) and B. PCs (22 ± 2 °C, 60rpm). Results are presented as a mean of 3 independent trials. Error bars with standard deviation ±SD. Figure 13B from paper by Paredes et al (2025) ^[1], copyrights approval to reproduce the figure available in page xv.

Table 11 – Summary of Growth rate (slope) and Doubling time parameters (including 95% Confidence Interval) derived from growth curves analysed ^[194]. Slope statistical comparison was performed using an unpaired t-test. “wt” – wild type.

Log phase	Strain	CBS 2016-05	CI/BAC/ 25/13/W	PS/BAC/ 169/17/W	PS/BAC/ 317/16/W	RN6390 “wt”	RN6390 $\Delta norB$	RN6390 $\Delta mgrA$	
TSB	Growth rate	0.65	1.08	0.60	0.83	0.65	0.50	0.56	
	Log(CFU/mL)/h								
	Doubling Time (hours)	1.07	0.64	1.15	0.84	1.07	1.38	1.24	
PCs	Growth rate	0.06	0.07	0.03	0.05	0.08	0.08	0.15	
	Log(CFU/mL)/h								
	Doubling Time (hours)	10.97	10.19	21.08	13.15	8.73	8.30	4.56	
Slope statistical comparison: Unpaired t-test									
	CBS vs CI/25	CBS vs PS/317	CBS vs PS/317	CI25 vs PS/169	CI25 vs PS/317	PS/169 vs PS/317	RN6390 [“wt” vs $\Delta mgrA$]	RN6390 [“wt” vs $\Delta norB$]	RN6390 [$\Delta mgrA$ vs $\Delta norB$]
TSB	0.427	0.198	0.198	0.474	0.275	0.233	0.159	0.216	0.712
PCs	0.216	0.628	0.628	0.003	0.008	0.177	0.648	0.804	0.564

3.1.6 *Staphylococcus aureus* biofilm formation in TSB and PCs

Biofilm formation results of the seven *S. aureus* strains, including four TRS, *S. aureus* RN6390 and RN6390 Δ *norB* and RN6390 Δ *mgrA*, are presented in Figure 14 and Table 12. Formation of biofilms was evaluated using a semi-quantitative crystal violet assay and strains were categorized as strong, moderate or weak biofilm formers based on the intensity of crystal violet staining compared to unspiked samples (negative controls).

Biofilm formation assays in TSBg showed that *S. aureus* CI/BAC/25/13/W is a weak biofilm former, whereas the other three TRS and the RN6390 isolates formed strong biofilms (Figure 14A, Table 12).

As expected, based on previous work in the Ramirez' lab [34,35], all *S. aureus* strains formed biofilms in PCs. *S. aureus* CI/BAC/25/13/W is a moderate biofilm former in this milieu, while the other three TRS and the RN6390 isolates are strong biofilm formers (Figure 14B, Table 12). Statistical analysis showed that the formation of biofilms is significantly higher in PCs compared to TSB ($p < 0.05$, Table 6) for all strains except for PS/BAC/169/17/W ($p = 0.189673$, Table 12). The variability in the biofilm formation data obtained in *S. aureus* grown in PCs compared to TSB can be attributed to blood donor variability.

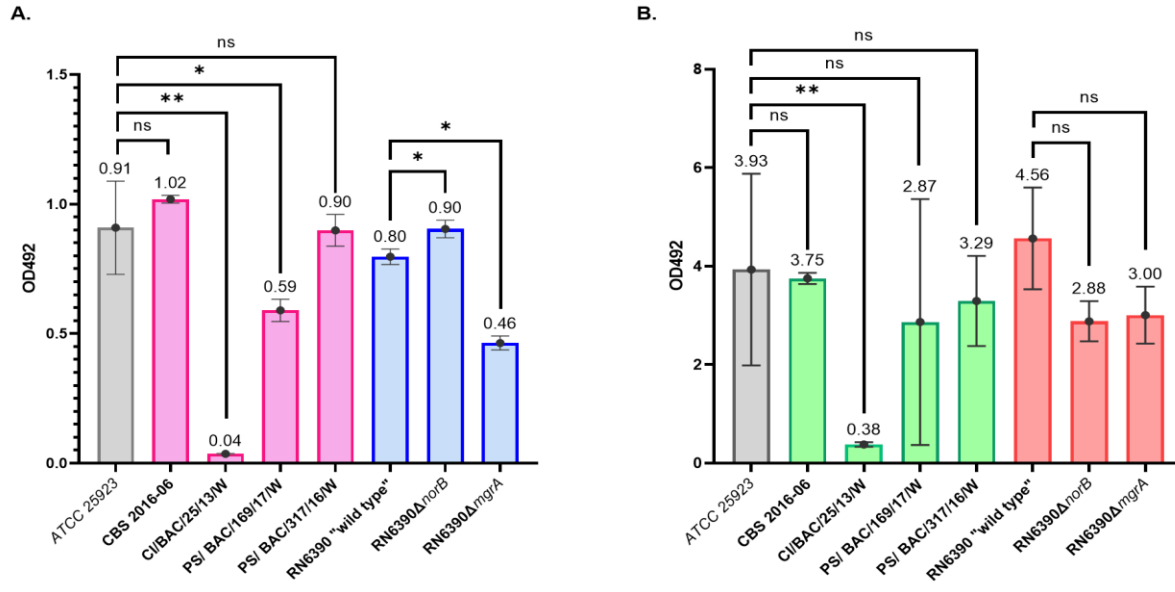


Figure 14 – Biofilm formation by *Staphylococcus aureus*. A. in TSB, B. in PCs. Unspiked TSBg and PCs were used as a negative control for biofilm formation. *S. aureus* ATCC 25925 served as positive control for biofilm formation and for comparison in the statistical analysis. Results performed in $n \geq 3$ independent trials with each assay performed in duplicate. Error bars with standard deviation \pm SE, Statistical analysis performed using a student t-test. ns: Not significant; *: $p < .05$; **: $p < .01$.

Table 12 – Biofilm formation assay results for all isolates in TSB and PCs, biofilm capability classification and statistical comparison (PCs vs TSB).

Strains	TSB		PCs	
	OD492	Classification	OD492	Classification
ATCC 25923	0.909 ±0.1804	Strong	3.930 ±1.9466	Strong
CBS 2016-06	1.019 ±0.0149	Strong	3.752 ±0.1137	Strong
CI/BAC/ 25/13/W	0.036 ±0.0022	Weak	0.378 ±0.0454	Moderate
PS/BAC/ 169/17/W	0.590 ±0.0433	Strong	2.866 ±2.4975	Strong
PS/BAC/ 317/16/W	0.899 ±0.0607	Strong	3.292 ±0.9147	Strong
RN6390 "wild type"	0.797 ±0.0299	Strong	4.563 ±1.0330	Strong
RN6390 <i>ΔnorB</i>	0.904 ±0.0344	Strong	2.881 ±0.4082	Strong
RN6390 <i>ΔmgrA</i>	0.464 ±0.0267	Strong	3.004 ±0.5779	Strong

Comparison of biofilm formation in TSB versus PCs

Strain	ATCC 25923	CBS 2016-06	CI/BAC/ 25/13/W	PS/BAC/ 169/17/W	PS/ BAC/ 317/16/W	RN6390 "wild type"	RN6390 <i>ΔnorB</i>	RN6390 <i>ΔmgrA</i>
P value	0.0473	2.449 E-05	5.301 E-05	0.189673	0.01588	0.0032	0.0011	0.0016

3.1.7 Comparative genomic analyses of *Staphylococcus aureus* strains

Genomic comparison between the TRS and *S. aureus* RN639036 was performed, and genome characteristics of the isolates are described in Table 13. Genome size is within the reported range size for *S. aureus* (2.5 to 2.9 Mbp) ^[63], with the genome of isolate PS/BAC/317/16/W being the smallest (2,665,983 bp) and the genome of the CBS 2016-05 strain being the largest (2,766,936 bp) among all isolates. Other features such as GC content (%), CDS (2392 – 2741), rRNAs (19), tRNA (58 – 60) and ncRNA (4) were also similar among isolates.

Table 13 – Overview of *Staphylococcus aureus* genome features of all isolates in study. Table retrieved from paper by Paredes et al (2025) ^[1], copyrights approval to reproduce the table available in page xv.

	CBS 2016-05	CI/BAC/ 25/13/W	PS/BAC/ 169/17/W	PS/BAC/ 317/16/W	RN6390
Accession number	NZ_CP070991	NZ_CP071102	NZ_CP071100	NZ_CP071104	NZ_CP090001
Origin	PC				Laboratory
Genome size (bp)	2,766,936	2,719,347	2,753,746	2,665,983	2,740,225
Genes (total)	2,823	2715	2,739	2,609	2,717
GC content (%)	32.87	32.88	32.85	32.93	32.90
CDSs	2,741	2,629	2,658	2,392	2,635
rRNA	19	19	19	19	19
tRNA	59	60	58	58	59
ncRNA	4	4	4	4	4
Reference	[186]	[187]	[188]	[189]	[190]

Multiple genome analysis using the Mauve Progressive algorithm showed a similar chromosome architecture of the five *S. aureus* strains which features eleven co-linear genomic blocks that exhibit similar genome rearrangements (Figure 15).

S. aureus RN6390 presents an inversion in its genome consistent with prophage phage SAP40 – ϕ 6390, as previously reported ^[190]. Additionally, this strain has a 11-bp deletion in the *rsbU* gene (Appendix A4) which encodes for the RsbU phosphatase that forms part of the sigma B regulon-^[190]. In contrast, the four TRS carry a wild-type copy of *rsbU*.

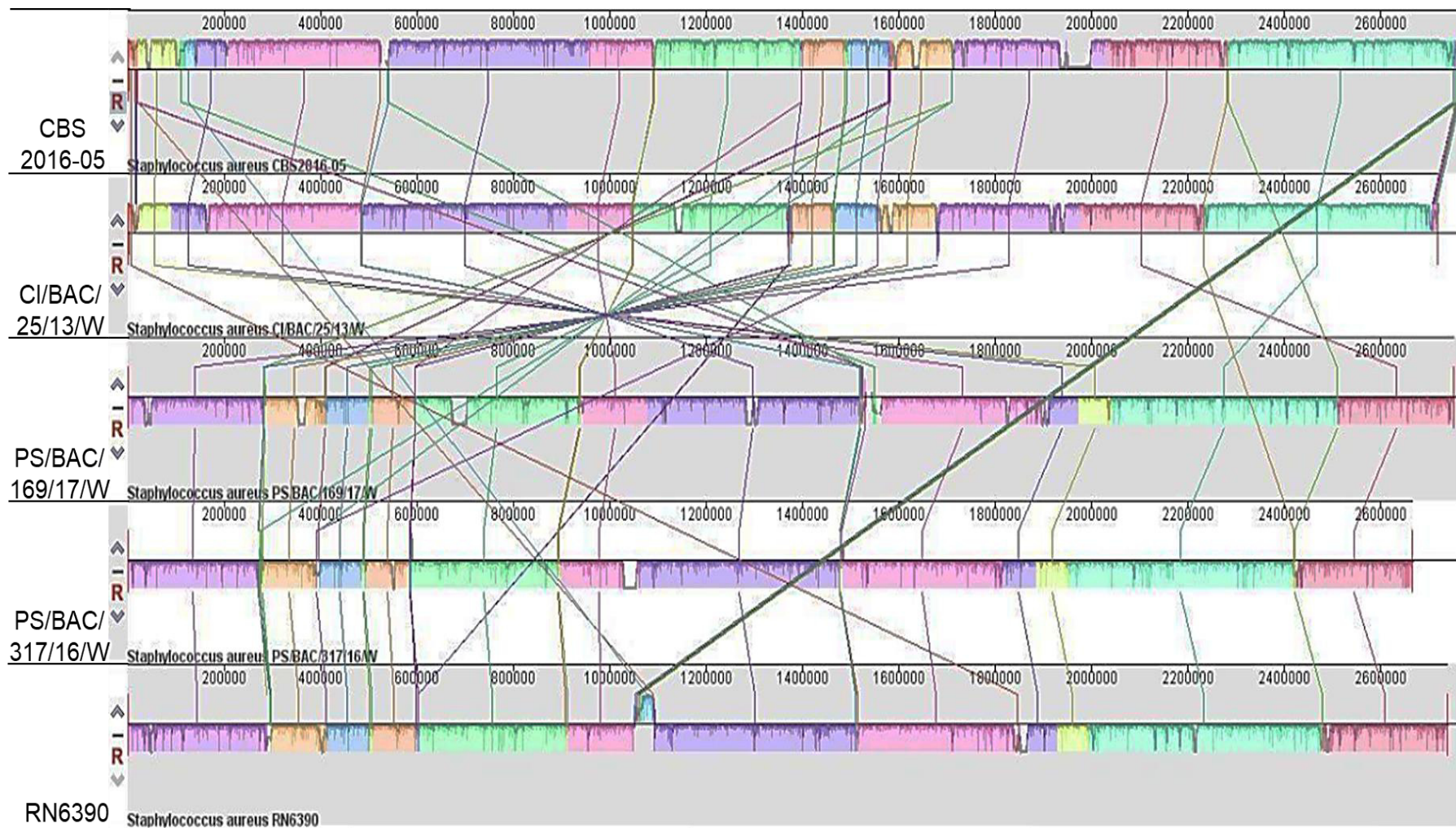


Figure 15 – Multiple genome alignment of *Staphylococcus aureus* TRS and *Staphylococcus aureus* RN6390 using Mauve progressive algorithm. Local collinear blocks are identical in color and represent homologous DNA regions. The scale (base pairs) refers to the genome position. Genome of the TRS *Staphylococcus aureus* CBS2016-05 served as the reference strain ^[1]. Figure retrieved from paper by Paredes et al (2025), copyrights approval to reproduce the figure available in page xv.

3.1.8 *Staphylococcus norB* genomic analysis

Genomic analysis of the *norB* gene in the five *S. aureus* isolates used in this study showed that the gene is 1,392 bp long. In all isolates, *norB* is part of a gene cluster that includes three upstream genes that encode for an alanine dehydrogenase, a threonine deaminase and an aa permease (Figure 16). The *norB* gene is separated from these three genes by a 158 bp intergenic region. Downstream of *norB*, there is a 398 bp intergenic region and then a gene encoding for an extracellular matrix binding protein, which is transcribed in the opposite orientation (Figure 16). Bioinformatic analysis of this gene cluster indicates that *norB* is transcribed independently and does not seem to be part of an operon.

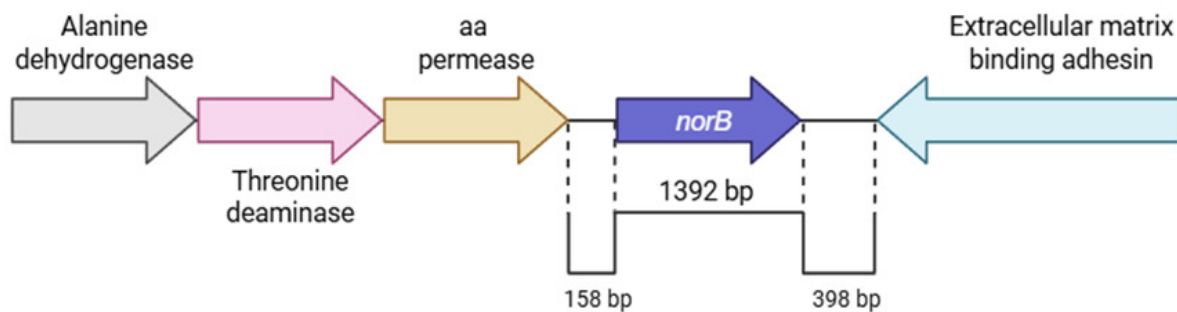


Figure 16 – Schematic representation of the orientation of *Staphylococcus aureus norB* and neighboring ORFs. Image prepared with Biorender.

3.1.9 Comparative analysis of virulence genes in *Staphylococcus aureus* genomes

Comparative genomic analyses of the four *S. aureus* TRS and RN6390, display a similar virulome profile; the isolates carry 60 to 75 genes encoding virulence factors involved in cell adherence, immune modulation, biofilm formation, enzymes and exotoxins as

illustrated in Figure 17 and Appendix A8. Additionally, the isolates carry several genes encoding for virulence regulators such as two component systems that were manually identified in each bacterial genome (Appendix A9).

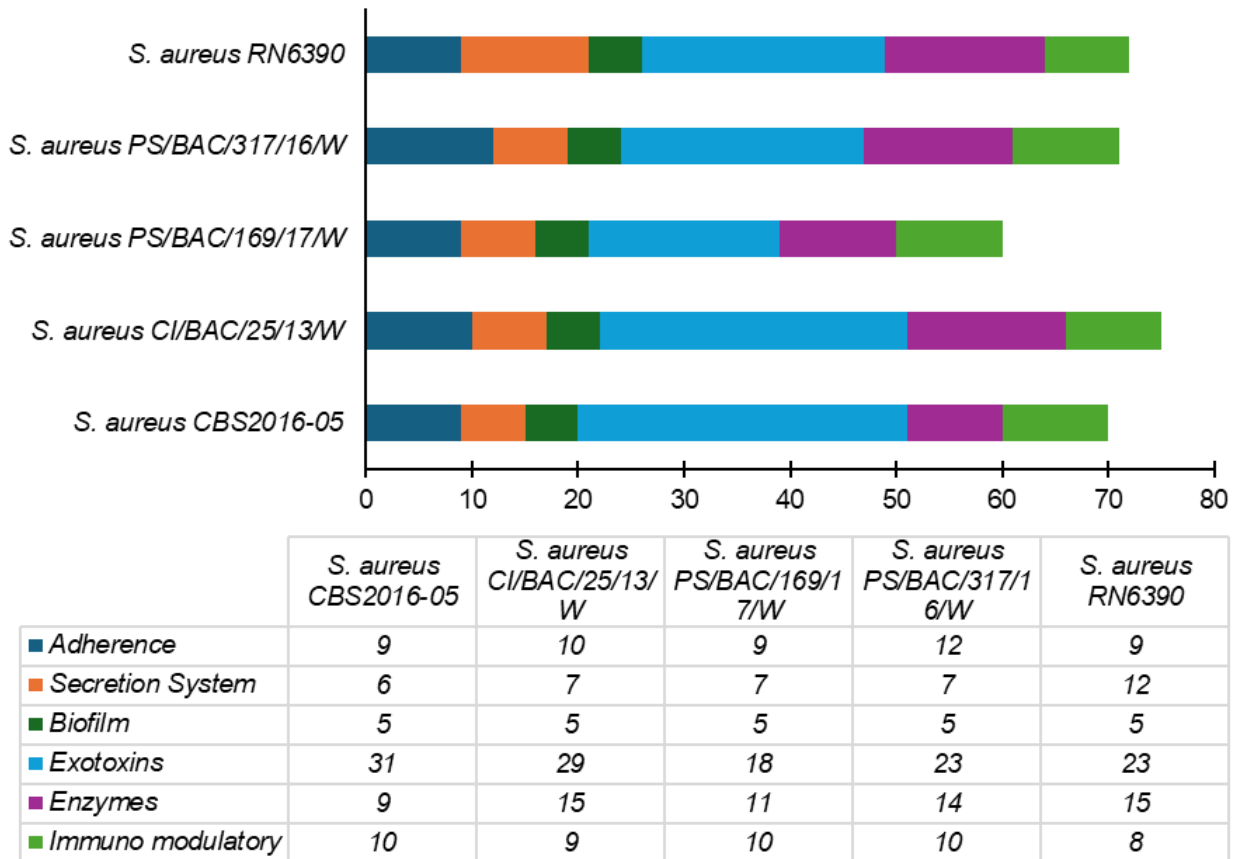


Figure 17 – Virulence factors category and number of genes detected in *Staphylococcus aureus* (four TRS – CBS 2016-05, CI/BAC/25/13/W, PS/BAC/169/17/W and PS/BAC/317/16/W, and *S. aureus* RN6390 using VFDB-VFalyzer9 data base.

3.1.9.1 *Staphylococcus aureus* genes involved in adherence and biofilm formation

Genes encoding for proteins involved in adherence, such as *eap*, *fnbA*, *sdrC* (encode for binding proteins - Eap: extracellular adherence protein; FnBPA: fibronectin-binding protein A; SdrC: serine-aspartate repeat protein family, respectively), *clfA*, *clfB* (encode for clumping factors ClfA and ClfB: cell wall-anchored proteins), *spa* (encodes for protein A), *coa* (encodes for staphylocoagulase) and all isolates carry over 14 genes involved in capsular biosynthesis.. However, presence of the *fnbB*, *sdrD*, and *sdrG* genes which encode for fibronectin-binding protein B (FnBPB), serine-aspartate repeat protein D (SdrD), and serine-aspartate repeat protein (SdrG), respectively, varied amount the strains. Moreover, biofilm genes of the *icaABCD* operon and repressor (*icaR*), which are associated with synthesis of the polysaccharide intercellular adhesin (PIA), are conserved in all isolates.

3.1.9.2 *Staphylococcus aureus* genes encoding toxins

Genes encoding for hemolysins, *hla* (α-hemolysin), *hld* (δ-hemolysin), and *hlg* (γ-hemolysin), were found in all genomes using the VFDB tool. Although the gene *hly* (encodes for β-hemolysin) was not identified as a virulence gene by the VFDB, manual search (wild-type gene blast against each genome) revealed the presence of the gene in all genomes ^[211]. As shown in Appendix A3 and Table 10, all strains, with the exception of PS/BAC/169/17/W, presented β-hemolysis. Expression of different hemolysins within

isolates may vary depending on environmental conditions and isolate origin (e.g., *hla* expression is higher in CA-MRSA strains compared HA-MRSA) [211,212].

Genes encoding for other exotoxins, including Panton-Valentine leucocidin (*lukD*, *lukG*) and enterotoxin SeIX (*seIX*) were found in all TRS while RN6390 lacks the *lukG* gene. Genes encoding for enterotoxins such as *seg*, *sei* and *seo* were present in *S. aureus* CBS 2016-05 and PS/BAC/169/17/W, and absent in the other isolates. Interesting, *S. aureus* RN6390 does not carry enterotoxin genes but carries enterotoxin-like *ssI1* to *ssI9* genes. The operon *crtM-Q*, which encodes for staphyloxanthin production is present in all isolates. Transcriptome data reveals upregulation only in *S. aureus* CBS2016-05^[34,186] (Appendix 10), which is validated by the difference in the tone of yellow colony pigmentation among isolates (Appendix A3)^[39].

3.1.9.3 *Staphylococcus aureus* genes encoding enzymes

The presence of genes encoding for enzymes varied among the genomes. For instance, the cysteine protease operon (*sspABC*) was present in all isolates while the staphylokinase (*sak*) gene was absent in strains PS/BAC/169/17/W and PS/BAC/317/W. Furthermore, the operon encoding for serine protease-like proteins (*spIABCDEFG*) was found in *S. aureus* CI/BAC/25/13/W, PS/BAC/317/16/W and RN6390, while three genes of this operon (*spIABD*) were not present in the PS/BAC/169/17/W isolate. Also, the full operon was absent from *S. aureus* CBS2016-05.

3.1.9.4 *Staphylococcus aureus* genes encoding antibiotic resistance genes

The resistome of the five *S. aureus* strains has a comparable number of antimicrobial resistance genes (~ 25 genes / isolate) coding for efflux pumps, enzymatic inactivation, target alteration and target protection (Appendix A11).

All genomes carry the same genes encoding for efflux of the Major Facilitator Superfamily, ATP-Binding Cassette, Small Multidrug Resistance, Multidrug and Toxic Compound Extrusion, and Resistance-Nodulation-Division.

Genes involved in enzymatic inactivation of antibiotics were identified in some of the isolates, for instance the gene *blaZ* (involved in β -lactam resistance) was present in three out of the five isolates (CBS2016-05, PS/BAC/169/17/W and PS/BAC/317/16/W) and *fosB* (involved in fosfomycin resistance) was absent in CBS2016-05. Genes involved in the resistance to aminoglycosides and macrolide antibiotics were not identified. Genes encoding for enzymes responsible for target modification, *glpT* and *murA* (involved in fosfomycin resistance), *fusA* (involved in fusidic acid resistance), *mecA* (involved in methicillin resistance), *gyrA*, *gyrB* and *parC* (involved in quinolone resistance) were present in all isolates. Additionally, manual search (gene and protein blast analyses) revealed the presence of the *parE* gene in all genomes. Sequence alignments of the GyrA, GyrB, ParC and ParE proteins showed amino acid changes within the different *S. aureus* isolates (Appendix A5), which could potentially affect protein function and be related to changes in quinolone resistance. The gene *msrA* (involved in erythromycin resistance) encoding for target protection was found in all genomes. Additionally,

regulators involved in the expression of resistance mechanisms (*arlR*, *arlS*, *mgrA*, *sdrM*, *lmrs*) were found in all isolates.

3.2 Global Comparative transcriptome analysis of *Staphylococcus aureus* TRS grown in PCs and TSB

A global transcriptome analysis of the TRS comparing *S. aureus* grown in PCs versus TSB was previously conducted in the Ramirez' lab with focus on metabolic and virulence genes (Appendix 10). For instance, transcriptome data revealed upregulation of genes encoding for surface adhesion factors like *clfA* (clumping factor A), *spA* (Protein A), and the capsule biosynthesis operon (*capA-H*), which facilitates adhesion to platelets, immune evasion, and biofilm formation, which are critical for survival and proliferation in PCs [39,63,67]. These transcriptional changes demonstrate *S. aureus*' capability to adapt to the PC storage environment, enhancing its virulence, its ability to escape detection, and being able to cause severe septic transfusion reactions as exemplified by the transfusion event involving *S. aureus* CBS 2016-05 [34].

3.2.1 Transcriptome analysis of antibiotic resistance genes in *Staphylococcus aureus*

My work complemented previous studies by expanding the transcriptome analysis to antibiotic resistance genes. Differential expression of virulence factors between staphylococci grown in PCs and media have shown that genes involved in antibiotic

resistance are upregulated in PC-grown *S. epidermidis* [213], and therefore we tested whether a similar phenotype was observed in *S. aureus*. The comparative transcriptome analyses revealed differentially expressed genes involved in various mechanisms of resistance to antibiotics, including the Major Facilitator Superfamily, the Multidrug and toxin extrusion family, ATP-binding cassette superfamily, and genes encoding for enzymes that modify the cellular targets of antibiotics and enzymes that modify or metabolize antimicrobial drugs (Figure 18).



Figure 18 – Heatmap of *Staphylococcus aureus* differentially expressed genes encoding antibiotic resistance mechanisms (PCs vs. TSB) [CBS: CBS2016-05, CI25: CI/BAC/25/13/W; PS169: PS/BAC/169/17/W and PS317: PS/BAC/317/16/W]. Red represents upregulated genes and blue represents downregulated genes. *nde*: Not differentially expressed. Heatmap prepared with GraphPad Prism (version 9.0.0). Figure retrieved from paper by Paredes et al (2025) [1], copyrights approval to reproduce the figure available in page xv.

The *norB* gene was the only one that was upregulated in the four TRS with a significant log₂ fold change ranging from 1.23 to 4.71 when *S. aureus* was grown in PCs compared to TSB (Figure 18). However, the other efflux pump genes of the *nor* family, *norA* and *norC*, were either downregulated or not differentially expressed (i.e., log₂ fold change = 0) in PC-grown TRS compared to TSB cultures (Figure 18). The *norB* gene encodes for the efflux pump NorB, which is involved in quinolone resistance and is negatively regulated by MgrA [135,136,140]. Transcriptome data were verified with RT-qPCR assays, which confirmed the upregulation of *norB* in PC-grown *S. aureus* compared to TSB cultures in all four TRSs (Figure 19). The housekeeping gene, 16S rRNA, was used as control to verify the transcriptome data. This gene was the only one that did not show differential expression from a list of potential housekeeping genes based on transcriptome data of the Ramirez lab (Appendix A12). Additionally, a literature review revealed that 16S rRNA is often used as a housekeeping gene in RT-qPCR assays [214–216]. The upregulation of *norB* in the TRS suggests that NorB efflux pump supports bacterial survival in the immunological challenging PC storage environment. Supporting my observations, Ding, et al. (2008) also showed a role of NorB in bacterial survival in a mouse skin abscess model [126].

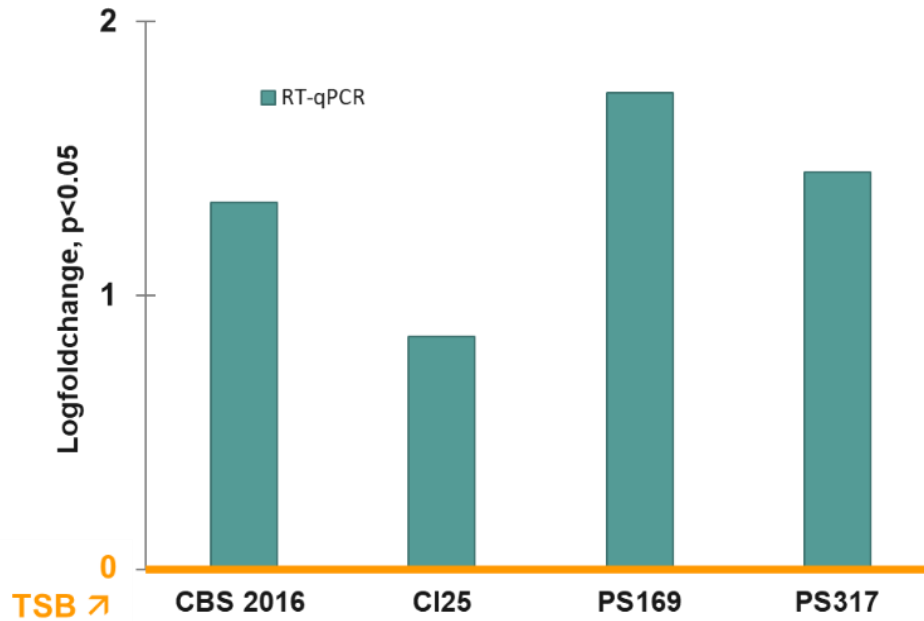


Figure 19 – RT-qPCR of *norB* expression in PCs compared to TSB (yellow line). Relative expression of *norB* in transfusion-relevant *Staphylococcus aureus* strains [CBS: CBS2016-05, CI25: CI/BAC/25/13/W; PS169: PS/BAC/169/17/W and PS317: PS/BAC/317/16/W] cultured in platelet concentrates (PCs) compared to trypticase soy broth (TSB). TSB is the baseline (yellow line). Gene expression levels were normalized to the housekeeping gene (16S RNA) and calculated using the $\Delta\Delta C_t$ method. Bars represent mean fold change from three pooled replicates. Expression of *norB* in PCs versus TSB was significantly different ($p < 0.05$). Figure retrieved from paper by Paredes et al (2025) ^[1], copyrights approval to reproduce the figure available in page xv.

3.2.2 Mutagenesis and overexpression of *Staphylococcus aureus norB*

3.2.2.1 Deletion of *norB* via CRISPR-Cas9 technology

Based on the transcriptome results, *S. aureus* PS/BAC/169/17/W was selected for downstream studies and construction of a *norB* deletion mutant using a CRISPR-Cas9 protocol. Table 14 & shows the steps of the mutation process and results. Efforts to generate a deletion of the *norB* gene in *S. aureus* PS/BAC/169/17/W were unsuccessful.

This outcome indicates a potential failure that may be due to Cas9-induced toxicity, inefficient delivery of the CRISPR components, inadequate repair of the DNA double-strand breaks and off-target effects [217]. Studies have demonstrated that the Cas9 enzyme can induce toxicity resulting in impaired cell growth and cell death, limiting the applications of the CRISPR-Cas9 system. Inefficient delivery of both the Cas9 enzyme and the guide RNA (gRNA) to the target cells reduces efficient and specific resulting limited loading capacity and lack the ability to integrate into the genome. Failure to repair of DNA double-strand breaks after Cas9 activity leading to unintended mutations or genomic instability. CRISPR-Cas9 can also induce mutations at unintended locations in the genome, known as off-target effects, additionally the Cas9 can cut the plasmid impairing the process [218]. Plasmid incompatibility was assessed to determine if pCasSA can coexist with the 2.7 Kb plasmid carried by *S. aureus* PS/BAC/1669/17W. The pCasSA vector belongs to plasmid incompatibility group A and carries a ColE1 origin of replication [205]. The sequence alignment of ColE1 against compared with the sequence the 2.7 Kb plasmid of *S. aureus* PS/BAC/1669/17W revealed no homology. Additionally, the presence of incompatibility groups in both plasmids was investigated using the bioinformatic tool "PlasmidFinder (v2.1)". This analysis revealed the absence of incompatibility groups in the PS/BAC/169/17W plasmid and the presence of the repUS16 incompatibility group in pCasSA. These results indicate that there are no overlapping regions between the origin of replication and incompatibility groups between the two plasmids, and therefore both could co-exist in *S. aureus*. This helped in part rule out this issue as the caused for the failed transformation during my mutagenesis assays.

Table 14 – Steps of CRISPR-Cas9 protocol to obtain a *norB* mutant in *Staphylococcus aureus* PS/BAC/169/17/W.

CRISPR-Cas9 protocol	Steps
1. Cloning upstream and downstream regions of <i>norB</i> into vector pCasSA resulting in plasmid “pHR” which was successfully transformed into <i>Escherichia coli</i> DC10b*	✓
2. Cloning of phosphorylated “small guided” RNA (sgRNA) into “pHR” resulting in the new plasmid “pHR-sgRNA”, which was again transformed into <i>E. coli</i> DC10b*	✓
3. Electroporation of <i>S. aureus</i> RN4220* with plasmid pHR-sgRNA isolated from <i>E. coli</i> DC10b, which was confirmed by colony PCR	✓ (Figure 20)
4. Electroporation of <i>S. aureus</i> PS/BAC/169/17/W with plasmid pHR-sgRNA isolated from <i>S. aureus</i> RN4220	✗

Steps achieved (✓) and unachieved (✗).

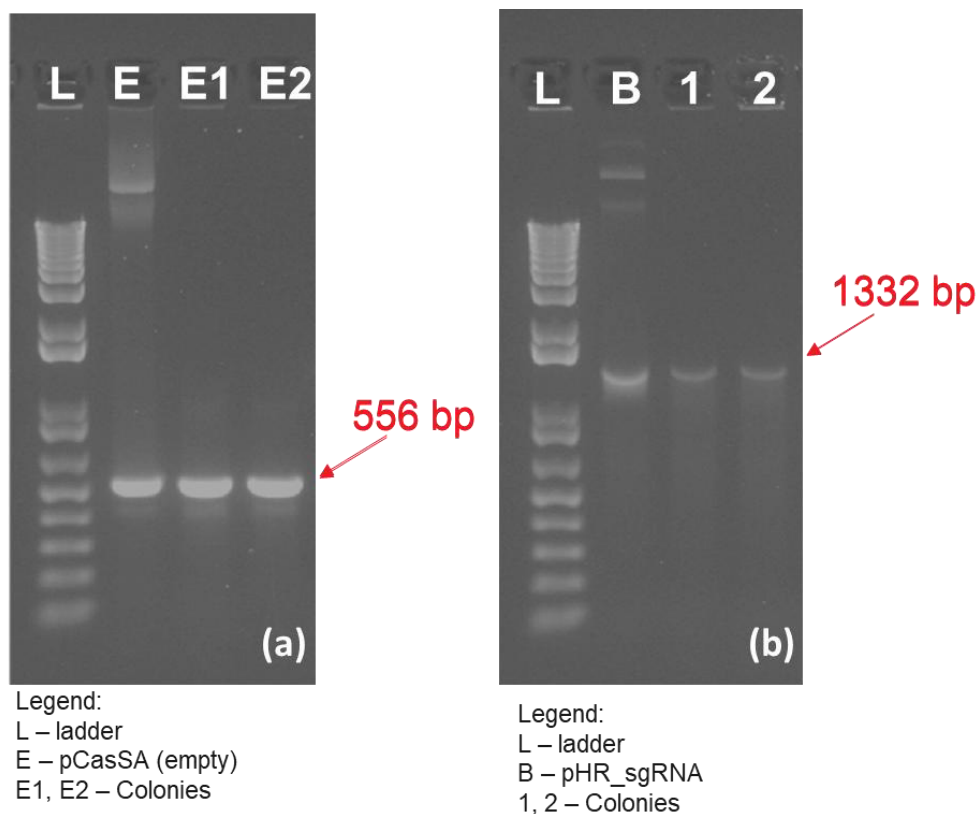


Figure 20 – Electroporation of *Staphylococcus aureus* RN4220 (CRISPR-Cas9). (a) Colony PCR of *S. aureus* RN4220 transformed with the empty pCasSA vector: (Table 14), (b) Colony PCR of *S. aureus* RN4220 transformed with plasmid pHR-sgRNA (Table 14).

3.2.2.2 Deletion of *norB* via allelic exchange recombination

Allelic exchange was attempted using the low-copy, temperature sensitive plasmid pIMAY to generate a *norB* deletion mutant, which was also unsuccessful as shown in the step-by-step description of Table 15. This failure may be attributed to low homologous recombination (i.e., the ability to repair DNA double-strand breaks using the homologous recombination repair pathway may be compromised) ^[219], or insufficient expression of the recombinase machinery as expression of recombinases that play a crucial role in homologous recombination and DNA repair ^[220].

Table 15 – Steps of allelic recombination exchange protocol to obtain a *norB* mutant in *Staphylococcus aureus* RN6390.

Allelic exchange protocol	Steps
1. Cloning upstream and downstream regions of <i>norB</i> into the plasmid pIMAY (pIMAY_HR) which was successfully transformed into <i>Escherichia coli</i> DC10b	✓
2. Electroporation of <i>S. aureus</i> RN4220 with plasmid pIMAY_HR isolated from <i>E. coli</i> DC10b, which was confirmed by colony PCR	✓ (Figure 21)
3. Electroporation of <i>S. aureus</i> RN6390 with plasmid pIMAY_HR isolated from <i>S. aureus</i> RN4220	✗

Steps achieved (✓) and unachieved (✗).

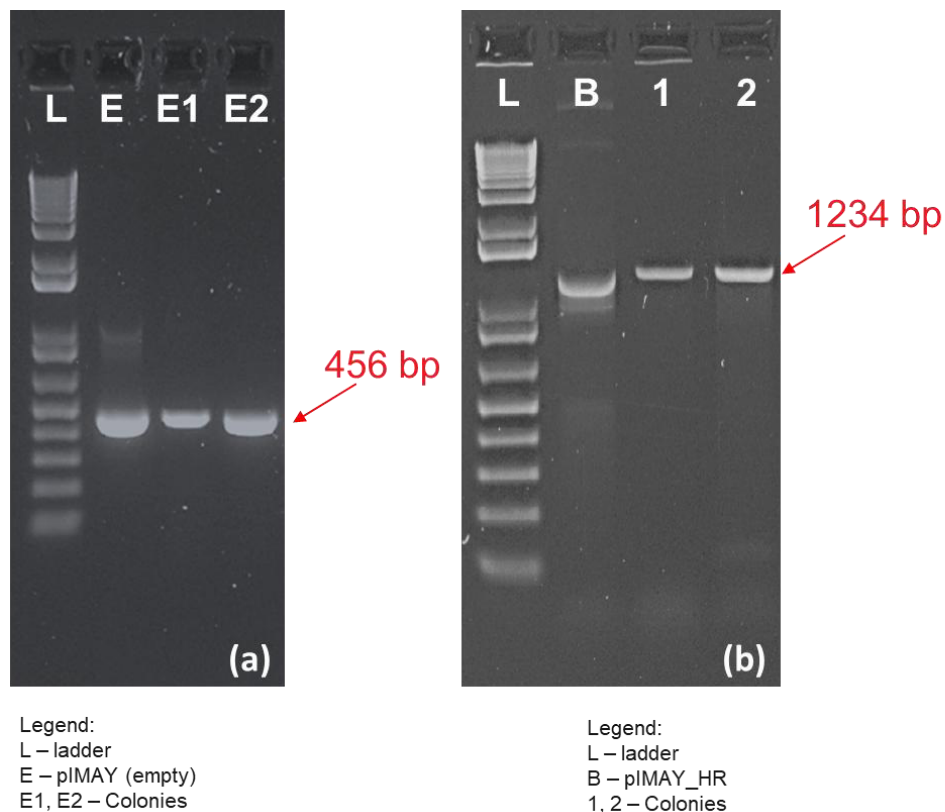


Figure 21 – Electroporation of *Staphylococcus aureus* RN4220 (Allelic Exchange). (a) Colony PCR of *S. aureus* RN4220 transformed with the empty pIMAY vector: (Table 15), (b) Colony PCR of *S. aureus* RN4220 transformed with plasmid pIMAY_HR (Table 15).

3.2.2.3 Overexpression of the *norB* gene in *Staphylococcus aureus*

Overexpression of *norB* in *S. aureus* was also attempted as an alternative to mutagenesis to study the function of NorB in quinolone resistance (Table 16). I constructed plasmid the pSK::*norBp*, which carries *norB* and its promoter from TRS CBS2016-05. This plasmid was successfully transformed into *S. aureus* RN4220. However, despite multiple attempts, electroporation of *S. aureus* CBS 2016-05 with pSK::*norBp* isolated from *S. aureus* RN4220 was unsuccessful. This suggests that the transformation efficiency was compromised by unknown factors, which I could not identify despite troubleshooting.

Table 16 – Steps of overexpression protocol.

Overexpression protocol	Steps
1. Cloning the <i>norB</i> gene and promoter into vector pSK5632 resulting in plasmid pSK:: <i>norBp</i> which was successfully transformed into <i>E. coli</i> DC10b	✓
2. Electroporation of <i>S. aureus</i> RN4220 with plasmid pSK:: <i>norBp</i> isolated from <i>E. coli</i> DC10b, which was confirmed by colony PCR	✓ (Figure 22)
3. Electroporation of <i>S. aureus</i> CBS2016-05 with plasmid pSK:: <i>norBp</i> isolated from <i>S. aureus</i> RN4220	✗

Steps achieved (✓) and unachieved (✗).

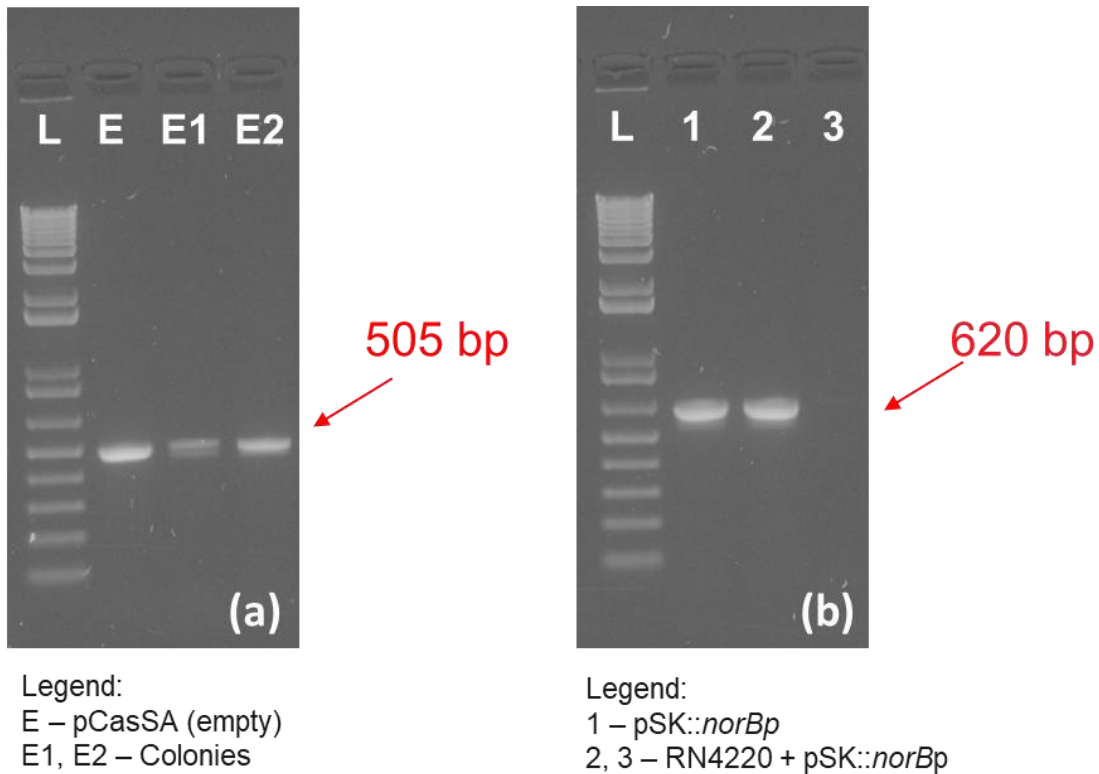


Figure 22 – Electroporation of *Staphylococcus aureus* RN4220 (Overexpression). (a) Colony PCR of *S. aureus* RN4220 transformed with the empty pSK5632 vector: (Table 16), (b) Colony PCR of *S. aureus* RN4220 transformed with plasmid pSK::*norBp* (Table 16).

3.2.2.4 *norB* expression in non-transfusion relevant strains of *Staphylococcus aureus*

As deleting and overexpressing *norB* in TRS proved challenging, functional assays were conducted with *S. aureus* RN6390, RN6390 Δ *norB* and RN6390 Δ *mgrA*. These isolates provide a genetic background of interest to study the function of *norB*: wild type RN6390, RN6390 Δ *norB* (deletion of the *norB* gene), and RN6390 Δ *mgrA* (overexpression of *norB*). Interestingly, RT-qPCR showed that expression of all three genes, *norA*, *norB*, and *norC*, was increased (one to six-fold) in *S. aureus* RN6390 when this strain was grown in PCs and expression of both *norA* and *norC* genes was enhanced in PC cultures of the *norB*

mutant (Figure 23). Unexpectedly, only *norB* was upregulated in the *mgrA* mutant despite that the global regulator *MgrA* represses expression of all three *nor* genes.

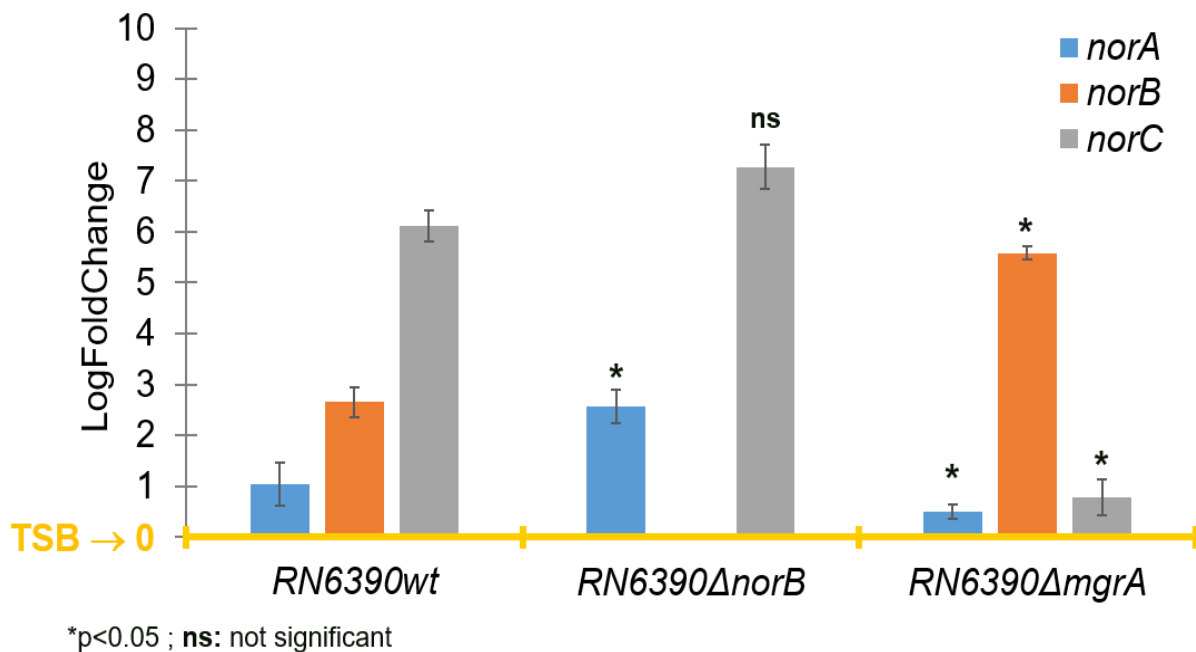


Figure 23 – Expression of efflux pumps genes *norA*, *norB*, and *norC* measured by RT-qPCR. Relative expression of *norA*, *norB*, and *norC* in *Staphylococcus aureus* RN6390 and its deletion mutants *norB* and *mgrA* cultured in platelet concentrates (PCs) compared to trypticase soy broth (TSB). TSB is the baseline (yellow line). Gene expression levels were normalized to the housekeeping gene 16SRNA and calculated using the $\Delta\Delta C_t$ method. Bars represent mean fold-change \pm standard deviation from three biological replicates. Statistical significance was determined by one-way ANOVA, * $p < 0.05$; ns: not significant. Figure retrieved from paper by Paredes et al (2025) ^[1], copyrights approval to reproduce the figure available in page xv.

3.3 Quinolone resistance assays of *Staphylococcus aureus* grown in media and PCs

In Canada, quinolones ciprofloxacin and norfloxacin are included as part of the treatment regimen for infections caused by *S. aureus* [221]. Therefore, these antibiotics were chosen to test quinolone resistance in PC-grown *S. aureus*. MIC and MBC assays for both antibiotics were determined for the four TRSs, *S. aureus* RN6390, RN6390 Δ *norB*, RN6390 Δ *mgrA*, and control *S. aureus* ATCC 29213.

3.3.1 MIC of ciprofloxacin and norfloxacin

The MIC of ciprofloxacin and norfloxacin were determined against the TRSs and *S. aureus* RN6390, RN6390 Δ *norB*, RN6390 Δ *mgrA* using the broth microdilution method (Table 17). The ATCC 29213 served as control strain. Ciprofloxacin exhibited a MIC ranging from 0.125 μ g/mL to 1 μ g/mL for all isolates while norfloxacin showed variable MICs among the isolates, ranging from 0.25 μ g/mL - 4 μ g/mL. As per classification of antibiotic resistance in the Clinical & Laboratory Standards Institute (CLSI) [146], all strains were sensitive to both quinolones.

Table 17 – Minimal Inhibitory Concentration (MIC) of ciprofloxacin and norfloxacin in *Staphylococcus aureus* grown in Mueller Hinton (n≥3) [209]. Table retrieved from paper by Paredes et al (2025), copyrights approval to reproduce the table available in page xv. Sensitive (S) [146]

<i>S. aureus</i> strains	Ciprofloxacin		Norfloxacin	
	µg/mL	S£1 µg/ml R≥4 µg/ml	µg/mL	S£4µg/ml R≥16 µg/ml
ATCC 29213 (Control)	0.125 – 0.5	S	1 – 2	S
CBS 2016-05	0.25 – 0.5	S	0.5	S
CI/BAC/25/13/W	0.5 – 1	S	2 – 4	S
PS/BAC/169/17/W	0.5 – 1	S	0.5 – 2	S
PS/BAC/317/16/W	0.5 – 1	S	0.25 – 1	S
RN6390	0.125 – 0.5	S	0.5 – 2	S
RN6390Δ <i>norB</i>	0.125 – 0.5	S	0.25 – 0.5	S
RN6390Δ <i>mgrA</i>	0.125 – 0.5	S	0.5 – 1	S

3.3.2 MBC of ciprofloxacin and norfloxacin

For MBC assays, all strains were cultured in PCs and TSB. MBC values in TSB were comparable to MIC results (Table 18 and Table 17, respectively). The MBC data showed a clear and consistent pattern in which all *S. aureus* strains exhibit an increase in ciprofloxacin and norfloxacin MBCs in PCs compared to TSB cultures, demonstrating that the PC environment triggers quinolone resistance in *S. aureus*. The ATCC 29213 strain served as control with known fluoroquinolone susceptibility, the MBC increase in this isolate grown in PCs validates that the increase in the resistance to ciprofloxacin and norfloxacin is due to the PC storage environment and not due to strain genetic variability. The MBC results for both quinolones were higher in PC-grown bacteria compared to TSB cultures reaching a significant difference for ciprofloxacin ($p < 0.05$) in all strains tested

except *S. aureus* PS/BAC/317/16/W, which was marginally different ($p = 0.057$) (Table 18).

Table 18 – Minimal Bactericidal Concentration (MBC) of ciprofloxacin and norfloxacin in *Staphylococcus aureus* grown in TSB and PCs, and statistical comparison ($n > 3$). Table retrieved from paper by Paredes et al (2025) [1], copyrights approval to reproduce the table available in page xv.

Strains	Ciprofloxacin ($\mu\text{g/mL}$)			Norfloxacin ($\mu\text{g/mL}$)		
	TSB	PCs	p Value	TSB	PCs	p Value
			(PCs vs. TSB)			(PCs vs. TSB)
ATCC 29213	0.25–2	16–64	<0.0001	1	2–128	<0.0001
CBS2016-05	0.5–1	1–8	0.0478	1–2	4–8	$p > 0.05$
CI/BAC/25/13/W	0.5–2	2–8	0.0303	1–4	1–4	$p > 0.05$
PS/BAC/169/17/W	1–8	8–32	0.0002	1–4	8–128	0.0571
PS/BAC/317/16/W	0.5–2	1–16	0.0571	1–2	1–16	$p > 0.05$
RN6390	0.125–1	0.5–16	<0.0001	1	1–16	<0.0001
RN6390 Δ <i>norB</i>	0.125– 0.5	0.5–4	<0.0001	0.5	1–8	<0.0001
RN6390 Δ <i>mgrA</i>	0.5–1	2–16	<0.0001	0.25–1	2–32	<0.0001
Comparison between (RN6390 “wild type” and deletion mutant isolates)						
Mann–Whitney U test						
Ciprofloxacin		p value	Norfloxacin		p value	
WT vs. Δ <i>norB</i> (PCs)		0.6501	WT vs. Δ <i>norB</i> (PCs)		0.2720	
WT vs. Δ <i>mgrA</i> (PCs)		0.0002	WT vs. Δ <i>mgrA</i> (PCs)		0.0011	

Importantly, MBC values of ciprofloxacin and norfloxacin in wild-type *S. aureus* RN6390 and RN6390 Δ *norB* grown in PCs were not significantly different ($p = 0.065$ and $p = 0.27$, respectively, Table 18) indicating that *norA* and *norC*, which are upregulated in the *norB* mutant (Figure 23) are activated in response to PC-associated stresses, may confer resistance to these quinolones in a *norB* negative background. However, significantly higher resistance to ciprofloxacin and norfloxacin in *S. aureus* RN6390 Δ *mgrA* compared

to the wild-type strain ($p = 0.0002$ and $p = 0.0011$, respectively; Table 18) was likely due mostly to the overexpression of *norB* and not to the overexpression of *norA* or *norC* (Figure 23).

3.4 *Staphylococcus aureus* virulence studies using a *Bombyx mori* model

3.4.1 NorB involvement in increased proliferation of *Staphylococcus aureus* in PCs

It has been shown that the PC storage environment enhances the virulence of transfusion-relevant *S. aureus* CBS2016-05 and that overexpression of NorB increases *S. aureus* survival in a mouse abscess model [126,159]. With this information, I hypothesized that NorB could be involved in increased growth in PCs and enhanced virulence of *S. aureus*.

Data shown in Figure 13A and Table 19 suggest faster growth of the wild-type RN6390 strain compared to RN6390 Δ *norB* and RN6390 Δ *mgrA* in TSB indicating that either lack of expression or overexpression of *norB* could impair growth in media. These results differ from the data obtained in PCs, in which the growth curves for the three strains overlap (Figure 13B).

3.4.2 NorB involvement in virulence of *Staphylococcus aureus*

In virulence studies using animal models, lethal dose (LD₅₀) values indicate the bacterial load needed to kill 50% of the population. In this study, three groups of 10 *B. mori* larvae per bacterial isolate (*S. aureus* RN6390, RN6390Δ*norB* and RN6390Δ*mgrA*) were injected with 10-fold bacterial suspensions to determine the bacterial load that kills 50% of each group. LD₅₀ studies in *B. mori* larvae showed that the *S. aureus* RN6390Δ*norB* had a higher LD₅₀ than the wild-type strain. Two-log more of *S. aureus* RN6390Δ*norB* were needed to kill 50% of larvae compared to wild-type *S. aureus* RN6390, indicating a decrease in the virulence of the mutant strain although no statistical significance was attained ($p > 0.05$) (Table 19). This provides novel evidence of the role of NorB in *S. aureus* virulence. As *norB* is overexpressed in the *S. aureus mgrA* mutant (Figure 23), it was expected to observe increased virulence of this mutant compared to the wild-type strain. However, LD₅₀ values of the *mgrA* mutant were higher than those of the wild-type strain.

Table 19 – LD50 results for wild type and mutants *norB* and *mgrA* *Staphylococcus aureus* strains in a silkworm animal model (n = 3, Student t-test p > 0.05). Table retrieved from paper by Paredes et al (2025) ^[1], copyrights approval to reproduce the table available in page xv.

<i>S. aureus</i> Isolates	LD₅₀ (Per Larvae)
RN6390 “wild type” (WT)	~1.02 × 10 ⁴ CFU (±1.01 × 10 ⁴)
RN6390Δ <i>norB</i>	~3.29 × 10 ⁶ CFU (±2.04 × 10 ⁶)
RN6390Δ <i>mgrA</i>	~2.85 × 10 ⁵ CFU (±1.90 × 10 ⁵)
Comparison between strains	
T-test with Welch’s correction (p value)	
WT vs. Δ <i>norB</i>	0.1518
WT vs. Δ <i>mgrA</i>	0.1773

3.4.3 Virulence assays in PC- versus TSB-derived *Staphylococcus aureus*

To determine the impact of the PC storage environment in *S. aureus* virulence driven by NorB, wild type *S. aureus* RN6390, RN6390Δ*norB* and RN6390Δ*mgrA* were grown in PCs and TSB. Bacterial suspensions were then adjusted to their respective LD₅₀ values and inoculated in silkworms to perform comparative killing assays. Results are shown in Figure 24.

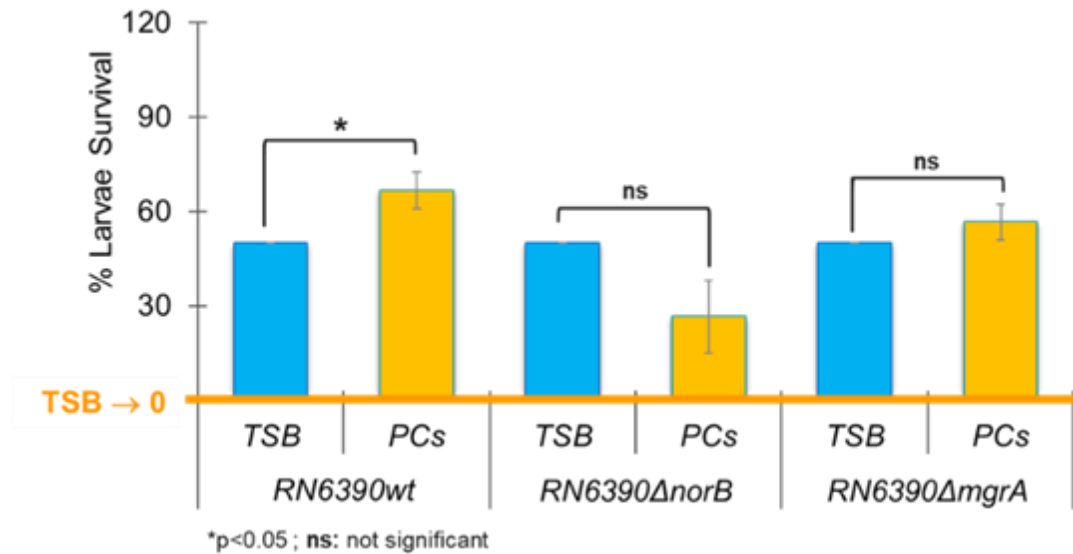


Figure 24 – Comparison of silkworm larvae survival after inoculation with *Staphylococcus aureus* derived from TSB and PCs. Silkworm larvae survival rates (%) in the presence of *S. aureus* RN6390 and deletion mutants *norB* and *mgrA*. Assays were performed using three independent PC units, tested on groups of ten larvae. Statistical analysis was performed using t-student test, $p < 0.05$; ns: not significant, $n = 3$.

Data previously obtained in the Ramirez' laboratory with the TRS CBS2016-05, showed significant increased virulence of PC-grown *S. aureus* CBS2016-05 compared to TSB-derived cultures [159]. Unexpectedly, in my assays, wild-type RN6390 and RN6390Δ*mgrA* showed reduced virulence when the isolates were grown in PCs compared to TSB cultures while the *norB* mutant grown in PCs demonstrated increased virulence compared to TSB-grown bacteria although no significance was attained (Figure 24).

4. Discussion

As a disclaimer, part of the discussion presented in this chapter has been published in the journal *Antibiotics* (MDPI), in which I am the first author ^[1]. Dr. Sandra Ramirez-Arcos was involved in data analysis, interpretation and discussion, and in editing the published manuscript.

PC storage at room temperature under agitation safeguards platelet functionality, which is critical for therapeutic efficacy. Unfortunately, these conditions are amenable for growth of most bacterial contaminants introduced during venipuncture ^[222]. Storage of PCs is limited to a maximum of seven days to minimize the platelet storage lesion (PSL), which encompasses a series of morphological and metabolic changes that platelets undergo as a result of an increase in lactate levels, with consequential decrease in pH, loss of surface membrane glycoproteins and reduced aggregation response ^[49,223]. A study by Yousuf et al, showed that *S. aureus* proliferation to clinically significant levels in PCs enhances the PSL ^[67]. Importantly, changes in the PC storage environment not only affects platelet metabolism but also impacts gene expression of bacterial contaminants. Immune stressors released by activated platelets during PC storage trigger differential expression of virulence genes such as those involve in biofilm formation and antimicrobial resistance in *S. aureus* and *S. epidermidis* ^[67,92,213]. Furthermore, gene expression studies conducted in the Ramirez' laboratory with *S. epidermidis* showed that antimicrobial resistance genes were upregulated and virulence was increased when the bacterium was grown in PCs versus TSB ^[213,224]. Therefore, I developed a series of experiments to test

whether the PC storage environment enhances antimicrobial resistance and virulence of *S. aureus*.

4.1. Role of NorB in quinolone resistance in *Staphylococcus aureus*

S. aureus is the predominant PC contaminant involved in septic transfusion reactions worldwide [39]. During my project, I performed comparative transcriptome analyses of four transfusion relevant strains grown in TSB and PCs with focus on genes involved in antibiotic resistance. Data from this analysis revealed differential expression of genes involved in resistance mechanisms to antibiotics, particularly the *norB* gene, which was upregulated in all strains. As *norB* encodes for the efflux pump NorB, which is involved in *S. aureus* resistance to quinolones such as ciprofloxacin and norfloxacin, I performed MBC assays for these antibiotics of the transfusion relevant strains grown in TSB and PCs showing increased resistance to the quinolones in PC-grown bacteria compared to TSB cultures. These results strongly suggested that NorB might be involved in quinolone resistance when *S. aureus* is grown in PCs. To confirm these data, MBC of ciprofloxacin and norfloxacin and RT-qPCR assays were performed with the non-transfusion relevant strains *S. aureus* RN6390 and its derivative *norB* and *mgrA* mutants. Data from those experiments indicated that not only NorB but potentially the efflux pumps NorA and NorC were also involved in the observed quinolone resistance.

Previous studies have shown that overexpression of *S. aureus norA* is directly related to increased resistance to ciprofloxacin [132,137,225]. Nevertheless, our results should be

analyzed with caution as *S. aureus* RN6390 lacks the RsbU phosphatase ^[190], which is involved in dephosphorylation of the global regulator MgrA ^[132]. It is intriguing to investigate whether other phosphatases (bacterial or platelet-derived) can change the phosphorylation status of MgrA and consequent expression of *nor* genes as repression of *norA* and *norB* depends on the phosphorylation state of MgrA ^[136]. Phosphorylated MgrA loses its ability to bind (repress) the *norA* promoter resulting in increased quinolone resistance ^[137]. Truong-Bolduc et al have shown that overexpression of the Serine/Threonine kinase gene *pknB*, which is involved in phosphorylation of MgrA, results in increased resistance of norfloxacin and ciprofloxacin in *S. aureus* RN6390 ^[132]. The quinolone resistance results presented herein are likely the consequence of complex interactive regulatory processes that merit further investigation.

Other potential mechanisms involved in quinolone resistance could be mutations in the *gyrA/B* and *parC/E* genes. A study from Solano-Galvez, et al (2021) ^[226], showed that genomic modification in these genes can result in the resistance to quinolones. Protein alignment of GyrA/B and ParC/E (Appendix A5) shows variation in amino acid residues among the TRS and RN6390 strain in comparison with the consensus sequence which merits further investigation to understand the impact of these sequence differences in quinolone resistance.

4.2. Role of NorB in growth of *Staphylococcus aureus* in PCs

S. aureus is a versatile pathogen that can adapt to different environments; the PC storage provides a harsh niche that triggers differential gene expression in bacteria to overcome

platelet-derived antimicrobial proteins and reduction of nutrients. The Ramirez lab has shown different patterns of bacterial growth in PCs compared to media particularly for *Staphylococcus* spp. For instance, Hamza, A. et al (2012) [227] and Taha, M. et al (2018) [228], have shown that coagulase negative staphylococci are able to grow in PCs at a lower growth rate compared to laboratory media, with marked differences between species and between isolates of the same species. Consistent to these previous data, my growth kinetics results of *S. aureus* grown under optimal conditions (TSB) versus PCs revealed a reduced growth rate in PCs. *S. aureus* growth rate in the PC bags is limited due to the harsh storage environment. Slow growth rates in PCs demonstrate that nutritional and immune challenges (e.g., antimicrobial peptides) reduce the rate of bacterial proliferation. Additionally, an increase in the concentration of host immune factors released by platelets due to PSL may contribute to the slower growth rates of *S. aureus* in PCs [67].

Interestingly, Chi, S. I. et al (2023) [92] have shown that staphylococcal enterotoxins impair growth of transfusion relevant *S. aureus* CBS 2016-05. I therefore investigated whether another virulence factor, the efflux pump NorB, affected growth to *S. aureus* in PCs as this protein has been shown to confer advantageous growth of *S. aureus* in skin abscesses [126]. My data showed overlapping growth curves of wild-type *S. aureus* RN6390 and its *norB* and *mgrA* mutants during PC storage. It is therefore not obvious that NorB alone confers advantageous proliferation of *S. aureus* in PCs.

It is important to acknowledge one caveat to these findings related to bacterial aggregation particularly in PCs, where multiple cells can adhere to form clumps that may underestimate colony counts. Despite this limitation, the data obtained from growth curve

assays remain robust due to reproducibility in the three independent replicates (Figures 12 and 13).

4.3. Role of NorB in virulence of *Staphylococcus aureus*

As shown in my genomic analysis, *S. aureus* comprises several virulence factors including exotoxins, immune evasion factors, and membrane proteins that facilitate bacterial infection, making this bacterium a major threat for PC recipients. Previous virulence studies from the Ramirez' lab with *S. epidermidis* using the nematode *C. elegans* animal model showed enhanced virulence in PC-grown bacteria in comparison to TSB cultures [224]. Similarly, it has been recently shown that the virulence of the transfusion relevant strain *S. aureus* CBS2016-05 is enhanced when grown in PCs compared to media using a *B. mori* animal model [159].

Since overexpression of NorB confers advantageous survival of *S. aureus* in skin abscesses [126]. I therefore decided to adapt a *B. mori* animal model optimized in our lab to study the role of NorB in virulence of *S. aureus*. My data showed a 2-log higher LD₅₀ for the *S. aureus norB* mutant compared to wild type *S. aureus* RN6390 indicating loss of virulence. Preliminary comparative studies in PCs vs TSB were inconclusive as the three strains grown in TSB showed 50% larvae mortality in each of three repetitions, which is statistically improbable and merits further assays.

It is important to recognise that the *rsbU* negative background of the RN6390 strains may have contributed to the virulence results obtained in silkworms which warrants more extensive studies using different *S. aureus* strains, animal models or cell cultures

[46,164,229]]. As RsbU has a major role in the SigB regulon, it is also critical to consider how the expression of other virulence factors driven by SigB played a role in the virulence results presented herein.

The overexpression of the NorB efflux pump in *S. aureus* results in increased survival and growth in a mouse abscess model [126], suggesting that this efflux pump may be involved in extrusion of host-derived antimicrobial factors. It is therefore possible that NorB is involved in extrusion of platelet-derived antimicrobial peptides in *S. aureus*-contaminated PCs. Furthermore, I propose that NorB is involved in a bacterial mechanism of defense by excreting antimicrobial peptides produced by silkworm larvae during infection as shown for other efflux pumps in *P. aeruginosa* [230].

It would therefore be interesting to investigate how expression of *norB* in a *rsbU*⁺ background influences virulence in silkworms as overexpression of *sigB* has been associated with in vitro resistance to antimicrobial peptides produced by nematodes in *S. aureus* [172]. This can be studied by performing comparative assays between *S. aureus* RN6390 and a *rsbU*⁺ strain such as *S. aureus* SH1000. This strain is ideal because SH1000 and RN6390 are isogenic; both are derived from *S. aureus* NCTC 8325 which harbors an 11-bp deletion in *rsbU* that was restored in the SH1000 strain [231].

The selection of a model to investigate the virulence of *S. aureus* grown in PCs, for instance when choosing between *B. mori* and a murine model, should be based on the aim of the experiment, model complexity (physiological and genetic similarities to humans), and practical considerations like ethics, cost and availability. The silkworm model was chosen to my project based on previous experience and availability of the larvae and protocols in our lab. Moreover, the silkworm innate immune response closely

reflects mammalian innate immune response and is an efficient, ethical, and low-cost tool to investigate basic virulence bacterial profiles [167,178]. Nonetheless, the lack of platelets in the silkworm hemolymph, the complex coagulation cascade, and adaptive immunity limit the applicability of this model [232]. Conversely, the mammal murine model is widely chosen as a model organism, as it comprises a full physiological system, including platelets [164]. Thus, this model has been previously used by other groups in the study the *S. aureus*' role in septic shock, resistance to mammalian immune clearance, and tissue infections like kidney abscesses [233–236]. Ultimately, my findings using silkworm larvae provide valid preliminary information that could be confirmed in a murine system.

5. Concluding Remarks

My studies aimed to investigate the impact of the PC storage environment on *S. aureus* transcriptional changes with a focus on genes involved in antibiotic resistance and virulence. Findings of this study demonstrate that the PC storage environment triggers *S. aureus* resistance to quinolones and upregulation of *nor* efflux pump genes in a strain-dependent manner. Additionally, I showed evidence of the potential role of NorB in *S. aureus* virulence using a silkworm model. My findings highlight the need to deepen our knowledge on the molecular mechanisms involved in resistance to antibiotics and virulence when bacteria proliferate in PCs. The increase of antibiotic resistance and bacterial virulence are a major concern worldwide. My work provides scientific insights that can add in the development of new rapid treatment drugs, or exploring non-antibiotic adjuvant therapies, such as efflux pump inhibitors, to restore antibiotic efficacy and improve patient outcomes. This is particularly important in the clinical setting to select antibiotics for the optimal treatment of patients suffering from transfusion-associated bacterial infections. Adding antibiotics to PCs is not viable due to ethical and regulatory considerations of transfusable PCs, which are considered a biological product. However, my research informs researchers and clinicians to develop novel therapies as described above. Overall, I have generated novel information advancing knowledge on platelet-*S. aureus* interaction in the unique PC storage environment opening avenues for future studies that can contribute with knowledge in the prevention of septic transfusion reactions involving contaminated PCs.

6. Future work

While my doctoral studies have provided valuable insights in the impact of the PC storage environment in *S. aureus* antibiotic resistance and virulence, several questions remain open for further exploration. Suggestions for future work that could build upon and extend the findings of my research studies are listed below.

- 1. Regulation of *nor* genes in a *mgrA* mutant may be driven by other regulators such as NorG.** Transcriptome and/or RT-qPCR could be used to confirm whether other regulators including NorG are upregulated in a *mgrA* mutant strain. These experiments could be complemented by the creation of a double $\Delta norG\Delta mgrA$ mutant and analyzing *nor* gene expression in this background.
- 2. Comparison of virulence studies between *rsbU*- and isogenic *rsbU*+ strains to investigate the role of NorB in virulence with a functional SigB regulon.** Comparative transcriptome and/or RT-qPCR analyses could be used to analyze the expression of *nor* genes in a functional SigB regulon compared to a deficient SigB regulon as the one used in my studies.
- 3. Investigating if NorB has a role in exporting antimicrobial peptides produced by activated platelets during PC storage to complement the role of this efflux pump in increased quinolone resistance.** Platelet-produced antimicrobial peptides could be tested with minimal inhibitory concentration assays using strains with different genetic backgrounds (e.g., wild type, $\Delta norB$ and $\Delta mgrA$) to assess the role of Nor efflux pumps in the survival and resistance to antimicrobial factors produced by activated platelets during PC storage.

7. Appendices

Figures

Appendix A1 – Supplementary information for Chapter 2 and 3

Figure 1A – *norB* primers efficiency for the TRS (CBS2016-06; CI/BAC/25/13/W; PS/BAC/169/17/W and PS/BAC/317/16/W)

Appendix A2 – Supplementary information for Chapter 2 and 3

Figure 2A – Primer efficiency for RN6390 “wild type”, and deletion mutants RN6390 Δ *norB* and RN6390 Δ *mgrA*

Appendix A3 – Supplementary information for Chapter 3

Figure 3A - *S. aureus* isolates grown in Blood Agar (BA) and Tryptic Soy Agar (TSA) plates

Appendix A4 – Supplementary information for Chapter 3

Figure 4A - Alignment of the *rsbU* gene for TRS and *S. aureus* RN6390

Appendix A5 – Supplementary information for Chapter 3

Figure 5A – Alignment of GyrA, GyrB, ParC and ParE proteins for TRS and *S. aureus* RN6390. Consensus sequences are highlighted in green and amino acid changes are highlighted in orange

Tables

Appendix A6 – Supplementary information for Chapter 2 and 3

Table 1A – List of primer (5' → 3') used in the experiments listed in this chapter

Appendix A7 – Supplementary information for Chapter 2 and 3

Table 2A – List of plasmids used in this chapter

Appendix A8 – Supplementary information for Chapter 3

Table 3A – List of virulence genes and associated virulence factor detected in *S. aureus* (four TRS and one laboratory strain) using VFDB-VFalyzer9 data base

Appendix A9 – Supplementary information for Chapter 3

Table 4A – List regulatory systems and two component systems (TCS) involved in virulence

Appendix A10 – Supplementary information for Chapter 2 and 3

Table 5A – Global Transcriptome analysis compiling

Appendix A11 – Supplementary information for Chapter 2 and 3

Table 6A – List of genes encoding for antibiotic resistance mechanism generated using the CARD curated data

Appendix A12 – Supplementary information for Chapter 2 and 3

Table 7A – List of housekeeping genes used in the literature and differential gene expression in the transcriptome data

Appendix A1 – Supplementary information for Chapter 3

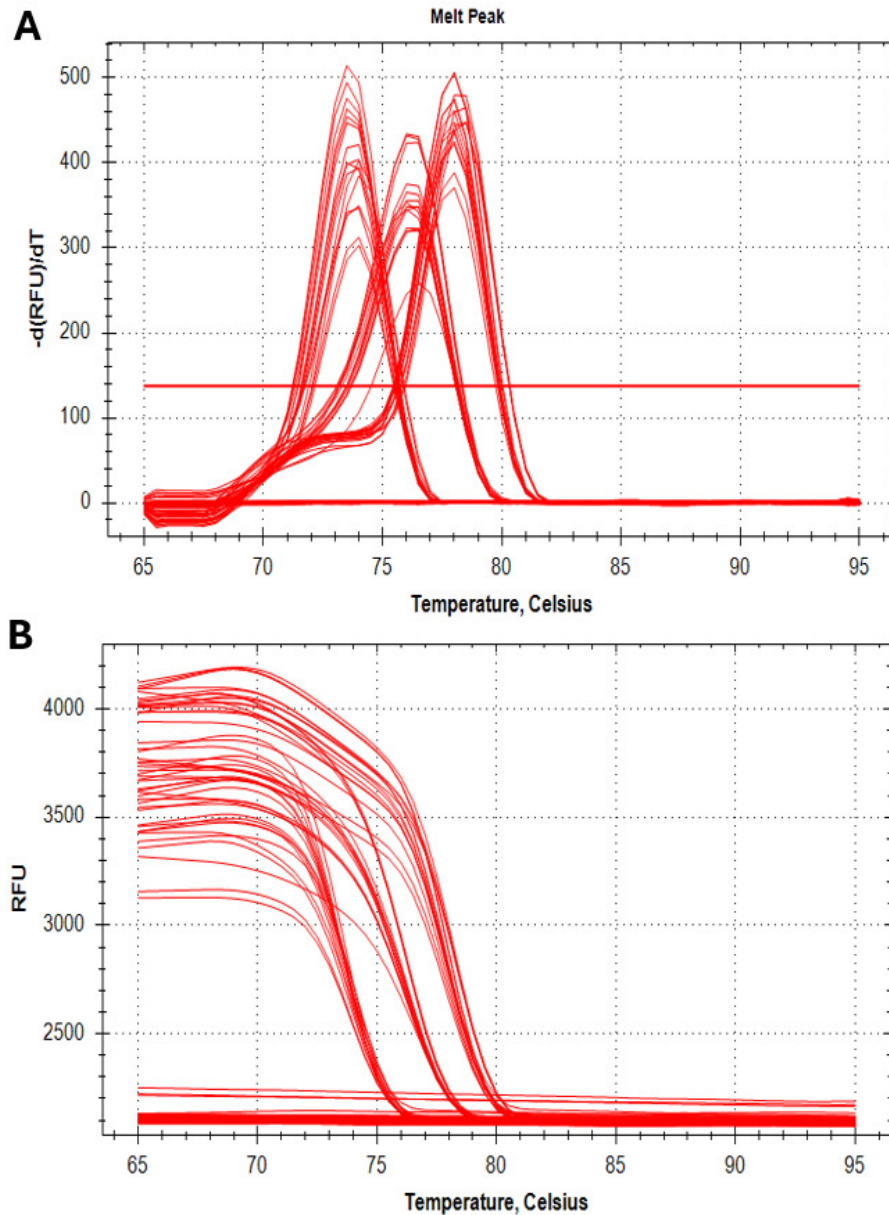


Figure 1A – *norB* primers efficiency for the TRS (CBS2016-06; CI/BAC/25/13/W; PS/BAC/169/17/W and PS/BAC/317/16/W). The Primers sets (forward and reverse) 16S rRNA, and *norB*. The graphs A and B demonstrate the reliability of the assay, indicated by the single-peak melt peaks and no peak corresponding to primer dimers or nonspecific products for the target gene or control in the melt curves, respectively. Figure retrieved from paper by Paredes et al (2025) ^[1], copyrights approval to reproduce the figure available in page xv.

Appendix A2 – Supplementary information for Chapter 3

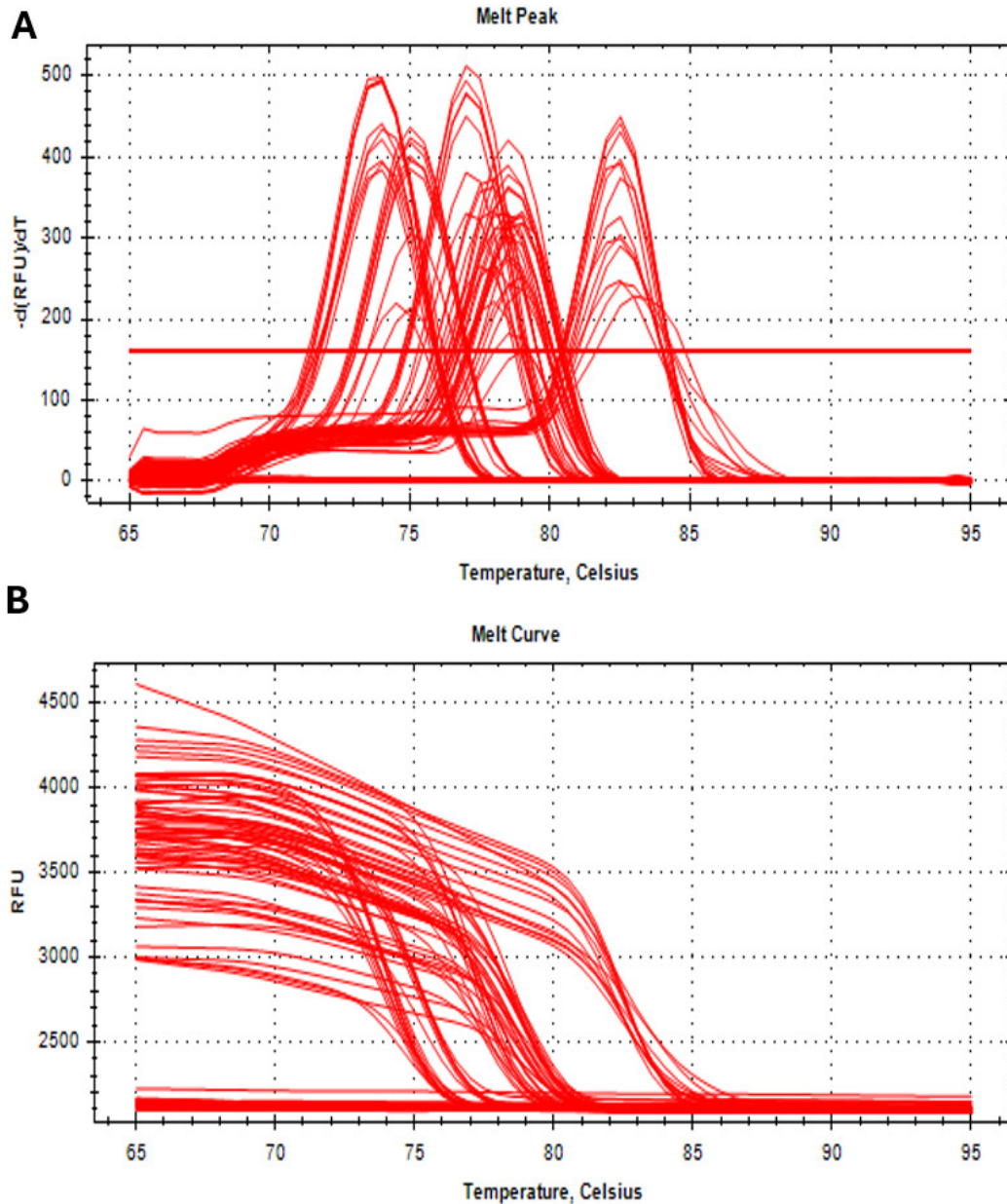


Figure 2A – Primer efficiency for RN6390 “wild type”, and deletion mutants RN6390 Δ *norB* and RN6390 Δ *mgrA*. Primers sets (forward and reverse) 16S rRNA, *norA*, *norB* and *norC*. The graphs A and B demonstrate the reliability of the assay, indicated by the single-peak melt peaks and no peak corresponding to primer dimers or nonspecific products for the target gene or control in the melt curves, respectively. Figure retrieved from paper by Paredes et al (2025) ^[1], copyrights approval to reproduce the figure available in page xv.

Appendix A3 – Supplementary information for Chapter 3

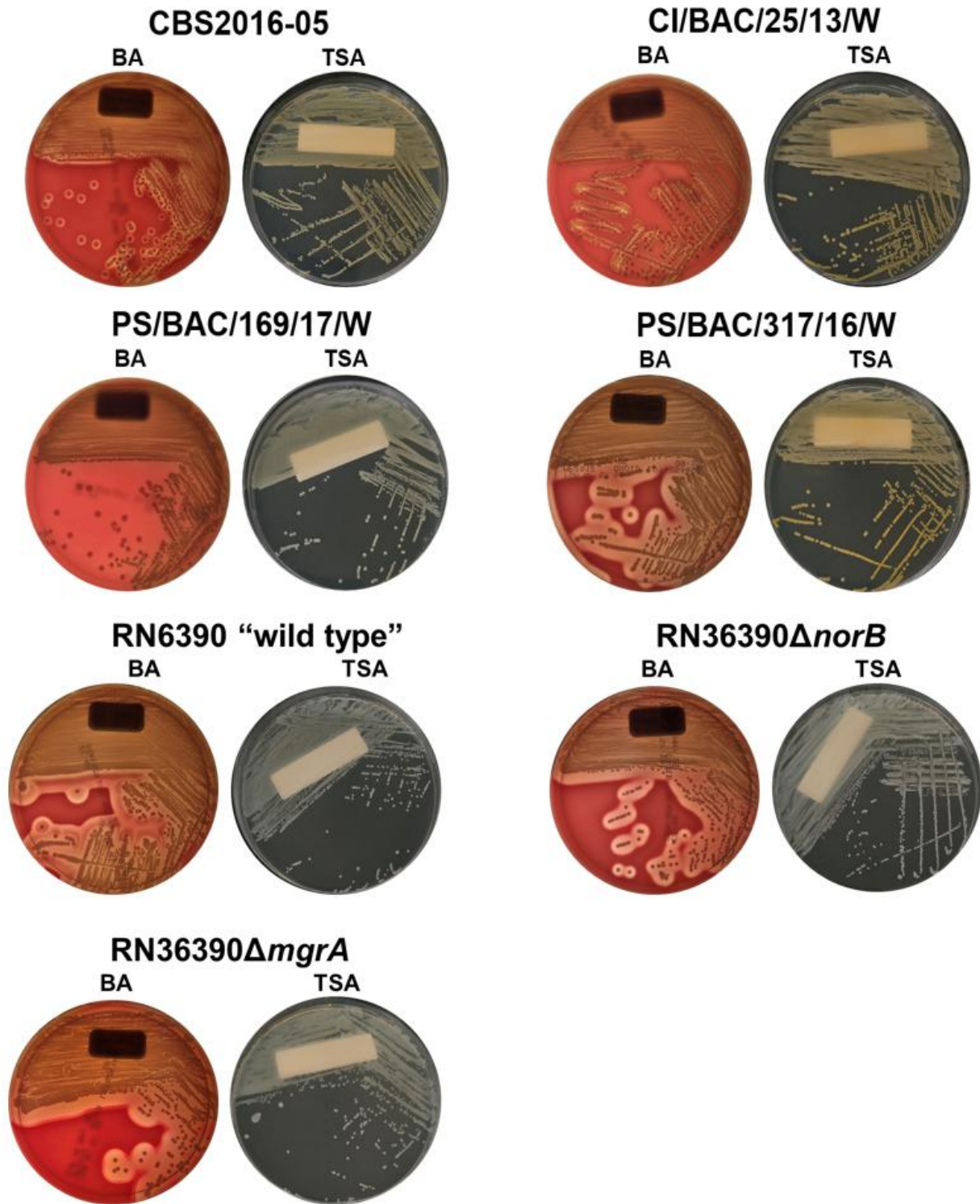


Figure 3A - *S. aureus* isolates grown in Blood Agar (BA) and Tryptic Soy Agar (TSA) plates. Isolates were streaked onto BA and TSA plates, incubated at 37 °C for 24h.

Appendix A4 – Supplementary information for Chapter 3

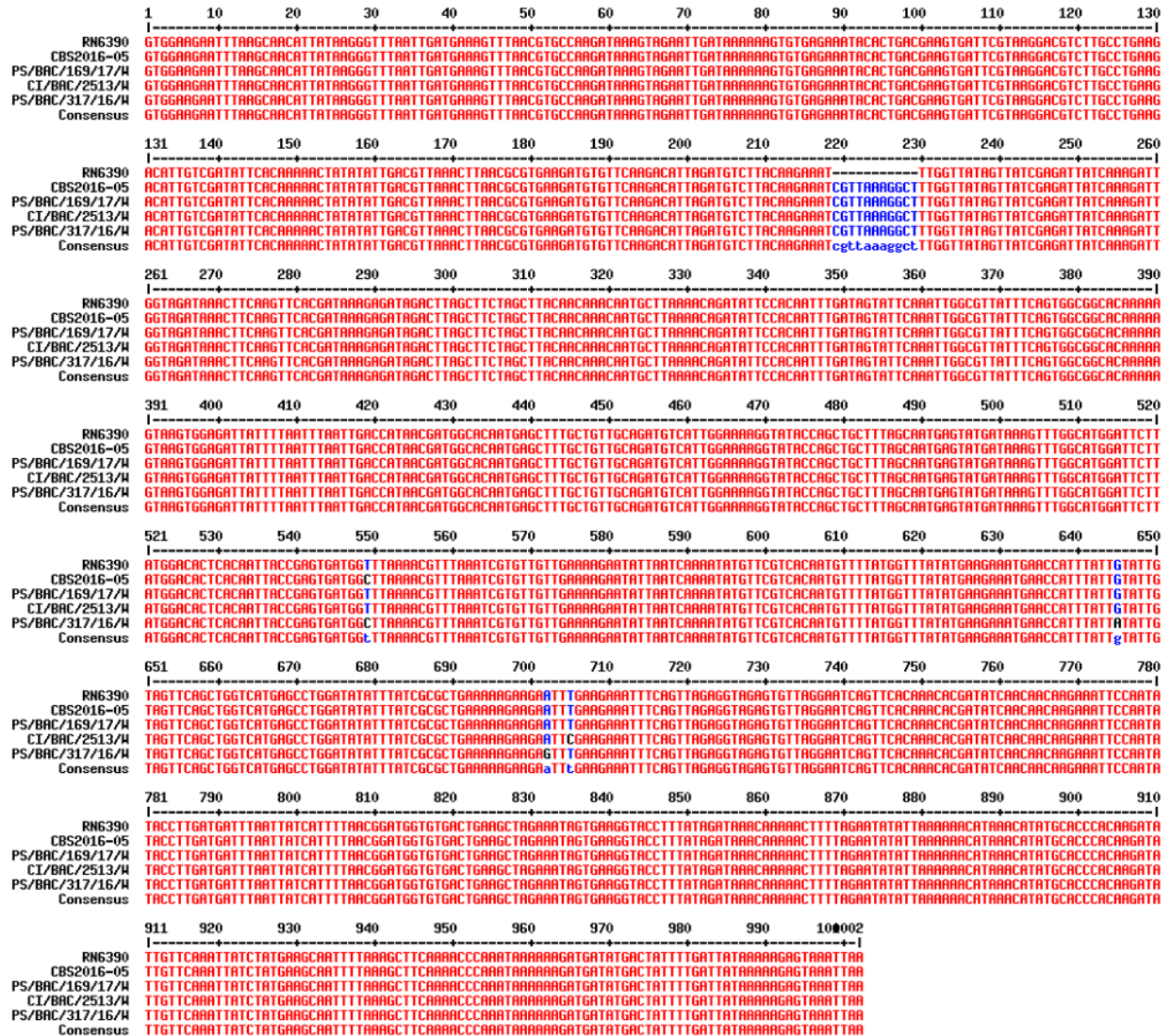


Figure 4A - Alignment of the *rsbU* gene for TRS and *S. aureus* RN6390 using MultAlin (last accessed on July 30th, 2025), with 11-bp deletion located between nucleotides 219 to 229 (inclusive).

Appendix A5 – Supplementary information for Chapter 3

GyrA DNA Gyrase subunit A

CLUSTAL O(1.2.4) multiple sequence alignment

PS169	MAELPQSRINERNITSEMRESFLDYAMSVIVARALPDVRDGLKPVHRRILYGLNEQGMTP	60
DNA_GyrA	MAELPQSRINERNITSEMRESFLDYAMSVIVARALPDVRDGLKPVHRRILYGLNEQGMTP	60
CI25	MAELPQSRINERNITSEMRESFLDYAMSVIVARALPDVRDGLKPVHRRILYGLNEQGMTP	60
RN6390	MAELPQSRINERNITSEMRESFLDYAMSVIVARALPDVRDGLKPVHRRILYGLNEQGMTP	60
CBS2016	MAELPQSRINERNITSEMRESFLDYAMSVIVARALPDVRDGLKPVHRRILYGLNEQGMTP	60
PS317	MAELPQSRINERNITSEMRESFLDYAMSVIVARALPDVRDGLKPVHRRILYGLNEQGMTP	60

PS169	DKSYKKSARIVGDVMGKYHPHGDSSIYEAMVRMAQDFSYRYPLVDGQGNFGSMDGDGAAA	120
DNA_GyrA	DKSYKKSARIVGDVMGKYHPHGDSSIYEAMVRMAQDFSYRYPLVDGQGNFGSMDGDGAAA	120
CI25	DKSYKKSARIVGDVMGKYHPHGDSSIYEAMVRMAQDFSYRYPLVDGQGNFGSMDGDGAAA	120
RN6390	DKSYKKSARIVGDVMGKYHPHGDSSIYEAMVRMAQDFSYRYPLVDGQGNFGSMDGDGAAA	120
CBS2016	DKSYKKSARIVGDVMGKYHPHGDSSIYEAMVRMAQDFSYRYPLVDGQGNFGSMDGDGAAA	120
PS317	DKSYKKSARIVGDVMGKYHPHGDSSIYEAMVRMAQDFSYRYPLVDGQGNFGSMDGDGAAA	120

PS169	MRYTEARMTKITLELLRDINKDTIDFIDNYDGNEREPSVLPARFPNLLANGASGIAVGMA	180
DNA_GyrA	MRYTEARMTKITLELLRDINKDTIDFIDNYDGNEREPSVLPARFPNLLANGASGIAVGMA	180
CI25	MRYTEARMTKITLELLRDINKDTIDFIDNYDGNEREPSVLPARFPNLLANGASGIAVGMA	180
RN6390	MRYTEARMTKITLELLRDINKDTIDFIDNYDGNEREPSVLPARFPNLLANGASGIAVGMA	180
CBS2016	MRYTEARMTKITLELLRDINKDTIDFIDNYDGNEREPSVLPARFPNLLANGASGIAVGMA	180
PS317	MRYTEARMTKITLELLRDINKDTIDFIDNYDGNEREPSVLPARFPNLLANGASGIAVGMA	180

PS169	TNIPPHNLTELINGVLSLSKNPDISIAELMEDIEGPDFPTAGLILGKSGIRRAYETGRGS	240
DNA_GyrA	TNIPPHNLTELINGVLSLSKNPDISIAELMEDIEGPDFPTAGLILGKSGIRRAYETGRGS	240
CI25	TNIPPHNLTELINGVLSLSKNPDISIAELMEDIEGPDFPTAGLILGKSGIRRAYETGRGS	240
RN6390	TNIPPHNLTELINGVLSLSKNPDISIAELMEDIEGPDFPTAGLILGKSGIRRAYETGRGS	240
CBS2016	TNIPPHNLTELINGVLSLSKNPDISIAELMEDIEGPDFPTAGLILGKSGIRRAYETGRGS	240
PS317	TNIPPHNLTELINGVLSLSKNPDISIAELMEDIEGPDFPTAGLILGKSGIRRAYETGRGS	240

PS169	IQMRSRAVIEERGGGRQRIVVTEIPFQVNKARMIEKIAELVRDCKIDGITDLRDETSVRT	300
DNA_GyrA	IQMRSRAVIEERGGGRQRIVVTEIPFQVNKARMIEKIAELVRDCKIDGITDLRDETSVRT	300
CI25	IQMRSRAVIEERGGGRQRIVVTEIPFQVNKARMIEKIAELVRDCKIDGITDLRDETSVRT	300
RN6390	IQMRSRAVIEERGGGRQRIVVTEIPFQVNKARMIEKIAELVRDCKIDGITDLRDETSVRT	300
CBS2016	IQMRSRAVIEERGGGRQRIVVTEIPFQVNKARMIEKIAELVRDCKIDGITDLRDETSVRT	300
PS317	IQMRSRAVIEERGGGRQRIVVTEIPFQVNKARMIEKIAELVRDCKIDGITDLRDETSVRT	300

PS169	GVRVVIDVRKDNASVILNPLYKQTPQTSGVNMIALVNGRPKLIINLKEALVHYLEHQK	360

DNA_GyrA	GVRVVIDVRKDANASVILNPLYKQTPQTSTFGVNMIALVNGRPKLINLKEALVHYLEHQK	360
CI25	GVRVVIDVRKDANASVILNPLYKQTPQTSTFGVNMIALVNGRPKLINLKEALVHYLEHQK	360
RN6390	GVRVVIDVRKDANASVILNPLYKQTPQTSTFGVNMIALVNGRPKLINLKEALVHYLEHQK	360
CBS2016	GVRVVIDVRKDANASVILNPLYKQTPQTSTFGVNMIALVNGRPKLINLKEALVHYLEHQK	360
PS317	GVRVVIDVRKDANASVILNPLYKQTPQTSTFGVNMIALVNGRPKLINLKEALVHYLEHQK *****	360
PS169	TVRRRTQYNLRKAKDRAHILEGLRIALDHIDEIISTIRESDDTKVAMESLQQRFKLSEK	420
DNA_GyrA	TVRRRTQYNLRKAKDRAHILEGLRIALDHIDEIISTIRESDDTKVAMESLQQRFKLSEK	420
CI25	TVRRRTQYNLRKAKDRAHILEGLRIALDHIDEIISTIRESDDTKVAMESLQQRFKLSEK	420
RN6390	TVRRRTQYNLRKAKDRAHILEGLRIALDHIDEIISTIRESDDTKVAMESLQQRFKLSEK	420
CBS2016	TVRRRTQYNLRKAKDRAHILEGLRIALDHIDEIISTIRESDDTKVAMESLQQRFKLSEK	420
PS317	TVRRRTQYNLRKAKDRAHILEGLRIALDHIDEIISTIRESEDDTKVAMESLQQRFKLSEK *****	420
PS169	QAQAILDMRLRRLTGLERDKIEAEYNELLYISELEAILADEEVLQLVRDELTEIRDRF	480
DNA_GyrA	QAQAILDMRLRRLTGLERDKIEAEYNELLYISELEAILADEEVLQLVRDELTEIRDRF	480
CI25	QAQAILDMRLRRLTGLERDKIEAEYNELLYISELEAILADEEVLQLVRDELTEIRDRF	480
RN6390	QAQAILDMRLRRLTGLERDKIEAEYNELLYISELEAILADEEVLQLVRDELTEIRDRF	480
CBS2016	QAQAILDMRLRRLTGLERDKIEAEYNELLYISELEAILADEEVLQLVRDELTEIRDRF	480
PS317	QAQAILDMRLRRLTGLERDKIEAEYNELLYISELEAILADEEVLQLVRDELTEIRDRF *****	480
PS169	GDDRRTEIQLGGFEDLEDEDLIPPEEQIVITLSHNNYIKRLLPVSTYRAQNRGGRGVQGMNT	540
DNA_GyrA	GDDRRTEIQLGGFEDLEDEDLIPPEEQIVITLSHNNYIKRLLPVSTYRAQNRGGRGVQGMNT	540
CI25	GDDRRTEIQLGGFEDLEDEDLIPPEEQIVITLSHNNYIKRLLPVSTYRAQNRGGRGVQGMNT	540
RN6390	GDDRRTEIQLGGFEDLEDEDLIPPEEQIVITLSHNNYIKRLLPVSTYRAQNRGGRGVQGMNT	540
CBS2016	GDDRRTEIQLGGFEDLEDEDLIPPEEQIVITLSHNNYIKRLLPVSTYRAQNRGGRGVQGMNT	540
PS317	GDDRRTEIQLGGFEDLEDEDLIPPEEQIVITLSHNNYIKRLLPVSTYRAQNRGGRGVQGMNT ** : *****	540
PS169	LEEDFVSQLVTLSTHDHVLFFTNKGRVYKLGVEPELSRQSKGIPVVNAIELENDEVIS	600
DNA_GyrA	LEEDFVSQLVTLSTHDHVLFFTNKGRVYKLGVEPELSRQSKGIPVVNAIELENDEVIS	600
CI25	LEEDFVSQLVTLSTHDHVLFFTNKGRVYKLGVEPELSRQSKGIPVVNAIELENDEVIS	600
RN6390	LEEDFVSQLVTLSTHDHVLFFTNKGRVYKLGVEPELSRQSKGIPVVNAIELENDEVIS	600
CBS2016	LEEDFVSQLVTLSTHDHVLFFTNKGRVYKLGVEPELSRQSKGIPVVNAIELENDEVIS	600
PS317	LEEDFVSQLVTLSTHDHVLFFTNKGRVYKLGVEPELSRQSKGIPVVNAIELENDEVIS ***** ** . **	600
PS169	TMIAVKDLESEDNLFVATKRGVVKRSALSNFSRINRNGKIAISFREDELIAVRLTSGQ	660
DNA_GyrA	TMIAVKDLESEDNLFVATKRGVVKRSALSNFSRINRNGKIAISFREDELIAVRLTSGQ	660
CI25	TMIAVKDLESEDNLFVATKRGVVKRSALSNFSRINRNGKIAISFREDELIAVRLTSGQ	660
RN6390	TMIAVKDLESEDNLFVATKRGVVKRSALSNFSRINRNGKIAISFREDELIAVRLTSGQ	660
CBS2016	TMIAVKDLESEDNLFVATKRGVVKRSALSNFSRINRNGKIAISFREDELIAVRLTSGQ	660

PS317	TMIAVKDLESEDNFLVFATKRGVVKRSALSNFSRINRNGKIAISFREDELIAVRLTSGQ	660

PS169	EDILIGTSHASLIRFPESTLRPLGRTATGVKGITLREGDEVGLDVAHENSDEVLVVTE	720
DNA_GyrA	EDILIGTSHASLIRFPESTLRPLGRTATGVKGITLREGDEVGLDVAHANSDEVLVVTE	720
CI25	EDILIGTSHASLIRFPESTLRPLGRTATGVKGITLREGDEVGLDVAHANSDEVLVVTE	720
RN6390	EDILIGTSHASLIRFPESTLRPLGRTATGVKGITLREGDEVGLDVAHANSDEVLVVTE	720
CBS2016	EDILIGTSHASLIRFPESTLRPLGRTATGVKGITLREGDEVGLDVAHANSDEVLVVTE	720
PS317	EDILIGTSHASLIRFPESTLRPLGRTATGVKGITLREGDEVGLDVAHANSDEVLVVTE	720

PS169	NGYGK RTPVNDYRLSNRGGKGIKTATITERNGNVVCITVTGEEDLMIVTNAGVIIRLDV	780
DNA_GyrA	NGYGK RTPVNDYRLSNRGGKGIKTATITERNGNVVCITVTGEEDLMIVTNAGVIIRLDV	780
CI25	NGYGK RTPVNDYRLSNRGGKGIKTATITERNGNVVCITVTGEEDLMIVTNAGVIIRLDV	780
RN6390	NGYGK RTPVNDYRLSNRGGKGIKTATITERNGNVVCITVTGEEDLMIVTNAGVIIRLDV	780
CBS2016	NGYGK RTPVNDYRLSNRGGKGIKTATITERNGNVVCITVTGEEDLMIVTNAGVIIRLDV	780
PS317	NGYGK RTPVNDYRLSNRGGKGIKTATITERNGNVVCITVTGEEDLMIVTNAGVIIRLDV	780

PS169	ADISQNGRAAQGVRLIRLGDDQFVSTVAKVKEDAEDETNEDEQSTSTVSEDGTEQQREAV	840
DNA_GyrA	ADISQNGRAAQGVRLIRLGDDQFVSTVAKVKEDAEDETNEDEQSTSTVSEDGTEQQREAV	840
CI25	ADISQNGRAAQGVRLIRLGDDQFVSTVAKVKEDAEDETNEDEQSTSTVSEDGTEQQREAV	840
RN6390	ADISQNGRAAQGVRLIRLGDDQFVSTVAKVKEDAEDETNEDEQSTSTVSEDGTEQQREAV	840
CBS2016	ADISQNGRAAQGVRLIRLGDDQFVSTVAKVKEDADEVN--EDEQSTVSEDGTEQQREAV	837
PS317	ADISQNGRAAQGVRLIRLGDDQFVSTVAKVKEDADEEN--EDEQSTVSEDGTEQQREAV	837
	*****:: . *:. *****	
PS169	VNDETPGNAIHTEVIESEEIDDGRIEVRQDFMDRVEEDIQQSLDEE-- 887	
DNA_GyrA	VNDETPGNAIHTEVIDSEENEDGRIEVRQDFMDRVEEDIQQSLDEE 889	
CI25	VNDETPGNAIHTEVIDSEENEDGRIEVRQDFMDRVEEDIQQSSDEE 889	
RN6390	VNDETPGNAIHTEVIDSEENEDGRIEVRQDFMDRVEEDIQQSSDEE-- 887	
CBS2016	VNDETPGNAIHTEVIDSEENEDGRIEVRQDFMDRVEEDIQQSSNEDEE 886	
PS317	VNDETPGNAIHTEVIDSEVNDGRIEVRQDFMDRVEEDIQQSSDDEE 886	
	*****:* .*:***** :::	

GyrB DNA Gyrase
subunit B

CLUSTAL O(1.2.4) multiple sequence alignment

PS317	MVTALSDVNNTDNYGAGQIQVLEGLEAVRKRPGMYIGSTSERGLHHLVWEIVDNSIDEAL	60
DNA_GyrB	MVTALSDVNNTDNYGAGQIQVLEGLEAVRKRPGMYIGSTSERGLHHLVWEIVDNSIDEAL	60
CBS2016	MVTALSDVNNTDNYGAGQIQVLEGLEAVRKRPGMYIGSTSERGLHHLVWEIVDNSIDEAL	60
RN6390	MVTALSDVNNTDNYGAGQIQVLEGLEAVRKRPGMYIGSTSERGLHHLVWEIVDNSIDEAL	60
CI25	MVTALSDVNNTDNYGAGQIQVLEGLEAVRKRPGMYIGSTSERGLHHLVWEIVDNSIDEAL	60
PS16	MVTALSDVNNTDNYGAGQIQVLEGLEAVRKRPGMYIGSTSERGLHHLVWEIVDNSIDEAL	60

PS317	AGYANQIEVVIEKDNWIKVTDNDRGIPVDIQEKMRPAVEVILTVLHAGGKFGGGGYKVS	120
DNA_GyrB	AGYANQIEVVIEKDNWIKVTDNDRGIPVDIQEKMRPAVEVILTVLHAGGKFGGGGYKVS	120
CBS2016	AGYANQIEVVIEKDNWIKVTDNDRGIPVDIQEKMRPAVEVILTVLHAGGKFGGGGYKVS	120
RN6390	AGYANQIEVVIEKDNWIKVTDNDRGIPVDIQEKMRPAVEVILTVLHAGGKFGGGGYKVS	120
CI25	AGYANKIEVVIEKDNWIKVTDNDRGIPVDIQEKMRPAVEVILTVLHAGGKFGGGGYKVS	120
PS16	AGYANKIEVVIEKDNWIKVTDNDRGIPVDIQEKMRPAVEVILTVLHAGGKFGGGGYKVS	120
	**** . *****	
PS317	GGLHGVGSSVNNALSQDLEVVVHRNETIYHQAYKKGVPQFDLKEVGTDDKTGTVIRFKAD	180
DNA_GyrB	GGLHGVGSSVNNALSQDLEVVVHRNETIYHQAYKKGVPQFDLKEVGTDDKTGTVIRFKAD	180
CBS2016	GGLHGVGSSVNNALSQDLEVVVHRNETIYHQAYKKGVPQFDLKEVGTDDKTGTVIRFKAD	180
RN6390	GGLHGVGSSVNNALSQDLEVVVHRNETIYHQAYKKGVPQFDLKEVGTDDKTGTVIRFKAD	180
CI25	GGLHGVGSSVNNALSQDLEVVVHRNETIYHQAYKKGVPQFDLKEVGTDDKTGTVIRFKAD	180
PS16	GGLHGVGSSVNNALSQDLEVVVHRNETIYHQAYKKGVPQFDLKEVGTDDKTGTVIRFKAD	180

PS317	GEIFTETTVYNYETLQQRIRELAFLNKGIQITLRDERDEENVREDSYHYEGGIKSYVELL	240
DNA_GyrB	GEIFTETTVYNYETLQQRIRELAFLNKGIQITLRDERDEENVREDSYHYEGGIKSYVELL	240
CBS2016	GEIFTETTVYNYETLQQRIRELAFLNKGIQITLRDERDEENVREDSYHYEGGIKSYVELL	240
RN6390	GEIFTETTVYNYETLQQRIRELAFLNKGIQITLRDERDEENVREDSYHYEGGIKSYVELL	240
CI25	GEIFTETTVYNYETLQQRIRELAFLNKGIQITLRDERDEENVREDSYHYEGGIKSYVELL	240
PS16	GEIFTETTVYNYETLQQRIRELAFLNKGIQITLRDERDEENVREDSYHYEGGIKSYVELL	240

PS317	NENKEPIHDEPIYIHQSKDDIEVEIAIQNSGYATNLLTYANNIHTYEGGTHEDGFKRAL	300
DNA_GyrB	NENKEPIHDEPIYIHQSKDDIEVEIAIQNSGYATNLLTYANNIHTYEGGTHEDGFKRAL	300
CBS2016	NENKEPIHDEPIYIHQSKDDIEVEIAIQNSGYATNLLTYANNIHTYEGGTHEDGFKRAL	300
RN6390	NENKEPIHDEPIYIHQSKDDIEVEIAIQNSGYATNLLTYANNIHTYEGGTHEDGFKRAL	300
CI25	NENKEPIHDEPIYIHQSKDDIEVEIAIQNSGYATNLLTYANNIHTYEGGTHEDGFKRAL	300
PS16	NENKEPIHDEPIYIHQSKDDIEVEIAIQNSGYATNLLTYANNIHTYEGGTHEDGFKRAL	300

PS317	TRVLSYGLSSKIMKEDRRLSGEDTREGMTAIISIKHGDPQFEGQTKTKLGNSEVRQVV	360

DNA_GyrB	TRVLNSYGLSSKIMKEEKDRLSGEDTREGMTAIISIKHGDPQFEGQTKKLGNSEVRQVV	360
CBS2016	TRVLNSYGLSSKIMKEEKDRLSGEDTREGMTAIISIKHGDPQFEGQTKKLGNSEVRQVV	360
RN6390	TRVLNSYGLSSKIMKEEKDRLSGEDTREGMTAIISIKHGDPQFEGQTKKLGNSEVRQVV	360
CI25	TRVLNSYGLSSKIMKEEKDRLSGEDTREGMTAIISIKHGDPQFEGQTKKLGNSEVRQVV	360
PS16	TRVLNSYGLSSKIMKEEKDRLSGEDTREGMTAIISIKHGDPQFEGQTKKLGNSEVRQVV	360
	*****.*****	
PS317	DKLFSEHFERFLYENPQVARTVVEKGIMAAARVAACKAREVTRRKSALDVASLPGKLAD	420
DNA_GyrB	DKLFSEHFERFLYENPQVARTVVEKGIMAAARVAACKAREVTRRKSALDVASLPGKLAD	420
CBS2016	DKLFSEHFERFLYENPQVARTVVEKGIMAAARVAACKAREVTRRKSALDVASLPGKLAD	420
RN6390	DKLFSEHFERFLYENPQVARTVVEKGIMAAARVAACKAREVTRRKSALDVASLPGKLAD	420
CI25	DKLFSEHFERFLYENPQVARTVVEKGIMAAARVAACKAREVTRRKSALDVASLPGKLAD	420
PS16	DKLFSEHFERFLYENPQVARTVVEKGIMAAARVAACKAREVTRRKSALDVASLPGKLAD	420

PS317	CSSKSPEECEIFLVEGDSAGGSTKSGRDSRTQAILPLRGKILNVEKARLDRILNNEIRQ	480
DNA_GyrB	CSSKSPEECEIFLVEGDSAGGSTKSGRDSRTQAILPLRGKILNVEKARLDRILNNEIRQ	480
CBS2016	CSSKSPEECEIFLVEGDSAGGSTKSGRDSRTQAILPLRGKILNVEKARLDRILNNEIRQ	480
RN6390	CSSKSPEECEIFLVEGDSAGGSTKSGRDSRTQAILPLRGKILNVEKARLDRILNNEIRQ	480
CI25	CSSKSPEECEIFLVEGDSAGGSTKSGRDSRTQAILPLRGKILNVEKARLDRILNNEIRQ	480
PS16	CSSKSPEECEIFLVEGDSAGGSTKSGRDSRTQAILPLRGKILNVEKARLDRILNNEIRQ	480

PS317	MITAFGTGIGGDFDLAKARYHKIVIMTDADVDGAHIRTLLLTFYRFMRPLIEAGYVYIA	540
DNA_GyrB	MITAFGTGIGGDFDLAKARYHKIVIMTDADVDGAHIRTLLLTFYRFMRPLIEAGYVYIA	540
CBS2016	MITAFGTGIGGDFDLAKARYHKIVIMTDADVDGAHIRTLLLTFYRFMRPLIEAGYVYIA	540
RN6390	MITAFGTGIGGDFDLAKARYHKIVIMTDADVDGAHIRTLLLTFYRFMRPLIEAGYVYIA	540
CI25	MITAFGTGIGGDFDLAKARYHKIVIMTDADVDGAHIRTLLLTFYRFMRPLIEAGYVYIA	540
PS16	MITAFGTGIGGDFDLAKARYHKIVIMTDADVDGAHIRTLLLTFYRFMRPLIEAGYVYIA	540

PS317	QPPLYKLTQGKQKYYVYNDRELDKDKSELNPTPKWSIARYKGLGEMNADQLWETTMNPEH	600
DNA_GyrB	QPPLYKLTQGKQKYYVYNDRELDKDKSELNPTPKWSIARYKGLGEMNADQLWETTMNPEH	600
CBS2016	QPPLYKLTQGKQKYYVYNDRELDKDKSELNPTPKWSIARYKGLGEMNADQLWETTMNPEH	600
RN6390	QPPLYKLTQGKQKYYVYNDRELDKDKSELNPTPKWSIARYKGLGEMNADQLWETTMNPEH	600
CI25	QPPLYKLTQGKQKYYVYNDRELDKDKSELNPTPKWSIARYKGLGEMNADQLWETTMNPEH	600
PS16	QPPLYKLTQGKQKYYVYNDRELDKDKSELNPTPKWSIARYKGLGEMNADQLWETTMNPEH	600

PS317	RALLQVKLEDAIEADQTFEMLMGDVVENRRQFIEDNAVYANLDF	644
DNA_GyrB	RALLQVKLEDAIEADQTFEMLMGDVVENRRQFIEDNAVYANLDF	644
CBS2016	RALLQVKLEDAIEADQTFEMLMGDVVENRRQFIEDNAVYANLDF	644
RN6390	RALLQVKLEDAIEADQTFEMLMGDVVENRRQFIEDNAVYANLDF	644
CI25	RALLQVKLEDAIEADQTFEMLMGDVVENRRQFIEDNAVYANLDF	644

PS16

RALLQVKLEDAIEADQTFEMLMGDVVENRRQFIEDNAVYANLDF

644

ParC TopoisomeraseIV
subunit A

CLUSTAL O(1.2.4) multiple sequence alignment

PS317	MSEIIQDLSLEDVLGDRFGRYSKYIIQERALPDVRDGLKPVQRRILYAMYSSGNTHDKNF	60
CBS2016	MSEIIQDLSLEDVLGDRFGRYSKYIIQERALPDVRDGLKPVQRRILYAMYSSGNTHDKNF	60
RN6390	MSEIIQDLSLEDVLGDRFGRYSKYIIQERALPDVRDGLKPVQRRILYAMYSSGNTHDKNF	60
Topoisomerase_ParC	MSEIIQDLSLEDVLGDRFGRYSKYIIQERALPDVRDGLKPVQRRILYAMYSSGNTHDKNF	60
CI25	MSEIIQDLSLEDVLGDRFGRYSKYIIQERALPDVRDGLKPVQRRILYAMYSSGNTHDKNF	60
PS169	MSEIIQDLSLEDVLGDRFGRYSKYIIQERALPDVRDGLKPVQRRILYAMYSSGNTHDKNF	60

PS317	RKSAKTVGDVIGQYHPHGDSSVYEAMVRLSQDWKLRHVL IEMHGNGSIDNDPPAAMRYT	120
CBS2016	RKSAKTVGDVIGQYHPHGDSSVYEAMVRLSQDWKLRHVL IEMHGNGSIDNDPPAAMRYT	120
RN6390	RKSAKTVGDVIGQYHPHGDSSVYEAMVRLSQDWKLRHVL IEMHGNGSIDNDPPAAMRYT	120
Topoisomerase_ParC	RKSAKTVGDVIGQYHPHGDSSVYEAMVRLSQDWKLRHVL IEMHGNGSIDNDPPAAMRYT	120
CI25	RKSAKTVGDVIGQYHPHGDSSVYEAMVRLSQDWKLRHVL IEMHGNGSIDNDPPAAMRYT	120
PS169	RKSAKTVGDVIGQYHPHGDSSVYEAMVRLSQDWKLRHVL IEMHGNGSIDNDPPAAMRYT	120
	***** **:	
PS317	EAKLSLLAEELLRDINKETVSFISNYDDTTLEPMVLPSRFPNLLVNGSTGISAGYATDIP	180
CBS2016	EAKLSLLAEELLRDINKETVSFIPNYDDTTLEPMVLPSRFPNLLVNGSTGISAGYATDIP	180
RN6390	EAKLSLLAEELLRDINKETVSFIPNYDDTTLEPMVLPSRFPNLLVNGSTGISAGYATDIP	180
Topoisomerase_ParC	EAKLSLLAEELLRDINKETVSFIPNYDDTTLEPMVLPSRFPNLLVNGSTGISAGYATDIP	180
CI25	EAKLSLLAEELLRDINKETVSFIPNYDDTTLEPMVLPSRFPNLLVNGSTGISAGYATDIP	180
PS169	EAKLSLLAEELLRDINKETVSFIPNYDDTTLEPMVLPSRFPNLLVNGSTGISAGYATDIP	180

PS317	PHNLAEVIQATLKYIDNPDITVNQLMKYIKGPDFPTGGIIQGIDGIKKAYESGKGRIIVR	240
CBS2016	PHNLAEVIQATLKYIDNPDITVNQLMKYIKGPDFPTGGIIQGIDGIKKAYESGKGRIIVR	240
RN6390	PHNLAEVIQATLKYIDNPDITVNQLMKYIKGPDFPTGGIIQGIDGIKKAYESGKGRIIVR	240
Topoisomerase_ParC	PHNLAEVIQATLKYIDNPDITVNQLMKYIKGPDFPTGGIIQGIDGIKKAYESGKGRIIVR	240
CI25	PHNLAEVIQATLKYIDNPDITVNQLMKYIKGPDFPTGGIIQGVGIDGIKKAYESGKGRIIVR	240
PS169	PHNLAEVIQATLKYIDNPDITVNQLMKYIKGPDFPTGGIIQGVGIDGIKKAYESGKGRIIVR	240

PS317	SKVEEETLRNGRKQLIITEIPYEVNKSSLVKRIDE LRADKKVDGIVEVRDETDRTGLRIA	300
CBS2016	SKVEEETLRNGRKQLIITEIPYEVNKSSLVKRIDE LRADKKVDGIVEVRDETDRTGLRIA	300
RN6390	SKVEEETLRNGRKQLIITEIPYEVNKSSLVKRIDE LRADKKVDGIVEVRDETDRTGLRIA	300
Topoisomerase_ParC	SKVEEETLRNGRKQLIITEIPYEVNKSSLVKRIDE LRADKKVDGIVEVRDETDRTGLRIA	300
CI25	SKVEEETLRNGRKQLIITEIPYEVNKSSLVKRIDE LRADKKVDGIVEVRDETDRTGLRIA	300
PS169	SKVEEETLRNGRKQLIITEIPYEVNKSSLVKRIDE LRADKKVDGIVEVRDETDRTGLRIA	300

PS317	IELKKDVNSESIKNYLKNSDLQISYFNMFVAISDGRPKLMGIRQIIDSYLNHQIEVVAN	360

CBS2016	IELKKDVNSESIGNYLYKNSDLQISYNFMVAISDGRPKLMGIRQIIDSYLNHQIEVVAN	360
RN6390	IELKKDVNSESIGNYLYKNSDLQISYNFMVAISDGRPKLMGIRQIIDSYLNHQIEVVAN	360
Topoisomerase_ParC	IELKKDVNSESIGNYLYKNSDLQISYNFMVAISDGRPKLMGIRQIIDSYLNHQIEVVAN	360
CI25	IELKKDVNSESIGNYLYKNSDLQISYNFMVAISDGRPKLMGIRQIIDSYLNHQIEVVAN	360
PS169	IELKKDVNSESIGNYLYKNSDLQISYNFMVAISDGRPKLMGIRQIIDSYLNHQIEVVAN	360

PS317	RTKFELDNAEKRMHIVEGLIKALSILDKVIELIRSSKNKRDAKENLIEVYEFTEEQAEAI	420
CBS2016	RTKFELDNAEKRMHIVEGLIKALSILDKVIELIRSSKNKRDAKENLIEVYEFTEEQAEAI	420
RN6390	RTKFELDNAEKRMHIVEGLIKALSILDKVIELIRSSKNKRDAKENLIEVYEFTEEQAEAI	420
Topoisomerase_ParC	RTKFELDNAEKRMHIVEGLIKALSILDKVIELIRSSKNKRDAKENLIEVFEFTEEQAEAI	420
CI25	RTKFELDNAEKRMHIVEGLIKALSILDKVIELIRSSKNKRDAKENLIEVFEFTEEQAEAI	420
PS169	RTKFELDNAEKRMHIVEGLIKALSILDKVIELIRSSKNKRDAKENLIEVFEFTEEQAEAI	420

PS317	VMLQLYRLTNTDIVALERGEHKELEALIKQLRHILDNDHALLNVIKEELNEIKKKFKSERL	480
CBS2016	VMLQLYRLTNTDIVALERGEHKELEALIKQLRHILDNDHALLNVIKEELNEIKKKFKSERL	480
RN6390	VMLQLYRLTNTDIVALERGEHKELEALIKQLRHILDNDHALLNVIKEELNEIKKKFKSERL	480
Topoisomerase_ParC	VMLQLYRLTNTDIVALERGEHKELEALIKQLRHILDNDHALLNVIKEELNEIKKKFKSERL	480
CI25	VMLQLYRLTNTDIVALERGEHKELEALIKQLRHILDNDHALLNVIKEELNEIKKKFKSERL	480
PS169	VMLQLYRLTNTDIVALERGEHKELEALIKQLRHILDNDHALLNVIKEELNEIKKKFKSERL	480

PS317	SLIEAEIEEIKIDKEVMVPSEEVILSMTRHGYIKRTSIRSYNASGVEDIGLDGDSLLKH	540
CBS2016	SLIEAEIEEIKIDKEVMVPSEEVILSMTRHGYIKRTSIRSFNASGVEDIGLDGDSLLKH	540
RN6390	SLIEAEIEEIKIDKEVMVPSEEVILSMTRHGYIKRTSIRSFNASGVEDIGLDGDSLLKH	540
Topoisomerase_ParC	SLIEAEIEEIKIDKEVMVPSEEVILSMTRHGYIKRTSIRSFNASGVEDIGLDGDSLLKH	540
CI25	SLIEAEIEEIKIDKEVMVPSEEVILSMTRHGYIKRTSIRSFNASGVEDIGLDGDSLLKH	540
PS169	SLIEAEIEEIKIDKEVMVPSEEVILSMTRHGYIKRTSIRSFNASGVEDIGLDGDSLLKH	540

PS317	QEVNTQDQTVLVFTNKGRYLFIPVHKLADIRWKELGQHSQIVPIEEDEVVINFNEKDFN	600
CBS2016	QEVNTQDQTVLVFTNKGRYLFIPVHKLADIRWKELGQHSQIVPIEEDEVVINFNEKDFN	600
RN6390	QEVNTQDQTVLVFTNKGRYLFIPVHKLADIRWKELGQHSQIVPIEEDEVVINFNEKDFN	600
Topoisomerase_ParC	QEVNTQDQTVLVFTNKGRYLFIPVHKLADIRWKELGQHSQIVPIEEDEVVINFNEKDFN	600
CI25	QEVNTQDQTVLVFTNKGRYLFIPVHKLADIRWKELGQHSQIVPIEEDEVVINFNEKDFN	600
PS169	QEVNTQDQTVLVFTNKGRYLFIPVHKLADIRWKELGQHSQIVPIEEDEVVINFNEKDFN	600

PS317	TDAFYVFATQNGMIKKSTVPLFKTTRFNKPLIATKVKENDDLISVMRFEKDLITITNK	660
CBS2016	TDAFYVFATQNGMIKKSTVPLFKTTRFNKPLIATKVKENDDLISVMRFEKDLITITNK	660
RN6390	TDAFYVFATQNGMIKKSTVPLFKTTRFNKPLIATKVKENDDLISVMRFEKDLITITNK	660
Topoisomerase_ParC	TDAFYVFATQNGMIKKSTVPLFKTTRFNKPLIATKVKENDDLISVMRFEKDLITITNK	660
CI25	TDAFYVFATQNGMIKKSTVPLFKTTRFNKPLIATKVKENDDLISVMRFEKDLITITNK	660

PS169	TDAFYVFATQNGMIKKSTVPLFKTTRFNKPLIATKVKENDDLISVMRFEKDQLITVITNK	660
	*****.*****.****	
PS317	GMSLTYNTSELSDTGLRAAGVKSINLKAEDFVVMTEGVSENDTILMATQRGSLKRISFKI	720
CBS2016	GMSLTYNTSELSDTGLRAAGVKSINLKAEDFVVMTEGVSENDTILMATQRGSLKRISFKI	720
RN6390	GMSLTYNTSELSDTGLRAAGVKSINLKAEDFVVMTEGVSENDTILMATQRGSLKRISFKI	720
Topoisomerase_ParC	GMSLTYNTSELSDTGLRAAGVKSINLKAEDFVVMTEGVSENDTILMATQRGSLKRISFKI	720
CI25	GMSLTYNTSELSDTGLRAAGVKSINLKAEDFVVMTEGVSENDTILMATQRGSLKRISFKI	720
PS169	GMSLTYNTSELSDTGLRAAGVKSINLKAEDFVVMTEGVSENDTILMATQRGSLKRISFKI	720

PS317	LQVAKRAQRGITLLKELKKNPHRIVAAHVVTGEHSQYTLYSKSNEEHGLINDIHKSEQYT	780
CBS2016	LQVAKRAQRGITLLKELKKNPHRIVAAHVVTGEHSQYTLYSKSNEEHGLINDIHKSEQYT	780
RN6390	LQVAKRAQRGITLLKELKKNPHRIVAAHVVTGEHSQYTLYSKSNEEHGLINDIHKSEQYT	780
Topoisomerase_ParC	LQVAKRAQRGITLLKELKKNPHRIVAAHVVTGEHSQYTLYSKSNEEHGLINDIHKSEQYT	780
CI25	LQVAKRAQRGITLLKELKKNPHRIVAAHVVTGEHSQYTLYSKSNEEHGLINDIHKSEQYT	780
PS169	LQVAKRAQRGITLLKELKKNPHRIVAAHVVTGEHSQYTLYSKSNEEHGLINDIHKSEQYT	780

PS317	NGSFIVDTDDFGEVIDMYIS	800
CBS2016	NGSFIVDTDDFGEVIDMYIS	800
RN6390	NGSFIVDTDDFGEVIDMYIS	800
Topoisomerase_ParC	NGSFIVDTDDFGEVIDMYIS	800
CI25	NGSFIVDTDDFGEVIDMYIS	800
PS169	NGSFIVDTDDFGEVIDMYIS	800

ParE TopoisomeraseIV
Subunit B

CLUSTAL O(1.2.4) multiple sequence alignment

PS169	MNKQNNYSDDSIQVLEGLEAVRKRPGMYIGSTDKRGLHHLVYEIVDNSVDEVLNQYGNIEI	60
Topoisomerase_ParE	MNKQNNYSDDSIQVLEGLEAVRKRPGMYIGSTDKRGLHHLVYEIVDNSVDEVLNQYGNIEI	60
CI25	MNKQNNYSDDSIQVLEGLEAVRKRPGMYIGSTDKRGLHHLVYEIVDNSVDEVLNQYGNIEI	60
RN6390	MNKQNNYSDDSIQVLEGLEAVRKRPGMYIGSTDKRGLHHLVYEIVDNSVDEVLNQYGNIEI	60
CBS2016	MNKQNNYSDDSIQVLEGLEAVRKRPGMYIGSTDKRGLHHLVYEIVDNSVDEVLNQYGNIEI	60
PS317	MNKQNNYSDDSIQVLEGLEAVRKRPGMYIGSTDKRGLHHLVYEIVDNSVDEVLNQYGNIEI	60

PS169	DVTINKDGSISIEDNDRGMPTGIHKSGKPTVEVIFTVLHAGGKFGQGGYKTSGLLHGVA	120
Topoisomerase_ParE	DVTINKDGSISIEDNDRGMPTGIHKSGKPTVEVIFTVLHAGGKFGQGGYKTSGLLHGVA	120
CI25	DVTINKDGSISIEDNDRGMPTGIHKSGKPTVEVIFTVLHAGGKFGQGGYKTSGLLHGVA	120
RN6390	DVTINKDGSISIEDNDRGMPTGIHKSGKPTVEVIFTVLHAGGKFGQGGYKTSGLLHGVA	120
CBS2016	DVTINKDGSISIEDNDRGMPTGIHKSGKPTVEVIFTVLHAGGKFGQGGYKTSGLLHGVA	120
PS317	DVTINKDGSISIEDNDRGMPTGIHKSGKPTVEVIFTVLHAGGKFGQGGYKTSGLLHGVA	120

PS169	SVNNALSEWLEVEIHRDGNIIHQSFKNNGSPSSGLVKKGKTKKTGKVTFKPDDTIFKAS	180
Topoisomerase_ParE	SVNNALSEWLEVEIHRDGNIIHQSFKNNGSPSSGLVKKGKTKKTGKVTFKPDDTIFKAS	180
CI25	SVNNALSEWLEVEIHRDGNIIHQSFKNNGSPSSGLVKKGKTKKTGKVTFKPDDTIFKAS	180
RN6390	SVNNALSEWLEVEIHRDGNIIHQSFKNNGSPSSGLVKKGKTKKTGKVTFKPDDTIFKAS	180
CBS2016	SVNNALSEWLEVEIHRDGNIIHQSFKNNGSPSSGLVKKGKTKKTGKVTFKPDDTIFKAS	180
PS317	SVNNALSEWLEVEIHRDGNIIHQSFKNNGSPSSGLVKKGKTKKTGKVTFKPDDTIFKAS	180

PS169	TSFNFDVLSERLQESAFLLKNLKITLNDLRSGKERQEHYHYEEGIKEFVSYVNEGKEVLH	240
Topoisomerase_ParE	TSFNFDVLSERLQESAFLLKNLKITLNDLRSGKERQEHYHYEEGIKEFVSYVNEGKEVLH	240
CI25	TSFNFDVLSERLQESAFLLKNLKITLNDLRSGKERQEHYHYEEGIKEFVSYVNEGKEVLH	240
RN6390	TSFNFDVLSERLQESAFLLKNLKITLNDLRSGKERQEHYHYEEGIKEFVSYVNEGKEVLH	240
CBS2016	TSFNFDVLSERLQESAFLLKNLKITLNDLRSGKERQEHYHYEEGIKEFVSYVNEGKEVLH	240
PS317	TSFNFDVLSERLQESAFLLKNLKITLNDLRSGKERQEHYHYEEGIKEFVSYVNEGKEVLH	240

PS169	DVATFSGEANGIEVDVAFQYNDQYSESILSFVNNVRTKGGTHEVGFKTAMTRVFNDYAR	300
Topoisomerase_ParE	DVATFSGEANGIEVDVAFQYNDQYSESILSFVNNVRTKGGTHEVGFKTAMTRVFNDYAR	300
CI25	DVATFSGEANGIEVDVAFQYNDQYSESILSFVNNVRTKGGTHEVGFKTAMTRVFNDYAR	300
RN6390	DVATFSGEANGIEVDVAFQYNDQYSESILSFVNNVRTKGGTHEVGFKTAMTRVFNDYAR	300
CBS2016	DVATFSGEANGIEVDVAFQYNDQYSESILSFVNNVRTKGGTHEVGFKTAMTRVFNDYAR	300
PS317	DVATFSGEANGIEVDVAFQYNDQYSESILSFVNNVRTKGGTHEVGFKTAMTRVFNDYAR	300

PS169	RINELKTKDKNLDGNDIREGLTAVVSVRIPEELLQFEGQTKSKLGTSEARSAVDSVVADK	360

Topoisomerase_ParE	RINELKTKDKNLDGNDIREGLTAVVSVRIPEELLQFEGQTKSKLGTSEARSAVDSVVADK	360
CI25	RINELKTKDKNLDGNDIREGLTAVVSVRIPEELLQFEGQTKSKLGTSEARSAVDSVVADK	360
RN6390	RINELKTKDKNLDGNDIREGLTAVVSVRIPEELLQFEGQTKSKLGTSEARSAVDSVVADK	360
CBS2016	RINELKTKDKNLDGNDIREGLTAVVSVRIPEELLQFEGQTKSKLGTSEARSAVDSVVADK	360
PS317	RINELKTKDKNLDGNDIREGLTAVVSVRIPEELLQFEGQTKSKLGTSEARSAVDSVVADK	360

PS169	LPFYLEEKGQLSKSLVKKAIKAQQAREAAARKAREDARSGKKNKRKDTLLSGKLTPAQSKN	420
Topoisomerase_ParE	LPFYLEEKGQLSKSLVKKAIKAQQAREAAARKAREDARSGKKNKRKDTLLSGKLTPAQSKN	420
CI25	LPFYLEEKGQLSKSLVKKAIKAQQAREAAARKAREDARSGKKNKRKDTLLSGKLTPAQSKN	420
RN6390	LPFYLEEKGQLSKSLVKKAIKAQQAREAAARKAREDARSGKKNKRKDTLLSGKLTPAQSKN	420
CBS2016	LPFYLEEKGQLSKSLVKKAIKAQQAREAAARKAREDARSGKKNKRKDTLLSGKLTPAQSKN	420
PS317	LPFYLEEKGQLSKSLVKKAIKAQQAREAAARKAREDARSGKKNKRKDTLLSGKLTPAQSKN	420

PS169	TEKNELYLVEGDSAGGSAKLGRDRKFQAILPLRGKVINTEKARLEDIFKNEEINTIITYTI	480
Topoisomerase_ParE	TEKNELYLVEGDSAGGSAKLGRDRKFQAILPLRGKVINTEKARLEDIFKNEEINTIITIHTI	480
CI25	TEKNELYLVEGDSAGGSAKLGRDRKFQAILPLRGKVINTEKARLEDIFKNEEINTIITIHTI	480
RN6390	TEKNELYLVEGDSAGGSAKLGRDRKFQAILPLRGKVINTEKARLEDIFKNEEINTIITIHTI	480
CBS2016	TDKNELYLVEGDSAGGSAKLGRDRKFQAILPLRGKVINTEKARLEDIFKNEEINTIITIHTI	480
PS317	TDKNELYLVEGDSAGGSAKLGRDRKFQAILPLRGKVINTEKARLEDIFKNEEINTIITIHTI	480
	*.*****.*	
PS169	GAGVGTDKIEDSNYNRVIIMTDADTDGAHIQVLLLTFFFKYMKPLVQAGRVFIALPPLY	540
Topoisomerase_ParE	GAGVGTDKIEDSNYNRVIIMTDADTDGAHIQVLLLTFFFKYMKPLVQAGRVFIALPPLY	540
CI25	GAGVGTDKIEDSNYNRVIIMTDADTDGAHIQVLLLTFFFKYMKPLVQAGRVFIALPPLY	540
RN6390	GAGVGTDKIEDSNYNRVIIMTDADTDGAHIQVLLLTFFFKYMKPLVQAGRVFIALPPLY	540
CBS2016	GAGVGTDKIEDSNYNRVIIMTDADTDGAHIQVLLLTFFFKYMKPLVQAGRVFIALPPLY	540
PS317	GAGVGTDKIEDSNYNRVIIMTDADTDGAHIQVLLLTFFFKYMKPLVQAGRVFIALPPLY	540

PS169	KLEKGGKTKRVEYAWTDEELNKLQKELGKGFTLQRYKGLGEMNPEQLWETTMNPETRTL	600
Topoisomerase_ParE	KLEKGGKTKRVEYAWTDEELNKLQKELGKGFTLQRYKGLGEMNPEQLWETTMNPETRTL	600
CI25	KLEKGGKTKRVEYAWTDEELNKLQKELGKGFTLQRYKGLGEMNPEQLWETTMNPETRTL	600
RN6390	KLEKGGKTKRVEYAWTDEELNKLQKELGKGFTLQRYKGLGEMNPEQLWETTMNPETRTL	600
CBS2016	KLEKGGKTKRVEYAWTDEELNKLQKELGKGFTLQRYKGLGEMNPEQLWETTMNPETRTL	600
PS317	KLEKGGKTKRVEYAWTDEELNKLQKELGKGFTLQRYKGLGEMNPEQLWETTMNPETRTL	600

PS169	IRVQVEDEVSSKRVTLLMGDKVQPRREWIEKHVEFGMQEDQSILDNSEVQVLENDQFDE	660
Topoisomerase_ParE	IRVQVEDEVSSKRVTLLMGDKVQPRREWIEKHVEFGMQEDQSILDNSEVQVLENDQFDE	660
CI25	IRVQVEDEVSSKRVTLLMGDKVQPRREWIEKHVEFGMQEDQSILDNSEVQVLENDQFDE	660
RN6390	IRVQVEDEVSSKRVTLLMGDKVQPRREWIEKHVEFGMQEDQSILDNSEVQVLENDQFDE	660
CBS2016	IRVQVEDEVSSKRVTLLMGDKVQPRREWIEKHVEFGMQEDQSILDNSEVQVLENDQFDE	660

```

PS317          IRVQVEDEVRSKRVTTLMGDKVQPREWIEKHVEFGMQEDQSILDNSEVQVLENDQFDE    660
                *****

PS169          EEI      663
Topoisomerase_ParE  EEI      663
CI25           EEI      663
RN6390        EEI      663
CBS2016       EEI      663
PS317         EEI      663
                ***

```

Figure 5A – Alignment of GyrA, GyrB, ParC and ParE proteins for TRS and *S. aureus* RN6390. Consensus sequences are highlighted in green and amino acid changes are highlighted in orange

Appendix A6 – Supplementary information for Chapter 2 and 3

Table 1A – List of primer (5' → 3') used in the experiments listed in this chapter.

Primer	Sequence*
RT-qPCR	
16S RNA (forward)	AAG TCG ATG GGC AAG ATG ATA C
16S RNA (reverse)	TCC TTC GTG AAG CTC CAT TTC
<i>norA</i> (forward)	GAC CAG GGA TTG GTG GAT TTA T
<i>norA</i> (reverse)	GGA AAC CAC TTG TCG TAG ACT T
<i>norB</i> (forward)	GAA TTA GGT GTA ACC TCA CTT CTT T
<i>norB</i> (reverse)	GTT GCA CCT GTG TAA GCT TAT
<i>norC</i> (forward)	TGG CAG TGG TAT CTG TTC AC
<i>norC</i> (reverse)	GGC GTC CCT TTG ATG AGT AA
CRISPR-Cas9	
pCasSA (forward)	GGGAAACGCCTGGTATCTTTA
pCasSA (reverse)	CATGTGATATGTCCCTCCTCTCTTC
HR1 (forward)	tttgagatctgtccatacccatggTCTAGATCGCAATGACAGTTGAAAATGT
HR1 (reverse)	AGGGAGGCAAATAGAGATGGATGTGCCTAAACAAAACGACACT
HR2 (forward)	AGTGTCGTTTTGTTTAGGCACATCCATCTCTATTTGCCTCCCT
HR2 (reverse)	aagatacaggtatattttctgaCTCGAGTGGTTTGGCGCAATTATACAAC
<i>norB</i> _spacer-F1	GAAAGTACTAATTATGATTCGTGT
<i>norB</i> _spacer-R1	AAACGAAATATTCTATGTCATTTG
<i>norB</i> _spacer-F2	GAAACAACGCTTTTAGGTTGGCGT
<i>norB</i> _spacer-R2	AAACACACGAATCATAATTAGTAC
<i>norB</i> _WtSeq-F	CCTGCTCCTACTACAAACATTCC
<i>norB</i> _MtSeq-F	CGATTCAATACAATTTTCGCAATCTATCC
<i>norB</i> _MtSeq-R	GCAGCATAAGGTAAGATAACTAGCA
Overexpression	
<i>norB</i> _promoter (forward)	GCGCGGATCCGCATTGAGAATAAATGGATGGACTAC
<i>norB</i> _promoter (reverse)	GCGCGAATTCTCATAATTGAGTGTCGTTTTGTTTA
pSK_backbone (forward)	GGTTACAATAGCGACGGAGAG
pSK_backbone (reverse)	TTCTAATGTCACTAACCTGCC
<i>norB</i> _confirmation (forward)	CAAACACTCGGATGCAAGAAAC
<i>norB</i> _confirmation (reverse)	GGTGTGAAATACCGCACAGA
Allelic exchange - <i>norB</i> mutant	
<i>norB</i> -A(<i>KpnI</i>)	ATGCGGTACCATTCGCAAATTAACAAAAT
<i>norB</i> -B	CATCTCTATTTGCCTCCCTATACTTTTGA
<i>norB</i> -C	GGCAAATAGAGATGTAATTGAGAATTAATTGAAATCATACAAGTCGC
<i>norB</i> -D (<i>SacI</i>)	CTCGAGCTCGATTCTCAGTCTGTTTCATTATTAC

Appendix A7 – Supplementary information for Chapter 2 and 3

Table 2A – List of plasmids used in this thesis.

Plasmid	Characteristics	Size (bp)	Reference
CRISPR-Cas9			
<i>E. coli</i> / <i>S. aureus</i> plasmid			
pCasSA	Bacterial Resistance(s) – Kanamycin and Chloramphenicol Growth Temperature – 30 °C (temperature sensitive) Copy number – High Copy	10240	[205]
Overexpression			
<i>Shuttle plasmid</i>			
pSK5632	Bacterial Resistance(s) – Ampicillin and Chloramphenicol Growth Temperature – 37 °C Copy number – Low Copy	5920	[237]
Allelic exchange			
<i>E. coli</i> / <i>Staphylococcal</i> spp. temperature-sensitive plasmid for allelic exchange			
pIMAY	Bacterial Resistance – Chloramphenicol Growth Temperature – 37 °C Copy number – Low Copy	5743	[202]

Appendix A8 – Supplementary information for Chapter 3

Table 3A – List of virulence genes and associated virulence factor detected in *S. aureus* (four TRS and one laboratory strain) using VFDB-VFalyzer9 data base (✓ - gene present, ✗ - gene absent).

Gene	<i>S. aureus</i> CBS 2016-05	<i>S. aureus</i> CI/BAC/ 25/13/W	<i>S. aureus</i> PS/BAC/ 169/17/W	<i>S. aureus</i> PS/BAC/ 317/16/W	<i>S. aureus</i> RN6390
Adherence					
<i>atl</i>	✓	✓	✓	✓	✓
<i>clfA</i>	✓	✓	✓	✓	✓
<i>clfB</i>	✓	✓	✓	✓	✓
<i>cna</i>	✓	✓	✓	✓	✗
<i>eap/map</i>	✓	✓	✓	✓	✗
<i>ebps</i>	✓	✓	✓	✓	✓
<i>fnbA</i>	✓	✓	✓	✓	✓
<i>fnbB</i>	✗	✓	✗	✓	✓
<i>sdrC</i>	✓	✓	✓	✓	✓
<i>sdrD</i>	✗	✗	✗	✓	✓
<i>sdrE</i>	✗	✗	✗	✗	✗
<i>sdrF</i>	✗	✗	✗	✗	✗
<i>sdrG</i>	✗	✗	✗	✓	✗
<i>sdrH</i>	✓	✓	✓	✓	✓
Secretion system					
<i>esxA</i>	✗	✓	✓	✓	✓
<i>esaA</i>	✗	✓	✓	✓	✓
<i>essA</i>	✗	✓	✓	✓	✓
<i>esaB</i>	✗	✓	✓	✓	✓
<i>essB</i>	✗	✓	✓	✓	✓
<i>essC</i>	✓	✓	✓	✓	✓
<i>esxC</i>	✓	✗	✗	✗	✓
<i>esxB</i>	✓	✗	✗	✗	✓
<i>esaE</i>	✓	✗	✗	✗	✓
<i>esxD</i>	✓	✗	✗	✗	✓
<i>esaD</i>	✗	✗	✗	✗	✓
<i>esaG</i>	✓	✓	✓	✓	✓
Biofilm					
<i>icaR</i>	✓	✓	✓	✓	✓
<i>icaA</i>	✓	✓	✓	✓	✓
<i>icaD</i>	✓	✓	✓	✓	✓
<i>icaB</i>	✓	✓	✓	✓	✓
<i>icaC</i>	✓	✓	✓	✓	✓

Table 3A – List of virulence genes and associated virulence factor detected in *S. aureus* (cont.)

Gene	<i>S. aureus</i> CBS 2016-05	<i>S. aureus</i> CI/BAC/ 25/13/W	<i>S. aureus</i> PS/BAC/ 169/17/W	<i>S. aureus</i> PS/BAC/ 317/16/W	<i>S. aureus</i> RN6390
Exotoxins					
<i>hly/hla</i>	✓	✓	✓	✓	✓
<i>hlb</i>	✗	✗	✗	✗	✗
<i>hld</i>	✓	✓	✓	✓	✓
<i>hlgA</i>	✓	✓	✓	✓	✓
<i>hlgC</i>	✓	✓	✓	✓	✓
<i>hlgB</i>	✓	✓	✓	✓	✓
<i>lukD</i>	✗	✓	✗	✓	✓
<i>lukE</i>	✗	✓	✗	✓	✓
<i>lukH</i>	✓	✓	✓	✓	✓
<i>lukG</i>	✓	✓	✓	✓	✗
<i>sea</i>	✗	✓	✗	✗	✗
<i>seb</i>	✗	✓	✗	✗	✗
<i>seg</i>	✓	✗	✓	✗	✗
<i>seh</i>	✓	✗	✗	✗	✗
<i>sei</i>	✓	✗	✓	✗	✗
<i>sem</i>	✓	✗	✓	✗	✗
<i>sen</i>	✓	✗	✓	✗	✗
<i>seo</i>	✓	✗	✓	✗	✗
<i>selp</i>	✗	✓	✗	✗	✗
<i>ses</i>	✓	✗	✗	✗	✗
<i>seu</i>	✓	✗	✓	✗	✗
<i>selw</i>	✓	✓	✓	✓	✗
<i>selx</i>	✓	✓	✗	✗	✗
<i>sely</i>	✓	✗	✗	✗	✗
<i>selz</i>	✗	✗	✗	✗	✗
<i>se(exo)</i>	✓	✗	✗	✗	✗
<i>spa</i>	✓	✓	✓	✓	✓
<i>ssl1</i>	✓	✓	✓	✓	✓
<i>ssl2</i>	✗	✓	✓	✓	✓
<i>ssl3</i>	✗	✓	✓	✓	✓
<i>ssl4</i>	✓	✓	✓	✓	✓
<i>ssl5</i>	✓	✓	✓	✓	✓
<i>ssl6</i>	✗	✗	✗	✗	✓
<i>ssl7</i>	✓	✓	✓	✓	✓

Table 3A – List of virulence genes and associated virulence factor detected in *S. aureus* (cont.)

Gene	<i>S. aureus</i> CBS 2016-05	<i>S. aureus</i> CI/BAC/ 25/13/W	<i>S. aureus</i> PS/BAC/ 169/17/W	<i>S. aureus</i> PS/BAC/ 317/16/W	<i>S. aureus</i> RN6390
<i>ssl8</i>	✓	✓	✗	✗	✓
<i>ssl9</i>	✓	✓	✓	✓	✓
<i>ssl10</i>	✓	✓	✓	✓	✓
<i>ssl11</i>	✓	✓	✓	✓	✓
<i>ssl12</i>	✓	✓	✓	✓	✓
<i>ssl13</i>	✓	✓	✓	✓	✓
<i>ssl14</i>	✓	✓	✓	✓	✓
<i>tsst-1</i>	✗	✗	✗	✗	✗
Enzymes					
<i>hysA</i>	✓	✓	✓	✓	✓
<i>lip</i>	✓	✓	✓	✓	✓
<i>geh</i>	✓	✓	✓	✓	✓
<i>spIA</i>	✗	✓	✗	✓	✓
<i>spIB</i>	✗	✓	✗	✓	✓
<i>spIC</i>	✗	✓	✓	✓	✓
<i>spID</i>	✗	✓	✗	✓	✓
<i>spIE</i>	✗	✓	✓	✓	✓
<i>spIF</i>	✗	✓	✓	✓	✓
<i>sspB</i>	✓	✓	✓	✓	✓
<i>sspC</i>	✓	✓	✓	✓	✓
<i>coa</i>	✓	✓	✓	✓	✓
<i>sak</i>	✓	✓	✗	✗	✓
<i>nuc</i>	✓	✓	✓	✓	✓
<i>sspA</i>	✓	✓	✓	✓	✓
Immune modulation					
<i>adsA</i>	✓	✓	✓	✓	✓
<i>capsular</i>	✓	✓	✓	✓	✓
<i>ebh</i>	✓	✓	✓	✓	✓
<i>chp</i>	✓	✗	✓	✓	✗
<i>efb</i>	✓	✓	✓	✓	✓
<i>sbi</i>	✓	✓	✓	✓	✓
<i>scn</i>	✓	✓	✓	✓	✗
<i>crtL</i>	✓	✓	✓	✓	✓
<i>crtQ</i>	✓	✓	✓	✓	✓
<i>crtP</i>	✓	✓	✓	✓	✓
<i>crtM</i>	✓	✓	✓	✓	✓
<i>crtN</i>	✓	✓	✓	✓	✓

Appendix A9 – Supplementary information for Chapter 3

Table 4A – List regulatory systems and two component systems (TCS) involved in virulence (✓ - gene present, ✗ - gene absent).

Regulator system	Genes	<i>S. aureus</i> CBS 2016-05	<i>S. aureus</i> CI/BAC/ 25/13/W	<i>S. aureus</i> PS/BAC/ 169/17/W	<i>S. aureus</i> PS/BAC/ 317/16/W	<i>S. aureus</i> RN6390
Cell-to-cell communication (quorum sensing)	<i>agrA</i>	✓	✓	✓	✓	✓
	<i>agrB</i>	✓	✓	✓	✓	✓
	<i>agrC</i>	✓	✓	✓	✓	✓
	<i>agrD</i>	✓	✓	✓	✓	✓
Induction of exo-protein production	<i>saeR</i>	✓	✓	✓	✓	✓
	<i>saeS</i>	✓	✓	✓	✓	✓
Oxygen-responsive TCS; repression of <i>agr</i> , TSST-1, and <i>spa</i>	<i>srrA</i>	✓	✓	✓	✓	✓
	<i>srrB</i>	✓	✓	✓	✓	✓
Autolysis and cell surface TCS and repression of <i>agr</i> and autolysis	<i>arlR</i>	✓	✓	✓	✓	✓
	<i>arlS</i>	✓	✓	✓	✓	✓
Cytoplasmic regulator; induction of exo-proteins and repression of <i>spa</i>	<i>sarA</i>	✓	✓	✓	✓	✓
Cytoplasmic regulator of toxins and extracellular proteases	<i>rot</i>	✓	✓	✓	✓	✓
Cytoplasmic regulator; induction of efflux pumps	<i>mgrA</i>	✓	✓	✓	✓	✓
RNAP (RNA polymerase holoenzyme)	<i>sigB</i>	✓	✓	✓	✓	✓
Virulence transcription factor	<i>kdpD</i>	✓	✓	✓	✓	✓
	<i>kdpE</i>	✓	✓	✓	✓	✓

Appendix A10 – Supplementary information for Chapter 3

Table 5A – List of possible housekeeping genes and their differential gene expression (RNA-seq data, PCs vs TSB).

Proteins	Genes	CBS 2016-05	PS/BAC/ 317/16/W	CI/BAC/ 25/13/W	PS/BAC/ 169/17/W	Pathways
Multidrug H+ antiporter, MFS transporter	<i>norA</i>	-0.55	-1.26	<i>nde</i>	-1.22	Efflux Pump
Quinolone resistance protein; Integral membrane efflux protein;	<i>norB</i>	1.97	2.83	4.71	1.23	
Transmembrane efflux protein; Integral membrane efflux protein;	<i>norC</i>	<i>nde</i>	<i>nde</i>	<i>nde</i>	<i>nde</i>	
Transmembrane efflux transporter; Drug: H+ antiporter-2 family; Multidrug efflux transporter	<i>mdeA</i>	<i>nde</i>	-1.29	0.37	-1.46	
Drug resistance transporter; Putative transport protein, Drug: H+ SAV1866 family putative multidrug efflux ABC transporter	<i>lmrS</i>	-1.24	-2.5	-0.77	-0.62	
ATP-binding protein	<i>msbA</i>	0.63	0.4	-1.42	<i>nde</i>	
Peptide-methionine (S)-S-oxide reductase	<i>bmrA</i>	-2.29	-0.46	-0.88	-3.17	
ABC-F type ribosomal protection protein	<i>msrA</i>	<i>nde</i>	-1.02	0.4	-1.62	
Multidrug efflux transporter	<i>yheS</i>	<i>nde</i>	<i>nde</i>	0.51	<i>nde</i>	
SepA	<i>sepA</i>	-0.87	-0.89	-8.47	<i>nde</i>	

Proteins	Genes	CBS 2016-05	PS/BAC/ 317/16/W	CI/BAC/ 25/13/W	PS/BAC/ 169/17/W	Pathways	
Methicillin resistance regulatory protein; Beta- lactamase regulator protein	<i>mecI</i>	-1.64	<i>nde</i>	<i>nde</i>	0.7	Enzymes	
Glycosyltransferase; Penicillin- binding protein 2A	<i>mgt</i>	1.32	<i>nde</i>	2.9	<i>nde</i>		
D-alanyl-D- alanine carboxypeptidase; Penicillin binding protein PBP4	<i>dacA</i>	-1.12	1.85	-1.08	1.1		
DNA Topoisomerase IV subunit A	<i>parC</i>	-1.59	<i>nde</i>	<i>nde</i>	<i>nde</i>		
DNA Topoisomerase IV subunit B	<i>parE</i>	-0.93	<i>nde</i>	<i>nde</i>	<i>nde</i>		
DNA gyrase subunit A	<i>gyrA</i>	<i>nde</i>	<i>nde</i>	0.8	<i>nde</i>		
DNA gyrase subunit B	<i>gyrB</i>	0.73	<i>nde</i>	0.69	-0.62		
DNA-dependent RNA polymerase auxiliary subunit epsilon family protein	<i>rpoY</i>	0.98	1.27	<i>nde</i>	1.14		
16S rRNA (adenine(1518)- N(6)/adenine(15 19)-N(6))- dimethyltransferase RsmA	<i>rsmA</i>	-0.94	<i>nde</i>	0.98	<i>nde</i>		
23S rRNA (pseudouridine(1 915)-N(3))- methyltransferase RlmH	<i>rlmH</i>	0.57	<i>nde</i>	<i>nde</i>	-1.53		
Isochorismatase; Cysteine hydrolase; Nicotinamidase; Pyrazinamidase	<i>rutB</i>	-0.37	0.5	<i>nde</i>	1.7		
accessory gene regulator AgrB	<i>agrB</i>	-2	-1.8	-3.7	<i>nde</i>		Agr quorum sensing/ surface proteins
cyclic lactone autoinducer peptide	<i>agrD</i>	-1.99	-2.0	-3.7	<i>nde</i>		

Proteins	Genes	CBS 2016-05	PS/BAC/ 317/16/W	CI/BAC/ 25/13/W	PS/BAC/ 169/17/W	Pathways
GHKL domain- containing protein response regulator	<i>agrC</i>	-2	-1.8	-3.6	<i>nde</i>	
transcription factor	<i>agrA</i>	-2.11	-1.6	-3.5	0.1	
bi-component gamma- hemolysin	<i>hlgB</i>	-3.21	-2.44	0.42	0.43	
HlgAB/HlgCB bi-component gamma- hemolysin HlgCB subunit C	<i>hlgC</i>	-2.82	-2.5	-7.77	0.43	
bi-component gamma- hemolysin HlgAB subunit A	<i>hlgA</i>	-2.92	-5.26	-8.92	0.43	
delta-hemolysin	<i>hld</i>	-7.55	-2.19	-2.8	1.1	
alpha-hemolysin	<i>hyl</i>	1.22	-1.68	<i>nde</i>	<i>nde</i>	
phenol-soluble modulin PSM- alpha-1	<i>PSM- alpha- 1</i>	-11.93	-7.95	-6.06	-2.00	
phenol-soluble modulin PSM- alpha-2	<i>PSM- alpha- 2</i>	-11.48	<i>nde</i>	-5.83	<i>nde</i>	
phenol-soluble modulin PSM- alpha-3	<i>PSM- alpha- 3</i>	-9.91	-9.08	-8.09	<i>nde</i>	
phenol-soluble modulin PSM- alpha-4	<i>PSM- alpha- 4</i>	-4.63	<i>nde</i>	-5.54	<i>nde</i>	
beta-class phenol-soluble modulin-1	<i>psm beta1</i>	-8.71	-7.87	-5.01	-1.18	
beta-class phenol-soluble modulin-2	<i>psm beta2</i>	-8.06	<i>nde</i>	-4.43	<i>nde</i>	
Glu-specific serine endopeptidase	<i>sspA</i>	-5.13	2	-0.88	2.35	
cysteine protease	<i>sspB</i>	-4.09	<i>nde</i>	-0.92	1.74	
staphopain B	<i>sspC</i>	-4.09	<i>nde</i>	-0.94	1.61	
staphostatin B	<i>sspC</i>	-4.09	<i>nde</i>	-0.94	1.61	
cell-wall- anchored protein	<i>sasF</i>	1.7	<i>nde</i>	3.22	0.57	
LPXTG cell wall anchor domain- containing protein	<i>sasD</i>	2.82	-3.87	-2.87	0.23	

Proteins	Genes	CBS 2016-05	PS/BAC/ 317/16/W	CI/BAC/ 25/13/W	PS/BAC/ 169/17/W	Pathways
serine-rich repeat glycoprotein adhesin SasA	<i>sasA</i>	1.96	<i>nde</i>	0.82	1.13	
fibrinogen-binding adhesin SdrG C-terminal	<i>sdrG</i>	<i>nde</i>	1.34	<i>nde</i>	<i>nde</i>	
autolysin/adhesin MSCRAMM family adhesin clumping factor MSCRAMM family adhesin clumping factor	<i>aaa</i>	-2.45	2.79	1.04	0.34	
	<i>clfA</i>	1.55	-1.39	0.15	-0.56	
	<i>clfB</i>	2.24	2.58	2.11	-0.12	
staphylococcal protein A	<i>spa</i>	5.8	-1.52	-1.00	2.63	Immune evasion
myeloperoxidase inhibitor SPIN	<i>spn</i>	-5.94	-3.22	-10.18	-0.86	
complement inhibitor SCIN-A	<i>scn</i>	-3.04	-2.43	-3.31	0.03	
extracellular adherence protein Eap/Map	<i>eap</i>	-3.57	<i>nde</i>	-5.99	0.72	
MAP domain-containing protein	<i>map</i>	-2.8	<i>nde</i>	-0.30	0.58	
staphylocoagulase	<i>coa</i>	-3.89	<i>nde</i>	-0.50	0.48	Other virulence factors
von Willebrand factor binding protein Vwb	<i>vwb</i>	1.41	<i>nde</i>	1.46	-0.07	
YSIRK domain-containing triacylglycerol lipase	<i>lip1</i>	-2.24	-5.34	-2.41	-4.42	
YSIRK domain-containing triacylglycerol lipase	<i>lip2/geh</i>	2.28	-1.22	-0.62	5.47	
phosphatidylinositol-specific phospholipase C	<i>plc</i>	<i>nde</i>	2.61	4.13	4.76	
	<i>crtM</i>	2.25	-1.20	-0.48	-0.81	
	<i>crtN</i>	1.90	<i>nde</i>	-0.87	-0.82	
Staphyloxanthin	<i>crtO</i>	<i>nde</i>	-3.05	0.11	-1.12	
	<i>crtP</i>	2.08	-2.38	<i>nde</i>	<i>nde</i>	
	<i>crtQ</i>	2.51	-2.00	-0.49	<i>nde</i>	
type 8 capsular polysaccharide synthesis protein	<i>cap8P</i>	2.46	1.55	0.67	0.98	Capsule Biosynthesis

Proteins	Genes	CBS 2016-05	PS/BAC/ 317/16/W	CI/BAC/ 25/13/W	PS/BAC/ 169/17/W	Pathways
type 8 capsular polysaccharide synthesis protein	<i>cap8O</i>	4.11	1.5	0.31	0.99	
capsular polysaccharide type 5/8 biosynthesis epimerase	<i>capN</i>	4.35	1.8	0.61	1.00	
type 8 capsular polysaccharide synthesis protein	<i>cap8M</i>	4.52	<i>nde</i>	0.90	1.11	
type 8 capsular polysaccharide synthesis protein	<i>cap8L</i>	4.7	1.84	0.81	1.14	
capsular biosynthesis protein	<i>cap8K</i>	4.89	2.04	0.75	0.95	
O-antigen ligase family protein	<i>cap8J</i>	4.74	2.08	0.82	0.93	
glycosyltransferase	<i>cap8I</i>	4.94	2.03	0.98	0.99	
antibiotic acetyltransferase	<i>cap8H</i>	5.22	2.13	0.87	1.05	
type 8 capsular polysaccharide synthesis protein	<i>cap8G</i>	5.4	1.81	0.92	1.15	
type 8 capsular polysaccharide synthesis protein	<i>cap8F</i>	5.5	1.64	1.02	1.19	
type 8 capsular polysaccharide synthesis protein	<i>cap8E</i>	5.43	1.5	1.06	1.25	
type 8 capsular polysaccharide synthesis protein	<i>cap8D</i>	5.56	1.23	1.15	1.22	
type 8 capsular polysaccharide synthesis protein	<i>cap8C</i>	5.83	<i>nde</i>	1.48	1.17	
type 8 capsular polysaccharide synthesis protein	<i>cap8B</i>	5.93	<i>nde</i>	1.18	0.65	
capsular polysaccharide type 5/8 biosynthesis	<i>capA</i>	5.89	<i>nde</i>	1.35	0.60	
response regulator transcription factor	<i>kdpE</i>	2.24	1.86	2.83	2.68	Potassium transport
sensor histidine kinase KdpD	<i>kdpD</i>	2.57	2.01	3.25	2.95	
potassium-transporting	<i>kdpA</i>	4.97	2.62	4.52	5.17	

Proteins	Genes	CBS 2016-05	PS/BAC/ 317/16/W	CI/BAC/ 25/13/W	PS/BAC/ 169/17/W	Pathways
ATPase subunit A potassium- transporting	<i>kdpB</i>	3.77	1.38	nde	4.39	
ATPase subunit KdpB						
K(+)-transporting ATPase subunit C	<i>kdpC</i>	3.82	1.21	3.22	4.10	
K(+)-transporting ATPase subunit C	<i>kdpC</i>	7.06	nde	nde	nde	
K(+)-transporting ATPase subunit B	<i>kdpB</i>	6.79	nde	nde	nde	
potassium- transporting ATPase subunit A	<i>kdpA</i>	6.55	nde	nde	nde	
sensor histidine kinase KdpD	<i>kdpD</i>	2.99	nde	nde	nde	
response regulator transcription factor	<i>kdpE</i>	2.71	nde	nde	nde	
pyruvate formate lyase-activating protein	<i>pflA</i>	6.59	1.95	7.26	5.81	Anaerobic/ aerobic metabolism
formate C- acetyltransferase	<i>pflB</i>	4.44		6.21	4.84	
acetolactate synthase AlsS	<i>alsS</i>	6.89	5.73	5.01	5.79	
acetolactate decarboxylase	<i>budA</i>	6.76	5.79	5.24	6.21	
anaerobic ribonucleoside- triphosphate reductase	<i>nrdD</i>	3.12	1.09	1.72	2.45	
anaerobic ribonucleoside- triphosphate reductase	<i>nrdG</i>	5.05	2.65	4.04	3.46	
activating protein class 1b						
ribonucleoside- diphosphate reductase subunit beta class 1b	<i>nrdF</i>	nde	2.48	0.63	1.02	
ribonucleoside- diphosphate reductase subunit alpha	<i>nrdE</i>	nde	2.38	0.76	1.04	

Proteins	Genes	CBS 2016-05	PS/BAC/ 317/16/W	CI/BAC/ 25/13/W	PS/BAC/ 169/17/W	Pathways
class Ib ribonucleoside- diphosphate reductase assembly flavoprotein NrdI	<i>nrdI</i>	<i>nde</i>	2.32	1.03	1.44	
threonine ammonia-lyase IlvA 3-	<i>ilvA</i>	-4.94	1.22	-0.19	0.46	Amino Acid metabolism
isopropylmalate dehydratase small subunit 3-	<i>leuD</i>	-5.14	1.08	-0.47	0.48	
isopropylmalate dehydratase large subunit 3-	<i>leuC</i>	-5.18	<i>nde</i>	-0.33	0.38	
isopropylmalate dehydrogenase 2-	<i>leuB</i>	-5.38	<i>nde</i>	-0.32	0.45	
isopropylmalate synthase ketol-acid reductoisomeras e	<i>leuA</i>	-5.58	<i>nde</i>	-0.48	0.37	
ACT domain- containing protein	<i>ilvC</i>	-5.74	<i>nde</i>	-0.16	0.47	
ACT domain- containing protein	<i>ilvH</i>	-5.59	1.87	<i>nde</i>	<i>nde</i>	
biosynthetic-type acetolactate synthase large subunit	<i>ilvB</i>	-5.57	1.94	-0.19	0.85	
dihydroxy-acid dehydratase	<i>ilvD</i>	-4.93	2.25	-0.20	1.28	
branched-chain amino acid transport system II carrier protein	<i>brnQ</i>	1.68	2.5	1.45	0.54	
betaine-aldehyde dehydrogenase	<i>betB</i>	6.74	3.64	3.83	-0.77	
choline dehydrogenase	<i>betA</i>	3.46	2.75	2.81	-1.35	
superoxide dismutase	<i>sodA</i>	3.02	<i>nde</i>	-0.82	1.96	
superantigen-like protein SSL14	<i>SSL14</i>	6.66	<i>nde</i>	3.00	4.34	Superantigens
superantigen-like protein SSL13	<i>SSL13</i>	5.68	<i>nde</i>	2.65	<i>nde</i>	
superantigen-like protein SSL12	<i>SSL12</i>	4.75	<i>nde</i>	1.72	<i>nde</i>	
superantigen-like protein SSL11	<i>SSL11</i>	<i>nde</i>	<i>nde</i>	-1.86	-0.54	

Proteins	Genes	CBS 2016-05	PS/BAC/ 317/16/W	CI/BAC/ 25/13/W	PS/BAC/ 169/17/W	Pathways
superantigen-like protein SSL10	<i>SSL10</i>	1.41	<i>nde</i>	-0.05	0.11	
staphylococcal enterotoxin type H	<i>seh</i>	2.3	<i>nde</i>	<i>nde</i>	<i>nde</i>	
exotoxin		3.58	<i>nde</i>	<i>nde</i>	0.60	
oleate hydratase	<i>ohyA</i>	5.55	<i>nde</i>	3.55	2.46	
cell wall integrity	<i>lytS</i>	1	1.25	3.66	1.99	Regulators
	<i>lytR</i>	1.15	1.85	5.17	2.42	
membrane charge alternation	<i>graF</i>	1.23	1.19	-0.32	-1.41	
<i>vraXSR</i> (cell wall synthesis)	<i>vraX</i>	3.17	-3.53	2.12	-1.17	
	<i>vraS</i>	0.95	-0.5	2.44	0.15	
	<i>vraR</i>	0.99	-0.95	2.43	-0.16	
<i>sarVRX</i> (biofilm & virulence)	<i>sarV</i>	1.86	1.35	0.42	2.29	
	<i>sarR</i>	1.81	1.14	0.12	1.16	
	<i>sarX</i>	1.49	1.92	-0.84	2.73	
General stress response	<i>sigB</i>	1.1	0.7	-0.1	1.77	
	<i>sigA</i>	1.02	0.65	0.14	0.54	
	<i>sigS</i>	-0.71	0.65	1.77	0.66	
	<i>sigH</i>	-0.8	1.66	0.78	0.5	
	<i>perR</i>	0.35	-0.21	0.32	0.28	
<i>perR/spx</i> (antioxidants; ROS)	<i>spx</i>	0.07	1.84	0.91	2.28	
<i>ctsR</i> (chaperones & proteases)	<i>ctsR</i>	1.21	-0.28	-0.03	-1.94	
Oxygen-responsive TCS	<i>srrA</i>	1.4	<i>nde</i>	1.4	<i>nde</i>	
	<i>srrB</i>	0.08	1.41	0.05	0.55	
<i>walRK</i> (cell wall integrity)	<i>walR</i>	1.03	0.91	0.93	0.35	
	<i>walK</i>	0.57	0.54	0.85	0.18	
<i>arlSR</i> (general acid response)	<i>arlS</i>	1.36	0.45	-0.06	0.24	
	<i>arlR</i>	1.04	0.13	-0.32	-0.26	
<i>cadC</i> (<i>cadA</i>)	<i>cadC</i>	-0.03	-0.03	1	-0.03	
<i>fur</i> (acid)	<i>fur</i>	0.22	-0.56	-0.55	0.34	
<i>codY</i> (global nutrient regulator)	<i>codY</i>	0.28	0.02	0.97	-0.06	
<i>ccpA</i> (carbohydrates)	<i>ccpA</i>	-0.4	-0.14	-0.7	-0.01	
<i>phoRP</i> (phosphates)	<i>phoR</i>	-0.34	-1.37	-0.52	-2.19	
	<i>phoP</i>	-1.55	0.01	-1.03	-3.41	
<i>mntH</i> & <i>zntR</i> (Mn ²⁺ & Zn ²⁺)	<i>mntH</i>	-2.36	-3.12	-1.67	-0.37	

Proteins	Genes	CBS 2016-05	PS/BAC/ 317/16/W	CI/BAC/ 25/13/W	PS/BAC/ 169/17/W	Pathways
	<i>zntR</i>	3.08	1.08	3.37	-0.53	
<i>rot</i> (amino acids)	<i>rot</i>	1.05	-0.95	0.05	-0.65	
<i>rpiAR</i> (pentose)	<i>rpiA</i>	1.1	0.39	1	0.2	
	<i>rpiR</i>	-0.31	-0.13	-2.29	-0.46	
response regulator transcription factor	<i>saeR</i>	-3.15	-1.44	-5.7	0.2	
two-component system sensor histidine kinase	<i>saeS</i>	-3.33	-1.31	-5.8	0.2	

Appendix A11 – Supplementary information for Chapter 3

Table 6A – List of genes encoding for antibiotic resistance mechanism generated using the CARD curated data (✓ - gene present, ✗ - gene absent).

Resistant Mechanisms	Related genes	<i>S. aureus</i> CBS 2016-05	<i>S. aureus</i> CI/BAC/ 25/13/W	<i>S. aureus</i> PS/BAC/ 169/17/W	<i>S. aureus</i> PS/BAC/ 317/16/W	<i>S. aureus</i> RN6390
Efflux pumps						
Major Facilitator Superfamily (MFS)	<i>arlR</i>	✓	✓	✓	✓	✓
	<i>arlS</i>	✓	✓	✓	✓	✓
	<i>sdrM</i>	✓	✓	✓	✓	✓
	<i>lmrS</i>	✓	✓	✓	✓	✓
	<i>norC</i>	✓	✓	✓	✓	✓
	<i>norA</i>	✓	✓	✓	✓	✓
	<i>norB</i>	✓	✓	✓	✓	✓
Multidrug and toxic compound extrusion (MATE) transporter	<i>mepR</i>	✓	✓	✓	✓	✓
	<i>mepA</i>	✓	✓	✓	✓	✓
ATP-binding cassette (ABC)	<i>mgrA</i>	✓	✓	✓	✓	✓
	<i>sav1866</i>	✓	✓	✓	✓	✓
Small Multidrug Resistance (SMR)	<i>sepA</i>	✓	✓	✓	✓	✓
Resistance-Nodulation-Division (RND)	<i>farE</i>	✓	✓	✓	✓	✓
	<i>femT</i>	✓	✓	✓	✓	✓
	<i>secDF</i>	✓	✓	✓	✓	✓
Enzymatic inactivation						
Aminoglycoside resistance	<i>ANT(9)-Ia</i>	✗	✗	✗	✗	✗
	<i>ANT(4')-Ia</i>	✗	✗	✗	✗	✗
	<i>ANT(6)-Ia</i>	✗	✗	✗	✗	✗
	<i>APH(3')-IIIa</i>	✗	✗	✗	✗	✗
Fosfomycin resistance	<i>fosB</i>	✗	✓	✓	✓	✓
β-lactam resistance	<i>blaZ</i>	✓	✗	✓	✓	✗
Macrolite resistance	<i>mph(C)</i>	✗	✗	✗	✗	✗

Table 6A – List of genes encoding for antibiotic resistance mechanism generated using the CARD curated data (Cont.).

Resistant Mechanisms	Genes	<i>S. aureus</i> CBS 2016-05	<i>S. aureus</i> CI/BAC/ 25/13/W	<i>S. aureus</i> PS/BAC/ 169/17/W	<i>S. aureus</i> PS/BAC/ 317/16/W	<i>S. aureus</i> RN6390
Target modification						
Methicillin resistance (PBP2)	<i>mecA</i>	✓	✓	✓	✓	✓
	<i>mecR1</i>	✗	✗	✗	✗	✗
	<i>mecI</i>	✗	✗	✗	✗	✗
Trimethoprim resistance	<i>dfpG</i>	✗	✗	✗	✗	✗
Macrolides, Lincosamides, & Streptogramins resistance	<i>erm(A)</i>	✗	✗	✗	✗	✗
	<i>erm(T)</i>	✗	✗	✗	✗	✗
Quinolone resistance	<i>gyrA</i>	✓	✓	✓	✓	✓
	<i>gyrB</i>	✓	✓	✓	✓	✓
Fluoroquinolone resistance	<i>parC</i>	✓	✓	✓	✓	✓
Fosfomycin resistance	<i>murA</i>	✓	✓	✓	✓	✓
	<i>glpT</i>	✓	✓	✓	✓	✓
Fusidic Acid resistance	<i>fusA</i>	✓	✓	✓	✓	✓
Target protection						
Erythromycin resistance	<i>msrA</i>	✓	✓	✓	✓	✓

Appendix A12 – Supplementary information for Chapter 2 and 3

Table 7A – List of possible housekeeping genes and their differential gene expression (RNA-seq data, PCs vs TSB, *nde* – not differentially expressed).

Housekeeping genes	CBS 2016-05	CI/BAC/ 25/13/W	PS/BAC/ 169/17/W	PS/BAC/ 317/16/W
<i>gyrA</i> (DNA gyrase A)	<i>nde</i>	-0.24	0.80	<i>nde</i>
<i>gyrB</i> (DNA gyrase B)	0.73	-0.10	0.69	-0.62
<i>arcC</i> (Carbamate kinase)	4.77	3.71	4.91	0.38
<i>aroE</i> (Shikimate dehydrogenase)	<i>nde</i>	0.81	0.15	<i>nde</i>
<i>fabD</i> (Malonyl-CoA-acyl carrier protein transacylase)	-0.39	-0.74	0.05	-0.74
<i>glpF</i> (Glycerol kinase)	-0.30	0.54	-0.48	0.98
<i>gmk*</i> (Guanylate kinase)	<i>nde</i>	0.73	0.04	1.35
<i>pta</i> (Phosphate acetyltransferase)	-0.77	-0.69	0.59	-0.20
<i>proC</i> (Pyrroline-5- carboxylate reductase)	<i>nde</i>	-0.53	-0.44	<i>nde</i>
<i>rpoB</i> (RNA polymerase subunit B)	<i>nde</i>	0.32	0.51	<i>nde</i>
<i>tpi / tpiA</i> (Triosephosphate isomerase)	-0.80	-2.73	-0.94	-3.12
16S rRNA (16S ribosomal RNA)	<i>nde</i>	<i>nde</i>	<i>nde</i>	<i>nde</i>

References

1. Paredes, C., Truong-Bolduc, Q. C., Wang, Y., Hooper, D. C., & Ramirez-Arcos, S. (2025). Enhanced Quinolone Resistance and Differential Expression of Efflux Pump nor Genes in *Staphylococcus aureus* Grown in Platelet Concentrates. *Antibiotics*, *14*(7), 635. <https://doi.org/10.3390/antibiotics14070635>
2. Greenwalt, T. J. (1997). A short history of transfusion medicine. *Transfusion*, *37*(5), 550–563. <https://doi.org/10.1046/j.1537-2995.1997.37597293889.x>
3. Roseborough, A., & Sanatham, D. (2021). An infusion of history: Transfusion medicine from the 17th century to current emergency practices. *University of Western Ontario Medical Journal*. <https://doi.org/10.5206/uwomj.v89i2.10516>
4. Gullbring, B. (1964). The Use of Plastics in Blood Transfusion Equipment with Special Regard to Toxicity Problems: EDITORIAL. *Vox Sanguinis*, *9*(5), 513–529. <https://doi.org/10.1111/j.1423-0410.1964.tb03323.x>
5. Ramirez-Arcos, S., & Goldman, M. (2017). Bacterial Contamination. In *Practical Transfusion Medicine* (5th ed., pp. 177–184). Practical Transfusion Medicine.
6. Ramirez-Arcos, S., Evans, S., McIntyre, T., Pang, C., Yi, Q., DiFranco, C., & Goldman, M. (2020). Extension of platelet shelf life with an improved bacterial testing algorithm. *Transfusion*, *60*(12), 2918–2928. <https://doi.org/10.1111/trf.16112>
7. Sang, Y., Roest, M., De Laat, B., De Groot, P. G., & Huskens, D. (2021). Interplay between platelets and coagulation. *Blood Reviews*, *46*, 100733. <https://doi.org/10.1016/j.blre.2020.100733>

8. Cimmino, G., & Golino, P. (2013). Platelet Biology and Receptor Pathways. *Journal of Cardiovascular Translational Research*, 6(3), 299–309. <https://doi.org/10.1007/s12265-012-9445-9>
9. Stegner, D., vanEeuwijk, J. M. M., Angay, O., Gorelashvili, M. G., Semeniak, D., Pinnecker, J., Schmithausen, P., Meyer, I., Friedrich, M., Dütting, S., Brede, C., Beilhack, A., Schulze, H., Nieswandt, B., & Heinze, K. G. (2017). Thrombopoiesis is spatially regulated by the bone marrow vasculature. *Nature Communications*, 8(1), 127. <https://doi.org/10.1038/s41467-017-00201-7>
10. Machlus, K. R., & Italiano, J. E. (2013). The incredible journey: From megakaryocyte development to platelet formation. *Journal of Cell Biology*, 201(6), 785–796. <https://doi.org/10.1083/jcb.201304054>
11. Janus-Bell, E., & Mangin, P. H. (2023). The relative importance of platelet integrins in hemostasis, thrombosis and beyond. *Haematologica*, 108(7), 1734–1747. <https://doi.org/10.3324/haematol.2022.282136>
12. Golebiewska, E. M., & Poole, A. W. (2015). Platelet secretion: From haemostasis to wound healing and beyond. *Blood Reviews*, 29(3), 153–162. <https://doi.org/10.1016/j.blre.2014.10.003>
13. Flad, H.-D., & Brandt, E. (2010). Platelet-derived chemokines: Pathophysiology and therapeutic aspects. *Cellular and Molecular Life Sciences*, 67(14), 2363–2386. <https://doi.org/10.1007/s00018-010-0306-x>

14. Zarbock, A., Polanowska-Grabowska, R. K., & Ley, K. (2007). Platelet-neutrophil interactions: Linking hemostasis and inflammation. *Blood Reviews*, *21*(2), 99–111. <https://doi.org/10.1016/j.blre.2006.06.001>
15. Clark, S. R., Ma, A. C., Tavener, S. A., McDonald, B., Goodarzi, Z., Kelly, M. M., Patel, K. D., Chakrabarti, S., McAvoy, E., Sinclair, G. D., Keys, E. M., Allen-Vercoe, E., DeVinney, R., Doig, C. J., Green, F. H. Y., & Kubes, P. (2007). Platelet TLR4 activates neutrophil extracellular traps to ensnare bacteria in septic blood. *Nature Medicine*, *13*(4), 463–469. <https://doi.org/10.1038/nm1565>
16. Cognasse, F., Hamzeh-Cognasse, H., Lafarge, S., Delezay, O., Pozzetto, B., McNicol, A., & Garraud, O. (2008). Toll-like receptor 4 ligand can differentially modulate the release of cytokines by human platelets. *British Journal of Haematology*, *141*(1), 84–91. <https://doi.org/10.1111/j.1365-2141.2008.06999.x>
17. Aslam, R., Speck, E. R., Kim, M., Crow, A. R., Bang, K. W. A., Nestel, F. P., Ni, H., Lazarus, A. H., Freedman, J., & Semple, J. W. (2006). Platelet Toll-like receptor expression modulates lipopolysaccharide-induced thrombocytopenia and tumor necrosis factor- α production in vivo. *Blood*, *107*(2), 637–641. <https://doi.org/10.1182/blood-2005-06-2202>
18. Yeaman, M. R. (2010). Platelets in defense against bacterial pathogens. *Cellular and Molecular Life Sciences*, *67*(4), 525–544. <https://doi.org/10.1007/s00018-009-0210-4>
19. Liesenborghs, L., Meyers, S., Lox, M., Criel, M., Claes, J., Peetermans, M., Trenson, S., Vande Velde, G., Vanden Berghe, P., Baatsen, P., Missiakas, D., Schneewind, O., Peetermans, W. E., Hoylaerts, M. F., Vanassche, T., & Verhamme, P. (2019).

Staphylococcus aureus endocarditis: Distinct mechanisms of bacterial adhesion to damaged and inflamed heart valves. *European Heart Journal*, 40(39), 3248–3259. <https://doi.org/10.1093/eurheartj/ehz175>

20. Horth, R. Z., Jones, J. M., Kim, J. J., Lopansri, B. K., Ilstrup, S. J., Fridey, J., Kelley, W. E., Stramer, S. L., Nambiar, A., Ramirez-Avila, L., Nichols, A., Garcia, W., Oakeson, K. F., Vlachos, N., McAllister, G., Hunter, R., Nakashima, A. K., & Basavaraju, S. V. (2018). Fatal Sepsis Associated with Bacterial Contamination of Platelets—Utah and California, August 2017. *MMWR. Morbidity and Mortality Weekly Report*, 67(25), 718–722. <https://doi.org/10.15585/mmwr.mm6725a4>

21. Rotin L & Mack J. (n.d.). Blood components, Chapter 2, Canadian Blood Services [Professional Education / Transfusion]. 2025. <https://professionaleducation.blood.ca>

22. Singh, R., Marwaha, N., Malhotra, P., & Dash, S. (2009). Quality assessment of platelet concentrates prepared by platelet rich plasma-platelet concentrate, buffy coat poor-platelet concentrate (BC-PC) and apheresis-PC methods. *Asian Journal of Transfusion Science*, 3(2), 86. <https://doi.org/10.4103/0973-6247.53882>

23. Blais-Normandin I, Tordon B, Anani W, Ning S. (n.d.). Clinical Guide to Transfusion, Pathogen-reduced platelets Chapter 19. *Pathogen-Reduced Platelets*. Retrieved April 12, 2025, from <https://professionaleducation.blood.ca>

24. Kelly, K., Finlon, J., Fulciniti, S., Lee, D., Jones, M., & Marschner, S. (2025). Effect of the added plasma rinseback on residual cell types in plateletpheresis leukoreduction systems. *Transfusion*, 65(1), 202–210. <https://doi.org/10.1111/trf.18086>

25. Fijnheer, R., Pietersz, R. N. I., Korte, D. D., & Roos, D. (1989). Monitoring of platelet morphology during storage of platelet concentrates. *Transfusion*, 29(1), 36–40. <https://doi.org/10.1046/j.1537-2995.1989.29189101162.x>
26. Green, S. M., Padula, M. P., Marks, D. C., & Johnson, L. (2020). The Lipid Composition of Platelets and the Impact of Storage: An Overview. *Transfusion Medicine Reviews*, 34(2), 108–116. <https://doi.org/10.1016/j.tmr.2019.12.001>
27. Liu, C., Su, Y., Guo, W., Ma, X., & Qiao, R. (2024). The platelet storage lesion, what are we working for? *Journal of Clinical Laboratory Analysis*, 38(1–2), e24994. <https://doi.org/10.1002/jcla.24994>
28. Yun, S.-H., Sim, E.-H., Goh, R.-Y., Park, J.-I., & Han, J.-Y. (2016). Platelet Activation: The Mechanisms and Potential Biomarkers. *BioMed Research International*, 2016, 1–5. <https://doi.org/10.1155/2016/9060143>
29. Suddock, J. T., & Crookston, K. P. (2025). Transfusion Reactions. In *StatPearls*. StatPearls Publishing. <http://www.ncbi.nlm.nih.gov/books/NBK482202/>
30. Delaney, M., Wendel, S., Bercovitz, R. S., Cid, J., Cohn, C., Dunbar, N. M., Apolseth, T. O., Popovsky, M., Stanworth, S. J., Tinmouth, A., Van De Watering, L., Waters, J. H., Yazer, M., & Ziman, A. (2016). Transfusion reactions: Prevention, diagnosis, and treatment. *The Lancet*, 388(10061), 2825–2836. [https://doi.org/10.1016/S0140-6736\(15\)01313-6](https://doi.org/10.1016/S0140-6736(15)01313-6)
31. McDonald, C., Allen, J., Brailsford, S., Roy, A., Ball, J., Moule, R., Vasconcelos, M., Morrison, R., & Pitt, T. (2017). Bacterial screening of platelet components by National

Health Service Blood and Transplant, an effective risk reduction measure. *Transfusion*, 57(5), 1122–1131. <https://doi.org/10.1111/trf.14085>

32. Walther-Wenke, G., & Schmidt, M. (2011). Impact of Bacterial Contamination on Blood Supply. *Transfusion Medicine and Hemotherapy*, 38(4), 229–230. <https://doi.org/10.1159/000330431>

33. Hong, H., Xiao, W., Lazarus, H. M., Good, C. E., Maitta, R. W., & Jacobs, M. R. (2016). Detection of septic transfusion reactions to platelet transfusions by active and passive surveillance. *Blood*, 127(4), 496–502. <https://doi.org/10.1182/blood-2015-07-655944>

34. Loza-Correa, M., Kou, Y., Taha, M., Kalab, M., Ronholm, J., Schlievert, P. M., Cahill, M. P., Skeate, R., Cserti-Gazdewich, C., & Ramirez-Arcos, S. (2017). Septic transfusion case caused by a platelet pool with visible clotting due to contamination with *Staphylococcus aureus*. *Transfusion*, 57(5), 1299–1303. <https://doi.org/10.1111/trf.14049>

35. Chi, S. I., Kumaran, D., Zeller, M. P., & Ramirez-Arcos, S. (2022). Transfusion of a platelet pool contaminated with exotoxin-producing *Staphylococcus aureus*: A case report. *Annals of Blood*, 7(0). <https://doi.org/10.21037/aob-21-38>

36. Kou, Y., Pagotto, F., Hannach, B., & Ramirez-Arcos, S. (2015). Fatal false-negative transfusion infection involving a buffy coat platelet pool contaminated with biofilm-positive *Staphylococcus epidermidis*: A case report. *Transfusion*, 55(10), 2384–2389. <https://doi.org/10.1111/trf.13154>

37. Walther-Wenke, G., Schrezenmeier, H., Deitenbeck, R., Geis, G., Burkhart, J., Höchsmann, B., Sireis, W., Schmidt, M., Seifried, E., Gebauer, W., Liebscher, U.-M., Weinauer, F., & Müller, T. H. (2010). Screening of platelet concentrates for bacterial

contamination: Spectrum of bacteria detected, proportion of transfused units, and clinical follow-up. *Annals of Hematology*, 89(1), 83–91. <https://doi.org/10.1007/s00277-009-0762-2>

38. Greco-Stewart, V. S., Brown, E. E., Parr, C., Kalab, M., Jacobs, M. R., Yomtovian, R. A., & Ramírez-Arcos, S. M. (2012). *Serratia marcescens* strains implicated in adverse transfusion reactions form biofilms in platelet concentrates and demonstrate reduced detection by automated culture. *Vox Sanguinis*, 102(3), 212–220. <https://doi.org/10.1111/j.1423-0410.2011.01550.x>

39. Chi, S. I., & Ramirez-Arcos, S. (2025). Platelet concentrates safety: A focus on the challenging pathogen *Staphylococcus aureus* - a narrative review. *Annals of Blood*, 10, 5–5. <https://doi.org/10.21037/aob-24-31>

40. Ramachandran, G. (2014). Gram-positive and gram-negative bacterial toxins in sepsis: A brief review. *Virulence*, 5(1), 213–218. <https://doi.org/10.4161/viru.27024>

41. Mazgaeen, L., & Gurung, P. (2020). Recent Advances in Lipopolysaccharide Recognition Systems. *International Journal of Molecular Sciences*, 21(2), 379. <https://doi.org/10.3390/ijms21020379>

42. Shumba, P., Mairpady Shambat, S., & Siemens, N. (2019). The Role of Streptococcal and Staphylococcal Exotoxins and Proteases in Human Necrotizing Soft Tissue Infections. *Toxins*, 11(6), 332. <https://doi.org/10.3390/toxins11060332>

43. Jacobs, M. R., Zhou, B., Tayal, A., & Maitta, R. W. (2024). Bacterial Contamination of Platelet Products. *Microorganisms*, 12(2), 258. <https://doi.org/10.3390/microorganisms12020258>

44. Canadian Blood Services. (2024). *Donor questionnaire for blood, platelets and plasma*. <https://www.blood.ca/en/blood/donating-blood/donor-questionnaire>
45. Ramirez-Arcos, S., Taha, M., Kou, Y., & Goldman, M. (2017). *Skin disinfection methods: Prospective evaluation and postimplementation results*. x
46. Jenkins, C., Ramírez-Arcos, S., Goldman, M., & Devine, D. V. (2011). Bacterial contamination in platelets: Incremental improvements drive down but do not eliminate risk. *Transfusion*, 51(12), 2555–2565. <https://doi.org/10.1111/j.1537-2995.2011.03187.x>
47. Mastronardi, C., Perkins, H., Derksen, P., denAdmirant, M., & Ramírez-Arcos, S. (2010). Evaluation of the BacT/ALERT® 3D system for the implementation of in-house quality control sterility testing at Canadian Blood Services. *Cclm*, 48(8), 1179–1187. <https://doi.org/10.1515/cclm.2010.240>
48. Totty, H., Ullery, M., Spontak, J., Viray, J., Adamik, M., Katzin, B., Dunne, W. M., & Deol, P. (2017). A controlled comparison of the BacT/ALERT® 3D and VIRTUO™ microbial detection systems. *European Journal of Clinical Microbiology & Infectious Diseases: Official Publication of the European Society of Clinical Microbiology*, 36(10), 1795–1800. <https://doi.org/10.1007/s10096-017-2994-8>
49. Liu, H., & Wang, X. (2021). Pathogen reduction technology for blood component: A promising solution for prevention of emerging infectious disease and bacterial contamination in blood transfusion services. *Journal of Photochemistry and Photobiology*, 8, 100079. <https://doi.org/10.1016/j.jpap.2021.100079>

50. Ramirez-Arcos, S., DiFranco, C., McIntyre, T., & Goldman, M. (2017). Residual risk of bacterial contamination of platelets: Six years of experience with sterility testing. *Transfusion*, 57(9), 2174–2181. <https://doi.org/10.1111/trf.14202>
51. Richard, P., Pouchol, E., Sandid, I., Aoustin, L., Lefort, C., Chartois, A., Baima, A., Malard, L., Bacquet, C., Ferrera-Tourenc, V., Gallian, P., Laperche, S., Bliem, C., Morel, P., & Tiberghien, P. (2024). Implementation of amotosalen plus ultraviolet A -mediated pathogen reduction for all platelet concentrates in FRANCE: Impact on the risk of transfusion-transmitted infections. *Vox Sanguinis*, 119(3), 212–218. <https://doi.org/10.1111/vox.13574>
52. U.S. Food and Drug Administration. (2022, December 22). *Important Information for Blood Establishments and Transfusion Services Regarding Bacterial Contamination of Platelets for Transfusion*. U.S. Food and Drug Administration. <https://www.fda.gov/vaccines-blood-biologics/safety-availability-biologics/important-information-blood-establishments-and-transfusion-services-regarding-bacterial-0>
53. García-Otálora, M.-A., McDonald, C., Bearne, J., Brown, B., Cheng, A., Humbrecht, C., Tiberghien, P., Ramirez-Arcos, S., & ISBT Transfusion-Transmitted Infectious Diseases Working Party Subgroup on Bacteria. (2025). Platelet component safety in the era of new advancements in bacterial screening and pathogen reduction: A congress report of the 2024 ISBT Transfusion-Transmitted Infectious Diseases Working Party, Bacteria Subgroup. *Vox Sanguinis*. <https://doi.org/10.1111/vox.70053>
54. Haass, K. A., Sapiano, M. R. P., Savinkina, A., Kuehnert, M. J., & Basavaraju, S. V. (2019). Transfusion-Transmitted Infections Reported to the National Healthcare Safety

Network Hemovigilance Module. *Transfusion Medicine Reviews*, 33(2), 84–91.
<https://doi.org/10.1016/j.tmr.2019.01.001>

55. Abela, M. A., Fenning, S., Maguire, K. A., & Morris, K. G. (2018). Bacterial contamination of platelet components not detected by BacT/ALERT®. *Transfusion Medicine*, 28(1), 65–70. <https://doi.org/10.1111/tme.12458>

56. Myles, I. A., & Datta, S. K. (2012). *Staphylococcus aureus*: An introduction. *Seminars in Immunopathology*, 34(2), 181–184. <https://doi.org/10.1007/s00281-011-0301-9>

57. Jenul, C., & Horswill, A. R. (2019). Regulation of *Staphylococcus aureus* Virulence. *Microbiology Spectrum*, 7(2), 7.2.29. <https://doi.org/10.1128/microbiolspec.GPP3-0031-2018>

58. Qadan, M., & Cheadle, W. G. (2009). Common Microbial Pathogens in Surgical Practice. *Surgical Clinics of North America*, 89(2), 295–310.
<https://doi.org/10.1016/j.suc.2008.09.002>

59. Stephen, J., Salam, F., Lekshmi, M., Kumar, S. H., & Varela, M. F. (2023). The Major Facilitator Superfamily and Antimicrobial Resistance Efflux Pumps of the ESKAPEE Pathogen *Staphylococcus aureus*. *Antibiotics*, 12(2), 343.
<https://doi.org/10.3390/antibiotics12020343>

60. Taylor, T. A., & Unakal, C. G. (2025). *Staphylococcus aureus* Infection. In *StatPearls*. StatPearls Publishing. <http://www.ncbi.nlm.nih.gov/books/NBK441868/>

61. Nikolic, P., & Mudgil, P. (2023). The Cell Wall, Cell Membrane and Virulence Factors of *Staphylococcus aureus* and Their Role in Antibiotic Resistance. *Microorganisms*, 11(2), 259. <https://doi.org/10.3390/microorganisms11020259>
62. Wang, M., Buist, G., & van Dijk, J. M. (2022). *Staphylococcus aureus* cell wall maintenance—The multifaceted roles of peptidoglycan hydrolases in bacterial growth, fitness, and virulence. *FEMS Microbiology Reviews*, 46(5), fuac025. <https://doi.org/10.1093/femsre/fuac025>
63. Ighem Chi, S., Flint, A., Weedmark, K., Pagotto, F., & Ramirez-Arcos, S. (2024). Comparative genome analyses of *Staphylococcus aureus* from platelet concentrates reveal rearrangements involving loss of type VII secretion genes. *Access Microbiology*, 6(9). <https://doi.org/10.1099/acmi.0.000820.v4>
64. Iqbal, Z., Seleem, M. N., Hussain, H. I., Huang, L., Hao, H., & Yuan, Z. (2016). Comparative virulence studies and transcriptome analysis of *Staphylococcus aureus* strains isolated from animals. *Scientific Reports*, 6(1), 35442. <https://doi.org/10.1038/srep35442>
65. Cheung, G. Y. C., Bae, J. S., & Otto, M. (2021). Pathogenicity and virulence of *Staphylococcus aureus*. *Virulence*, 12(1), 547–569. <https://doi.org/10.1080/21505594.2021.1878688>
66. Cox, D., Kerrigan, S. W., & Watson, S. P. (2011). Platelets and the innate immune system: Mechanisms of bacterial-induced platelet activation. *Journal of Thrombosis and Haemostasis*, 9(6), 1097–1107. <https://doi.org/10.1111/j.1538-7836.2011.04264.x>

67. Yousuf, B., Pasha, R., Pineault, N., & Ramirez-Arcos, S. (2024). Modulation of *Staphylococcus aureus* gene expression during proliferation in platelet concentrates with focus on virulence and platelet functionality. *PLOS ONE*, *19*(7), e0307920. <https://doi.org/10.1371/journal.pone.0307920>
68. Liesenborghs, L., Verhamme, P., & Vanassche, T. (2018). *Staphylococcus aureus*, master manipulator of the human hemostatic system. *Journal of Thrombosis and Haemostasis*, *16*(3), 441–454. <https://doi.org/10.1111/jth.13928>
69. Foster, T. J. (2024). Cell Wall-Anchored Surface Proteins of *Staphylococcus aureus*. In A. Nakane & K. Asano (Eds.), *Staphylococcus aureus* (pp. 41–80). Springer Nature Singapore. https://doi.org/10.1007/978-981-99-9428-1_2
70. Foster, T. J. (2019). The MSCRAMM Family of Cell-Wall-Anchored Surface Proteins of Gram-Positive Cocci. *Trends in Microbiology*, *27*(11), 927–941. <https://doi.org/10.1016/j.tim.2019.06.007>
71. Kim, H. K., Emolo, C., DeDent, A. C., Falugi, F., Missiakas, D. M., & Schneewind, O. (2012). Protein A-specific monoclonal antibodies and prevention of *Staphylococcus aureus* disease in mice. *Infection and Immunity*, *80*(10), 3460–3470. <https://doi.org/10.1128/IAI.00230-12>
72. O'Brien, L., Kerrigan, S. W., Kaw, G., Hogan, M., Penadés, J., Litt, D., Fitzgerald, D. J., Foster, T. J., & Cox, D. (2002). Multiple mechanisms for the activation of human platelet aggregation by *Staphylococcus aureus*: Roles for the clumping factors ClfA and ClfB, the serine–aspartate repeat protein SdrE and protein A. *Molecular Microbiology*, *44*(4), 1033–1044. <https://doi.org/10.1046/j.1365-2958.2002.02935.x>

73. Shinji, H., Yosizawa, Y., Tajima, A., Iwase, T., Sugimoto, S., Seki, K., & Mizunoe, Y. (2011). Role of fibronectin-binding proteins A and B in in vitro cellular infections and in vivo septic infections by *Staphylococcus aureus*. *Infection and Immunity*, *79*(6), 2215–2223. <https://doi.org/10.1128/IAI.00133-11>
74. Bertling, A., Niemann, S., Hussain, M., Holbrook, L., Stanley, R. G., Brodde, M. F., Pohl, S., Schifferdecker, T., Roth, J., Jurk, K., Müller, A., Lahav, J., Peters, G., Heilmann, C., Gibbins, J. M., & Kehrel, B. E. (2012). Staphylococcal Extracellular Adherence Protein Induces Platelet Activation by Stimulation of Thiol Isomerases. *Arteriosclerosis, Thrombosis, and Vascular Biology*, *32*(8), 1979–1990. <https://doi.org/10.1161/ATVBAHA.112.246249>
75. Alfeo, M. J., Pagotto, A., Barbieri, G., Foster, T. J., Vanhoorelbeke, K., De Filippis, V., Speziale, P., & Pietrocola, G. (2021). *Staphylococcus aureus* iron-regulated surface determinant B (IsdB) protein interacts with von Willebrand factor and promotes adherence to endothelial cells. *Scientific Reports*, *11*(1), 22799. <https://doi.org/10.1038/s41598-021-02065-w>
76. Ali, R. A., Wuescher, L. M., Dona, K. R., & Worth, R. G. (2017). Platelets Mediate Host Defense against *Staphylococcus aureus* through Direct Bactericidal Activity and by Enhancing Macrophage Activities. *Journal of Immunology (Baltimore, Md.: 1950)*, *198*(1), 344–351. <https://doi.org/10.4049/jimmunol.1601178>
77. Koupenova, M., Clancy, L., Corkrey, H. A., & Freedman, J. E. (2018). Circulating Platelets as Mediators of Immunity, Inflammation, and Thrombosis. *Circulation Research*, *122*(2), 337–351. <https://doi.org/10.1161/CIRCRESAHA.117.310795>

78. Surewaard, B. G. J., Thanabalasuriar, A., Zeng, Z., Tkaczyk, C., Cohen, T. S., Bardoel, B. W., Jorch, S. K., Deppermann, C., Bubeck Wardenburg, J., Davis, R. P., Jenne, C. N., Stover, K. C., Sellman, B. R., & Kubes, P. (2018). α -Toxin Induces Platelet Aggregation and Liver Injury during *Staphylococcus aureus* Sepsis. *Cell Host & Microbe*, *24*(2), 271-284.e3. <https://doi.org/10.1016/j.chom.2018.06.017>
79. Alabdullatif, M., & Alzahrani, A. (2022). Expression of biofilm-associated genes in *Staphylococcus aureus* during storage of platelet concentrates. *Transfusion and Apheresis Science*, *61*(6), 103456. <https://doi.org/10.1016/j.transci.2022.103456>
80. Spaan, A. N., van Strijp, J. A. G., & Torres, V. J. (2017). Leukocidins: Staphylococcal bi-component pore-forming toxins find their receptors. *Nature Reviews. Microbiology*, *15*(7), 435–447. <https://doi.org/10.1038/nrmicro.2017.27>
81. Tam, K., & Torres, V. J. (2019). *Staphylococcus aureus* Secreted Toxins and Extracellular Enzymes. *Microbiology Spectrum*, *7*(2). <https://doi.org/10.1128/microbiolspec.GPP3-0039-2018>
82. Li, X., Busch, L. M., Piersma, S., Wang, M., Liu, L., Gesell Salazar, M., Surmann, K., Mäder, U., Völker, U., Buist, G., & van Dijk, J. M. (2024). Functional and Proteomic Dissection of the Contributions of CodY, SigB and the Hibernation Promoting Factor HPF to Interactions of *Staphylococcus aureus* USA300 with Human Lung Epithelial Cells. *Journal of Proteome Research*, *23*(10), 4742–4760. <https://doi.org/10.1021/acs.jproteome.4c00724>
83. Sultan, A. R., Swierstra, J. W., Lemmens-den Toom, N. A., Snijders, S. V., Hansenová Maňásková, S., Verbon, A., & Van Wamel, W. J. B. (2018). Production of Staphylococcal

Complement Inhibitor (SCIN) and Other Immune Modulators during the Early Stages of *Staphylococcus aureus* Biofilm Formation in a Mammalian Cell Culture Medium. *Infection and Immunity*, 86(8), e00352-18. <https://doi.org/10.1128/IAI.00352-18>

84. Wazir, H. U., Narang, P., Silvani, G., Mehner, C., Poole, K., Burke, C., & Chou, J. (2023). Bacterial Virulence and Prevention for Human Spaceflight. *Life (Basel, Switzerland)*, 13(3), 656. <https://doi.org/10.3390/life13030656>

85. Le, K. Y., & Otto, M. (2015). Quorum-sensing regulation in staphylococci-an overview. *Frontiers in Microbiology*, 6, 1174. <https://doi.org/10.3389/fmicb.2015.01174>

86. Vinodhini, V., & Kavitha, M. (2024). Deciphering agr quorum sensing in *Staphylococcus aureus*: Insights and therapeutic prospects. *Molecular Biology Reports*, 51(1), 155. <https://doi.org/10.1007/s11033-023-08930-3>

87. Bien, J., Sokolova, O., & Bozko, P. (2011). Characterization of Virulence Factors of *Staphylococcus aureus*: Novel Function of Known Virulence Factors That Are Implicated in Activation of Airway Epithelial Proinflammatory Response. *Journal of Pathogens*, 2011, 1–13. <https://doi.org/10.4061/2011/601905>

88. Jiang, J.-H., Cameron, D. R., Nethercott, C., Aires-de-Sousa, M., & Peleg, A. Y. (2023). Virulence attributes of successful methicillin-resistant *Staphylococcus aureus* lineages. *Clinical Microbiology Reviews*, 36(4), e00148-22. <https://doi.org/10.1128/cmr.00148-22>

89. van Kessel, K. P. M., Bestebroer, J., & van Strijp, J. A. G. (2014). Neutrophil-Mediated Phagocytosis of *Staphylococcus aureus*. *Frontiers in Immunology*, 5, 467. <https://doi.org/10.3389/fimmu.2014.00467>

90. Jahn, K., Handtke, S., Palankar, R., Kohler, T. P., Wesche, J., Wolff, M., Bayer, J., Wolz, C., Greinacher, A., & Hammerschmidt, S. (2022). A-hemolysin of *Staphylococcus aureus* impairs thrombus formation. *Journal of Thrombosis and Haemostasis*, *20*(6), 1464–1475. <https://doi.org/10.1111/jth.15703>
91. Francis, D., Bhairaddy, A., Joy, A., Hari, G. V., & Francis, A. (2023). Secretory proteins in the orchestration of microbial virulence: The curious case of *Staphylococcus aureus*. In *Advances in Protein Chemistry and Structural Biology* (Vol. 133, pp. 271–350). Elsevier. <https://doi.org/10.1016/bs.apcsb.2022.10.004>
92. Chi, S. I., Yousuf, B., Paredes, C., Bearn, J., McDonald, C., & Ramirez-Arcos, S. (2023). Proof of concept for detection of staphylococcal enterotoxins in platelet concentrates as a novel safety mitigation strategy. *Vox Sanguinis*, *118*(7), 543–550. <https://doi.org/10.1111/vox.13440>
93. Goda, K., Kenzaka, T., Hoshijima, M., Yachie, A., & Akita, H. (2021). Toxic shock syndrome with a cytokine storm caused by *Staphylococcus simulans*: A case report. *BMC Infectious Diseases*, *21*(1), 19. <https://doi.org/10.1186/s12879-020-05731-y>
94. Postma, B., Poppelier, M. J., van Galen, J. C., Prossnitz, E. R., van Strijp, J. A. G., de Haas, C. J. C., & van Kessel, K. P. M. (2004). Chemotaxis inhibitory protein of *Staphylococcus aureus* binds specifically to the C5a and formylated peptide receptor. *Journal of Immunology (Baltimore, Md.: 1950)*, *172*(11), 6994–7001. <https://doi.org/10.4049/jimmunol.172.11.6994>
95. Clauditz, A., Resch, A., Wieland, K.-P., Peschel, A., & Götz, F. (2006). Staphyloxanthin Plays a Role in the Fitness of *Staphylococcus aureus* and Its Ability To Cope with

Oxidative Stress. *Infection and Immunity*, 74(8), 4950–4953.
<https://doi.org/10.1128/IAI.00204-06>

96. Elmesserri, R. A., Saleh, S. E., Elsherif, H. M., Yahia, I. S., & Aboshanab, K. M. (2022). Staphyloxanthin as a Potential Novel Target for Deciphering Promising Anti-*Staphylococcus aureus* Agents. *Antibiotics*, 11(3), 298.
<https://doi.org/10.3390/antibiotics11030298>

97. Yu, J., Shen, L., Yang, J., Shi, J., Huang, Y., Shang, Y., & Yu, F. (2025). Staphyloxanthin-enriched extracts promote biofilm formation and oxidative stress resistance in *Staphylococcus aureus*. *Microbiology Spectrum*, e00996-25.
<https://doi.org/10.1128/spectrum.00996-25>

98. Parastan, R., Kargar, M., Solhjoo, K., & Kafilzadeh, F. (2020). A synergistic association between adhesion-related genes and multidrug resistance patterns of *Staphylococcus aureus* isolates from different patients and healthy individuals. *Journal of Global Antimicrobial Resistance*, 22, 379–385. <https://doi.org/10.1016/j.jgar.2020.02.025>

99. Cramton, S. E., Gerke, C., Schnell, N. F., Nichols, W. W., & Götz, F. (1999). The Intercellular Adhesion (*ica*) Locus Is Present in *Staphylococcus aureus* and Is Required for Biofilm Formation. *Infection and Immunity*, 67(10), 5427–5433.
<https://doi.org/10.1128/IAI.67.10.5427-5433.1999>

100. Kwiecinski, J., Peetermans, M., Liesenborghs, L., Na, M., Björnsdottir, H., Zhu, X., Jacobsson, G., Johansson, B. R., Geoghegan, J. A., Foster, T. J., Josefsson, E., Bylund, J., Verhamme, P., & Jin, T. (2016). Staphylokinase Control of *Staphylococcus aureus*

Biofilm Formation and Detachment Through Host Plasminogen Activation. *Journal of Infectious Diseases*, 213(1), 139–148. <https://doi.org/10.1093/infdis/jiv360>

101. Pietrocola, G., Campoccia, D., Motta, C., Montanaro, L., Arciola, C. R., & Speziale, P. (2022). Colonization and Infection of Indwelling Medical Devices by *Staphylococcus aureus* with an Emphasis on Orthopedic Implants. *International Journal of Molecular Sciences*, 23(11), 5958. <https://doi.org/10.3390/ijms23115958>

102. Tsouklidis, N., Kumar, R., Heindl, S. E., Soni, R., & Khan, S. (2020). Understanding the Fight Against Resistance: Hospital-Acquired Methicillin-Resistant *Staphylococcus aureus* vs. Community-Acquired Methicillin-Resistant *Staphylococcus aureus*. *Cureus*, 12(6), e8867. <https://doi.org/10.7759/cureus.8867>

103. Nicolle, L. (2006). Community-acquired MRSA: A practitioner's guide. *Canadian Medical Association Journal*, 175(2), 145–145. <https://doi.org/10.1503/cmaj.060457>

104. David, M. Z., & Daum, R. S. (2010). Community-Associated Methicillin-Resistant *Staphylococcus aureus*: Epidemiology and Clinical Consequences of an Emerging Epidemic. *Clinical Microbiology Reviews*, 23(3), 616–687. <https://doi.org/10.1128/CMR.00081-09>

105. Antimicrobial Resistance Taskforce (AMRTF). (2022). *Canadian Antimicrobial Resistance Surveillance System (CARSS) Report 2022*. Public Health Agency of Canada (PHAC). <https://doi.org/10.58333/e241022>

106. Miller, W. R., & Arias, C. A. (2024). ESKAPE pathogens: Antimicrobial resistance, epidemiology, clinical impact and therapeutics. *Nature Reviews Microbiology*, 22(10), 598–616. <https://doi.org/10.1038/s41579-024-01054-w>

107. Brdová, D., Ruml, T., & Viktorová, J. (2024). Mechanism of staphylococcal resistance to clinically relevant antibiotics. *Drug Resistance Updates*, 77, 101147. <https://doi.org/10.1016/j.drup.2024.101147>
108. Foster, T. J. (2017). Antibiotic resistance in *Staphylococcus aureus*. Current status and future prospects. *FEMS Microbiology Reviews*, 41(3), 430–449. <https://doi.org/10.1093/femsre/fux007>
109. Ernst, C. M., Staubitz, P., Mishra, N. N., Yang, S.-J., Hornig, G., Kalbacher, H., Bayer, A. S., Kraus, D., & Peschel, A. (2009). The Bacterial Defensin Resistance Protein MprF Consists of Separable Domains for Lipid Lysinylation and Antimicrobial Peptide Repulsion. *PLoS Pathogens*, 5(11), e1000660. <https://doi.org/10.1371/journal.ppat.1000660>
110. Coupri, D., Verneuil, N., Hartke, A., Liebaut, A., Lequeux, T., Pfund, E., & Budin-Verneuil, A. (2021). Inhibition of D -alanylation of teichoic acids overcomes resistance of methicillin-resistant *Staphylococcus aureus*. *Journal of Antimicrobial Chemotherapy*, 76(11), 2778–2786. <https://doi.org/10.1093/jac/dkab287>
111. DeMars, Z., Singh, V. K., & Bose, J. L. (2020). Exogenous Fatty Acids Remodel *Staphylococcus aureus* Lipid Composition through Fatty Acid Kinase. *Journal of Bacteriology*, 202(14). <https://doi.org/10.1128/JB.00128-20>
112. Tiwari, K., Gatto, C., & Wilkinson, B. (2018). Interrelationships among Fatty Acid Composition, Staphyloxanthin Content, Fluidity, and Carbon Flow in the *Staphylococcus aureus* Membrane. *Molecules*, 23(5), 1201. <https://doi.org/10.3390/molecules23051201>

113. Fisher, J. F., & Mobashery, S. (2021). β -Lactams against the Fortress of the Gram-Positive *Staphylococcus aureus* Bacterium. *Chemical Reviews*, 121(6), 3412–3463. <https://doi.org/10.1021/acs.chemrev.0c01010>
114. Nomura, R., Nakaminami, H., Takasao, K., Muramatsu, S., Kato, Y., Wajima, T., & Noguchi, N. (2020). A class A β -lactamase produced by borderline oxacillin-resistant *Staphylococcus aureus* hydrolyses oxacillin. *Journal of Global Antimicrobial Resistance*, 22, 244–247. <https://doi.org/10.1016/j.jgar.2020.03.002>
115. Fathi, J., Hashemizadeh, Z., Dehkordi, R. S., Bazargani, A., Javadi, K., Hosseini-Nave, H., & Hadadi, M. (2022). Evaluation of aminoglycoside modifying enzymes, SCCmec, coagulase gene and PCR-RFLP coagulase gene typing of *Staphylococcus aureus* isolates from hospitals in Shiraz, southwest of Iran. *Heliyon*, 8(8), e10230. <https://doi.org/10.1016/j.heliyon.2022.e10230>
116. Lade, H., & Kim, J.-S. (2023). Molecular Determinants of β -Lactam Resistance in Methicillin-Resistant *Staphylococcus aureus* (MRSA): An Updated Review. *Antibiotics*, 12(9), 1362. <https://doi.org/10.3390/antibiotics12091362>
117. Shokravi, Z., Mehrad, L., & Ramazani, A. (2017). Detecting the frequency of aminoglycoside modifying enzyme encoding genes among clinical isolates of methicillin-resistant *Staphylococcus aureus*. *BioImpacts*, 5(2), 87–91. <https://doi.org/10.15171/bi.2015.15>
118. Fergestad, M. E., Stamsås, G. A., Morales Angeles, D., Salehian, Z., Wasteson, Y., & Kjos, M. (2020). Penicillin-binding protein PBP2a provides variable levels of protection

toward different β -lactams in *Staphylococcus aureus* RN4220. *MicrobiologyOpen*, 9(8), e1057. <https://doi.org/10.1002/mbo3.1057>

119. Hooper, D. C., & Jacoby, G. A. (2015). Mechanisms of drug resistance: Quinolone resistance. *Annals of the New York Academy of Sciences*, 1354(1), 12–31. <https://doi.org/10.1111/nyas.12830>

120. Khodabandeh, M., Mohammadi, M., Abdolsalehi, M. R., Alvandimanesh, A., Gholami, M., Bibalan, M. H., Pournajaf, A., Kafshgari, R., & Rajabnia, R. (2019). Analysis of Resistance to Macrolide–Lincosamide–Streptogramin B Among *mecA*-Positive *Staphylococcus aureus* Isolates. *Osong Public Health and Research Perspectives*, 10(1), 25–31. <https://doi.org/10.24171/j.phrp.2019.10.1.06>

121. Fergestad, M. E., Stamsås, G. A., Morales Angeles, D., Salehian, Z., Wasteson, Y., & Kjos, M. (2020). Penicillin-binding protein PBP2a provides variable levels of protection toward different β -lactams in *Staphylococcus aureus* RN4220. *MicrobiologyOpen*, 9(8), e1057. <https://doi.org/10.1002/mbo3.1057>

122. Hosseini, S. S., Niakan, M., Saderi, H., Motallebi, M., Taherikalani, M., Asadollahi, K., & Emaneini, M. (2016). Frequency of genes encoding erythromycin ribosomal methylases among *Staphylococcus aureus* clinical isolates with different D-phenotypes in Tehran, Iran. *Iranian Journal of Microbiology*, 8(3), 161–167.

123. Afzal, M., Vijay, A. K., Stapleton, F., & Willcox, M. (2022). The Relationship between Ciprofloxacin Resistance and Genotypic Changes in *S. aureus* Ocular Isolates. *Pathogens*, 11(11), 1354. <https://doi.org/10.3390/pathogens11111354>

124. Sinha, S., Aggarwal, S., & Singh, D. V. (2024). Efflux pumps: Gatekeepers of antibiotic resistance in *Staphylococcus aureus* biofilms. *Microbial Cell*, *11*, 368–377. <https://doi.org/10.15698/mic2024.11.839>
125. Dashtbani-Roozbehani, A., & Brown, M. H. (2021). Efflux Pump Mediated Antimicrobial Resistance by Staphylococci in Health-Related Environments: Challenges and the Quest for Inhibition. *Antibiotics*, *10*(12), 1502. <https://doi.org/10.3390/antibiotics10121502>
126. Ding, Y., Onodera, Y., Lee, J. C., & Hooper, D. C. (2008). NorB, an Efflux Pump in *Staphylococcus aureus* Strain MW2, Contributes to Bacterial Fitness in Abscesses. *Journal of Bacteriology*, *190*(21), 7123–7129. <https://doi.org/10.1128/JB.00655-08>
127. Lekshmi, M., Stephen, J., Ojha, M., Kumar, S., & Varela, M. (2022). *Staphylococcus aureus* antimicrobial efflux pumps and their inhibitors: Recent developments. *AIMS Medical Science*, *9*(3), 367–393. <https://doi.org/10.3934/medsci.2022018>
128. Costa, S. S., Viveiros, M., Amaral, L., & Couto, I. (2013). Multidrug Efflux Pumps in *Staphylococcus aureus*: An Update. *The Open Microbiology Journal*, *7*(1), 59–71. <https://doi.org/10.2174/1874285801307010059>
129. Sonstein, S. A., & Burnham, J. C. (1993). Effect of low concentrations of quinolone antibiotics on bacterial virulence mechanisms. *Diagnostic Microbiology and Infectious Disease*, *16*(4), 277–289. [https://doi.org/10.1016/0732-8893\(93\)90078-L](https://doi.org/10.1016/0732-8893(93)90078-L)
130. Gao, W., Monk, I. R., Tobias, N. J., Gladman, S. L., Seemann, T., Stinear, T. P., & Howden, B. P. (2015). Large tandem chromosome expansions facilitate niche adaptation

during persistent infection with drug-resistant *Staphylococcus aureus*. *Microbial Genomics*, 1(2). <https://doi.org/10.1099/mgen.0.000026>

131. Shapiro, R. S. (2015). Antimicrobial-induced DNA damage and genomic instability in microbial pathogens. *PLoS Pathogens*, 11(3), e1004678. <https://doi.org/10.1371/journal.ppat.1004678>

132. Truong-Bolduc, Q. C., & Hooper, D. C. (2010). Phosphorylation of MgrA and Its Effect on Expression of the NorA and NorB Efflux Pumps of *Staphylococcus aureus*. *Journal of Bacteriology*, 192(10), 2525–2534. <https://doi.org/10.1128/JB.00018-10>

133. Lekshmi, M., Ammini, P., Adjei, J., Sanford, L. M., Shrestha, U., Kumar, S., & Varela, M. F. (2018). Modulation of antimicrobial efflux pumps of the major facilitator superfamily in *Staphylococcus aureus*. *AIMS Microbiology*, 4(1), 1–18. <https://doi.org/10.3934/microbiol.2018.1.1>

134. Kumar, S., Athreya, A., Gulati, A., Nair, R. M., Mahendran, I., Ranjan, R., & Penmatsa, A. (2021). Structural basis of inhibition of a transporter from *Staphylococcus aureus*, NorC, through a single-domain camelid antibody. *Communications Biology*, 4(1), 836. <https://doi.org/10.1038/s42003-021-02357-x>

135. Truong-Bolduc, Q. C., & Hooper, D. C. (2007). The Transcriptional Regulators NorG and MgrA Modulate Resistance to both Quinolones and β -Lactams in *Staphylococcus aureus*. *Journal of Bacteriology*, 189(8), 2996–3005. <https://doi.org/10.1128/JB.01819-06>

136. Truong-Bolduc, Q. C., Dunman, P. M., Strahilevitz, J., Projan, S. J., & Hooper, D. C. (2005). MgrA Is a Multiple Regulator of Two New Efflux Pumps in *Staphylococcus aureus*.

Journal of Bacteriology, 187(7), 2395–2405. <https://doi.org/10.1128/JB.187.7.2395-2405.2005>

137. Truong-Bolduc, Q. C., Ding, Y., & Hooper, D. C. (2008). Posttranslational modification influences the effects of MgrA on *norA* expression in *Staphylococcus aureus*. *Journal of Bacteriology*, 190(22), 7375–7381. <https://doi.org/10.1128/JB.01068-08>

138. Crosby, H. A., Schlievert, P. M., Merriman, J. A., King, J. M., Salgado-Pabón, W., & Horswill, A. R. (2016). The *Staphylococcus aureus* Global Regulator MgrA Modulates Clumping and Virulence by Controlling Surface Protein Expression. *PLOS Pathogens*, 12(5), e1005604. <https://doi.org/10.1371/journal.ppat.1005604>

139. Crosby, H. A., Tiwari, N., Kwiecinski, J. M., Xu, Z., Dykstra, A., Jenul, C., Fuentes, E. J., & Horswill, A. R. (2020). The *Staphylococcus aureus* ArlRS two-component system regulates virulence factor expression through MgrA. *Molecular Microbiology*, 113(1), 103–122. <https://doi.org/10.1111/mmi.14404>

140. Truong-Bolduc, Q. C., Dunman, P. M., Eidem, T., & Hooper, D. C. (2011). Transcriptional profiling analysis of the global regulator NorG, a GntR-like protein of *Staphylococcus aureus*. *Journal of Bacteriology*, 193(22), 6207–6214. <https://doi.org/10.1128/JB.05847-11>

141. Giachino, P., Engelmann, S., & Bischoff, M. (2001). ζ^B Activity Depends on RsbU in *Staphylococcus aureus*. *Journal of Bacteriology*, 183(6), 1843–1852. <https://doi.org/10.1128/JB.183.6.1843-1852.2001>

142. Pané-Farré, J., Jonas, B., Hardwick, S. W., Gronau, K., Lewis, R. J., Hecker, M., & Engelmann, S. (2009). Role of RsbU in Controlling SigB Activity in *Staphylococcus aureus*

following Alkaline Stress. *Journal of Bacteriology*, 191(8), 2561–2573.
<https://doi.org/10.1128/JB.01514-08>

143. Yuan, L., Liu, Q., Xu, L., Wu, B., & Feng, Y. (2024). Structural basis of promoter recognition by *Staphylococcus aureus* RNA polymerase. *Nature Communications*, 15(1), 4850. <https://doi.org/10.1038/s41467-024-49229-6>

144. Lee, J., Carda-Diéguez, M., Žiemytė, M., Vreugde, S., Cooksley, C., Crosby, H. A., Horswill, A. R., Mira, A., Zilm, P. S., & Kidd, S. P. (2022). Functional *mgrA* Influences Genetic Changes within a *Staphylococcus aureus* Cell Population over Time. *Journal of Bacteriology*, 204(10), e00138-22. <https://doi.org/10.1128/jb.00138-22>

145. Truong-Bolduc, Q. C., Hsing, L. C., Villet, R., Bolduc, G. R., Estabrooks, Z., Taguezem, G. F., & Hooper, D. C. (2012). Reduced aeration affects the expression of the NorB efflux pump of *Staphylococcus aureus* by posttranslational modification of MgrA. *Journal of Bacteriology*, 194(7), 1823–1834. <https://doi.org/10.1128/JB.06503-11>

146. Gupta, R. Kr., Alba, J., Xiong, Y. Q., Bayer, A. S., & Lee, C. Y. (2013). MgrA Activates Expression of Capsule Genes, but Not the α -Toxin Gene in Experimental *Staphylococcus aureus* Endocarditis. *The Journal of Infectious Diseases*, 208(11), 1841–1848. <https://doi.org/10.1093/infdis/jit367>

147. Chen, P. R., Bae, T., Williams, W. A., Duguid, E. M., Rice, P. A., Schneewind, O., & He, C. (2006). An oxidation-sensing mechanism is used by the global regulator MgrA in *Staphylococcus aureus*. *Nature Chemical Biology*, 2(11), 591–595. <https://doi.org/10.1038/nchembio820>

148. Sun, F., Ding, Y., Ji, Q., Liang, Z., Deng, X., Wong, C. C. L., Yi, C., Zhang, L., Xie, S., Alvarez, S., Hicks, L. M., Luo, C., Jiang, H., Lan, L., & He, C. (2012). Protein cysteine phosphorylation of SarA/MgrA family transcriptional regulators mediates bacterial virulence and antibiotic resistance. *Proceedings of the National Academy of Sciences*, *109*(38), 15461–15466. <https://doi.org/10.1073/pnas.1205952109>
149. Luong, T. T., Dunman, P. M., Murphy, E., Projan, S. J., & Lee, C. Y. (2006). Transcription Profiling of the *mgrA* Regulon in *Staphylococcus aureus*. *Journal of Bacteriology*, *188*(5), 1899–1910. <https://doi.org/10.1128/JB.188.5.1899-1910.2006>
150. Wang, H. H. (2012). *Unraveling gene regulation of MDR and ABC-transporters in bacteria* [Bachelor thesis Life Science & Technology, University of Groningen]. https://fse.studenttheses.ub.rug.nl/10095/1/LST_Bc_2012_HWang.pdf
151. Mukherjee, P., Roy, S., Ghosh, D., & Nandi, S. K. (2022). Role of animal models in biomedical research: A review. *Laboratory Animal Research*, *38*(1), 18. <https://doi.org/10.1186/s42826-022-00128-1>
152. Trübe, P., Hertlein, T., Mrochen, D. M., Schulz, D., Jorde, I., Krause, B., Zeun, J., Fischer, S., Wolf, S. A., Walther, B., Semmler, T., Bröker, B. M., Ulrich, R. G., Ohlsen, K., & Holtfreter, S. (2019). Bringing together what belongs together: Optimizing murine infection models by using mouse-adapted *Staphylococcus aureus* strains. *International Journal of Medical Microbiology*, *309*(1), 26–38. <https://doi.org/10.1016/j.ijmm.2018.10.007>
153. Ferro, T. A. F., Araújo, J. M. M., Dos Santos Pinto, B. L., Dos Santos, J. S., Souza, E. B., Da Silva, B. L. R., Colares, V. L. P., Novais, T. M. G., Filho, C. M. B., Struve, C.,

Calixto, J. B., Monteiro-Neto, V., Da Silva, L. C. N., & Fernandes, E. S. (2016). Cinnamaldehyde Inhibits *Staphylococcus aureus* Virulence Factors and Protects against Infection in a *Galleria mellonella* Model. *Frontiers in Microbiology*, 7, 2052. <https://doi.org/10.3389/fmicb.2016.02052>

154. Irazoqui, J. E., Troemel, E. R., Feinbaum, R. L., Luhachack, L. G., Cezairliyan, B. O., & Ausubel, F. M. (2010). Distinct Pathogenesis and Host Responses during Infection of *C. elegans* by *P. aeruginosa* and *S. aureus*. *PLoS Pathogens*, 6(7), e1000982. <https://doi.org/10.1371/journal.ppat.1000982>

155. Reddy A, H., & C, S. (2016). A Critical Assessment of *Bombyx mori* Haemolymph Extract on *Staphylococcus aureus* an In vitro and In silico Approach. *Journal of Proteomics & Bioinformatics*, 9(9). <https://doi.org/10.4172/jpb.1000410>

156. Ségalat, L. (2007). Invertebrate Animal Models of Diseases as Screening Tools in Drug Discovery. *ACS Chemical Biology*, 2(4), 231–236. <https://doi.org/10.1021/cb700009m>

157. Ashraf, H., & Qamar, A. (2023). Silkworm *Bombyx mori* as a model organism: A review. *Physiological Entomology*, 48(4), 107–121. <https://doi.org/10.1111/phen.12421>

158. Montali, A., Berini, F., Saviane, A., Cappelozza, S., Marinelli, F., & Tettamanti, G. (2022). A *Bombyx mori* Infection Model for Screening Antibiotics against *Staphylococcus epidermidis*. *Insects*, 13(8), 748. <https://doi.org/10.3390/insects13080748>

159. Kumaran, D. (2024). *Assessing the Impact of Collection, Production, and Storage of Platelet Concentrates on Bacterial Contamination and Product Safety* [University of

Ottawa]. <https://ruor.uottawa.ca/server/api/core/bitstreams/8c06e3dd-af9c-42ad-a866-a72918cb941f/content>

160. Kaito, C., & Sekimizu, K. (2007). A silkworm model of pathogenic bacterial infection. *Drug Discoveries & Therapeutics*, 1(2), 89–93.

161. Garc a-Lara, J., Needham, A. J., & Foster, S. J. (2005). Invertebrates as animal models for *Staphylococcus aureus* pathogenesis: A window into host–pathogen interaction. *FEMS Immunology & Medical Microbiology*, 43(3), 311–323. <https://doi.org/10.1016/j.femsim.2004.11.003>

162. Yu, H., Xu, Y., Imani, S., Zhao, Z., Ullah, S., & Wang, Q. (2024). Navigating ESKAPE Pathogens: Considerations and Caveats for Animal Infection Models Development. *ACS Infectious Diseases*, 10(7), 2336–2355. <https://doi.org/10.1021/acsinfecdis.4c00007>

163. Zheng, P., Liu, F., Long, J., Jin, Y., Chen, S., Duan, G., & Yang, H. (2023). Latest Advances in the Application of Humanized Mouse Model for *Staphylococcus aureus*. *The Journal of Infectious Diseases*, 228(6), 800–809. <https://doi.org/10.1093/infdis/jiad253>

164. Kebaier, C., Chamberland, R. R., Allen, I. C., Gao, X., Broglie, P. M., Hall, J. D., Jania, C., Doerschuk, C. M., Tilley, S. L., & Duncan, J. A. (2012). *Staphylococcus aureus* α -hemolysin mediates virulence in a murine model of severe pneumonia through activation of the NLRP3 inflammasome. *The Journal of Infectious Diseases*, 205(5), 807–817. <https://doi.org/10.1093/infdis/jir846>

165. Parker, D. (2017). Humanized Mouse Models of *Staphylococcus aureus* Infection. *Frontiers in Immunology*, 8, 512. <https://doi.org/10.3389/fimmu.2017.00512>

166. Zeng, M., Wang, Y., Liu, F., Long, J., & Yang, H. (2025). Rabbit Models for Infectious Diseases Caused by *Staphylococcus aureus*. *Microbiology Research*, 16(4), 76. <https://doi.org/10.3390/microbiolres16040076>
167. Kumaran, D., & Ramirez-Arcos, S. (2025). The platelet concentrate storage environment may enhance the ability of *Cutibacterium acnes* to establish chronic infections. *Transfusion*, 65(10), 1851–1860. <https://doi.org/10.1111/trf.18368>
168. Ménard, G., Rouillon, A., Ghukasyan, G., Emily, M., Felden, B., & Donnio, P.-Y. (2021). *Galleria mellonella* Larvae as an Infection Model to Investigate sRNA-Mediated Pathogenesis in *Staphylococcus aureus*. *Frontiers in Cellular and Infection Microbiology*, 11, 631710. <https://doi.org/10.3389/fcimb.2021.631710>
169. Alnezary, F. S., Almutairi, M. S., Alhifany, A. A., & Almangour, T. A. (2023). Assessing *Galleria mellonella* as a preliminary model for systemic *Staphylococcus aureus* infection: Evaluating the efficacy and impact of vancomycin and *Nigella sativa* oil on gut microbiota. *Saudi Pharmaceutical Journal*, 31(12), 101824. <https://doi.org/10.1016/j.jsps.2023.101824>
170. Mannala, G. (2020). *Galleria mellonella* as an alternative in vivo model to study bacterial biofilms on stainless steel and titanium implants. *ALTEX*. <https://doi.org/10.14573/altex.2003211>
171. Sheehan, G., Dixon, A., & Kavanagh, K. (2019). Utilization of *Galleria mellonella* larvae to characterize the development of *Staphylococcus aureus* infection. *Microbiology*, 165(8), 863–875. <https://doi.org/10.1099/mic.0.000813>

172. Sifri, C. D., Begun, J., Ausubel, F. M., & Calderwood, S. B. (2003). *Caenorhabditis elegans* as a Model Host for *Staphylococcus aureus* Pathogenesis. *Infection and Immunity*, *71*(4), 2208–2217. <https://doi.org/10.1128/IAI.71.4.2208-2217.2003>
173. Begun, J., Sifri, C. D., Goldman, S., Calderwood, S. B., & Ausubel, F. M. (2005). *Staphylococcus aureus* Virulence Factors Identified by Using a High-Throughput *Caenorhabditis elegans*-Killing Model. *Infection and Immunity*, *73*(2), 872–877. <https://doi.org/10.1128/IAI.73.2.872-877.2005>
174. Kao, L.-T., Yang, T.-Y., Hung, W.-C., Yang, W.-T., He, P., Chen, B.-X., Wang, Y.-C., Chen, S.-S., Lai, Y.-W., Wang, H.-Y., & Tseng, S.-P. (2024). In Vivo Effect of Halicin on Methicillin-Resistant *Staphylococcus aureus* -Infected *Caenorhabditis elegans* and Its Clinical Potential. *Antibiotics*, *13*(9), 906. <https://doi.org/10.3390/antibiotics13090906>
175. Li, J., Mao, Y., Yi, J., Lin, M., Xu, H., Cheng, Y., Wu, H., & Liu, J. (2023). Induced expression modes of genes related to Toll, Imd, and JAK/STAT signaling pathway-mediated immune response in *Spodoptera frugiperda* infected with *Beauveria bassiana*. *Frontiers in Physiology*, *14*, 1249662. <https://doi.org/10.3389/fphys.2023.1249662>
176. Wang, J.-H. (2010). *Drosophila* as a model for antiviral immunity. *World Journal of Biological Chemistry*, *1*(5), 151. <https://doi.org/10.4331/wjbc.v1.i5.151>
177. Younes, S., Al-Sulaiti, A., Nasser, E. A. A., Najjar, H., & Kamareddine, L. (2020). *Drosophila* as a Model Organism in Host–Pathogen Interaction Studies. *Frontiers in Cellular and Infection Microbiology*, *10*, 214. <https://doi.org/10.3389/fcimb.2020.00214>
178. Ghani, M. U., Liu, G., Zhang, Q., Liu, C., Li, S., Yang, Y., Ahmad, M., & Cui, H. (2025). A Comprehensive review of humoral immune defense in the silkworm, *Bombyx mori*:

Mechanistic insights and responses to microbial pathogens. *Developmental & Comparative Immunology*, 170, 105418. <https://doi.org/10.1016/j.dci.2025.105418>

179. Romoli, O., Saviane, A., Bozzato, A., D'Antona, P., Tettamanti, G., Squartini, A., Cappellozza, S., & Sandrelli, F. (2017). Differential sensitivity to infections and antimicrobial peptide-mediated immune response in four silkworm strains with different geographical origin. *Scientific Reports*, 7(1), 1048. <https://doi.org/10.1038/s41598-017-01162-z>

180. Tan, J., Xu, M., Zhang, K., Wang, X., Chen, S., Li, T., Xiang, Z., & Cui, H. (2013). Characterization of hemocytes proliferation in larval silkworm, *Bombyx mori*. *Journal of Insect Physiology*, 59(6), 595–603. <https://doi.org/10.1016/j.jinsphys.2013.03.008>

181. Ghani, M. U., Liu, G., Zhang, Q., Liu, C., Li, S., Yang, Y., Ahmad, M., & Cui, H. (2025). A Comprehensive review of humoral immune defense in the silkworm, *Bombyx mori*: Mechanistic insights and responses to microbial pathogens. *Developmental & Comparative Immunology*, 170, 105418. <https://doi.org/10.1016/j.dci.2025.105418>

182. Shambat, S. M., Chen, P., Hoang, A. T. N., Bergsten, H., Vandenesch, F., Siemens, N., Lina, G., Monk, I. R., Foster, T. J., Arakere, G., Svensson, M., & Norrby-Teglund, A. (2015). Modeling staphylococcal pneumonia in a human 3D lung tissue model system delineates toxin-mediated pathology. *Disease Models & Mechanisms*, dmm.021923. <https://doi.org/10.1242/dmm.021923>

183. Kurow, O., Nuwayhid, R., Stock, P., Steinert, M., Langer, S., Krämer, S., & Metelmann, I. B. (2023). Organotypic 3D Co-Culture of Human Pleura as a Novel In Vitro

Model of *Staphylococcus aureus* Infection and Biofilm Development. *Bioengineering*, 10(5), 537. <https://doi.org/10.3390/bioengineering10050537>

184. Kohda, K., Li, X., Soga, N., Nagura, R., Duerna, T., Nakajima, S., Nakagawa, I., Ito, M., & Ikeuchi, A. (2021). An In Vitro Mixed Infection Model With Commensal and Pathogenic Staphylococci for the Exploration of Interspecific Interactions and Their Impacts on Skin Physiology. *Frontiers in Cellular and Infection Microbiology*, 11, 712360. <https://doi.org/10.3389/fcimb.2021.712360>

185. Guzmán-Soto, I., McTiernan, C., Gonzalez-Gomez, M., Ross, A., Gupta, K., Suuronen, E. J., Mah, T.-F., Griffith, M., & Alarcon, E. I. (2021). Mimicking biofilm formation and development: Recent progress in in vitro and in vivo biofilm models. *iScience*, 24(5), 102443. <https://doi.org/10.1016/j.isci.2021.102443>

186. Yousuf, B., Flint, A., Weedmark, K., Pagotto, F., & Ramirez-Arcos, S. (2021). Genome Sequence of *Staphylococcus aureus* Strain CBS2016-05, Isolated from Contaminated Platelet Concentrates in Canada. *Microbiology Resource Announcements*, 10(34), e00288-21. <https://doi.org/10.1128/MRA.00288-21>

187. Paredes, C., Chi, S. I., Flint, A., Weedmark, K., McDonald, C., Bearne, J., Ramirez-Arcos, S., & Pagotto, F. (2021). Complete Genome Sequence of *Staphylococcus aureus* CI/BAC/25/13/W, Isolated from Contaminated Platelet Concentrates in England. *Microbiology Resource Announcements*, 10(45), e00840-21. <https://doi.org/10.1128/MRA.00840-21>

188. Paredes, C., Chi, S. I., Flint, A., Weedmark, K., McDonald, C., Bearne, J., Ramirez-Arcos, S., & Pagotto, F. (2021). Complete Genome Sequence of *Staphylococcus aureus*

PS/BAC/169/17/W, Isolated from a Contaminated Platelet Concentrate in England. *Microbiology Resource Announcements*, 10(45), e00841-21. <https://doi.org/10.1128/MRA.00841-21>

189. Yousuf, B., Flint, A., Weedmark, K., McDonald, C., Bearne, J., Pagotto, F., & Ramirez-Arcos, S. (2021). Genome Sequence of *Staphylococcus aureus* Strain PS/BAC/317/16/W, Isolated from Contaminated Platelet Concentrates in England. *Microbiology Resource Announcements*, 10(35), e00577-21. <https://doi.org/10.1128/MRA.00577-21>

190. Garrett, S. R., Mariano, G., & Palmer, T. (2022). Genomic analysis of the progenitor strains of *Staphylococcus aureus* RN6390. *Access Microbiology*, 4(11). <https://doi.org/10.1099/acmi.0.000464.v3>

191. Truong-Bolduc, Q. C., Zhang, X., & Hooper, D. C. (2003). Characterization of NorR Protein, a Multifunctional Regulator of *norA* Expression in *Staphylococcus aureus*. *Journal of Bacteriology*, 185(10), 3127–3138. <https://doi.org/10.1128/JB.185.10.3127-3138.2003>

192. Wang, L.-J., Yang, X., Qian, S.-Y., Liu, Y.-C., Yao, K.-H., Dong, F., & Song, W.-Q. (2019). Identification of hemolytic activity and hemolytic genes of Methicillin-resistant *Staphylococcus aureus* isolated from Chinese children. *Chinese Medical Journal*, 133(1), 88–90. <https://doi.org/10.1097/cm9.0000000000000571>

193. BIOMERIEUX. (2021, April). *VITEK 2 GP*. BIOMERIEUX.

194. Navarro-Pérez, M. L., Fernández-Calderón, M. C., & Vadillo-Rodríguez, V. (2022). Decomposition of Growth Curves into Growth Rate and Acceleration: A Novel Procedure

To Monitor Bacterial Growth and the Time-Dependent Effect of Antimicrobials. *Applied and Environmental Microbiology*, 88(3). <https://doi.org/10.1128/aem.01849-21>

195. Lin, M.-F., Lin, Y.-Y., & Lan, C.-Y. (2020). Characterization of biofilm production in different strains of *Acinetobacter baumannii* and the effects of chemical compounds on biofilm formation. *PeerJ*, 8, e9020. <https://doi.org/10.7717/peerj.9020>

196. Wick, R. R., Judd, L. M., Gorrie, C. L., & Holt, K. E. (2017). Unicycler: Resolving bacterial genome assemblies from short and long sequencing reads. *PLOS Computational Biology*, 13(6), e1005595. <https://doi.org/10.1371/journal.pcbi.1005595>

197. Taboada, B., Estrada, K., Ciria, R., & Merino, E. (2018). Operon-mapper: A web server for precise operon identification in bacterial and archaeal genomes. *Bioinformatics*, 34(23), 4118–4120. <https://doi.org/10.1093/bioinformatics/bty496>

198. Camacho, C., Coulouris, G., Avagyan, V., Ma, N., Papadopoulos, J., Bealer, K., & Madden, T. L. (2009). BLAST+: Architecture and applications. *BMC Bioinformatics*, 10(1). <https://doi.org/10.1186/1471-2105-10-421>

199. Lim, H. G., Gao, Y., Rychel, K., Lamoureux, C., Lou, X. A., & Palsson, B. O. (2025). Revealing systematic changes in the transcriptome during the transition from exponential growth to stationary phase. *mSystems*, 10(1), e01315-24. <https://doi.org/10.1128/msystems.01315-24>

200. Jaishankar, J., & Srivastava, P. (2017). Molecular Basis of Stationary Phase Survival and Applications. *Frontiers in Microbiology*, 8, 2000. <https://doi.org/10.3389/fmicb.2017.02000>

201. Love, M. I., Huber, W., & Anders, S. (2014). Moderated estimation of fold change and dispersion for RNA-seq data with DESeq2. *Genome Biology*, 15(12), 550. <https://doi.org/10.1186/s13059-014-0550-8>
202. Monk, I. R. (2012). Genetic manipulation of Staphylococci—Breaking through the barrier. *Frontiers in Cellular and Infection Microbiology*, 2. <https://doi.org/10.3389/fcimb.2012.00049>
203. Monk, I. R., Shah, I. M., Xu, M., Tan, M.-W., & Foster, T. J. (2012). Transforming the Untransformable: Application of Direct Transformation To Manipulate Genetically *Staphylococcus aureus* and *Staphylococcus epidermidis*. *mBio*, 3(2), e00277-11. <https://doi.org/10.1128/mBio.00277-11>
204. Ebrahimi, S., Khosravi, M. A., Raz, A., Karimipoor, M., & Parvizi, P. (2023). CRISPR-Cas Technology as a Revolutionary Genome Editing tool: Mechanisms and Biomedical Applications. *Iranian Biomedical Journal*, 27(5), 219–246. <https://doi.org/10.61186/ibj.27.5.219>
205. Chen, W., Zhang, Y., Yeo, W.-S., Bae, T., & Ji, Q. (2017). Rapid and Efficient Genome Editing in *Staphylococcus aureus* by Using an Engineered CRISPR/Cas9 System. *Journal of the American Chemical Society*, 139(10), 3790–3795. <https://doi.org/10.1021/jacs.6b13317>
206. Carattoli, A., & Hasman, H. (2020). PlasmidFinder and In Silico pMLST: Identification and Typing of Plasmid Replicons in Whole-Genome Sequencing (WGS). In F. De La Cruz (Ed.), *Horizontal Gene Transfer* (Vol. 2075, pp. 285–294). Springer US. https://doi.org/10.1007/978-1-4939-9877-7_20

207. Truong-Bolduc, Q. C., Wang, Y., & Hooper, D. C. (2022). Role of *Staphylococcus aureus* Tet38 in Transport of Tetracycline and Its Regulation in a Salt Stress Environment. *Journal of Bacteriology*, *204*(7), e0014222. <https://doi.org/10.1128/jb.00142-22>
208. Grkovic, S., Brown, M. H., Hardie, K. M., Firth, N., & Skurray, R. A. (2003). Stable low-copy-number *Staphylococcus aureus* shuttle vectors. *Microbiology (Reading, England)*, *149*(Pt 3), 785–794. <https://doi.org/10.1099/mic.0.25951-0>
209. Clinical and Laboratory Standards Institute. (2024). *Performance Standards for Antimicrobial Susceptibility Testing (Table 2C)* (Version CLSI M100, 34th Edition). CLSI.
210. Mah, T.-F. (2014). Establishing the Minimal Bactericidal Concentration of an Antimicrobial Agent for Planktonic Cells (MBC-P) and Biofilm Cells (MBC-B). *Journal of Visualized Experiments*, *83*, 50854. <https://doi.org/10.3791/50854>
211. Vandenesch, F., Lina, G., & Henry, T. (2012). *Staphylococcus aureus* hemolysins, bi-component leukocidins, and cytolytic peptides: A redundant arsenal of membrane-damaging virulence factors? *Frontiers in Cellular and Infection Microbiology*, *2*, 12. <https://doi.org/10.3389/fcimb.2012.00012>
212. Di Bella, S., Marini, B., Stroffolini, G., Geremia, N., Giacobbe, D. R., Campanile, F., Bartoletti, M., Allosio, G., Di Risio, L., Viglietti, G., Principe, L., Costantino, V., Buseti, M., Zerbato, V., Mearelli, F., Biolo, G., Nunnari, A., Cafiero, C. M., & Di Masi, A. (2025). The virulence toolkit of *Staphylococcus aureus*: A comprehensive review of toxin diversity, molecular mechanisms, and clinical implications. *European Journal of Clinical Microbiology & Infectious Diseases*. <https://doi.org/10.1007/s10096-025-05148-y>

213. Loza-Correa, M., Yousuf, B., & Ramirez-Arcos, S. (2021). *Staphylococcus epidermidis* undergoes global changes in gene expression during biofilm maturation in platelet concentrates. *Transfusion*, 61(7), 2146–2158. <https://doi.org/10.1111/trf.16418>
214. Saad Latteef, N., Salih, W. Y., Aziz Abdulhassan, A., & Jasim Obeed, R. (2022). Evaluation of Gene Expression of *norA* and *norB* Gene in Ciproflaxin and Levofloxacin Resistant *Staphylococcus aureus*. *Archives of Razi Institute*, 77(5), 1987–1993. <https://doi.org/10.22092/ARI.2022.358335.2197>
215. Ates, A., Tastan, C., & Ermertcan, S. (2024). *Precision Genome Editing Unveils a Breakthrough in Reversing Antibiotic Resistance: CRISPR/Cas9 Targeting of Multi-Drug Resistance Genes in Methicillin-Resistant Staphylococcus aureus*. *Microbiology*. <https://doi.org/10.1101/2023.12.31.573511>
216. Mello, P. L., Riboli, D. F. M., Martins, L. D. A., Brito, M. A. V. P., Victória, C., Calixto Romero, L., & Ribeiro De Souza Da Cunha, M. D. L. (2020). *Staphylococcus spp.* Isolated from Bovine Subclinical Mastitis in Different Regions of Brazil: Molecular Typing and Biofilm Gene Expression Analysis by RT-qPCR. *Antibiotics*, 9(12), 888. <https://doi.org/10.3390/antibiotics9120888>
217. Peng, R., Lin, G., & Li, J. (2016). Potential pitfalls of CRISPR/Cas9-mediated genome editing. *The FEBS Journal*, 283(7), 1218–1231. <https://doi.org/10.1111/febs.13586>
218. Sioson, V. A., Kim, M., & Joo, J. (2021). Challenges in delivery systems for CRISPR-based genome editing and opportunities of nanomedicine. *Biomedical Engineering Letters*, 11(3), 217–233. <https://doi.org/10.1007/s13534-021-00199-4>

219. Stewart, M. D., Merino Vega, D., Arend, R. C., Baden, J. F., Barbash, O., Beaubier, N., Collins, G., French, T., Ghahramani, N., Hinson, P., Jelinic, P., Marton, M. J., McGregor, K., Parsons, J., Ramamurthy, L., Sausen, M., Sokol, E. S., Stenzinger, A., Stires, H., ... Allen, J. (2022). Homologous Recombination Deficiency: Concepts, Definitions, and Assays. *The Oncologist*, 27(3), 167–174. <https://doi.org/10.1093/oncolo/oyab053>
220. Everitt, R. G., Didelot, X., Batty, E. M., Miller, R. R., Knox, K., Young, B. C., Bowden, R., Auton, A., Votintseva, A., Lerner-Svensson, H., Charlesworth, J., Golubchik, T., Ip, C. L. C., Godwin, H., Fung, R., Peto, T. E. A., Walker, A. S., Crook, D. W., & Wilson, D. J. (2014). Mobile elements drive recombination hotspots in the core genome of *Staphylococcus aureus*. *Nature Communications*, 5(1). <https://doi.org/10.1038/ncomms4956>
221. LeBlanc, L., Pepin, J., Toulouse, K., Ouellette, M.-F., Coulombe, M.-A., Corriveau, M.-P., & Alary, M.-E. (2006). Fluoroquinolones and Risk for Methicillin-Resistant *Staphylococcus aureus* , Canada. *Emerging Infectious Diseases*, 12(7), 1398–1405. <https://doi.org/10.3201/eid1209.060397>
222. Ramírez-Arcos, S., & Goldman, M. (2022). Bacterial Contamination. In M. F. Murphy, D. J. Roberts, M. H. Yazer, & N. M. Dunbar (Eds.), *Practical Transfusion Medicine* (1st ed., pp. 221–228). Wiley. <https://doi.org/10.1002/9781119665885.ch18>
223. Trochanowska-Pauk, N., Walski, T., Bohara, R., Mikolas, J., & Kubica, K. (2024). Platelet Storage—Problems, Improvements, and New Perspectives. *International Journal of Molecular Sciences*, 25(14), 7779. <https://doi.org/10.3390/ijms25147779>

224. Hodgson, S. D., Greco-Stewart, V., Jimenez, C. S., Sifri, C. D., Brassinga, A. K. C., & Ramirez-Arcos, S. (2014). Enhanced pathogenicity of biofilm-negative *S taphylococcus epidermidis* isolated from platelet preparations. *Transfusion*, *54*(2), 461–470. <https://doi.org/10.1111/trf.12308>
225. Hamady, A. B., Abd El-Fadeal, N. M., Imbaby, S., Nassar, H. M., Sakr, M. G., & Marei, Y. E. (2024). Expression of *norA*, *norB* and *norC* efflux pump genes mediating fluoroquinolones resistance in MRSA isolates. *The Journal of Infection in Developing Countries*, *18*(03), 399–406. <https://doi.org/10.3855/jidc.18877>
226. Mechanisms of Resistance to Quinolones. (2021). In S. Georgina Solano-Gálvez, M. Fernanda Valencia-Segrove, M. José Ostos Prado, A. Berenice López Bouciguez, D. Abelardo Álvarez-Hernández, & R. Vázquez-López, *Antimicrobial Resistance—A One Health Perspective*. IntechOpen. <https://doi.org/10.5772/intechopen.92577>
227. Hamza, A. (2012). *Growth and Biofilm Formation of Bacteria Isolated from Contaminated Platelet Units*. <https://doi.org/10.20381/RUOR-5784>
228. Taha, M., Kohnen, C., Mallya, S., Kou, Y., Zapata, A., & Ramirez-Arcos, S. (2018). Comparative characterisation of the biofilm-production abilities of *Staphylococcus epidermidis* isolated from human skin and platelet concentrates. *Journal of Medical Microbiology*, *67*(2), 190–197. <https://doi.org/10.1099/jmm.0.000673>
229. Rollin, G., Tan, X., Tros, F., Dupuis, M., Nassif, X., Charbit, A., & Coureuil, M. (2017). Intracellular Survival of *Staphylococcus aureus* in Endothelial Cells: A Matter of Growth or Persistence. *Frontiers in Microbiology*, *8*, 1354. <https://doi.org/10.3389/fmicb.2017.01354>

230. Neidig, A., Stempel, N., Waeber, N. B., Nizer, W. S. da C., & Overhage, J. (2023). Knock-out of multidrug efflux pump MexXY-OprM results in increased susceptibility to antimicrobial peptides in *Pseudomonas aeruginosa*. *Microbiology and Immunology*, 67(9), 422–427. <https://doi.org/10.1111/1348-0421.13089>
231. Kullik, I., & Giachino, P. (1997). The alternative sigma factor sigmaB in *Staphylococcus aureus*: Regulation of the *sigB* operon in response to growth phase and heat shock. *Archives of Microbiology*, 167(2–3), 151–159. <https://doi.org/10.1007/s002030050428>
232. Chen, K., & Lu, Z. (2018). Immune responses to bacterial and fungal infections in the silkworm, *Bombyx mori*. *Developmental & Comparative Immunology*, 83, 3–11. <https://doi.org/10.1016/j.dci.2017.12.024>
233. Pidwill, G. R., Gibson, J. F., Cole, J., Renshaw, S. A., & Foster, S. J. (2021). The Role of Macrophages in *Staphylococcus aureus* Infection. *Frontiers in Immunology*, 11, 620339. <https://doi.org/10.3389/fimmu.2020.620339>
234. Bertram, T., Reimers, D., Lory, N. C., Schmidt, C., Schmid, J., C. Heinig, L., Bradtke, P., Rattay, G., Zielinski, S., Hellmig, M., Bartsch, P., Rohde, H., Nuñez, S., Roseblatt, M. V., Bono, M. R., Gagliani, N., Sandrock, I., Panzer, U., Krebs, C. F., ... Mittrücker, H.-W. (2023). Kidney-resident innate-like memory $\gamma\delta$ T cells control chronic *Staphylococcus aureus* infection of mice. *Proceedings of the National Academy of Sciences*, 120(1), e2210490120. <https://doi.org/10.1073/pnas.2210490120>

235. Kim, H. K., Missiakas, D., & Schneewind, O. (2014). Mouse models for infectious diseases caused by *Staphylococcus aureus*. *Journal of Immunological Methods*, 410, 88–99. <https://doi.org/10.1016/j.jim.2014.04.007>
236. Klopfenstein, N., Cassat, J. E., Monteith, A., Miller, A., Drury, S., Skaar, E., & Serezani, C. H. (2021). Murine Models for Staphylococcal Infection. *Current Protocols*, 1(3), e52. <https://doi.org/10.1002/cpz1.52>
237. Grkovic, S., Brown, M. H., Hardie, K. M., Firth, N., & Skurray, R. A. (2003). Stable low-copy-number *Staphylococcus aureus* shuttle vectors. *Microbiology*, 149(3), 785–794. <https://doi.org/10.1099/mic.0.25951-0>